Newcastle
University

The role of DNA-dependent protein kinase (DNA-PK) and ataxia telangiectasia mutated (ATM) kinase in the cellular response to microtubule-targeting drugs

Emily Victoria Alinda Mould

Thesis submitted for the degree of Doctor of Philosophy

Newcastle University

Faculty of Medical Sciences

Northern Institute for Cancer Research

November 2014

Abstract

DNA-dependent protein kinase (DNA-PK) and ataxia telangiectasia mutated (ATM) kinase are DNA-damage activated kinases that play central roles in the non-homologous end joining (NHEJ) and homologous recombination (HR) DNA double-strand break repair pathways, respectively. DNA-PK and ATM have both been shown to have roles in addition to DNA repair, involving localisation at the centrosome during mitosis and mitotic regulation. Pilot studies demonstrated that the selective DNA-PK and ATM inhibitors, NU7441 and KU55933, respectively, caused greater sensitisation to DNA-damaging and microtubule-targeting agents in multidrug-resistant cells compared with parental cells. This observation led to the hypothesis that inhibition of DNA-PK and ATM using NU7441 and KU55933, respectively, or loss of DNA-PK function in DNA-PK deficient cells, would sensitise cells to agents that interfere with the formation of the mitotic spindle, e.g. microtubule-targeting agents such as vincristine, docetaxel and paclitaxel.

Growth inhibition assays in four different paired parental sensitive and multidrug-resistant cell lines (resistant through overexpression of the drug efflux transporter, MDR1) demonstrated that 1 µM NU7441 and 10 µM KU55933 sensitised the multidrug-resistant cells to vincristine and either docetaxel or paclitaxel to a significantly greater extent than in parental cells. Phosphorylation of DNA-PK at a DNA-damage-associated autophosphorylation site (Ser2056) was observed in response to vincristine, which did not cause DNA damage as determined using the COMET assay. Unexpectedly, three MDR1-overexpressing multidrug-resistant cell lines were found to be not only chemo-resistant but also radio-resistant.

Investigations into the effects of NU7441 and KU55933 on drug transport demonstrated that in MDR1-overexpressing canine kidney MDCKII-MDR1 cells, 1µM NU7441 significantly increased doxorubicin cellular accumulation, measured by fluorescence microscopy, *via* an MDR1-dependent mechanism. NU7441 (1 µM), three structurally-related compounds (NU7742 (an inactive NU7441 analogue), DRN1 and DRN2 (DNA-PK-inhibitory and DNA-PK non-inhibitory atropisomeric NU7441 derivatives, respectively)) at 1 µM, and KU55933 at 1 µM and 10 µM, all increased intracellular vincristine accumulation in the MDR1-overexpressing CCRF-CEM VCR/R cells to a level similar to that induced by verapamil, as measured by LC-MS.

Growth inhibition and cytotoxicity studies using an isogenic panel of DNA-PK proficient and deficient cell lines, with varying DNA-PK catalytic subunit expression levels (parental DNA-PK +/+, DNA-PK +/-, DNA-PK -/- and DNA-PK -/- cells with PRKDC cDNA re-expression (DNA-PK RE)) established that DNA-PK -/- cells were more sensitive to ionising radiation, vincristine and docetaxel, thereby demonstrating a role for DNA-PK in the response of cells to all of these agents. KU55933 (10 µM) caused significant sensitisation in the HCT116 DNA-PK +/+, DNA-PK +/- and DNA-PK -/- cells to ionising radiation, vincristine and docetaxel, suggesting an additional role for ATM. The combination of vincristine and ionising radiation was significantly more active in the absence of DNA-PK or following inhibition of DNA-PK.

Confocal microscopy studies demonstrated that phosphorylated DNA-PK localised to mitotic structures and that lack or inhibition of DNA-PKcs caused an increase in aberrant mitotic events, such as chromosome misalignment, increases in centrosome number and multipolar spindle formation.

Overall, the studies described in this thesis demonstrate that DNA-PK and ATM play a role in mitosis and in the response of cancer cells to microtubule-targeting agents. Dual DNA-PK and MDR1 inhibitors, and dual ATM and MDR1 inhibitors, were identified. These results extend the clinical potential of targeted inhibition of DNA-PK and ATM to use in combination with microtubule-targeting agents.

Acknowledgements

Firstly, I would like to thank my supervisors Dr Elaine Willmore and Professor Herbie Newell for giving me the opportunity to undertake my PhD project here in Newcastle. Elaine has provided so much help, support and endless patience. She has been not only a fantastic supervisor but also a great friend. Herbie has been incredibly generous with his time, support and optimism (along with being a source of many cat stories) throughout my PhD project, for which I am extremely grateful. I am also very thankful for the help I received from both Elaine and Herbie to publish a number of the results explained in Chapter 4; the journal article is included in the Appendices.

I would like to thank all of the people who have provided me with lab help over the years; without which I would not have made it through! I am grateful to all of the past and present members of the Drug Discovery and Imaging group for their help and for making the NICR such a nice place to work. Particular mention has to go to Sue Tudhope who has been the source of much help, knowledge (both science and Formula 1), endless laughs and bananas along the way, and I am so grateful for everything she has done for me. The other people who deserve a special mention are Nicole Phillips, Lindi Chen, Phil Berry, David Jamieson, Chris Hill, Suzanne Kyle, Emma Haagensen, Jill Hunter and Evan Mulligan.

This work would not have been possible without the generous financial support of Cancer Research UK for which I am very grateful. I would also like to thank Professor Iain McNeish (University of Glasgow) for kindly providing the SKOV3 and SKOV3-TR, and the A2780 and A2780-TX1000, paired cell lines for use in these studies.

All of the data in the results section of this thesis are my own work except where indicated. I had the pleasure of supervising Stephanie Burnell during her MRes project and her work contributed to a number of the figures in Chapter 3; indicated in the figure legends. Also, a small proportion of the work in Chapter 3 with the KK47 cell line has been previously presented as part of my MRes thesis; which is clearly indicated in the figure legends and was included for comparative purposes.

Finally, I would like to thank my parents for all of their love and guidance over the years (despite them not really knowing what this thesis is about!). My extended family and friends have been extremely supportive, and particular mention goes to Laura Mottram who has been a great fellow PhD stress-head! Lastly, special thanks must go to Will for his unwavering optimism and belief in me, along with being an excellent proof-reader, my best friend, and my future husband.

Table of Contents

List of Figures, Tables and Equations

Figures

Chapter 1 : Introduction

Chapter 2 : Materials and Methods

Chapter 3 : The effects of the DNA-PK inhibitor NU7441 and the ATM kinase inhibitor KU55933 on the growth inhibitory and cytotoxic activities of microtubule-targeting agents in paired parental and multidrug-resistant cell lines

Chapter 4 : Identification of dual DNA-PK and MDR1 inhibitors, and ATM kinase and MDR1 inhibitors, for the potentiation of cytotoxic drug activity

Chapter 5 : Investigation into the response of paired parental and multidrug-resistant cells to ionising radiation alone and in combination with NU7441 or KU55933

Chapter 6 : Investigation of the role of DNA-PK and ATM as a determinant of ionising radiation and vincristine response using paired DNA-PK proficient and deficient cell lines

Chapter 7 : The effect of ionising radiation, microtubule-targeting agents and DNA-PK deletion or inhibition on mitosis, and the subcellular localisation and activity of DNA-PK

Tables

Chapter 5 : Investigation into the response of paired parental and multidrug-resistant cells to ionising radiation alone and in combination with NU7441 or KU55933

Chapter 6 : Investigation of the role of DNA-PK and ATM as a determinant of ionising radiation and vincristine response using paired DNA-PK proficient and deficient cell lines

Equations

Chapter 2: Materials and Methods

List of Abbreviations

°C	Degrees Celsius
µg	Microgram
µl	Microlitre
µM	Micromole
53BP1	p53 binding protein 1
ABC	ATP-binding cassette
ABCB1	ATP-binding cassette, subfamily B 1, gene that codes for MDR1 protein
ABCC1	ATP-binding cassette, subfamily C 1
ABCG2	ATP-binding cassette, subfamily G 2, gene that codes for BCRP
AFC	Amino-4-trifluoromethyl coumarin
AIRE	Autoimmune regulator
AKT	Protein kinase B
ALL	Acute lymphoblastic leukaemia
AML	Acute myeloid leukaemia
AMP	5' adenosine monophosphate
AMPK	AMP-activated protein kinase
ANOVA	Analysis of variance
APC	Anaphase-promoting complex
AT	Ataxia telangiectasia
ATLD	Ataxia telangiectasia–like disorder
ATM	Ataxia telangiectasia mutated kinase
ATP	Adenosine tri-phosphate
ATPase	Adenosine 5'-tri-phosphatase
ATR	Ataxia telangiectasia and Rad3 related
BCA	Bicinchoninic acid
Bcl-2	B-cell lymphoma-2
BCR-Abl	Breakpoint cluster region – Abelson, fusion gene formed by chromosome 9 and 22 translocation
BCRP	Breast cancer resistance protein

BER	Base excision repair
BH3	Bcl-2 homology domain 3
BLM	Bloom syndrome helicase
B-Raf	Cellular proto-oncogene B homolog of the V-raf murine sarcoma viral oncogene
B-Raf^{V600E}	V600E mutant form of B-Raf
BRCA1	Breast cancer type 1 susceptibility protein
BRCA2	Breast cancer type 2 susceptibility protein
BSA	Bovine serum albumin
BUB1	Budding uninhibited by benzimidazoles 1 protein
BUB1B	Budding uninhibited by benzimidazoles 1 protein kinase B
BUB3	Budding uninhibited by benzimidazoles 3 protein
BUBR1	BUB-related 1
CA	California
CDC20	Cell division cycle 20
cDNA	Complementary DNA
Chk1	Checkpoint kinase 1
Chk2	Checkpoint kinase 2
Chk2 T68	Phosphorylation site at threonine 68 on Chk2
CLL	Chronic lymphocytic leukaemia
c-Met	Cellular proto-oncogene which encodes HGF receptor
c-Myc	Cellular proto-oncogene homolog of v-Myc, the avian myelocytomatosis viral oncogene
CNS	Central nervous system
CO_2	Carbon dioxide
COSMIC	Catalogue of somatic mutations in cancer
CT	Cycle threshold, PCR
CT	Connecticut
CtIP	C-terminal binding protein-interacting protein
CTLA4	Cytotoxic T-lymphocyte antigen 4
Da	Daltons

DAPI	4',6-diamidino-2-phenylindole
DDR	DNA damage response
dH$_2$O	Deionised water
DMEM	Dulbecco's Modified Eagle Medium
DMSO	Dimethyl sulphoxide
DNA	Deoxyribonucleic acid
DNA-PK	DNA-dependent protein kinase
DNA-PKcs	Catalytic subunit of DNA-dependent kinase
dNTPs	Deoxyribonucleoside triphosphates
DOC	Docetaxel
DOX	Doxorubicin
DSB	DNA double-strand break
ECL	Enhanced chemiluminescence
EDTA	Ethylenediaminetetraacetic acid
EGFR	Epidermal growth factor receptor
ELISA	Enzyme-linked immunosorbent assay
EM	Emily Mould
ERK	Extracellular signal-regulated kinase
Exo1	Exonuclease 1
EZH2	Enhancer of zeste homolog 2 (Drosophila), a histone-lysine N-methyltransferase
FAM	Synthetic equivalent of fluorescein dye
FAT	Focal adhesion targeting region, consisting of FRAP, ATM and TRRAP
FATC	COOH-terminal FAT domain
FBS	Foetal bovine serum
FLT3	FMS-related tyrosine kinase 3, also known as CD135
FRAP	FKBP12-rapamycin-associated protein
g	Gram
GDP	Guanosine di-phosphate
GEN1	Holliday junction 5' flap endonuclease
GI$_{50}$	Half maximal growth inhibitory concentration

GLUT1	Glucose transporter 1
GTP	Guanosine tri-phosphate
GTPase	Family of hydrolase enzymes that bind and hydrolyse GTP
H2AX	Histone H2A family, X member
H_2O	Water
HCC	Hepatocellular carcinoma
HEAT	Huntingtin, Elongation Factor 3, PP2A and Tor1
HGF	Hepatocyte growth factor
HIF-1α	Hypoxia-inducible factor-1 alpha
HPLC	High-performance liquid chromatography
HR	Homologous recombination
HRP	Horse-radish peroxidase
hSMG-1	Human suppressor of morphogenesis in genitalia-1
IAAP	$[^{125}I]$-iodoarylazidoprazosin
IC_{50}	Half maximal inhibitory concentration
IFN	Type 1 interferon
IgG	Immunoglobulin G
INCENP	Inner centromere protein
IR	Ionising radiation
IRF-3	Interferon regulatory factor-3
KAP1	Krüppel associated box (KRAB)-associated protein-1
KCl	Potassium chloride
KCM	Buffer containing 120 mM KCl, 20 mM NaCl, 10 mM Tris-HCl, pH 8.0, 1 mM EDTA
KCM-T	0.1 % (v/v) Triton X-100 in KCM buffer
kDa	Kilodaltons
KSP	Kinesin spindle protein
Ku	Heterodimeric protein involved in NHEJ consisting of Ku70 and Ku80
Ku70	Ku protein of approximately 70 kDa mass
Ku80	Ku protein of approximately 80 kDa mass
l	Litre

LC$_{90}$	90 % lethal concentration
LC-MS	Liquid chromatography-mass spectrometry
LoxP	locus of X-over P1, sequence recognised by Cre recombinase in site-specific recombinase technology
LRP	Lung resistance-related protein
mAb	Monoclonal antibody
MAD1	Mitotic arrest deficient-1 like protein
MAD2	Mitotic arrest deficient-2 like protein
MAP2	Microtubule-associated protein 2
MAP4	Microtubule-associated protein 4
MAPs	Microtubule-associated proteins
MD	Maryland
MDC assay	Assay which evaluates incorporation of monodansylcadaverine into vacuoles by fluorescent microscopy
MDC1	Mediator of DNA-damage checkpoint 1
MDM2	Mouse double minute 2 protein
MDR	Multidrug-resistance
MDR1	Multidrug-resistance protein 1
MEM	Minimum Essential Medium
MITOX	Mitoxantrone
ml	Millilitre
mM	Millimoles
mm	Millimetres
MMR	Mismatch repair
MOPS	Buffer containing 3-(N-morpholino)propanesulfonic acid
Mre11	Meiotic recombination 11 homolog A (*S.cerevisiae*), DNA repair protein
MRN	Complex consisting of Mre11, Rad50 and Nbs1
mRNA	Messenger RNA
MRP1	Multidrug resistance-associated protein 1
MS	Mass spectrometry

MSP1	Monopolar spindle protein 1
MTA	Microtubule-targeting agent
mTOR	Mammalian or mechanistic target of rapamycin
MTT	Methylthiazolyldiphenyl-tetrazolium bromide
NaOH	Sodium hydroxide
NBS	Nijmegen breakage syndrome
Nbs1	Nijmegen breakage syndrome 1 protein
NER	Nucleotide excision repair
NF-κB	Nuclear factor kappa B
ng	Nanogram
NHEJ	Non-homologous end-joining
NK cells	Natural killer cells
nl	Nanolitre
nM	Nanomole
nm	Nanometres
NSCLC	Non-small cell lung cancer
NuMA1	Nuclear mitotic apparatus protein 1
OTM	Olive tail moment, COMET assay measurement, [(tail mean – head mean) * tail % DNA] / 100
p21	Protein of 21 kDa molecular mass also known as cyclin dependent kinase inhibitor 1A
p53	Tumour suppressor transcription factor protein of 53 kDa mass
PAR	Poly ADP ribose
PARP	Poly ADP ribose polymerase
PARP1	Poly ADP ribose polymerase 1
PBL	Peripheral blood lymphocytes
PBS	Phosphate buffered saline
PCR	Polymerase chain reaction
PF_{50}	Half maximal potentiation factor
PI3K	Phosphoinositide 3-kinase
PI3KA	Gene encoding the 110 kDa catalytic subunit of class 1 PI3K

PIKK	PI3K-like-kinase family consisting of DNA-PKcs, ATM, ATR, mTOR, hSMG-1 and TRRAP
PLK	Polo-like kinase
PLK1	Polo-like kinase 1
PLK4	Polo-like kinase 4
PMS	N-methyl dibenzopyrazine methyl sulphate in phosphate buffered saline
Pol μ	DNA polymerase mu
Pol λ	DNA polymerase lambda
PP2A	Protein phosphatase 2
PP6	Protein phosphatase 6
PRKDC	Gene encoding DNA-PKcs
qRT-PCR	Quantitative real time-polymerase chain reaction
rAAV	Recombinant adeno-associated virus vectors
Rad50	Rad50 (*S. cerevisiae*) homolog, DNA repair protein
Rad51	Rad51 (*S. cerevisiae*) homolog recombinase, DNA repair protein
Rad52	Rad 52 (*S. cerevisiae*) homolog, DNA repair protein
RAG-1	Recombination-activating gene-1
RAG-2	Recombination-activating gene-2
Rb	Retinoblastoma protein
RING-finger	Really interesting new gene-finger, domain
RNA	Ribonucleic acid
RNase	Ribonuclease
RNF168	RING finger protein 168
RNF8	RING finger protein 8
RPA	Replication protein A
RPA32	32 kDa subunit of replication protein A
RPMI	Roswell Park Memorial Institute Medium
RR-AFC	Ac-RR-amino-4-trifluoromethyl coumarin, substrate for Cathepsin B Activity Assay kit
RT	Real time
SAC	Spindle assembly checkpoint

SB	Stephanie Burnell
SCID	Severe combined immunodeficiency disease
SD	Standard deviation
SDS	Sodium dodecyl sulphate
SDS-PAGE	Sodium dodecyl sulphate – polyacrylamide gel electrophoresis
SEM	Standard error of the mean
Ser1981	ATM autophosphorylation site at serine 1981
Ser2056	DNA-PKcs autophosphorylation site at serine 2056
siRNA	Small interfering RNA
Skp2	S-phase kinase-associated protein 2
SLX1	Structure-Specific Endonuclease Subunit 1 Homolog A (*S. cerevisiae*)
SLX4	Structure-Specific Endonuclease Subunit 4 Homolog (*S. cerevisiae*)
SNP	Single nucleotide polymorphisms
SYBR Green	N',N'-dimethyl-N-[4-[(E)-(3-methyl-1,3-benzothiazol-2-ylidene)methyl]-1-phenylquinolin-1-ium-2-yl]-N-propylpropane-1,3-diamine, asymmetrical cyanine dye
TAMRA	5-Carboxytetramethylrhodamine
tATM	Total ATM protein of approximately 350 kDa
TBS	Tris-buffered saline
TBS-T	Tris-buffered saline with Tween 20
tDNA-PKcs	Total DNA-PKcs protein of approximately 460 kDa
TEMOZ	Temozolomide
Thr2609	DNA-PKcs phosphorylation site at threonine 2609
TNF	Tumour necrosis factor
TNKS1	Tankyrase 1
TopBP1	DNA topoisomerase 2-binding protein 1
Tor1	Target of rapamycin complex 1
TP53	Tumour suppressor gene encoding p53
TRA	Tissue-restricted antigen

Tris	Tris(hydroxymethyl)aminomethane
Tris-HCL	Tris-hydrochloric acid
TRRAP	Transformation/transcription domain-associated protein
UK	United Kingdom
USA	United States of America
USF-1	Upstream stimulatory transcription factor 1
V	Volts
V(D)J	Recombination targeting variable (V), diversity (D) and joining (J) gene segments
v/v	Volume in volume
VCAM-1	Vascular cell adhesion protein 1
VCR	Vincristine
VCR/R	Vincristine-resistant
VEGF	Vascular endothelial growth factor
VEGFR2	Vascular endothelial growth factor receptor 2
w/v	Weight in volume
WA	Washington State, USA
WRN	Werner syndrome protein
x g	Times gravity of the earth, in relation to centrifugation
XLF	XRCC4-like factor
XRCC4	X-ray repair complementing defective repair in Chinese hamster cells 4
XRCC5	X-ray repair complementing defective repair in Chinese hamster cells 5 encoding the protein Ku80
XRCC6	X-ray repair complementing defective repair in Chinese hamster cells 6 encoding the protein Ku70
XTT	Sodium 3'-[1-(phenylaminocarbonyl)- 3,4-tetrazolium]-bis (4-methoxy-6-nitro) benzene sulphonic acid hydrate
γH2AX	H2AX phosphorylated on serine 139, called gamma-H2AX
ΔCT	Delta cycle threshold, difference of expression between 2 genes determined by PCR
λ_{em}	Emission wavelength
λ_{ex}	Excitation wavelength

Chapter 1: Introduction

1.1 Cancer

Cancer is the name given to a large, heterogeneous group of diseases that have developed particular genetic alterations to allow malignant growth. There are over 200 different cell types in the body and therefore over 200 different types of cancer.

In the UK, more than 331,000 people were diagnosed with cancer in 2011 and more than 1 in 3 people will develop cancer during their lifetime, with breast, lung, prostate and bowel cancers together accounting for over half of all new cancers diagnosed every year (Cancer Research UK, 2014). Cancer incidence rates in the UK have risen 23 % in males and 43 % in females over the last 40 years, but in that time cancer survival rates have doubled and now 50 % of people will survive for at least 10 years after diagnosis (Cancer Research UK, 2014).

Hanahan and Weinberg originally proposed that, despite the large number of different cancers, all cancer cells have 6 biological capabilities, or "Hallmarks", in common that are acquired during the multistep development of a human tumour; self-sufficiency in growth signals, evasion of apoptosis, insensitivity to anti-growth signals, sustained angiogenesis, limitless replicative potential and tissue invasion and metastasis (Hanahan and Weinberg, 2000). In 2011, a further two "Hallmarks" were added, and these are "deregulating cellular energy metabolism" and "avoiding immune destruction" (Hanahan and Weinberg, 2011) (Figure 1-1). It was also noted that there are two "enabling characteristics" that make the acquisition of the biological capabilities possible and these are "genome instability" and "mutation and tumour-promoting inflammation".
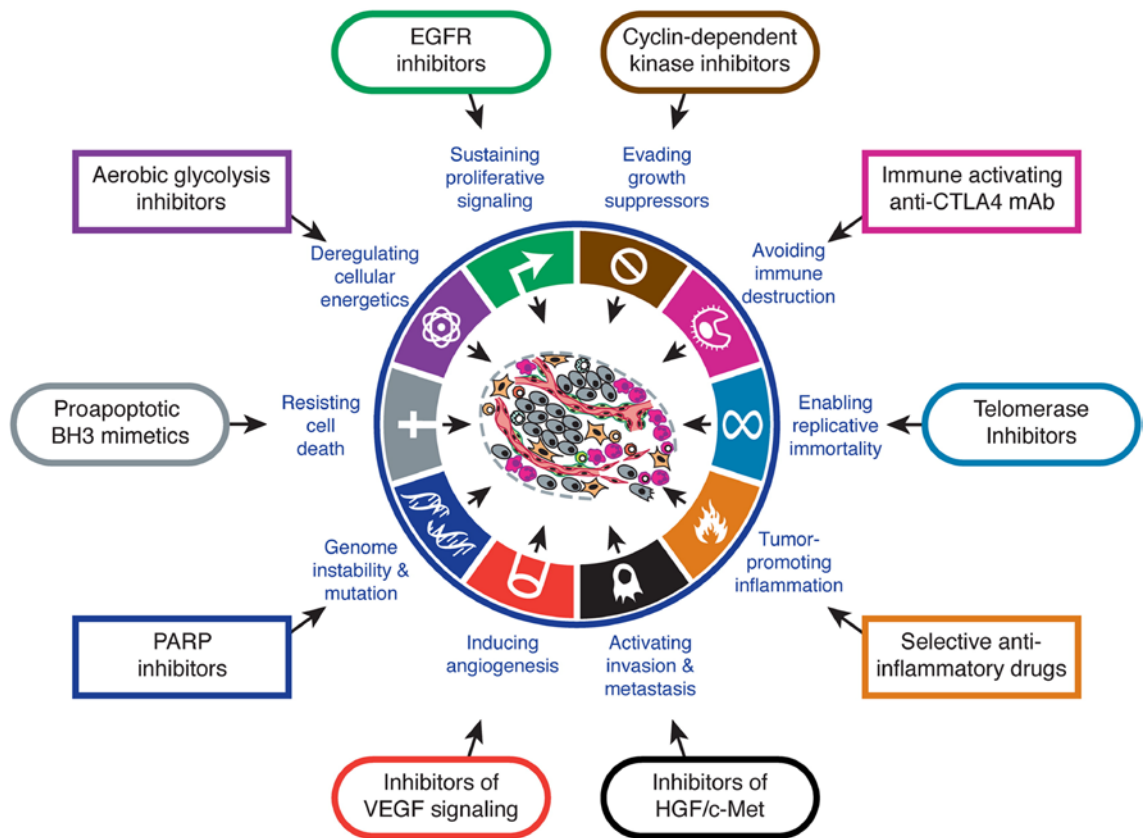
Figure 1-1: The Hallmarks of Cancer. Hanahan and Weinberg (2011) have postulated that these are the main 10 acquired hallmarks of cancer and associated examples of therapeutic targeting of each of these features are given.

Chemotherapy originated in the early 1900s with the German chemist Paul Ehrlich. It was defined as the "use of chemicals to treat diseases", and Paul Ehrlich postulated that it would be possible to create "magic bullets", which would be drugs that would travel straight to their intended targets; i.e. the beginnings of targeted therapy (Strebhardt and Ullrich, 2008). Radiotherapy and surgery dominated cancer treatment until the development of combination chemotherapy followed by cancer sequencing, which together with patient-derived cancer cell lines and improved *in vivo* models to test novel agents, have led to the recent advancement of targeted therapies (DeVita and Chu, 2008).

The majority of cancer patients are treated with a combination of cytotoxic chemotherapeutics and/or radiation therapy, which tend not to distinguish between normal "healthy" rapidly-dividing cells and cancer cells, and therefore result in toxic side-effects to tissues such as bone marrow, the gastrointestinal tract and hair follicles. Ionising radiation acts to damage DNA directly or indirectly by the ionisation of atoms in the DNA and the formation of hydroxyl radicals from water molecules that attack the

DNA (Mahaney *et al.*, 2009). There are many different classes of chemotherapeutics that act through different mechanisms to result in cell killing such as alkylating agents, anti-metabolites, topoisomerase inhibitors and microtubule-targeting agents. However, the development of resistance to chemotherapeutic agents is a major clinical problem.

Many cytotoxic chemotherapeutics and radiation, along with environmental damage, ultraviolet light and cell cycle replication errors, result in the formation of single- or double-strand breaks in the DNA. There are a number of mechanisms which repair different DNA lesions, and key proteins in these pathways can display altered expression in cancer cells.

1.2   DNA repair

DNA strand breaks result in arrest at a cell cycle checkpoint and either cell death *via* apoptosis or the engagement of a relevant repair pathway such as nucleotide excision repair (NER), base excision repair (BER), mismatch repair (MMR), or the double strand break repair pathways homologous recombination and non-homologous end-joining (Hoeijmakers, 2001). Together with cell cycle checkpoint activation, metabolic processes and stress responses, DNA repair allows for cell survival.

NER repairs helix-distorting lesions on one strand of the DNA caused mainly by exogenous factors, which interfere with base pairing and can impede replication, whereas BER repairs base changes caused as a result of predominantly endogenous damage (de Laat *et al.*, 1999; Lindahl and Wood, 1999; Hoeijmakers, 2001).

DNA double strand breaks (DSB) can be lethal to a cell and therefore correct repair is essential for a cell to survive. Incorrect repair of the double strand breaks can cause genomic rearrangements such as deletions, fusions and translocations; features of genomic instability which are commonly observed in cancer cells (Aplan, 2006). The two main double strand break repair pathways are non-homologous end-joining (NHEJ) and homologous recombination (HR), in which the major essential kinases are DNA-dependent protein kinase (DNA-PK) and ataxia telangiectasia mutated kinase (ATM), respectively. These proteins are the focus of studies in this thesis.

1.3   DNA-dependent protein kinase (DNA-PK)

1.3.1   Structure and function

DNA-dependent protein kinase (DNA-PK) is a serine/threonine kinase complex consisting of a heterodimer of Ku proteins (Ku70/Ku80) and the catalytic subunit of DNA-PK (DNA-PKcs). The gene for DNA-PKcs (*PRKDC)* is located on chromosome 8q11 and comprises of 4128 amino acids (approximately 469 kDa). The Ku70/Ku80 heterodimer consists of 609 amino acids (approximately 70 kDa) and 732 amino acids (approximately 80 kDa), respectively, encoded by *XRCC6* and *XRCC5* which are located on chromosomes 22q13 and 2q33-34, respectively (Koike, 2002). DNA-PKcs belongs to the phosphatidylinositol 3-kinase like kinase (PIKK) family (Hartley *et al.*, 1995), along with the other DNA damage-activated kinases ataxia telangiectasia mutated kinase (ATM) and ataxia telangiectasia- and Rad3-related kinase (ATR), and mammalian target of rapamycin (mTOR), human suppressor of morphogenesis in genitalia-1 (hSMG-1) and transformation/transcription domain-associated protein (TRRAP) (Shiloh, 2003; Lovejoy and Cortez, 2009) (Figure 1-2).
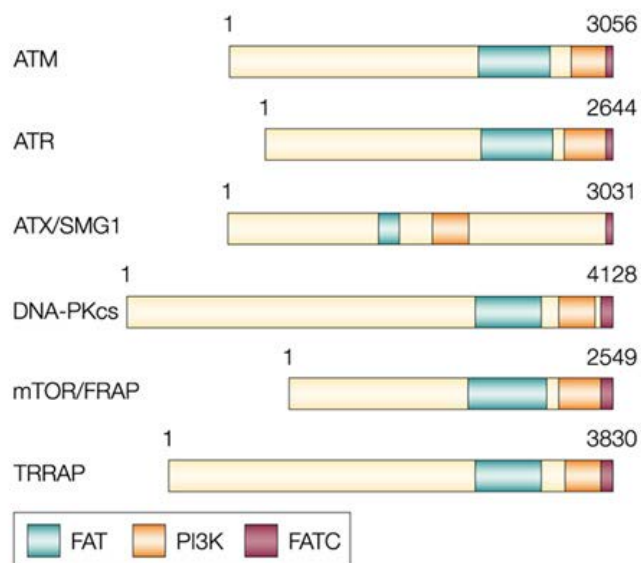
Figure 1-2: Size and common motifs in the PIKK family members. These family members share three motifs: the FAT (focal adhesion targeting) and FATC (COOH-terminal FAT) domains and the PI3K domain, and all possess protein kinase activity (apart from TRRAP) (Shiloh, 2003).

DNA-PKcs contains a large N-terminal domain consisting of helical elements, HEAT (Huntingtin, Elongation Factor 3, PP2A and Tor1) repeats and phosphorylation sites with important regulatory functions (JK, PQR and ABCDE clusters), a FAT domain (conserved amongst PIKK members), a kinase domain (conserved) and short C-terminal region called the FATC domain (Dobbs *et al.*, 2010) (Figure 1-3).
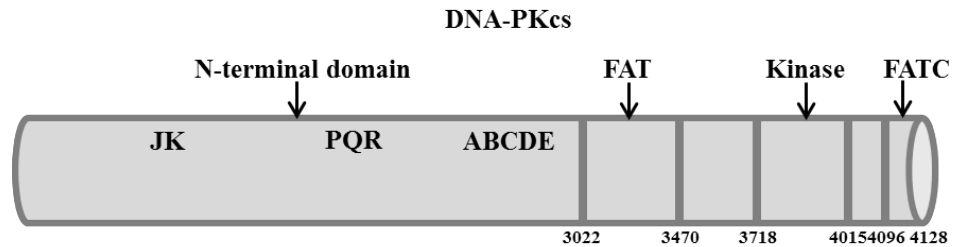
Figure 1-3: DNA-PKcs functional domains. Adapted from Goodwin and Knudsen (2014).

DNA-PK plays an essential role in NHEJ but has also been implicated in homologous recombination, hypoxia, lipogenesis and metabolic regulation, innate immunity and inflammation responses, and genomic stability (reviewed in Goodwin and Knudsen (2014)) (Figure 1-4).
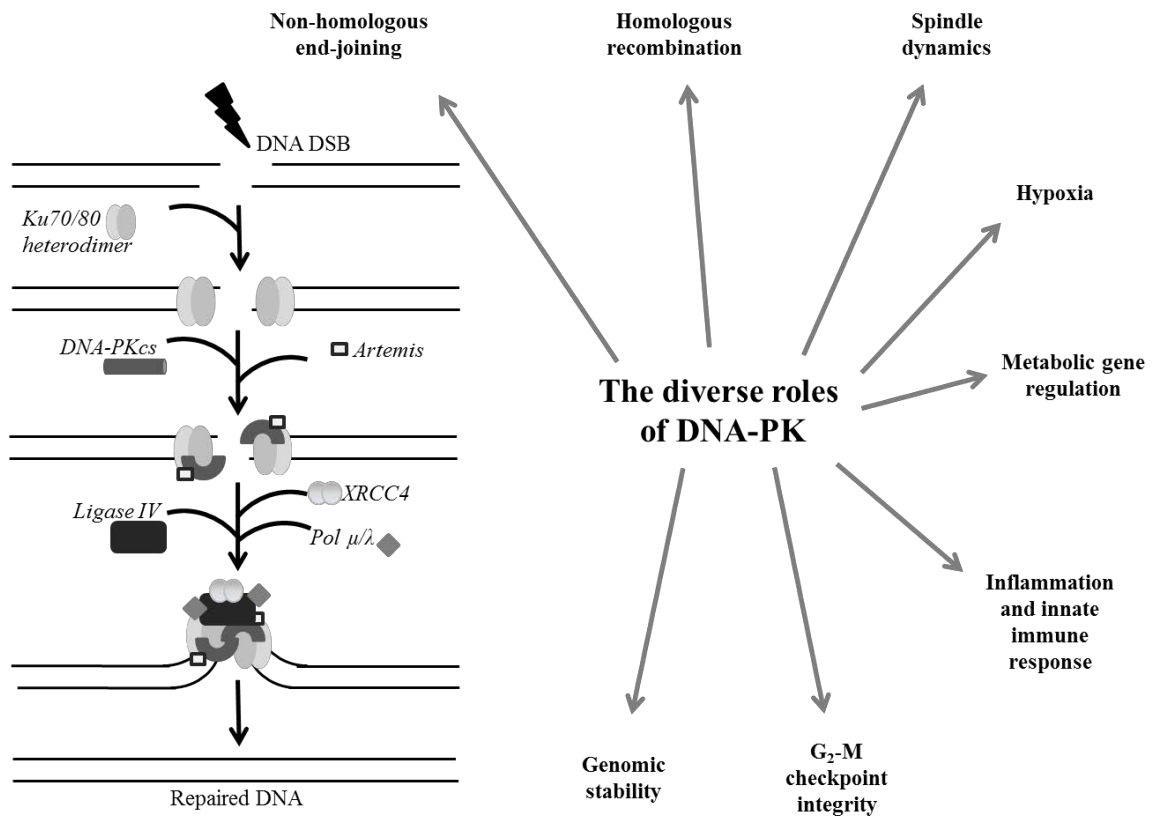
Figure 1-4: The role of DNA-PK in non-homologous end-joining and some of the additional roles of DNA-PK. NHEJ pathway adapted from (Goodwin and Knudsen, 2014).

1.3.2   Non-homologous end-joining (NHEJ)

The main factor in determining which double-strand break repair pathway is utilised is the phase of the cell cycle. NHEJ, thought to be the predominant pathway, is a rapid but inaccurate form of repair which predominates in G_0 and G_1. HR is slower and more accurate, and is dominant after DNA replication when a sister chromatid is present (Meek *et al.*, 2004). NHEJ is also required for the site-specific recombination process, somatic or V(D)J recombination, that assembles coding regions for the variable domains of immunoglobulin and T cell receptors from their different locations on the chromosome during lymphocyte development (Tonegawa, 1983; Meek *et al.*, 2004). DNA double-strand breaks occur at conserved recombination signal sequences flanking all variable (V), diversity (D) and joining (J) gene segments that are generated by two recombination-activating genes (RAG-1 and RAG-2). NHEJ resolves these recombination intermediates (Oettinger *et al.*, 1990; McBlane *et al.*, 1995).

There is a diverse range of DNA break ends that the NHEJ repair pathway components need to deal with and consequently NHEJ enzymes exhibit a large degree of multifunctionality, structural tolerance, iterative processing and mechanistic flexibility (Gu and Lieber, 2008). There are six main components involved in NHEJ: DNA-PKcs, Ku70, Ku80, XRCC4, DNA ligase IV and Artemis. When a DNA DSB arises, the ring-shaped Ku70/Ku80 heterodimer binds to the DNA ends forming a Ku: DNA complex which serves as a docking site for the nuclease, polymerases and ligase to bind (Figure 1-4). Ku is highly abundant in the cell with an estimated 400,000 molecules *per* cell and has a high binding constant for DSBs (2.4×10^{-9} M) (Mimori *et al.*, 1986; Blier *et al.*, 1993). DNA-PKcs is then recruited and induces the inward translocation of Ku by approximately one helical turn to allow DNA-PKcs to act as a tether for the broken DNA ends and to prevent exonucleolytic degredation (Yoo and Dynan, 1999; Goodwin and Knudsen, 2014). Once DNA-PKcs is bound, it initially undergoes phosphorylation at a number of autophosphorylation sites, the best characterised being serine 2056 (in the PQR cluster of five phosphorylation sites located at aa 2023-2056) and threonine 2609 (in the ABCDE cluster of six phosphorylation sites at aa 2609-2647), which causes conformational changes and enhances serine and threonine kinase activity.

DNA-PKcs also interacts with Artemis and the Artemis:DNA-PKcs complex has endonucleolytic activity and cuts various forms of damaged DNA ends (Ma *et al.*, 2005). Pol μ and pol λ can bind to the Ku:DNA complex and are capable of template-dependent and, in the case of pol μ, template-independent synthesis which is extremely important in NHEJ. DNA-PKcs also stimulates the ligase activity of the XLF: XRCC4: DNA ligase IV complex which can ligate across gaps and ligate incompatible DNA ends with high efficiency (Costantini *et al.*, 2007; Gu *et al.*, 2007a; Gu *et al.*, 2007b). Upon activation, DNA-PKcs also phosphorylates a large number of proteins, including serine 139 on H2AX (γH2AX), which is a well-known marker of DSBs and recruits repair proteins and organises repair signalling cascades (Paull *et al.*, 2000; An *et al.*, 2010).

In vivo, DNA-PKcs phosphorylation of threonine 2609 is critical for DSB repair and radio-resistance, and is catalysed not only by DNA-PKcs itself but also by ATM and ATR in response to a variety of stress-inducers (Yajima *et al.*, 2006; Chen *et al.*, 2007). However, no other proteins have been implicated in the phosphorylation of serine 2056 other than DNA-PKcs itself, and so this phosphorylation site is used a marker of DNA-PK activity (Chen *et al.*, 2005).

1.3.3 Additional roles of DNA-PK

When repairing DNA DSBs, homologous recombination (HR) is more accurate than NHEJ because it uses an undamaged sister chromatid as a template for repair but is therefore restricted to the S-G_2 phases of the cell cycle (described in Section 1.4.2) (San Filippo *et al.*, 2008). HR is a more complex form of repair and takes more than 7 hours to complete, whereas NHEJ can be completed in 30 minutes, and although NHEJ is thought to be the dominant form of DSB repair, a functional HR pathway is necessary for cell viability (Mao *et al.*, 2008). Potential crosstalk between HR and NHEJ mediated by DNA-PK has been investigated, and certain specific phosphorylation sites on DNA-PKcs identified which promote HR whilst inhibiting NHEJ (Convery *et al.*, 2005; Neal *et al.*, 2011).

DNA-PK has been shown to be activated by mild hypoxia, independently from DNA DSBs and NHEJ, and DNA-PKcs positively regulates the hypoxia-inducible factor-1 alpha (HIF-1α), which activates a number of oxygen-related genes and contributes to the adaptive response to hypoxic conditions, for example the glucose transporter, *GLUT1*, expression (Bouquet *et al.*, 2011).

A role for DNA-PK in metabolic gene regulation has been demonstrated in response to insulin through phosphorylation of the transcription factor USF-1 which activates fatty acid synthesis (Wong *et al.*, 2009). DNA-PK positively regulates the activation of the regulatory γ1 subunit of AMP-activated protein kinase (AMPK), an energy change sensor, under glucose-deprived conditions (Amatya *et al.*, 2012). DNA-PK has also recently been shown to be a critical regulator of the oxidative stress response and is required for suppression of reactive-oxygen species build-up in an NHEJ-independent role (Li *et al.*, 2014).

The DNA binding activity of nuclear factor kappa B (NF-κB) during inflammation is critical for VCAM-1 (vascular cell adhesion protein 1) expression, which facilitates transmigration, the accumulation of leukocytes and cell-cell interactions at inflammatory sites, and DNA-PK is required to phosphorylate the NF-κB p50 subunit for VCAM-1 expression in response to the cytokine TNF (tumour necrosis factor) (Ju *et al.*, 2010). DNA-PK activates innate immunity and subsequent inflammatory responses by recognising and binding to foreign DNA and initiating interferon regulatory factor-3 (IRF-3)-mediated transcription of type 1 interferon (IFN), and multiple cytokines and chemokines (Ferguson *et al.*, 2012). DNA-PKcs also modulates the innate immune response through recruitment of autoimmune regulator

(AIRE) to DNA, activating tissue-restricted antigen (TRA) genes and mediating central tolerance in the thymus (Zumer *et al.*, 2012).

DNA-PK has been shown to mediate genomic stability in a number of ways. NHEJ is an error-prone repair process due to the basic nature of the ligation of the broken DNA ends together, which can cause a loss of nucleotides and result in chromosomal rearrangements where more than one DSB occurs in close proximity. DNA-PK therefore affects inherent genomic stability due to its role in this process. However, activated DNA-PKcs phosphorylates Snail1, a transcriptional regulator shown to determine pathological epithelial to mesenchymal transition during tumour progression (Kajita *et al.*, 2004), and this phosphorylation leads to increased Snail1 stability. Increased Snail1 stability reciprocally inhibits DNA-PKcs activity and therefore causes defective DNA DSB repair; affecting genomic instability, and migration of tumour cells, characteristics of an aggressive tumour (Pyun *et al.*, 2013).

DNA-PK and ATM are required for the maintenance of G_2-M cell cycle checkpoint integrity through phosphorylation of threonine 21 of the 32 kDa subunit of replication protein A (RPA32) and mutations in both RPA32 and DNA-PKcs result in unrepaired DNA and the inappropriate entry into mitosis due to a G_2-M arrest defect (Block *et al.*, 2004b).

DNA-PK has been shown to localise to the centrosomes, kinetochores and midbody during mitosis and play a regulatory function in mitotic spindle dynamics and chromosomal segregation, attributed to activation of the Chk2-BRCA1 signalling pathway (Lee *et al.*, 2011; Shang *et al.*, 2014). Inhibition of DNA-PK following ionising radiation causes aberrant spindles and multinucleated cells leading to mitotic catastrophe, and therefore DNA-PKcs activation is important in the maintenance of microtubule dynamics during mitosis (Shang *et al.*, 2010).

1.3.4   DNA-PK expression and cancer

DNA-PK activity and expression have been examined in many human clinical tumour samples. The relationship between DNA-PK and prognosis, radiation response and cancer risk have been examined (reviewed in Hsu *et al.* (2012)). An elevation in DNA-PKcs expression has been observed in a variety of cancers. Increased DNA-PKcs expression in colorectal cancer, nasopharyngeal cancer and non-small cell lung cancer (NSCLC) has been reported by several groups, although some studies found no association with clinical outcome whilst others found overexpression to be associated with clinical stage and poor survival (Hosoi *et al.*, 2004; Lee *et al.*, 2005b; Xing *et al.*, 2008). Investigations into lymphoid malignancies revealed increased expression of DNA-PK in acute lymphoblastic leukaemia (ALL), chronic lymphocytic leukaemia (CLL) and lymphoma, which was associated with the degree of maturation, lymphoma grading and proliferation rate (Holgersson *et al.*, 2004). A separate study demonstrated that DNA-PK was an indicator of poor prognosis in CLL and that DNA-PK overexpression was associated with CLL patients displaying poor prognosis genetic aberrations del(11q) (associated with loss of ATM) and del(17p) (associated with loss of p53) (Willmore *et al.*, 2008). In contrast, a study in gastric cancer demonstrated that loss of DNA-PKcs expression was associated with tumour progression and a poorer survival (Lee *et al.*, 2005a; Lee *et al.*, 2007), and reduced DNA-PK repair activity has previously been associated with increased risk of developing lung cancer (Auckley *et al.*, 2001).

A number of studies have investigated DNA-PK expression in peripheral blood lymphocytes (PBLs). Lower DNA-PK activity was observed in PBLs in patients with uterine, cervix or breast cancer, and the frequency of chromosomal aberrations increased with decreased DNA-PK activity (Someya *et al.*, 2006). Decreased DNA-PK activity has been found in advanced cancer patients compared with early stage patients in a variety of cancers, e.g. breast, uterine, head and neck, oesophagus and non-Hodgkin's lymphoma, and lower DNA-PK activity in advanced cancer can be associated with decreased survival and an increased risk of developing distant metastasis following radiotherapy (Someya *et al.*, 2011).

1.3.5   Defects in NHEJ and mutations in the DNA-PKcs gene

Due to the importance of NHEJ, deficiencies in this pathway have been shown to lead to genomic instability and the suppression of translocations, amplifications and deletions, and germline defects that can result in soft tissue sarcomas and increased

breast cancer risk (Grawunder *et al.*, 1998; Ferguson *et al.*, 2000; Sharpless *et al.*, 2001; Fu *et al.*, 2003). Mutations in the various proteins involved in NHEJ, such as Ku70, Ku80, XRCC4 and DNA-PKcs, result in radiation sensitivity and a defect in V(D)J recombination (Kirchgessner *et al.*, 1995; Nussenzweig *et al.*, 1996; Gu *et al.*, 1997; Grawunder *et al.*, 1998).

Severe combined immunodeficiency disease (SCID) can occur in patients with defects in the NHEJ pathway, which normally have the phenotype of T-B-NK+ (absence of both T-cells and B-cells but with NK cells present). Mutations in Artemis, DNA Ligase IV, DNA-PKcs and Cernunnos-XLF have all been reported to cause SCID in humans (reviewed in Dvorak and Cowan (2010)). No defects in XRCC4 or Ku have been reported in humans, and XRCC4 defects are embryonically lethal in mice (Soulas-Sprauel *et al.*, 2007).

There have been four reported incidences of germline mutations in the DNA-PKcs gene *PRKDC* in animals; two in mice (Bosma *et al.*, 1983; Jhappan *et al.*, 1997), one in a horse (McGuire and Poppie, 1973) and one in a Jack Russell terrier dog (Meek *et al.*, 2001), and two incidences of *PRKDC* mutation in human patients (van der Burg *et al.*, 2009; Woodbine *et al.*, 2013). The first human germline mutation found was from a radiosensitive T-B-SCID patient that had a *PRKDC* missense mutation (Leu3062Arg), which did not affect DNA-PKcs expression but conferred impaired Artemis activation and NHEJ (van der Burg *et al.*, 2009). The second patient had compound heterozygous *PRKDC* mutations resulting in low expression and barely detectable DNA-PKcs kinase activity, impaired NHEJ and neurological abnormalities (Woodbine *et al.*, 2013). Several somatic mutations in the coding region of *PRKDC* have been identified in patients with breast and pancreatic cancers (Wang *et al.*, 2008b).

The *PRKDC* intron 8 6721 G to T variant has been implicated in bladder cancer and hepatocellular carcinoma (HCC). The 6721TT genotype was associated with a significant increase in bladder cancer, and was more frequent in patients older than 65 or who were smokers (Wang *et al.*, 2008a) in a study of 213 bladder cancer patients. However, 6721GG or 6721GT was associated with an increased risk of HCC compared with 6721TT in a study on 348 HCC patients from a high aflatoxin-exposed population (Long *et al.*, 2011). These examples demonstrate that single nucleotide polymorphisms (SNPs) in non-coding regions of DNA-PKcs may alter gene expression or function (Hsu *et al.*, 2012).

1.3.6 DNA-PK inhibitors

DNA damaging agents are an effective mainstay of cancer treatment and their therapeutic index may be improved by inhibition of DNA repair or cell cycle checkpoint inhibition, as many cancer cells lack DNA repair pathways compared with normal healthy tissue; such that targeting the DNA repair pathway on which the cancer cell depends for survival is an effective treatment strategy (Zhou and Bartek, 2004; Al-Ejeh *et al.*, 2010).

Wortmannin (Figure 1-5A) is a non-competitive, non-specific phosphatidylinositol 3-kinase (PI3K) inhibitor and was one of the first inhibitors of DNA-PK identified (DNA-PK IC_{50} = 150 nM), acting through irreversible alkylation of lysine 802 in the active site of DNA-PK that is critical for activity. Wortmannin was shown to be an effective radiosensitiser (Arcaro and Wymann, 1993; Price and Youmell, 1996). Caffeine (Figure 1-5B) has also been demonstrated to be an inhibitor of the PIKKs DNA-PK, ATM and ATR and is an effective radiosensitiser but lacks specificity (Sarkaria *et al.*, 1999; Block *et al.*, 2004a).

LY294002 (2-(4-morpholinyl)-8-phenyl-4H-1-benzopyran-4-one) (Figure 1-5C) is a morpholine derivative of the plant flavonoid quercetin and is a structurally-distinct pan PI3K inhibitor with DNA-PK inhibitory activity (DNA-PK IC_{50} = 360 nM). LY294002 has been shown to increase cellular sensitivity to radiation and chemotherapeutic agents (Vlahos *et al.*, 1994; Sarkaria *et al.*, 1999; Gharbi *et al.*, 2007). Although this compound is not suitable for *in vivo* investigation due to instability (Gupta *et al.*, 2003), the structure has proved to be a lead compound in the development of more potent DNA-PK inhibitors.

A number of compounds based on LY294002 were developed from the ICOS Corporation (Bothell, WA) small molecule library resulting in the synthesis of IC87361 (Figure 1-5D), a potent and selective DNA-PK inhibitor (DNA-PK IC_{50} = 34 nM). IC87361 directly inhibited the repair of DNA DSBs and displayed radiosensitisation and growth delay enhancement in xenograft studies. However, the pharmacokinetic limitations such as poor bioavailability and rapid clearance compromised the use of this class of compound (Kashishian *et al.*, 2003; Shinohara *et al.*, 2005).

NU7026 (2-(morpholin-4-yl)-benzo[h]chomen-4-one) (DNA-PK IC_{50} = 230 nM) (Figure 1-5E) is a LY294002-based ATP-competitive compound that demonstrated more than fifty-fold selectivity for DNA-PKcs over PI3K and is inactive against ATM and ATR (Veuger *et al.*, 2003). NU7026 potentiated the cytotoxicity of topoisomerase II poisons (Willmore *et al.*, 2004); however, metabolic lability and poor solubility

meant that this was not a suitable compound for *in vivo* investigation (Nutley *et al.*, 2005).

The DNA-PK inhibitor NU7441 (8-dibenzothiophen-4-yl-2-morpholin-4-yl-chromen-4-one) (DNA-PK IC_{50} = 14 nM) (Figure 1-5F), developed from the PI3K inhibitor LY294002 by screening chromenone libraries (Leahy *et al.*, 2004), has improved potency over NU7026. NU7441 has been shown to increase cellular sensitivity to radiation and topoisomerase II poisons in a number of solid and haematological cell lines, and increase etoposide-induced tumour growth delay in mice bearing SW620 xenografts (Zhao *et al.*, 2006; Willmore *et al.*, 2008; Elliott *et al.*, 2011; Shaheen *et al.*, 2011; Ciszewski *et al.*, 2014; Tichy *et al.*, 2014). It has been demonstrated that this sensitisation occurs because NU7441 attenuates the repair of both IR- and etoposide-induced DNA double strand breaks in a DNA-PK dependent manner (Zhao *et al.*, 2006; Tavecchio *et al.*, 2012). NU7441 is around 20-fold more selective for DNA-PK over PI3K in cellular assays (Tavecchio *et al.*, 2012). It has also been shown that inhibition of DNA-PK using NU7441, or knockdown using siRNA, led to accelerated senescence following radiation *in vitro* (Azad *et al.*, 2011); indicating an alternative mechanism of action. NU7441 is the DNA-PK inhibitor used throughout these studies.

NU7742 (8-dibenzothiophen-4-yl-2-piperidin-1-yl-chromen-4-one) (Figure 1-5H) is an inactive derivative of NU7441 (IC_{50} > 10 µM) in which the morpholine oxygen has been replaced with a methylene group, resulting in the loss of sensitisation of cells to DNA-damaging agents (Willmore *et al.*, 2008). The introduction of a methyl substituent at the 7-position of the chromen-4-one ring generated atropisomers DRN1 (DNA-PK IC_{50} = 2 nM) and DRN2 (DNA-PK IC_{50} = 7 µM) (Figure 1-5I). As expected, and due to restricted rotation between the chromen-4-one and dibenzothiophene rings, DNA-PK inhibitory activity resides exclusively in the laevorotatory enantiomer DRN1 (Clapham *et al.*, 2012).

NDD0004 (IC_{50} = 10 nM) (Figure 1-5G) is a Newcastle Drug Discovery compound recently synthesised, more water-soluble, potent and selective version of NU7441 (unpublished data).

The DNA-PK IC_{50} values cited above for these compounds were generated in a cell-free ELISA assay which used DNA-PK purified from HeLa cell nuclear extracts and examined the known ability of DNA-PK to phosphorylate the serine-15 residue of a p53 peptide, and the ability of compounds to inhibit this phosphorylation event (Griffin *et al.*, 2005).

14

There are three compounds currently in clinical trials that target DNA-PK, although all three compounds lack specificity and target multiple pathways. CC-122 is termed a pleiotropic pathway modifier and is a DNA-PK inhibitor with potent *in vitro* anti-proliferative, immunomodulatory and anti-angiogenic properties (Gandhi *et al.*, 2012). CC-122 is in Phase I clinical trial for advanced solid tumours, non-Hodgkin's lymphoma or multiple myeloma (NCT01421524) (Clinicaltrials.gov, 2014). CC-115 is a dual DNA-PK and mTOR kinase inhibitor in Phase I trials for patients with advanced solid tumours and haematological malignancies (NCT01353625) (Clinicaltrials.gov, 2014). ZSTK474 is a pan PI3K inhibitor and has some inhibitory effect on DNA-PK (Kong *et al.*, 2009). ZSTK474 is in Phase I trials, one active (NCT01682473) and one completed (NCT01280487), for patients with solid malignancies. However, all of these clinical compounds have multiple targets and so it is not possible to distinguish effects due to DNA-PK inhibition.
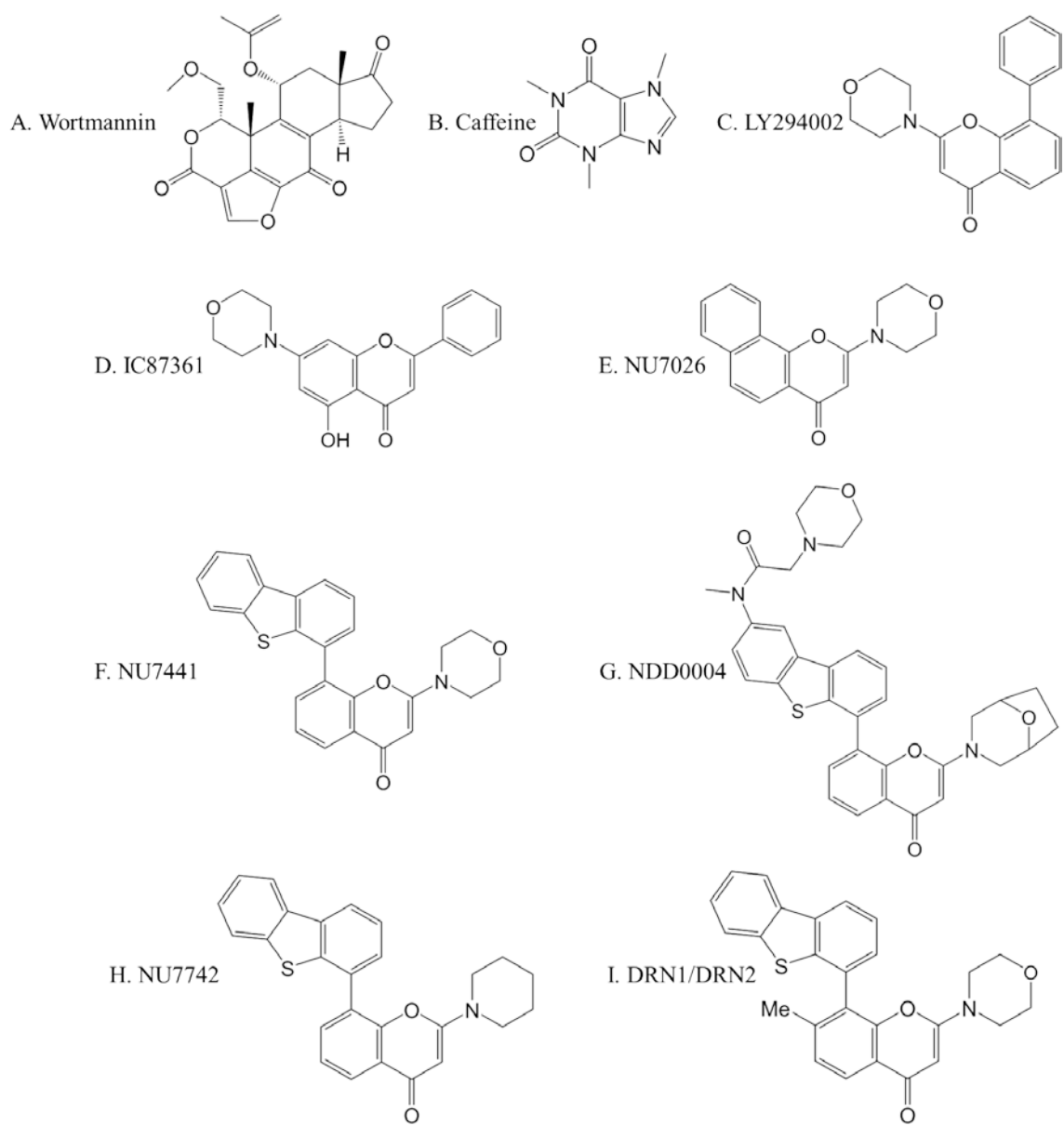
Figure 1-5: Structures of the DNA-PK inhibitors discussed in Section 1.3.6.

Compound Name	Cell free assay DNA-PK IC$_{50}$ (μM)	Structure-activity relationship
NU7441	0.014 ± 0.001	>100 fold selective for DNA-PK over PI3K and other PIKK family members
NU7742	>10	morpholine oxygen of NU7441 replaced by methylene group results in no DNA-PK inhibitory activity
DRN1	0.002 ± 0.001	laevorotatory enantiomer with DNA-PK inhibitory activity
DRN2	7	dextrorotatory enantiomer with no DNA-PK inhibitory activity
NDD0004	0.01	>100 fold selective for DNA-PK over PI3K and other PIKK family members. More potent and selective than NU7441

Table 1-1: DNA-PK inhibitory properties and structure-activity relationships of the compounds used in this study

1.4   Ataxia telangiectasia mutated kinase (ATM)

1.4.1   Structure and function

ATM is a large 370 kDa kinase encoded on human chromosome 11q22-23 and is another member of the PIKK family of enzymes (Shiloh, 2003). Like the other PIKK family members, ATM consists of a FAT domain, a PI3K domain and a FATC domain that represents a common C-terminal amino acid sequence found near the N-terminus of the protein (McKinnon, 2004).

ATM plays an essential role in HR pathway of DNA DSB repair, but ATM has also been implicated in playing a role in genomic stability, replication stress, telomere stability, redox sensing, transcription and mitotic spindle assembly; roles which will all be discussed in the following sections.

1.4.2   Homologous recombination (HR)

HR repairs DNA DSBs during the S and G$_2$ phases of the cell cycle when a sister chromatid is available to be used as a template for information exchange and accurate repair, making this DSB repair pathway more accurate than NHEJ.

HR is initiated by the MRN complex (Mre11, Rad50 and Nijmegen breakage syndrome 1 (Nbs1) proteins) which recognises the DSB and recruits ATM kinase to the site of damage (Mirzoeva and Petrini, 2001; Uziel *et al.*, 2003). ATM exists as an inactive dimer or multimer until recruited to sites of DNA damage where it autophosphorylates itself on several serine residues (367, 1893 and 1981), causing dissociation of ATM molecules into active monomers (Bakkenist and Kastan, 2003). ATM autophosphorylation at serine 1981 occurs within one minute of ionising radiation (Bakkenist and Kastan, 2003). Nbs1 interacts directly with ATM at DSB sites, where ATP-dependent Rad50 activity is required, and Nbs1 ubiquitination by Skp2 E3 ligase facilitates ATM recruitment and activity (Uziel *et al.*, 2003; Lee and Paull, 2005; Wu *et al.*, 2012). Activated ATM then signals to a large number of downstream targets such as checkpoint proteins (including Chk2), chromatin-remodelling and other DNA damage factors (including p53). C-terminal binding protein-interacting protein (CtIP) physically interacts with the MRN complex when it is recruited to DNA ends. Recruitment initiates 5'-3' end resection and generates a 3' single-stranded DNA overhang which is needed for strand exchange (Sartori *et al.*, 2007). Bloom syndrome helicase (BLM) stimulates further resection by the nucleolytic activity of exonucleases, including Exo1 (Nimonkar *et al.*, 2008), and the single-stranded DNA is bound by RPA protein. RPA is replaced by Rad51, a process mediated by Rad52 and BRCA2 (McIlwraith *et al.*, 2000; Jensen *et al.*, 2010), which forms Rad51-coated single-stranded DNA that allows strand invasion of the homologous DNA on the sister chromatid (New *et al.*, 1998), and the Rad51-coated strand is then extended by DNA polymerase η to form a D-loop (McIlwraith *et al.*, 2005). Recombining DNA strands are linked *via* a four-way junction by covalent bonds and this complex structure is known as a Holliday junction. DNA nucleases such as GEN1 and SLX1/SLX4, and DNA helicases such as Werner syndrome (WRN) and BLM, resolve and process these Holliday junctions (Constantinou *et al.*, 2000; Ip *et al.*, 2008; Fekairi *et al.*, 2009; Svendsen *et al.*, 2009), resulting in the accurate repair of the DSB using the sister chromatid template.

1.4.3 Additional roles of ATM

ATM has many roles beyond homologous recombination. These roles include replication stress through crosstalk with ATR (Burdak-Rothkamm *et al.*, 2008), redox sensing and regulating, in which ATM decreases reactive oxygen species (Alexander *et al.*, 2010) and is activated by hypoxia (Bencokova *et al.*, 2009), transcription through indirect activation of NF-κB (Wu *et al.*, 2006), insulin signalling through phosphorylation of eIF-4E-binding protein 1 (Yang and Kastan, 2000) and insulin secretion (Miles *et al.*, 2007), and in neuronal function through trafficking and function of synaptic vesicles (Li *et al.*, 2009).

In relation to this thesis, ATM has been shown to play multiple roles in mitosis and mitotic spindle assembly. A defective mitotic spindle checkpoint following ionising radiation in A-T cells (i.e. lacking in ATM protein) was previously observed (Takagi *et al.*, 1998; Shigeta *et al.*, 1999). ATM acts with p21 to suppress aneuploidy and chromosomal instability as demonstrated in an ATM -/- mouse model which displayed defective metaphase to anaphase transition and abnormal karyokinesis (Shen *et al.*, 2005). Furthermore, the inhibition of ATM using the specific ATM inhibitor KU55933 led to chromosomal aberrations (White *et al.*, 2008). ATM has recently been shown to be activated during mitosis in the absence of DNA damage by aurora-B-mediated phosphorylation of serine 1403, and activated ATM localises to the centrosomes and midbody during mitosis (Yang *et al.*, 2011). ATM was also demonstrated to phosphorylate a critical kinetochore protein, BUB1, at serine 314 which activates the spindle checkpoint (Yang *et al.*, 2011). ATM forms a complex with the poly(ADP)ribose polymerase (PARP) tankyrase (TNKS1), the spindle protein NuMA1 and BRCA1 in mitosis, and this complex promotes efficient poly(ADP)ribosylation of NuMA1 and correct bipolar spindle assembly (Palazzo *et al.*, 2014).
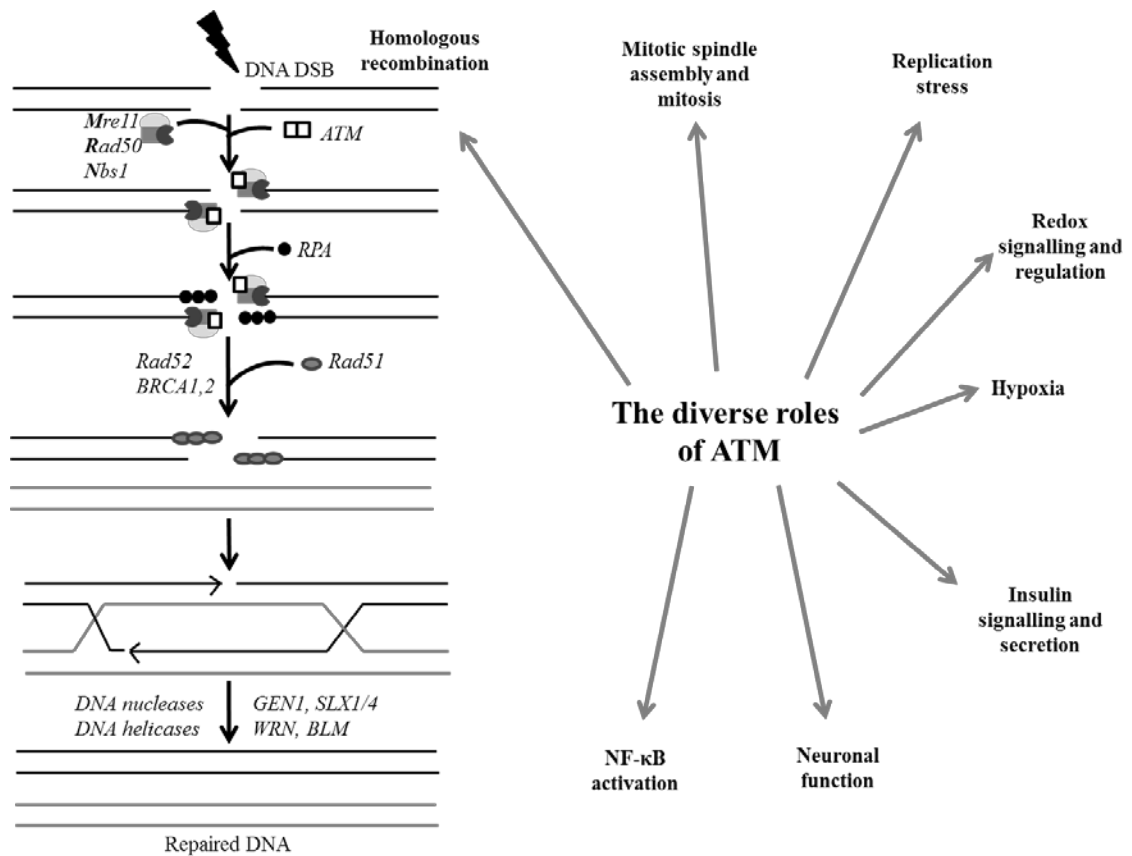
Figure 1-6: The role of ATM in homologous recombination and some of the additional roles of ATM. HR pathway adapted from Mostoslavsky (2008).

1.4.4 Germline and somatic mutations in ATM and defects in HR

Ataxia telangiectasia (AT) is an autosomal recessive disorder where ATM is defective, which affects around 1:40,000 – 1:100,000 live births. The disease is characterised by a 100-fold increase in the risk of some cancers (e.g. lymphomas) along with immunodeficiency, hypersensitivity to ionising radiation, progressive cerebellar ataxia, oculocutaneous telangiectasias, hypogonadism, growth retardation, premature ageing and genetic instability (Meyn, 1995). It was demonstrated in a cohort study of AT patients that those with no ATM kinase activity almost always develop lymphomas in childhood, whereas the AT patients with residual ATM kinase activity were protected from the lymphomas in childhood but had a 30-fold increased risk of breast cancer (Reiman *et al.*, 2011). There is an increased risk of breast cancer in heterozygous carriers of ATM mutations (Thompson *et al.*, 2005), and a number of well-characterised ATM mutations have been proven to be responsible for increased cancer susceptibility (Renwick *et al.*, 2006).

Patients with Nijmegen breakage syndrome (NBS), caused by mutant Nbs1 protein, have defective ATM activation and are predisposed to cancer (Digweed and Sperling, 2004). Those patients with ataxia telangiectasia–like disorder (ATLD) express a mutant form of Mre11 protein and also have defective ATM activation but not cancer predisposition (Stracker and Petrini, 2011).

There are a number of reported cases of somatic ATM mutations present in cancers. Approximately 25 % of CLL patients present at diagnosis with ATM mutations or deletions. The mutations or deletions are associated with a poor prognosis and shorter treatment-free interval (Guarini *et al.*, 2012). CLL patients with biallelic ATM alterations have a significantly reduced overall survival compared with those patients with monoallelic ATM mutation or deletion (Skowronska *et al.*, 2012). Many studies have reported ATM mutations in a number of solid and haematological cancers with the percentage of ATM aberrations in cancer being around 5 %, but this proportion varies according to tissue type ranging from 0.7 % in ovary tissue to 11.1 % in haematopoietic and lymphoid tissue (reviewed in Cremona and Behrens (2014)). To note, ATM mutations have been demonstrated to predispose to breast cancer and a recent study on 119 breast cancer samples found ATM to be downregulated in 55 % of the breast tumours compared with adjacent tissue (Salimi *et al.*, 2012).

1.4.5 ATM inhibitors

Both wortmannin (Figure 1-5A) and caffeine (Figure 1-5B) have previously been used as ATM inhibitors but, as discussed in Section 1.3.6, these inhibitors are non-selective PIKK and PI3K inhibitors. In addition, wortmannin cannot be used *in vivo* because wortmannin covalently modifies a large number of proteins.

KU55933 (2-morpholin-4-yl-6-thianthren-1-yl-pyran-4-one) (ATM IC_{50} = 13 nM) (Figure 1-7A) was derived from LY294002 (Section 1.3.6) and is an ATM inhibitor with demonstrated specificity over PI3K and the other PIKK family members (Hickson *et al.*, 2004). KU55933 can radio-sensitise and chemo-sensitise cells to DSB-inducing agents and inhibit a range of ionising radiation-induced ATM-dependent phosphorylation events (Hickson *et al.*, 2004). KU55933 is the ATM inhibitor that is used throughout the studies in this thesis.

The purified enzyme assay used to determine the cell-free ATM IC_{50} values is very similar to the assay to measure DNA-PK, described in Section 1.3.6. ATM was purified from HeLa nuclear extracts and the ability to phosphorylate p53 on serine 15 measured by an ELISA assay.

KU60019 (2-[(2R, 6S)-2, 6-dimethylmorpholin-4-yl]-N-[5-(6-morpholin-4-yl-4-oxo-4H-pyran-2-yl)-9H-thioxanthen-2-yl]-acetamide) (Figure 1-7B) is a more potent and water-soluble analogue of KU55933 (ATM IC_{50} = 6 nM) which also causes sensitivity to radiation, along with reducing ATM-mediated AKT and ERK prosurvival signalling and cell migration (Golding *et al.*, 2009).

CP466722 (Figure 1-7C) is another specific ATM inhibitor that is structurally distinct from KU55933, identified by Pfizer (Massachusetts, USA) using a 1500 targeted compound library (Rainey *et al.*, 2008). CP466722 is a rapidly reversible inhibitor of ATM kinase, which reduced ATM-dependent cellular phosphorylation events and function, and caused radiosensitisation (Rainey *et al.*, 2008).

The kinase assays used to identify ATM inhibitors use ATM protein from human cells isolated in multistep procedures as it is not possible to express full-length ATM protein in bacteria or baculovirus (Chan *et al.*, 2000), limiting screening procedures. However, a new immunoassay to screen novel ATM kinase inhibitors has been developed which sensitively and quantitatively measures protein signalling pathways through expression or phosphorylation of ATM and its downstream target, KAP1 (a heterochromatin protein) (Guo *et al.*, 2014). This new assay has identified two novel ATM inhibitors to date.
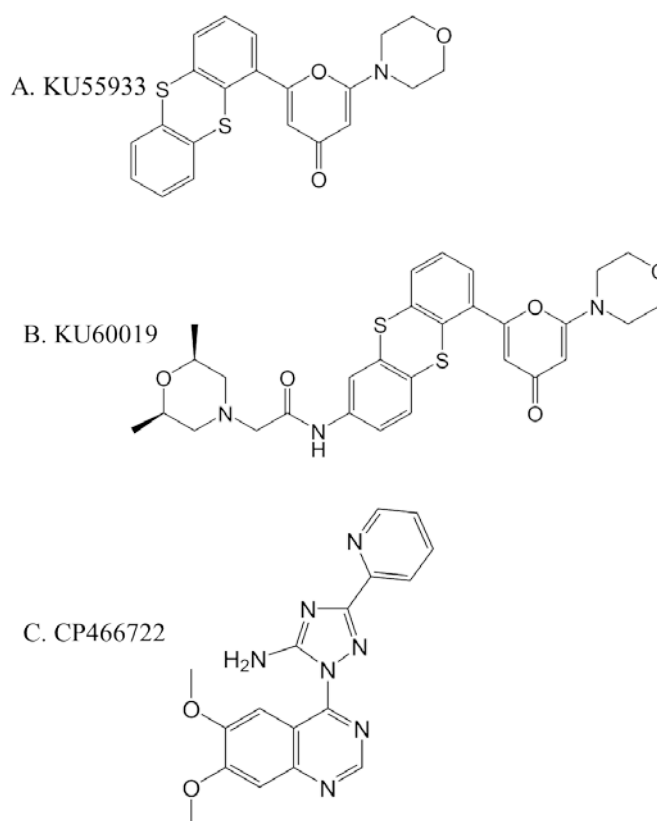
Figure 1-7: Structures of the ATM inhibitors discussed in Section 1.4.5.

1.5   The DNA damage response during mitosis

As previously discussed, DNA-PK and ATM have both been shown to localise to mitotic structures during mitosis in the absence of DNA damage, and play a regulatory role. Recently, the efficacy of the DNA damage response (DDR) during mitosis has been investigated.

It has been hypothesised that the DDR that occurs in interphase cells is comprised of two distinct stages (Giunta *et al.*, 2010). Firstly, there is the initial detection of the DNA strand breaks by the Mre11-Rad50-Nbs1 (MRN) and Ku70 and Ku80 complexes, recruitment of ATM and DNA-PKcs respectively, phosphorylation of H2AX and binding of the DDR mediator protein MDC1 (Rogakou *et al.*, 1998; Falck *et al.*, 2005; Stucki *et al.*, 2005). The second phase comprises the recruitment of RING-finger ubiquitin E3-ligases RNF8 and RNF168, which ubiquitylate γH2AX and cause remodelling of chromatin, and p53-binding protein 1 (53BP1) and BRCA1 accumulation (Kolas *et al.*, 2007; Doil *et al.*, 2009). The end result of the DDR is cell cycle arrest and the cellular fate is either survival or death.

Whilst the DDR in interphase cells has been extensively investigated, there is a relatively poor understanding of the process of the DDR in cells undergoing mitosis (mitotic cells). Treatment of mitotic cells with IR generally fails to halt cell cycle progression although vertebrate cells exposed to IR during late G2 to mid prophase (a phase called "antephase") can delay or reverse mitotic progression (Chin and Yeong, 2010).

After antephase the cells must complete mitosis, even in the presence of DNA strand breaks (Rieder and Cole, 1998). Recently it has been shown that cells in mitosis appear to undergo the primary DDR (involving DNA-PK, ATM and γH2AX phosphorylation) but do not recruit the ubiquitin ligases and complete the full DDR, suggesting that the mitotic cells mark the DSBs during mitosis before full repair during the next cell cycle (Giunta et al., 2010). Secondary DDR processes could be damaging to cells if chromatin is remodelled during mitosis. It was also shown that mitotic cells are more radiosensitive than interphase cells; inhibition of DNA-PK and ATM enhanced radiosensitivity and prolonged the repair of IR-induced foci in mitotic cells once they had progressed to G1 (Giunta et al., 2010).

Following the observation that DNA-PK and ATM, along with ATR, Chk1, Chk2, p53, BRCA1 and TopBP1, localise to the centrosome during mitosis (Hsu and White, 1998; Tsvetkov et al., 2003; Reini et al., 2004; Tritarelli et al., 2004; Zhang et al., 2007b; Lee et al., 2011), and that RNF8 and RNF168 localise at the kinetochores, it was suggested that the DDR proteins may be sequestered at mitotic structures to prevent them being recruited or accumulating at sites of damaged chromatin during mitosis, allowing the cell to prioritise passage through mitosis over repair of DNA breaks (Giunta and Jackson, 2011).

1.6   Microtubules structure and function

1.6.1   *Microtubules in interphase cells*

Microtubules are hollow cylindrical structures that are essential for a wide range of cellular functions and, together with actin microfilaments and intermediate filaments, form the cell cytoskeleton. The intracellular lattice-like structure of the microtubules during the majority of the cell cycle is involved in cellular growth and motility, intracellular molecule and organelle trafficking, modulation of enzyme activity and

protein-protein interaction scaffolding, and plays a major role in cell stress responses (extensively reviewed in (Parker *et al.*, 2014)) (Figure 1-8).

Microtubules are comprised of heterodimers of α-tubulin and β-tubulin which are arranged head-to-tail in 13 parallel protofilaments to form a hollow cylindrical structure (Stanton *et al.*, 2011). The microtubules are dynamic structures with the constant assembly and disassembly of tubulin heterodimers in a highly regulated manner, and the final structure is organised in a polar manner with α-tubulin subunit exposed at the 'minus' end and the β-tubulin subunit exposed at the 'plus' end of the microtubule (Risinger *et al.*, 2009). β-Tubulin has GTPase activity and must be bound to GTP to allow assembly into the microtubules, and this GTP is then irreversibly hydrolysed to GDP upon the addition of another β-tubulin molecule (Erickson and O'Brien, 1992). Most of the β-tubulin proteins are therefore GDP-bound, with the β-tubulins exposed at the 'plus' end forming a GTP cap that prevents microtubule depolymerisation. The relatively rapid addition and deletion of tubulin heterodimers at the 'plus' end, compared with the slower dynamics at the 'minus' end, is called dynamic instability (Mitchison and Kirschner, 1984).

The microtubules are organised by the microtubule-organising centre called the centrosome. The centrosome consists of a pair of centrioles surrounded by a fibrous network of pericentriolar material which binds many proteins including the γ-tubulin ring that nucleates the microtubules (reviewed in Hinchcliffe and Sluder (2001)). During interphase, the microtubules are nucleated by the centrosome (centrally located adjacent to nucleus) and organised into parallel, polarised arrays radiating out from the centrosomes with their 'plus' ends all orientated in the same direction towards the cell periphery (Bergen and Borisy, 1980; Bergen *et al.*, 1980). There are two motor proteins, kinesin and dynein, which are responsible for the movement of molecules along the microtubules (Hirokawa *et al.*, 2009; Kardon and Vale, 2009). Kinesin carries out 'plus' end –directed movement and traffics for example, protein-containing vesicles to be excreted from the cells to the cell periphery (Hirokawa *et al.*, 2009). Dynein is a 'minus' end-directed motor protein which carries signalling proteins towards the nucleus (Kardon and Vale, 2009) (Figure 1-8).

Microtubule structure

α/β tubulin heterodimers

Microtubule function in interphase

Cell growth and motility

Stress responses

Enzyme activity

Kinesin   Dynein

Intracellular trafficking

Cell cytoskeleton

Protein-protein interaction scaffolding

Centrosome

Nuclear pore complex

Cytoplasmic microtubule

Microtubule-capping protein (plus-end stabilization)

Microtubule function in mitosis

Interphase

Prophase

Telophase and cytokinesis

Aurora A

Aurora A   Aurora B

Polo-like kinase

Polo-like kinase

Aurora A

Polo-like kinase   Polo-like kinase

Aurora B   Aurora A   Aurora B   Aurora B   Aurora A

Aurora A

Polo-like kinase

Anaphase

Mitotic spindle checkpoint

Metaphase

Prometaphase

Figure 1-8: Microtubule structure and functions in both interphase and mitosis.
Figures adapted from (Kavallaris, 2010; Komlodi-Pasztor *et al.*, 2011).

1.6.2   *Microtubules in mitotic cells*

Mitosis is a highly complex and regulated process that ensures the correct segregation of sister chromatids to maintain genomic stability. Upon entry into mitosis, the centrosome duplicates and the daughter centrosomes form the two poles for the mitotic spindle following the breakdown of the nuclear envelope (Hinchcliffe and Sluder, 2001) (Figure 1-8). The interphase microtubule network disassembles and new, more dynamic, spindle microtubules are formed (Zhai *et al.*, 1996). The microtubules are organised to form the mitotic spindle and interact with the kinetochores creating

26

tension that allows the direction of the sister chromatids to opposite spindle poles (Jordan and Wilson, 2004). In prometaphase the microtubules are highly dynamic and lengthen and shorten rapidly, probing the cytoplasm for kinetochores (Hayden *et al.*, 1990). During metaphase the microtubules undergo a process called 'treadmilling' where tubulin is continually added at the kinetochores and removed at the spindle poles, causing the attached duplicated chromosomes to oscillate back and forth under high tension in the mitotic spindle region; which is necessary for correct spindle function (Mitchison, 1989; Shelby *et al.*, 1996). During anaphase the microtubules undergo controlled shortening to pull the sister chromatids to the opposite spindle poles (Jordan and Wilson, 2004).

The correct duplication of the centrosomes is very important because the cell does not have a checkpoint to terminate mitosis in response to extra centrosomes and therefore extra spindle poles (Sluder *et al.*, 1997). If the centrosome does not duplicate then cells return to interphase which causes polyploidy, whereas more than two centrosomes leads to multipolar spindles, unequal division of the chromosomes and genetic instability (Orr-Weaver and Weinberg, 1998).

The mitotic spindle assembly checkpoint (SAC) monitors the proper attachment of the mitotic spindles to kinetochores to ensure that there is the correct tension for sister chromatid separation; a single unattached chromosome or incorrect tension halts the cell cycle and prevents progression to anaphase (Foley and Kapoor, 2013). There are a wide range of proteins involved in the SAC, including mitotic arrest deficient 1 (MAD1), MAD2, budding uninhibited by benomyl 1 (BUB1), BUB3, BUB-related 1 (BUBR1) and monopolar spindle protein 1 (MSP1) kinases (Hoyt *et al.*, 1991; Li and Murray, 1991; Weiss and Winey, 1996), most of which target unattached kinetochores and are depleted from kinetochores when microtubules attach (Foley and Kapoor, 2013). Downstream of the SAC is an E3 ubiquitin ligase, known as the anaphase-promoting complex (APC), and the proteins in the SAC inhibit the APC by inactivating its cofactor CDC20, until all kinetochores are attached and the correct tension is detected (Hwang *et al.*, 1998).

There are a number of other proteins that localise to mitotic structures and play well-characterised functions. For example, the aurora kinases are a family of mitotic serine-threonine kinases. Aurora A kinase levels increase as the cell progresses through prophase, metaphase and anaphase, and the protein localises to the spindle poles and then to the midbody during telophase and cytokinesis, where it is involved in centrosome separation and maturation, and spindle stability (Dutertre *et al.*, 2002).

Auroras B and C kinases are chromosomal passenger proteins and both interact with the inner centromere protein (INCENP) (Sasai *et al.*, 2004). Aurora B kinase localises to microtubules near the kinetochores whereas aurora C kinase moves from the centromeres to the midbody during cell cycle progression (Sasai *et al.*, 2004). The knockdown of either aurora B or C kinase gave rise to multinucleated cells with an additive effect seen with knockdown of both proteins; demonstrating their importance in correct mitosis (Sasai *et al.*, 2004). The polo-like kinases (PLK1-4) are another family of proteins that play regulatory functions during mitosis and localise to the centrosomes, spindle poles and midbody during mitosis (van de Weerdt and Medema, 2006).

1.7   Microtubule-targeting agents

Due to the importance of microtubules in correct cell division, microtubules are important targets of anticancer agents and a wide variety of antimitotic drugs have been developed and used clinically in the treatment of cancer. Many microtubule-targeting agents (MTAs) were identified in large scale screens of natural products and act to inhibit cell proliferation by interfering with the essential spindle dynamics of the microtubules, causing a slowing or blocking of mitosis at the metaphase-anaphase transition and inducing apoptosis.

There are five different groups of MTAs based on their tubulin binding site, which are the vinca alkaloids, the taxanes, colchicine, the epothilones and laulimalide (Liu *et al.*, 2014). MTAs are generally sub-classified into two classes; the microtubule-destabilising agents and the microtubule-stabilising agents. However, these sub-classifications are overly simplistic because their effects on microtubule polymer mass (through destabilising or stabilising) occur at high concentrations but all of the compounds suppress microtubule spindle dynamics at much lower concentrations, causing the metaphase-anaphase block, and it is now thought that this is the more important mechanism of action of MTAs (reviewed in Jordan and Wilson (2004)).

1.7.1   Microtubule destabilisers

The vinca alkaloids group were originally derived from the Madagascan periwinkle, *Catharanthus roseus*, around 50 years ago (Bohannon *et al.*, 1963), and include the first generation compounds vincristine (Figure 1-9) and vinblastine, and the second generation compounds vinorelbine, vindesine and vinflunine.

At high concentrations, the vinca alkaloids bind near the GTP hydrolysis site at the plus end of the microtubules, modulate the gain and loss of this GTP cap and result in decreased dynamics, mitotic spindle destruction and disassembly of the microtubules (Cutts *et al.*, 1960; Toso *et al.*, 1993). At low but clinically-relevant concentrations, the vinca alkaloids do not act to depolymerise/disassemble the microtubules but cause the cells to arrest in mitosis (due to the suppression of microtubule dynamics) and undergo apoptosis (Jordan *et al.*, 1991). The vinca alkaloids bind reversibly to the β-tubulin subunit of the tubulin heterodimers in a distinct binding site called the vinca-binding domain, leading to a conformational change causing tubulin self-association (Wilson *et al.*, 1982; Bai *et al.*, 1990). Vinblastine was also shown to bind along the microtubules and cause loosening of the protofilaments, exposing further vinblastine binding sites and aiding in the depolymerisation of microtubules (Jordan *et al.*, 1986; Singer *et al.*, 1989). The binding of the vinca alkaloids to the microtubule ends to disrupt the microtubule dynamics is extremely sensitive. Only one or two molecules of vinblastine per microtubule end are required to cause a 50 % reduction in instability and "treadmilling" dynamics of microtubules, without causing depolymerisation; thereby reducing the ability of the cell to assemble a correct mitotic spindle and reducing the tension at the kinetochores (Jordan and Wilson, 2004).

Vincristine and vinblastine are widely used clinically in combination regimens in the treatment of a range of haematological malignancies, including acute lymphoblastic leukaemia, Hodgkin's and non-Hodgkin's lymphoma. The other agents in this group, vinorelbine and vinflunine, are used in the treatment of lung, breast and bladder cancers (Bennouna *et al.*, 2008; Pallis *et al.*, 2011). The vinca alkaloids are associated with severe toxicities such as myelosuppression and peripheral neuropathy (Swain and Arezzo, 2008), which are also observed with the taxane group of MTAs. Although not fully understood, neurotoxicity is caused by the effect of these agents on microtubules in neurons, which could disrupt axonal flow and cause neuronal retraction (Sahenk *et al.*, 1994).

Colchicine is another microtubule destabilising agent that is used clinically in the treatment of gout (Ben-Chetrit and Levy, 1998). Colchicine binds to a site at the interface between α-tubulin and β-tubulin in the heterodimer near to the α-tubulin GTP-binding site, and preferentially binds to free heterodimers which inhibits dynamics upon binding of the heterodimer to a microtubule (Ravelli *et al.*, 2004; Risinger *et al.*, 2009). As with the vinca alkaloids, at low concentrations colchicine stabilises microtubule dynamics and at higher concentrations causes depolymerisation of microtubules.

However, colchicine or its derivatives have not found a use in cancer therapy due to the severe toxicities seen at the concentrations necessary for anti-tumour activity, however, lower doses can be tolerated for gout treatment (Ben-Chetrit and Levy, 1998). There are a number of colchicine site-binding agents that are in development for use alone or in combination with other chemotherapeutics. For example ABT-751 has antimitotic and vascular-disrupting properties and clinical trials have shown efficacy against a range of solid and haematological malignancies (Mauer *et al.*, 2008) and CA4P, which depolymerises interphase microtubules in tumour vascular endothelial cells (Kanthou and Tozer, 2007) (reviewed in (Risinger *et al.*, 2009)).

1.7.2 Microtubule stabilisers

The taxanes are derived from *Taxus brevifolia*, the Pacific yew (Wani *et al.*, 1971) and consist of paclitaxel and its semi-synthetic analogue, docetaxel (Figure 1-9).

The taxanes bind to GDP-bound β-tubulin in assembled microtubules on the inner surface and cause a conformational change that resembles the GTP-bound form, which increases the tubulin affinity for neighbouring molecules and therefore causes microtubule polymerisation and stabilisation (Nogales *et al.*, 1995; Elie-Caille *et al.*, 2007). The ability of paclitaxel to increase microtubule polymerisation is associated with a 1:1 paclitaxel to tubulin heterodimer molar ratio, and paclitaxel has also been demonstrated to cause the formation of 12 protofilament microtubules compared with the usual 13 protofilaments (Andreu *et al.*, 1992). At low concentrations, the taxanes act in a similar manner to the microtubule-destabilising agents to decrease microtubule dynamics, with just one paclitaxel molecule bound per several hundred tubulin molecules in a microtubule being sufficient to reduce the dynamic rate of the microtubules by 50 % (Yvon *et al.*, 1999).

Paclitaxel and docetaxel are widely used in the treatment of solid tumours including breast, lung, ovarian, and prostate cancers (Clarke and Rivory, 1999). Neutropenia, hypersensitivity reactions, and fluid retention are frequently experienced by patients treated with these agents (Baker *et al.*, 2009), and their use is limited by the occurrence of inherent and acquired drug resistance. Paclitaxel is highly insoluble and therefore must be administered in cremophor, an agent that causes hypersensitivity reactions. There are a number of newer compounds that were developed to overcome the solubility and drug resistance problems encountered with paclitaxel and docetaxel. These include ABI-007 (albumin-bound paclitaxel with increased solubility which does not require cremophor formulation) (Gradishar *et al.*, 2005), ANG1005 (modified

paclitaxel with improved solubility conjugated to a receptor-targeting peptide to promote transport across blood-brain barrier) (Regina *et al.*, 2008), and XRP9881 and TP1287 (semi-synthetic derivatives of paclitaxel that are poor substrates of the drug-efflux transporter, MDR1) (Fitzgerald *et al.*, 2012) (Robert *et al.*, 2010).

The epothilones are a more recent group of pharmaceuticals to enter clinical development, which act as microtubule-stabilising agents by binding to a site near to the taxane-binding site with a similar mechanism of action to the taxanes whilst retaining activity in multidrug-resistant cells (Kowalski *et al.*, 1997). The epothilones are poor MDR1 substrates and also display good activity in βIII tubulin-overexpressing cancers, a subset of tumours that exhibit poor responses to the taxanes (Kowalski *et al.*, 1997; Edelman and Shvartsbeyn, 2012). Laulimalide and peloruside A are compounds that acts as microtubule stabilisers and bind to a novel microtubule-binding site on β-tubulin, allowing the co-administration of these agents with taxanes, which is not possible with the epothilones (Hamel *et al.*, 2006; Wilmes *et al.*, 2011).
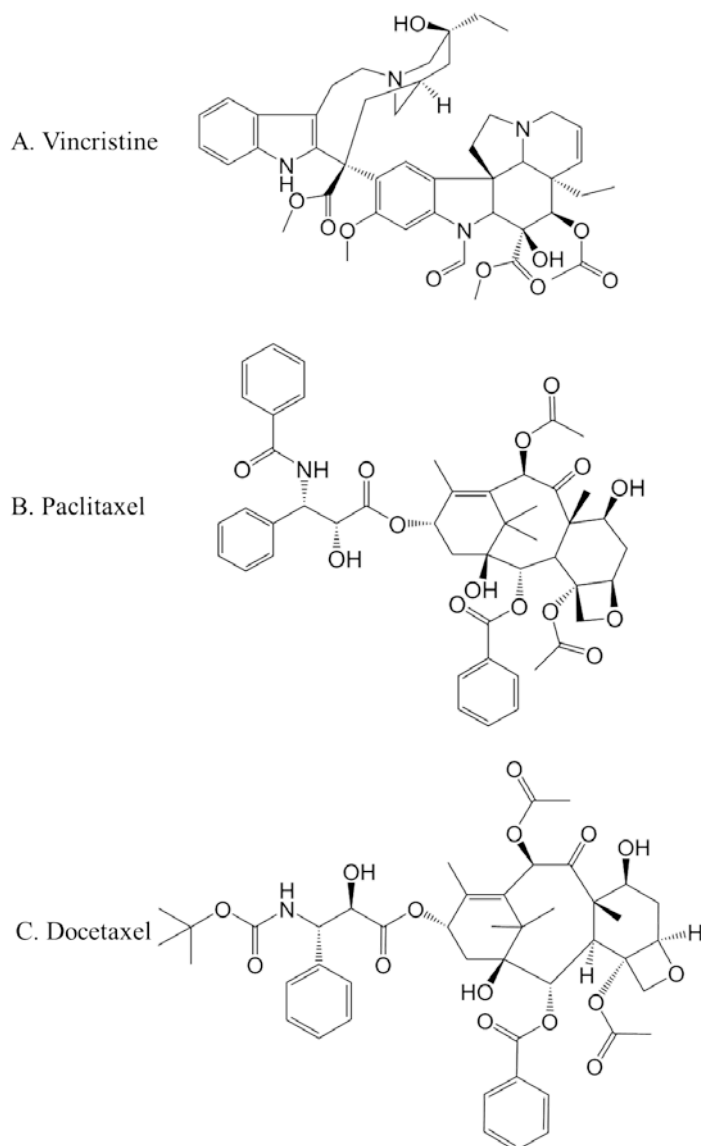
Figure 1-9: Structures of the three microtubules-targeting agents, vincristine, paclitaxel and docetaxel, used in this thesis.

1.7.3   The effect of microtubule-targeting agents in interphase cells

The hypothesis for the selectivity of agents which interfere with mitosis, e.g. the MTAs and some mitosis-specific kinase inhibitors, is that cancer cells are rapidly-dividing (compared with normal healthy tissue) and therefore should be selectively killed by agents that halt cell division. A number of inhibitors of mitotic kinases have been recently developed following this rationale, including inhibitors of aurora kinases A, B and C, polo-like kinases (PLK) and kinesin spindle protein (KSP). As explained in Section 1.6.2, aurora kinase A levels increase in mitosis and this protein localises to various mitotic structures and plays a regulatory function, demonstrating mitosis-

specific effects (Dutertre *et al.*, 2002), and aurora kinases B and C are chromosome passenger proteins which localise to mitotic structures and aid in the attachment of the kinetochores to mitotic spindle fibres (Sasai *et al.*, 2004). PLKs 1-4 act at the centrosomes, spindle poles and midbody during mitosis (Kishi *et al.*, 2009). KSP is a mitosis-specific protein that hydrolyses ATP to fuel the production of force for movement along microtubules to promote the assembly, maintenance and elongation of the mitotic spindle (Huszar *et al.*, 2009). Inhibitors of these kinases, and MTAs, disrupt mitosis effectively but none of these agents initiate mitosis and so the mitosis-specific inhibitors can only work when a cell is undergoing mitosis (reviewed in Komlodi-Pasztor *et al.* (2012)). Despite large pharmaceutical investment, there has been very limited clinical activity demonstrated with mitosis-specific kinase inhibitors.

Microtubules have many functions during interphase as well as mitosis and therefore MTAs can potentially target cells in all phases of the cell cycle. Komlodi-Pasztor *et al.* (2011) produced an excellent review entitled "Mitosis is not a key target of microtubule-targeting agents in patient tumours" in which they presented a well-balanced argument for the roles of MTAs in interphase cells. Cancer cell lines studied *in vitro* and xenograft models can have much faster doubling-times than clinical tumours. The median tumour doubling time presented in all of the studies combined in this review was 147 days, a sharp contrast to the 24-hour doubling time of cell lines *in vitro* or the 1-12 day doubling time of a tumour xenograft model (Komlodi-Pasztor *et al.*, 2011). Therefore the percentage of cells undergoing mitosis at any time in a human tumour is extremely low, and MTAs have demonstrated good clinical activity compared with mitosis-specific agents, implying that the main effects caused by MTAs in a human tumour may be mitosis-independent. The trafficking of important proteins along the microtubules is a vital feature of the microtubules in interphase, and many proteins have been identified that either associate with or traffic along the microtubules. These include p53, c-Myc, BRCA1, Rb, androgen receptor, protein kinase C and many others (Alexandrova *et al.*, 1995; Garcia-Rocha *et al.*, 1997; Hsu and White, 1998; Giannakakou *et al.*, 2000; Roth *et al.*, 2007; Zhu *et al.*, 2010). In addition, proteins relevant to the studies described in this thesis localise to mitotic structures e.g. DNA-PK and ATM (Zhang *et al.*, 2007b; Shang *et al.*, 2010), and therefore it is hypothesised that interfering with intracellular trafficking could disrupt cancer cells (Komlodi-Pasztor *et al.*, 2011). In addition, a number of mitosis-independent effects of MTA treatment have been identified, such as vascular disruption causing increased permeability of tumour blood vessels (Kanthou and Tozer, 2007), and effects on sensory neurones (which rarely

or never divide) causing the characteristic neuropathy experienced by patients treated with these agents (DeAngelis *et al.*, 1991; Mielke *et al.*, 2006). These findings lead to the proposal that MTAs demonstrate the majority of their effects on cancer cells in interphase, with the mitosis-specific effects demonstrated in cell lines *in vitro* and on bone marrow precursors *in vivo* causing neutropenia following treatment (Legha *et al.*, 1990).

1.7.4 Tubulin modifications and cancer

There are eight different isoforms of α-tubulin and seven different isoforms of β-tubulin, which make up the microtubules in a function- and tissue-dependent manner, and are distinguishable by differing C-terminal sequences (Sullivan and Cleveland, 1986; Luduena, 1993).

The main microtubule modifications documented in a range of cancers are altered expression of tubulin isotypes, alterations in tubulin post-translational modifications and changes in microtubule-associated protein (MAP) expression (reviewed in Parker *et al.* (2014)). Altered tubulin isotype expression (e.g. high βI-tubulin, βIII-tubulin, βIVa-tubulin, βV-tubulin and γ-tubulin) and altered post-translational modifications (e.g. high Δ2α-tubulin and detyrosinated tubulin) commonly correlate with poor prognosis, poor response to MTAs, more aggressive disease and poor survival in a range of cancers (Parker *et al.*, 2014). Changes in the expression of MAPs such as Tau, MAP2, MAP4, BRCA1 and kinesins have been related to chemotherapy resistance and disease progression (Parker *et al.*, 2014), however, these modifications are not clinically prevalent and so their importance in cancer progression is undetermined.

Centrosome amplification is tightly associated with the formation of multipolar spindles and chromosomal instability. Centrosome amplification frequently occurs in human cancers and is assumed to contribute to transformation or to be a consequence of cancer progression (Pihan *et al.*, 1998; Lingle *et al.*, 2002).

1.7.5 Mechanisms of resistance to microtubule-targeting agents

A well-reported mechanism of resistance to MTAs is changes in tubulin expression. Cell lines overexpressing βIII-tubulin display resistance to vinca alkaloids and taxanes (Risinger *et al.*, 2008), and cell lines made resistant to taxanes display changes in specific β-tubulin isotypes, including βI, βII-, βIII- and βIVa-tubulin (Kavallaris *et al.*, 1997; Galletti *et al.*, 2007; Gan and Kavallaris, 2008; McCarroll *et al.*, 2010; Wang *et al.*, 2014).

The most prominently reported cause of resistance to MTAs is the overexpression of the ATP-binding cassette drug efflux pump, multidrug resistance protein1 (MDR1). The classical taxanes and vinca alkaloids, including paclitaxel, docetaxel and vincristine, are substrates for MDR1 (Benard *et al.*, 1989; Mickisch *et al.*, 1991). MDR1 overexpression has been associated with taxane treatment, which led to multidrug resistance (Leonard *et al.*, 2003; Rottenberg *et al.*, 2007).

1.8 Multidrug-resistance

There are two classes of resistance to chemotherapeutic agents that are observed in cancer. The first is impaired delivery of drugs to cancer cells, which can result from poor absorption of orally administered drugs, increased drug metabolism or increased excretion, such that the drug concentration in the blood is lower and less drug diffuses from the blood into the tumour, which can involve changes to tumour vasculature (Jain, 2012). The second class of resistance encompasses genetic and epigenetic alterations in the cancer cells that affect drug sensitivity, such as changes to drug targets, increased repair of damage caused by anticancer agents, disruption of cell death apoptosis pathways, activation of detoxifying enzymes (e.g. cytochrome P450 enzymes), decreased drug influx into cells or increased drug efflux (*via* ATP-dependent efflux pumps) (reviewed in Gottesman *et al.* (2002)). Multidrug resistance is the simultaneous resistance to several structurally-related drugs that do not necessarily have a common mechanism of action. Multidrug resistance that occurs due to increased drug efflux *via* increased expression of ATP-dependent efflux pumps that have broad drug specificity, including the taxanes, the vinca alkaloids, the anthracyclines and actinomycin D, is often called classical multidrug resistance. MDR1, one of the ATP-binding cassette (ABC) family of drug efflux transporters related to this PhD study, will be discussed further.

1.9 Multidrug-resistance protein 1 (MDR1)

1.9.1 MDR1 structure and function

Multidrug-resistance protein 1 (also known as P-glycoprotein) is the product of the *ABCB1/MDR1* gene. MDR1 was first discovered almost 40 years ago through cell

surface membrane studies of resistant Chinese Hamster Ovary cells which demonstrated the presence of a 170 kDa glycoprotein that was not present in parental sensitive cells (Juliano and Ling, 1976). MDR1 was the first member of the ABC superfamily of transmembrane transporters to be cloned, and there are now 48 known ABC transporters, sub-classified into seven distinct, structure- and sequence-specific subfamilies (A-G) (Dean *et al.*, 2001). The MDR1 efflux pump consists of two homologous components, each with 6 transmembrane regions and an ATP-binding site (Chen *et al.*, 1986).
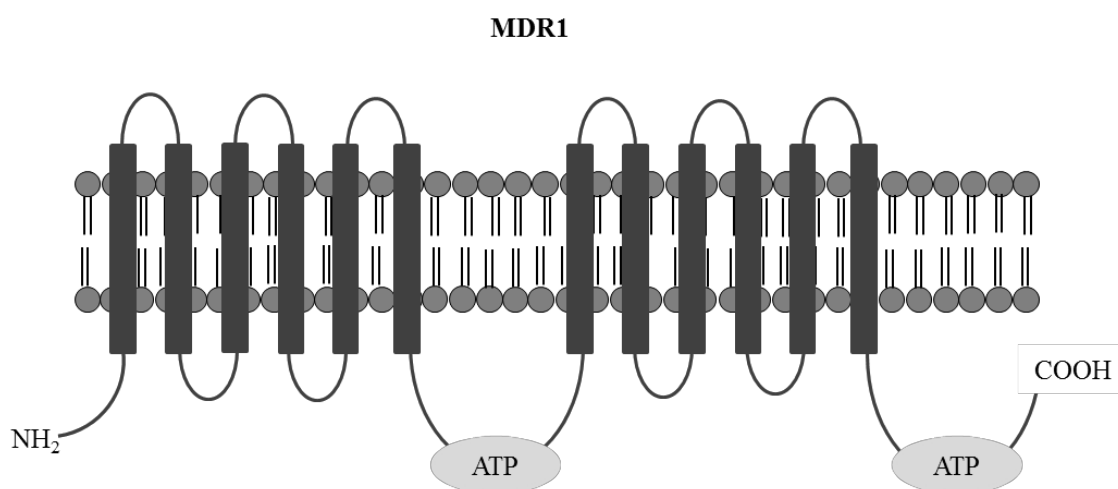
Figure 1-10: Structure of the ABC transporter, MDR1. Adapted from Gottesman *et al.* (2002).

The binding of hydrophobic drug substrates to the transmembrane regions induces ATPase activity at the first ATP site causing a conformational change to export the bound drug out of the cell, followed by ATPase activity at the second site to reset the conformation of the efflux pump (Ramachandra *et al.*, 1998; Gottesman *et al.*, 2002). MDR1 is located in the apical membrane of many cell types and acts as a drug efflux transporter in the liver, kidneys, gastrointestinal tract, and multiple blood barriers including the blood-brain and the blood-placental barriers (Sikic *et al.*, 1997; Gottesman *et al.*, 2002). MDR1 has been demonstrated to be an effective, apical membrane transporter of hydrophobic substrates, peptides, lipids, steroids and xenobiotics including hydrophobic drugs such as vinca alkaloids, taxanes, colchicine and anthracyclines (Allen *et al.*, 2000; Dean *et al.*, 2001). In relation to this thesis study on kinases, it is interesting to note that at least 8 distinct phosphorylation sites have been identified on MDR1 with protein kinase C, protein kinase A and casein kinase 2

implicated as major players in MDR1 phosphorylation (reviewed in Stolarczyk *et al.* (2011)). However, the role of phosphorylation on MDR1 function remains unclear it is suggested that the regulation of MDR1 phosphorylation will be due to multiple kinases acting at multiple phosphorylation sites,

1.9.2   MDR1 expression in human cancers

Although the overexpression of MDR1 in response to repeated treatment with an MDR1 substrate is easily demonstrated *in vitro*, the role of MDR1 in the clinical setting is widely debated. Early studies demonstrated that MDR1 was overexpressed in human cancers and that there was an increase in MDR1 expression upon relapse (Fojo *et al.*, 1987; Goldstein *et al.*, 1989), but the initial thought that this was the only mechanism of resistance was quickly disproven. The measurement of MDR1 levels in solid tumours is difficult because of tumour heterogeneity and interpretation of the data is complicated by the different methods used to measure MDR1. However, correlations between MDR1 expression and clinical outcome have been demonstrated in haematological cancers. For example, a study demonstrated that one-third of acute myeloid leukaemia (AML) patients expressed MDR1 at diagnosis, which increases to more than half at relapse, and MDR1 expression is correlated with a reduced complete remission rate, poorer prognosis and increased rate of resistant disease (Legrand *et al.*, 1999; Leith *et al.*, 1999; Michieli *et al.*, 1999; van der Kolk *et al.*, 2000).

Following the discovery of the ABC family of transporters and their role in multidrug resistance, many inhibitors of this family of transporters have been developed. MDR1 inhibitors cause large *in vitro* sensitisations with drugs known to be MDR1 substrates. However, there has been very limited clinical success with MDR1 inhibitors due to inefficacy, low bioavailability at tumour site or toxicity (reviewed in (Szakacs *et al.*, 2006). Primary toxicities observed included hypotension, ataxia and immunosuppression with secondary toxicities due to MDR1 inhibition in bone marrow stem cells. Many of the MDR1 substrates induced pharmacokinetic interactions that affected cytotoxic drug clearance and metabolism, resulting in high plasma cytotoxic drug concentrations and hence toxicity. Modification of the drug dose and patient-to-patient variation of the pharmacokinetic interaction effects resulted in patients being over-dosed or under-treated (Szakacs *et al.*, 2006). Until there are accurate methods for the measurement of MDR1 activity and inhibition in clinical trials, and the contribution of MDR1 to clinical resistance is fully established, there will be limited progress in the development of MDR1 inhibitors in cancer treatment.

1.10   Previous findings

Prior to the commencement of this project, a Master's degree project student demonstrated that the acute lymphoblastic leukaemia cell line, CCRF-CEM, was sensitised not only to DNA damaging agents but also to the microtubule-targeting agent vincristine, by the DNA-PK and ATM selective inhibitors NU7441 and KU55933, respectively (NJ Tan, unpublished results). An additional hypothesis for this Master's degree project was to test whether multidrug-resistant cells would be hypersensitive to the sensitisation effects of DNA-PK or ATM inhibition on topoisomerase II poisons and microtubule-targeting agents, and it was demonstrated that the vincristine-resistant CCRF-CEM VCR/R cell line was sensitised to both DNA-damaging and microtubule-targeting agents to a greater degree by NU7441 and KU55933 than the vincristine-sensitive parental CCRF-CEM cells.

1.11   Summary and hypothesis

The roles of DNA-PK and ATM in the DNA repair pathways of non-homologous end-joining and homologous recombination, respectively, are well established. However, recent findings suggest that DNA-PK and ATM may have roles beyond DNA repair, one of which is a regulatory function in the mitotic spindle assembly and mitotic progression. Microtubules are important intracellular structures that are involved in cell structure, polarity and intracellular protein trafficking, along with formation of the mitotic spindle to ensure the correct separation of chromosomes during cell division. Microtubule-targeting agents are widely used in the clinic but the development of resistance to these agents is a clinical problem. The hypothesis tested in this thesis was that DNA-PK and ATM play a role in the response of cells to microtubule-targeting agents and, therefore, that inhibition of DNA-PK and ATM, using the selective inhibitors NU7441 and KU55933, respectively, would sensitise cells to microtubule-targeting agents.

1.12 Aims

There were five overall aims of this thesis:

1. To investigate the sensitisation of paired parental and multidrug-resistant cell lines to microtubule-targeting agents using NU7441 and KU55933, and to examine DNA-PK and ATM expression and activity in response to these agents

2. To identify whether NU7441 and KU55933 were enhancing sensitivity in multidrug-resistant cell lines to MTAs *via* interaction with the drug efflux transporter, MDR1

3. To explore combinations of ionising radiation and microtubule-targeting agents, in the presence and absence of DNA-PK or ATM inhibition

4. To investigate the importance of DNA-PK and ATM in the response of cells to microtubule-targeting agents using DNA-PK deficient and proficient isogenic cell lines

5. To investigate the localisation and activation of DNA-PK in mitotic cells, and the effect of ionising radiation and microtubule-targeting agents on this localisation and activation, together with changes to the mitotic spindle structure and mitotic progression in DNA-PK proficient and deficient cells

Chapter 2: Materials and Methods

2.1   Materials

2.1.1   Chemicals and reagents

All chemicals and reagents were obtained from Sigma-Aldrich (Dorset, UK) unless otherwise specified.

2.1.2   General equipment

Balances: A&D FX-320 electronic balance (A&D Company Ltd, Tokyo, Japan) and Salter electroscale XF-3200 (Scientific Laboratory Supplies, Nottingham, UK)

Coulter counter: Beckman Coulter Z1 (Beckman Coulter, Buckinghamshire, UK)

Centrifuges: Eppendorf 5415D (Scientific Laboratory Supplies, Nottingham, UK) and Beckman Coulter Allegra X-12R (Beckman Coulter, Buckinghamshire, UK)

Heating blocks: Starlab dry bath system (Starlab UK, Milton Keynes, UK) and Grant heating block (BDH, Dorset, UK)

Incubators: Sanyo CO_2 incubators (Panasonic Biomedical Sales Europe BV, Leicestershire, UK)

Irradiator: Gulmay Medical RS320 Irradiation System (Gulmay, Surrey, UK)

Luminometer: BMG Labtech FLUOstar Omega multi-mode microplate reader (BMG Labtech GMBH, Ortenberg, Germany)

Microscopes: Leica DMIL inverted microscope (Leica Microsystems, Buckinghamshire, UK) and Leitz labovert (Leica Microsystems, Buckinghamshire, UK)

pH meters: Mettler Toledo SevenEasy (Mettler Toledo, Columbus, OH, USA)

Power pack: BioRad Powerpac HC (BioRad, Hertfordshire, UK)

Rollers: Stuart SRT6 and SRT1 roller mixers (Stuart Scientific, Surrey, UK)

Shakers: Stuart STR9 gyro rocker (Stuart Scientific, Surrey, UK)

Spectrophotometers: Spectromax 96-well microtitre plate reader (Molecular Devices, Berks, UK), BioRad Model 680 microplate reader (BioRad, Hertfordshire, UK) and BMG Labtech FLUOstar Omega multi-mode microplate reader (BMG Labtech GMBH, Ortenberg, Germany)

Stirrers: IKA C-MAG MS10 (IKA, Staufen, Germany)

Tissue culture hoods: BioMAT[2] Airology Centre (Medical Air Technology Ltd, Oldham, UK)

Waterbaths: Grant JB1 (Grant Instruments, Cambridgeshire, UK)

Western blotting tanks: BioRad Criterion Cell running tank and BioRad Criterion blotter transfer tank (BioRad, Hertfordshire, UK)

2.1.3 Small molecule inhibitors

The DNA-PK inhibitor NU7441 (8-dibenzothiophen-4-yl-2-morpholin-4-yl-chromen-4-one) (DNA-PK IC_{50} = 14 nM) was kindly provided by KuDOS and synthesised by Dr Marc Frigerio, Dr Mark Hummersone and Dr Keith Menear. NU7441 was used at a concentration of 1 µM which was previously shown to inhibit DNA-PK activity without inducing cellular toxicity (Zhao *et al.*, 2006).

NU7742 (8-dibenzothiophen-4-yl-2-piperidin-1-yl-chromen-4-one) was synthesised by Dr Celine Cano at Newcastle Cancer Centre and has been previously shown to be an inactive derivative of NU7441 with a methylene group replacing the morpholine oxygen (DNA-PK IC_{50} > 10 µM) as used in Willmore *et al.* (2008). NU7742 was used at 1 µM to allow direct comparison with NU7441.

DRN1 and DRN2 were previously synthesised by Dr Gavin Jones, Faye Craven, Dr Tommy Rennison and Dr Kate Clapham at the Newcastle Cancer Centre. The atropisomers DRN1 (DNA-PK IC_{50} = 2 nM) and DRN2 (DNA-PK IC_{50} = 7 µM) are derivatives of NU7441 with an additional methyl substituent at the 7-position of the chromen-4-one ring. The 7-methyl group restricts rotation of the O-dibenzothiophene moiety such that two atropisomers are formed, only one (DRN1) having appreciable DNA-PK-inhibitory activity (Clapham *et al.*, 2012).

The ATM inhibitor, KU55933 (2-morpholin-4-yl-6-thianthren-1-yl-pyran-4-one) (ATM IC_{50} = 13 nM), was routinely purchased from Tocris Bioscience (Abingdon, UK). KU55933 was used at 10 µM which has previously been shown to inhibit ATM function and ATM-dependent phosphorylation events (Hickson *et al.*, 2004).

All of the inhibitors were dissolved in DMSO and stored under light-protected conditions at -20 °C. NU7441 and NU7742 were stored at a concentration of 2 mM, DRN1 and DRN2 were stored at 1.5 mM, and KU55933 was stored at 20 mM.

2.1.4 Microtubule-targeting agents

Vincristine sulphate salt, paclitaxel and docetaxel were all dissolved in DMSO and were stored at concentrations of 1 mM, 5 mM and 6.2 mM, respectively, at -20 °C.

2.2 Mammalian cell culture

All tissue culture plasticware including Corning flasks, cell culture petri dishes and 6-well and 96-well cell culture multiwall plates were purchased from Fisher

Scientific International Ltd (Leicestershire, UK). Sterile plastic pipettes were purchased from Starlabs (Buckinghamshire, UK). Tissue culture medium, penicillin-streptomycin and trypsin-EDTA were obtained from Sigma-Aldrich (Dorset, UK). Foetal bovine serum (FBS) was purchased from Sigma-Aldrich until September 2012, after which time Gibco FBS was purchased from Life Technologies (Paisley, UK). Sterile phosphate buffered saline (PBS) was prepared in the Newcastle Cancer Centre.

2.2.1 Cell lines

The following cell lines were used during this study:

Cell Line	Details	Reference
CCRF-CEM	Suspension T-cell acute lymphoblastic leukaemia cell line derived from buffy coat of 4 year old female (1964)	(Foley *et al.*, 1965)
CCRF-CEM VCR/R	CCRF-CEM cells that were made multidrug-resistant by exposure to stepwise increments of vincristine and that overexpress MDR1	(Haber *et al.*, 1989)
M059J	Adherent human glioblastoma cell line that is spontaneously DNA-PKcs deficient	(Lees-Miller *et al.*, 1995)
M059J-Fus1	M059J cells that have been complemented with an extra copy of chromosome 8 containing the DNA-PKcs gene	(Hoppe *et al.*, 2000)
SKOV3	Adherent metastatic ovarian adenocarcinoma cell line originally derived from the ascites of a 64 year old female (1973)	(Fogh and Trempe, 1975)
SKOV3-TR	SKOV3 cells that were made paclitaxel resistant by exposure to stepwise increments and that overexpress MDR1	Kindly provided by Professor Iain McNeish (Glasgow)
A2780	Adherent human ovarian carcinoma established from the tumour tissue of an untreated patient	(Hamilton *et al.*, 1984)
A2780-TX1000	A2780 cells that were made paclitaxel resistant by exposure to stepwise increments and that overexpress MDR1	Kindly provided by Professor Iain McNeish
KK47	Adherent bladder cancer cell line derived from a transitional cell carcinoma of the bladder	(Hasegawa *et al.*, 1995)*
KK47A	KK47 cells that are multidrug-resistant created by exposure to stepwise increments of doxorubicin and that overexpress MDR1	(Kimiya *et al.*, 1992)
MDCKII	Adherent Madin-Darby canine kidney cell line strain II, originally derived from a whole normal adult dog kidney in 1958	(Louvard, 1980)
MDCKII-MDR1	MDCKII cell line that stably overexpresses MDR1	(Evers *et al.*, 1998)
HCT116 DNA-PK +/+	Adherent human colon cancer cell line derived from the colorectal carcinoma of an adult male	(Brattain *et al.*, 1981)
HCT116 DNA-PK +/-	HCT116 cells with heterozygous knockout of *PRKDC*, purchased from Horizon Discovery	(Ruis *et al.*, 2008)
HCT116 DNA-PK -/-	HCT116 cells with homozygous knockout of *PRKDC*, purchased from Horizon Discovery	(Ruis *et al.*, 2008)
HCT116 DNA-PK -/-, cDNA re-expression	HCT116 cells with homozygous knockout of *PRKDC* and *PRKDC* re-expressed using cDNA, purchased from Horizon Discovery	(Ruis *et al.*, 2008)

Table 2-1: Cell lines that were used in these studies

* KK47 cells referenced in this paper were stated to have been derived by Taya *et al.* (1977) but the article is in Japanese and a translation is not available. To note, the cell lines used were obtained from academic laboratories and were not submitted for authentication.

2.2.2 *Continuous culture of cell lines*

All cell lines, routinely grown in medium T-75 tissue culture flasks, were split every 3-5 days depending on the growth rate to maintain the cells in the exponential phase of growth and kept at 37 °C in a humidified atmosphere of 95 % (v/v) air and 5 % (v/v) CO_2. Adherent cells were split when the cells reached approximately 70 % confluency. Suspension cells were split to maintain the cell density between 3 x 10^5 and 2 x 10^6 viable cells/ml.

A2780 and A2780-TX1000 cells, CCRF-CEM and CCRF-CEM VCR/R cells and HCT116 cell line panel were all grown in RPMI-1640 medium containing 2 mM L-glutamine supplemented with 10 % (v/v) FBS and 1 % (v/v) penicillin (50 U/ml) – streptomycin (50 µg/ml). The A2780-TX1000 cells were routinely grown in the presence of paclitaxel at a final concentration of 1 µM which was added to the media from a stock of 5 mM paclitaxel. Drug-containing media was removed and replaced by drug-free full media at least 3 days before experiments were carried out. The HCT116 DNA-PK -/-, cDNA re-expression (RE) cells were maintained under antibiotic selection using puromycin (Invitrogen, Paisley, UK) at a final concentration in the media of 2 µg/ml.

M059J and M059J-Fus1 cells, SKOV3 and SKOV3-TR cells, and MDCKII and MDCKII-MDR1 cells were grown in Dulbecco's modified eagles medium (DMEM) containing 2 mM L-glutamine supplemented with 10 % (v/v) FBS and 1 % (v/v) penicillin (50 U/ml) – streptomycin (50 µg/ml). The SKOV3-TR cells were routinely grown in the presence of paclitaxel at a final concentration of 300 nM. Drug-containing media was removed and replaced by drug-free full media at least 3 days before experiments were carried out. The M059J-Fus1 cells were maintained under antibiotic selection using G418 disulfate at a final concentration of 200 µg/ml.

KK47 and KK47A cells were grown in MEM medium supplemented with 1 % (v/v) L-glutamine, 1.5 % (v/v) MEM vitamins solution, 1 % (v/v) MEM non-essential amino acids, 10 % (v/v) FBS and 1 % (v/v) penicillin (50 U/ml) – streptomycin (50 µg/ml).

During routine sub-culturing of adherent cells and for use in experiments, the growth medium was aspirated from the flask and the cells were washed in 1 x PBS. An appropriate volume of 1 x trypsin-EDTA solution (10 x trypsin stock solution diluted in PBS) to cover the cells was added and the cells were incubated for 5 minutes at 37 °C in a humidified atmosphere of 95 % (v/v) air and 5 % (v/v) CO_2. The cells were collected and the trypsin neutralised by the addition of at least an equal volume of cell media

before the cells were collected by centrifugation at 400 x g. Suspension cells were collected and centrifuged before resuspending in fresh media. The passage number was noted on the flask when the cells were recovered from the liquid nitrogen bank and cells were replaced after 30 passages.

2.2.3 Storage and recovery of cells from the liquid nitrogen bank

Before storage in liquid nitrogen, 1×10^6 cells per ml from a 70 % confluent flask were harvested, pelleted and resuspended in their normal growth medium supplemented with 10 % (v/v) DMSO. The HCT116 cells from Horizon were frozen in freezing medium comprised of RPMI 1640 medium with 50 % (v/v) FBS and 10 % (v/v) DMSO. A sample of 1 ml of cell suspension was aliquoted into labelled cryovials and stored for 24 hours at -80 ℃ before being placed in the liquid nitrogen bank for long term storage.

To recover samples from liquid nitrogen storage, the cells were rapidly defrosted by holding the cryovial in a 37 ℃ water bath followed by transfer to a 10 ml universal tube containing 9 ml of pre-warmed normal growth medium. The cells were collected by centrifugation at 400 x g for 5 minutes, the pellet was resuspended in growth medium and transferred to a medium tissue culture flask and the flask incubated at 37 °C in a humidified atmosphere of 95 % (v/v) air and 5 % (v/v) CO_2. The medium was changed after 24 hours to remove any residual DMSO.

The A2780-TX1000 and SKOV3-TR cells were revived in drug-free media for 24 hours before transfer to media containing 1 μM or 300 nM paclitaxel, respectively, for at least 10 days before starting experimental work.

2.2.4 Mycoplasma

Actively-growing cell cultures were routinely tested in-house every 8 weeks for mycoplasma infection using the Mycoalert Mycoplasma detection kit (Cambrex, Berkshire, UK).

2.2.5 Counting cells using a haemocytometer

For routine cell culture experiments, cells were counted using a haemocytometer. A Neubauer haemocytometer (Sigma-Aldrich, Dorset, UK) is a glass slide with two 3 mm^2 mirrored chambers with a laser-etched grid on the lower surface.
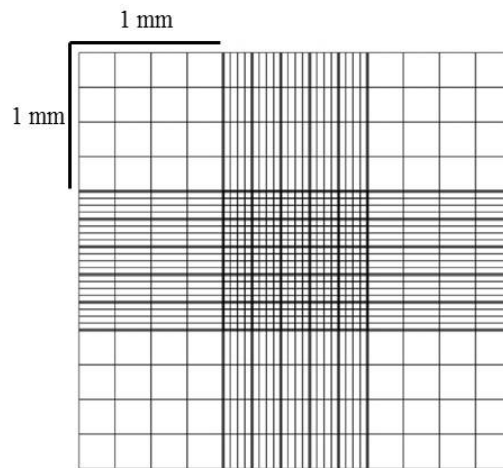
Figure 2-1: Grid layout of a haemocytometer chamber

Each chamber is divided into 9 equal large 1 mm^2 squares which are each subdivided into 16 smaller squares (Figure 2-1). When a cover slip is placed over the chambers, the depth is uniform at 0.1 mm and so the volume of each large square can be calculated as (1 mm x 1 mm) x 0.1 mm = 0.1 mm^3. One mm^3 = 1 µl, hence the number of cells *per* ml can be calculated using the following equation:

$$\frac{Mean\ cell\ count}{Number\ of\ squares} = cells/ml \times 10^4$$

Equation 2-1: Formula for the calculation of the number of cells *per* ml in a cell suspension using a haemocytometer

At least 100 cells were counted from at least 3 large squares and counts were carried out in duplicate.

2.2.6   Counting cells using a Coulter counter

Cells were counted using a Coulter counter during clonogenic cytotoxicity assays. Half a millilitre of cell suspension was added to a Coulter pot, along with 0.5 ml of media (1:2 dilution of cell suspension). Nine ml of Facs Flow (BD Biosciences, Oxford, UK) was added to the Coulter pot (1:20 dilution) and the number of cells in 0.5 ml of the cell suspension were counted using a Beckman Coulter cell counter. Counts were carried out in duplicate and the average count multiplied by 40 gave the cells *per* ml of the original cell suspension. Adherent cells were counted between the size boundaries of 8-24 µm. Suspension cells were counted between 6-21 µm.

2.3   Growth inhibition by XTT assay

2.3.1   *Principle*

The XTT assay measures the metabolic activity of cells. The assay is based on the cleavage of the yellow tetrazolium salt XTT, to form an orange formazan dye, by mitochondrial dehydrogenases, which only occurs in viable, metabolically active cells (Figure 2-2). The orange formazan dye is soluble and is quantified using a spectrophotometer and has a peak absorbance at approximately 450 nm.
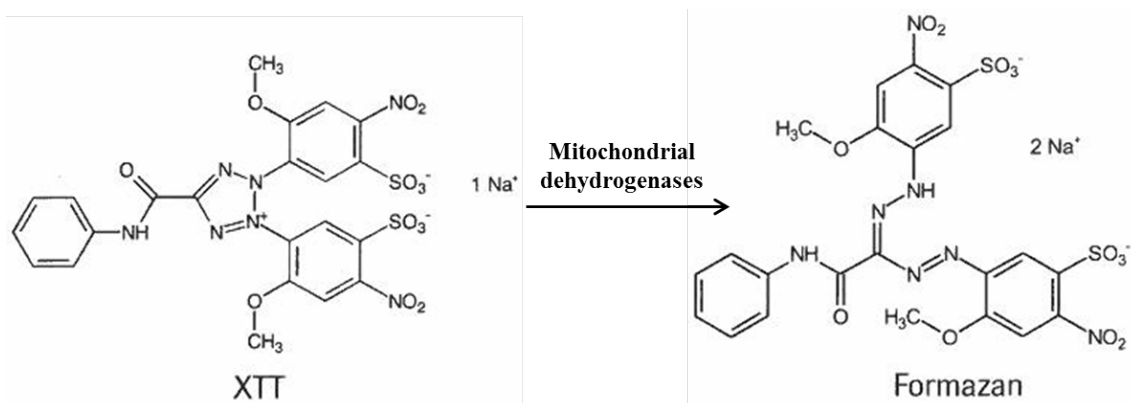
Figure 2-2: Reduction of the yellow tetrazolium salt, XTT, to the orange formazan dye in viable cells

An increase or decrease in the number of living cells can be measured indirectly as an increase or decrease in mitochondrial dehydrogenase activity which is measured as the amount of orange formazan formed.

2.3.2   *Method*

Exponentially growing cells were plated out into a 96 well plate (excluding outer wells) in 90 µl media and incubated for 24 hours at 37 °C in a humidified atmosphere of 95 % (v/v) air and 5 % (v/v) CO_2. PBS (100 µl) was added to the outer wells on three sides of the plate to prevent evaporation of the inner wells and a "blank" lane of 100 µl media was added to the remaining outer wells to allow for background subtraction. Media (10 µl) containing the required drug concentration was added in triplicate and the cells were incubated for a further 72 hours. If the cells were to be treated with ionising radiation, cells were plated out in 100 µl media, incubated for 24 hours and then irradiated with the desired dose before incubating for a further 72 hours.

The XTT assay (Roche, Herts, UK) reagents consisted of XTT labelling reagent (1mg/ml XTT (sodium 3'-[1-(phenylaminocarbonyl)- 3,4-tetrazolium]-bis (4-methoxy-6-nitro) benzene sulphonic acid hydrate in RPMI without Phenol red) and electron coupling reagent (1.25 mM PMS (N-methyl dibenzopyrazine methyl sulphate in phosphate buffered saline). Each 96 well plate required 3.5 ml XTT labelling reagent mixed with 70 µl electron coupling reagent, and 50 µl of this mixture was added to all the cell-containing wells and the media control wells, and the plates were incubated for 4 hours. The absorbance was then measured using a spectrometer at 450 nm at room temperature.

2.3.3   Analysis of results

Results were analysed using GraphPad Prism 6 software (GraphPad Prism Software, CA, USA). Data were normalised to the value for cells with no drug. If inhibitors were used in combination with a drug, data were normalised to the value for cells with inhibitor alone. Two-way analysis of variance (ANOVA) tests were carried out with data from 3 independent experiments to examine whether there was a significant interaction effect between two variables. Growth inhibitory concentration resulting in 50 % growth compared with control was calculated for each separate data set and then a Student's unpaired t-test was used to determine if there was a significant difference between data sets. Differences with a $p < 0.05$ were considered statistically significant.

2.4   Clonogenic assay for adherent cells

2.4.1   Principle

Cytotoxicity was measured by the clonogenic assay for cell survival. This assay examines the ability of a single adherent cell to survive after treatment and form a colony of more than 50 cells. This assay allows cytostatic and cytotoxic effects of drugs and inhibitors to be distinguished, which the XTT assay cannot do.

2.4.2   Method

Adherent cells were seeded into 6 well plates at a density of 1×10^5 cells/ml and left for 24 hours at 37 °C in a humidified atmosphere of 95 % (v/v) air and 5 % (v/v) CO_2. Cells were then treated with compounds or ionising radiation and incubated for the

required length of time. Cells were detached using trypsin as described in Section 2.2.2 and counted using the Coulter counter (Section 2.2.6). Using the cell count obtained, cell suspensions were diluted in an appropriate volume of media in order to produce 50-200 colonies in a 10 cm tissue culture dish. Each cell suspension was plated out in triplicate containing 1, 2 and 4 times the chosen density to ensure that, even at high drug concentrations, colonies would be detected. The plates were then were kept at 37 °C in a humidified atmosphere of 95 % (v/v) air and 5 % (v/v) CO_2 for 10-14 days to allow colony growth, depending on the cell line.

Once the cells had produced colonies of a suitable size to count (>50 cells/colony), the media was aspirated and the colonies were fixed using Carnoy's fixative (3 volumes of methanol (Fisher Scientific, Leicestershire, UK) to 1 volume of acetic acid (BDH, Dorset, UK)) for 5 minutes. The fixative was removed and the colonies were stained with 0.4 % (w/v) crystal violet in water for 5 minutes. The excess stain was removed by gently rinsing the plates in running water and the plates were left to dry overnight. Colonies of > 50 cells were counted using the automated ColCount colony counter (Oxford Optronix, Oxfordshire, UK).

2.4.3   *Analysis of results*

The plating efficiency of control DMSO-treated cells was calculated using Equation 2-2, and this value was used to calculate how many cells should be plated to ensure 50-200 colonies *per* plate.

$$Plating\ efficiency\ (\%) = \frac{Number\ of\ Colonies\ counted}{Number\ of\ cells\ seeded} \times 100$$

Equation 2-2: Calculation of plating efficiency

The cytotoxicity in drug-treated cells was expressed as a percentage of control DMSO-treated cell survival. Graphs were plotted using GraphPad Prism 6 and the drug concentration that was lethal to 90 % of the population (LC_{90}) was calculated. All data are the results of at least 3 independent experiments.

2.5   Methylcellulose clonogenic assay for suspension cells

2.5.1   Principle

The methylcellulose clonogenic assay has the same principle as the adherent cell clonogenic assay (Section 2.4). Methocult semi-solid methylcellulose-based media is used to study the ability of suspension cells to survive and form colonies following treatment.

Methylthiazolyldiphenyl-tetrazolium bromide (MTT) (Sigma) was used to identify and count the colonies. MTT is a yellow compound that is converted to dark blue/purple insoluble formazan crystals by mitochondrial dehydrogenases in viable cells. The solution can evenly distribute throughout the semi-solid methylcellulose and the blue crystals formed in the cells allow the colonies to be seen easily by eye, enabling the counting of colonies without the use of a microscope.

2.5.2   Method

Suspension cells were counted and then seeded in 6 well plates at a density of 1×10^6 cells *per* well. Plates were incubated for 24 hours at 37 °C in a humidified atmosphere of 95 % (v/v) air and 5 % (v/v) CO_2 before treatment with compounds or ionising radiation and then incubation for a further 24 hours. A bottle of Methocult H4230 methylcellulose media (Stemcell Technologies, Grenoble, France) was thawed overnight at 4 °C before use. Gibco Iscove's medium (20 ml) (Life Technologies, Paisley, UK) was added to the 80 ml bottle of Methocult along with 0.5 ml glutamine (1 mM) and the bottle was mixed and then warmed to 37 °C in the incubator.

The cells were transferred to 1.5 ml microfuge tubes, centrifuged for 5 minutes at 1500 rpm, resuspended in fresh full medium and then counted using the Coulter counter (Section 2.2.6). Methylcellulose media (1.5 ml) was transferred to microfuge tubes using a blunt-ended needle (Stemcell Technologies, Grenoble, France) and cells were added at a density selected to result in 50-200 colonies *per* well. Each cell suspension was plated out in triplicate with each containing 1, 2 and 4 times the chosen density. The tubes were vortexed to ensure even cell distribution in the methylcellulose medium, and incubated for 20 minutes to allow any bubbles in the tubes to clear. Using a 5 ml syringe fitted with a blunt-ended needle, 1 ml cell suspension in methylcellulose medium was transferred to each well of a 6 well plate, taking care to avoid introducing bubbles to the wells whilst achieving full well coverage. Plates were incubated for 14 days at 37 °C in a humidified atmosphere of 95 % (v/v) air and 5 % (v/v) CO_2.

To detect the colonies, MTT was diluted to a concentration of 1 mg/ml in PBS and 500 µl was spread evenly over the methylcellulose in each well and incubated for 2 hours to allow diffusion throughout the medium. Colonies were then visible and were counted by eye.

2.5.3 Analysis of results

Analysis was performed as described in Section 2.4.3. Plating efficiency was calculated using Equation 2-2 and cytotoxicity in drug-treated cultures was expressed as a percentage of control DMSO-treated cell survival. The plating efficiency of untreated CCRF-CEM and CCRF-CEM VCR/R cells was approximately 35-40%, which is considered high for a suspension cell line and is only achievable in this cell line with the use of Methocult. Graphs were generated using GraphPad Prism 6 software and the drug concentration that was lethal for 90 % of the population (LC_{90}) was calculated. All data are the results of at least 3 independent experiments.

2.6 Caspase-Glo 3/7 assay

2.6.1 Principle

The Caspase-Glo 3/7 assay measures the activity of caspase-3 and -7 and was obtained from Promega (Southampton, UK). Caspase-3 and -7 are members of the cysteine aspartic acid-specific protease (caspase) family whose activation plays a key role in the execution-phase of apoptosis in mammalian cells (Thornberry *et al.*, 1997). Caspases recognise tetra-peptide sequences and hydrolyse peptide bonds after aspartic acid (D) residues; caspase-3 and caspase-7 share similar substrate specificity by recognising D-x-x-D. The assay provides a luminogenic caspase-3/7 substrate containing the tetra-peptide sequence DEVD, and reagents optimised for caspase activity, luciferase signal and cell lysis. The Caspase-Glo assay contains a buffer and a lyophilised substrate that are mixed and added to cells causing cell lysis and allowing caspase cleavage of the substrate. Caspase substrate cleavage causes the release of aminoluciferin (a luciferase substrate), resulting in luciferase action and a luminescence signal that is proportional to the amount of caspase activity, measured using a luminometer (Figure 2-3).

One disadvantage of the caspase assay is that it relies on the absolute cell number being consistent in all wells, which is not always possible as cell number may change following treatment when compared to control wells.
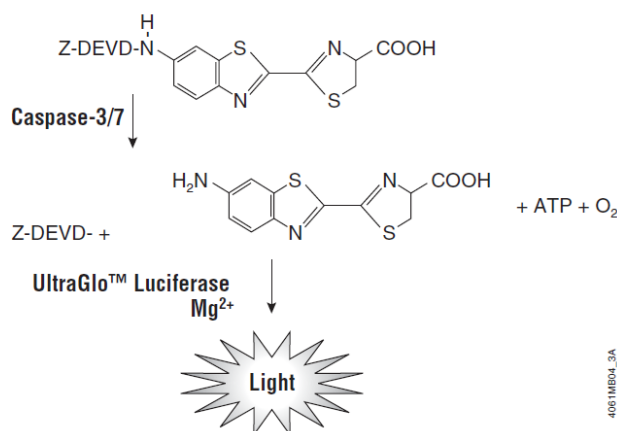
Figure 2-3: Caspase 3/7 cleavage of the luminescence substrate containing the DEVD tetra-peptide sequence.

From: www.promega.co.uk

2.6.2 Method

Cells were counted and 90 µl aliquots of cell suspension were plated in white solid-bottomed 96 well plates (Greiner Bio-One, Stonehouse, UK) and left to incubate for 24 hours at 37 °C in a humidified atmosphere of 95 % (v/v) air and 5 % (v/v) CO_2. Ten µl of the relevant drug treatments were added to wells in duplicate and plates were incubated for the desired length of time. Caspase-Glo 3/7 buffer (2.5 ml) was added to the bottle containing the lyophilised Caspase-Glo 3/7 substrate, and when carrying out this assay with adherent cells, 80 µl of media was removed from each well leaving 20 µl which was mixed with 20 µl of Caspase-Glo reagent following which plates were incubated for 30 minutes. Duplicate wells containing only media with Caspase-Glo reagent were used as blank controls. Luminescence was measured using the FLUOstar Omega luminometer with a gain of 3000. The gain setting was previously optimised to allow maximum sensitivity measurements without saturation of the detector.

2.6.3 Analysis of results

All values were blank-subtracted and data were presented as percentage increase in caspase-3/7 activity compared to untreated control cells. Graphs were plotted using GraphPad Prism 6.

2.7   Protein analysis

2.7.1   Preparation of whole cell extracts

Cell pellets were re-suspended in ice-cold Novagen Phosphosafe extraction reagent (EMD Millipore, MA, USA), supplemented with 25x protease inhibitor cocktail (Roche Diagnostics GMBH, Mannheim, Germany), at a volume of approximately two times the volume of the pellet in a 1.5 ml microfuge tube. Lysates were incubated at room temperature for 5 minutes before being centrifuged at 16,000 x g at 4 °C to pellet the cell debris. The supernatant was transferred to a new microfuge tube and a 5 µl aliquot was removed to be used for protein estimation before the remaining volume was snap frozen and stored at -80 °C.

2.7.2   Quantification of protein using the Pierce protein assay
2.7.2.1 Principle

The Pierce BCA protein assay employs the reagent bicinchoninic acid (BCA) and is used to determine protein concentration in a sample. The first reaction is the reduction of Cu^{2+} to Cu^{+} by peptide bonds in protein, in an alkaline medium, and the reduction of Cu^{2+} is in proportion to the amount of protein in the sample. The second reaction is the chelation of two molecules of BCA with one Cu^{+} ion, which results in the purple-coloured BCA-Cu^{+} complex product that strongly absorbs light at 562 nm and can be measured on a spectrophotometer.

2.7.2.2 Method

The Pierce BCA Protein Assay Kit (Pierce, Thermo Scientific, IL, USA), was used according to the manufacturer's instructions to estimate the protein concentration of whole cell extracts, or nuclear and cytoplasmic fractions. The supplied albumin standard containing 2 mg/ml BSA was used to make standards with final BSA concentrations of 0.2, 0.4, 0.6, 0.8, 1 and 1.2 mg/ml. The unknown samples were diluted 1:10 in dH_2O and 10 µl was added in quadruplicate to a 96 well plate along with the known standards and blanks containing H_2O. BCA reagent A and BCA reagent B were mixed in a ratio of 50:1, respectively. The mixed reagent (190 µl) was added to each well and the plate was incubated at 37 °C in a humidified atmosphere of 95 % (v/v) air and 5 % (v/v) CO_2 for 30 minutes. The absorbance was measured on the FLUOstar Omega spectrophotometer at 570 nm.

2.7.2.3 Analysis of results

A standard curve was created from the absorbance of the standards and the protein concentration of the unknown samples was calculated using the value obtained from the standard curve multiplied by 10 to account for the 1:10 dilution.

2.7.3   SDS-polyacrilamide gel electrophoresis
2.7.3.1 Principle

SDS-PAGE (sodium dodecyl sulphate – polyacrylamide gel electrophoresis) is used to separate proteins and peptides in a sample based on their molecular weights. When a current is applied to a sample containing a mixture of proteins in their native conformation, they migrate to either the anode or cathode depending on their isoelectric point. SDS is an amphiphillic anionic surfactant which denatures proteins and applies an equal negative charge to the unfolded proteins *per* unit mass. This results in all proteins retaining only their primary structures once unfolded and all of the proteins having a strong negative charge and therefore migrating towards the positively charged anode according to their molecular weight.

Polyacrylamide gel is used for the electrophoresis. Bisacrylamide creates cross-links between polyacrylamide molecules creating a gel through which the denatured proteins can pass. The ratio of acrylamide and bisacrylamide determines the size of the pores created in the gel which in turn determines the rate at which the proteins travel based on their molecular weight. A lower percentage of acrylamide results in better resolution of high molecular weight proteins and a higher percentage improving resolution of lower molecular weight proteins. This study investigated both high and low molecular weight proteins (e.g. DNA-PK at 460 kDa and β-actin at 42 kDa) and therefore gradient gels were used, allowing the resolution of both proteins on one gel.

2.7.3.2 Method

Cell lysates, collected as described in Section 2.7.1, were mixed with PBS and 4 x XT sample buffer (Bio-Rad, Hertfordshire, UK) to give 30 µg of total protein *per* well in the gel. The sample buffer contained SDS to denature the proteins and bromophenol blue loading dye. Proteins were denatured by heating the samples to 95 °C for 5 minutes before cooling on ice. Samples were centrifuged briefly to collect any condensation in the tubes. The majority of experiments used pre-cast 3-8 % Criterion Tris-Acetate 18-well polyacrylamide gels (Bio-Rad, Hertfordshire, UK) for electrophoresis. However, when examining MDM2, p53 and p21 levels, 4-20 % tris-glycine gels were used.

HiMark pre-stained molecular weight marker (Life Technologies, Paisley, UK) was loaded into at least 1 well of the 3-8 % gels and Precision Plus protein standard (BioRad, Hertfordshire, UK) was loaded onto the 4-20 % gels, in order to estimate the protein molecular weights in the samples. Tricine running buffer (1x) (BioRad, Hertfordshire, UK) was used with the 3-8 % gels and electrophoresis was carried out at 90 V for 2 hours. MOPS running buffer (1x) (BioRad, Hertfordshire, UK) was used with the 4-20 % gels to fill the BioRad criterion gel tank and electrophoresis was carried out at 150 V for 1 hour.

2.7.4   Western blotting

2.7.4.1 Principle

Western blotting is the process by which proteins are transferred from the polyacrylamide gel to a nitrocellulose protein-binding membrane using an electric current in a transfer buffer. Once the proteins are bound and immobilised, antibodies can be used for immune-detection of specific proteins of interest.

2.7.4.2 Method

The Western blotting apparatus was assembled in accordance to the manufacturer's guidelines (BioRad, Hertfordshire, UK). Fibre pads, 3 mm filter paper (Whatman, GE Healthcare, Amersham, UK) and Hybond C nitrocellulose membrane (GE Healthcare, Amersham, UK) were soaked for at least 10 minutes in 1x Tris-Glycine transfer buffer (Life Technologies, Paisley, UK) just prior to the end of each electrophoresis run. The gel was removed from its plastic cover and also soaked in transfer buffer for 5 minutes before assembly of the Western blotting cassette. The cassette was loaded as shown in Figure 2-4. A small roller was used to remove bubbles from between the different layers.
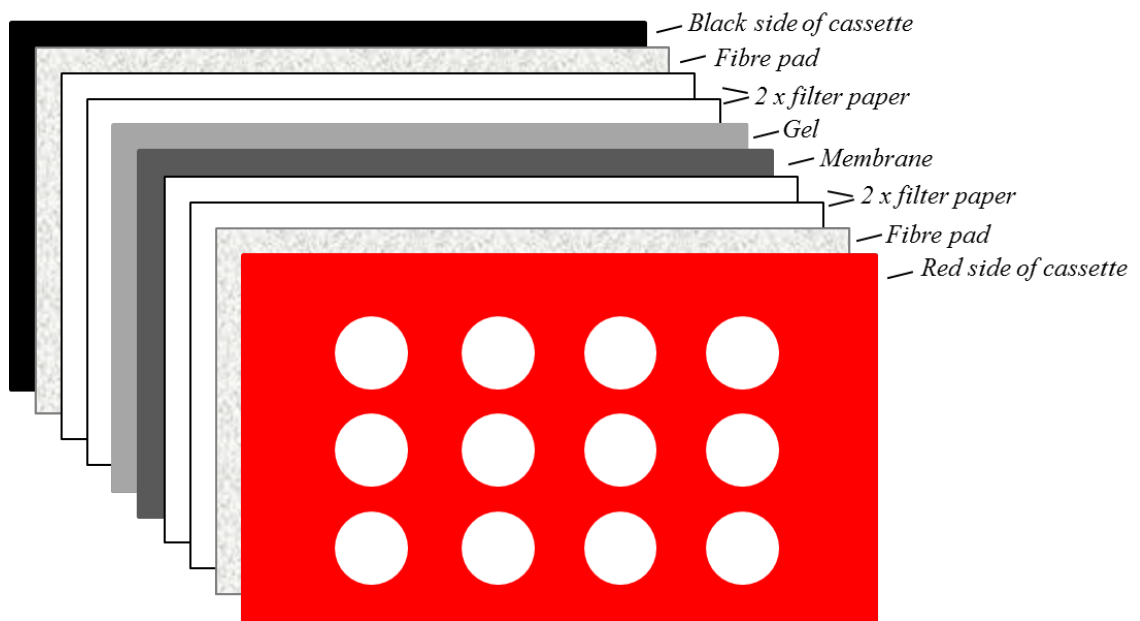
Figure 2-4: Schematic diagram of the assembly of a Western blot cassette

The cassette was loaded into a BioRad transfer tank filled with an ice block and transfer buffer and the proteins were transferred from the gel onto the nitrocellulose membrane using an electric current at 100 V for 45 minutes. The membrane was then removed from the cassette ready for immunodetection.

2.7.5 Immunodetection and enhanced chemiluminescence for protein detection

2.7.5.1 Principle

Proteins can be detected using specific antibodies, which can be selected to detect the total protein or forms of the protein phosphorylated at particular sites. A secondary horse-radish peroxidase (HRP)-conjugated antibody raised against the animal that produced the primary antibody is then used to recognise and bind to the primary antibody.

The enhanced chemiluminescence (ECL) system is robust, highly-sensitive and light-emitting. The HRP that is conjugated to the secondary antibody catalyses the oxidation of luminol resulting in the production of 3-aminophthalate, a reagent that emits light when it decays from the excited to the ground state (Figure 2-5). The amount and location of light emission that HRP catalyses is directly correlated with the location and amount of protein present on the membrane, and the phenol-enhanced luminol reagent in the ECL mix increases the light emission by more than 1000-fold. Light

emission occurs at a wavelength of 428 nm and this light can be captured using autoradiography imaging film.
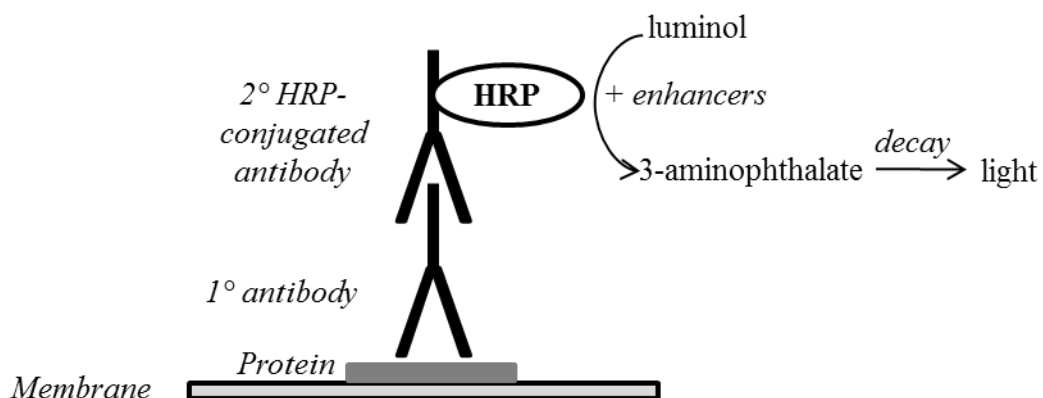
Figure 2-5: Schematic diagram of enhanced chemiluminescence

2.7.5.2 Method

The membrane was blocked for 1 hour in 1x tris-buffered saline (TBS) with 0.05 % (v/v) Tween 20 and 5 % (w/v) bovine serum albumin (BSA) powder. This blocking step reduces non-specific antibody binding on to the membrane, aided by the mild detergent Tween 20. The membranes were then probed using primary antibodies raised against the phosphorylated or total proteins of interest, as described in Table 2-2, and were incubated for the indicated time on a rocker. If overnight incubation at 4 °C was not possible, 4 hours incubation at room temperature was used. The membrane was then washed 3 times for 5 minutes with 0.05 % (v/v) Tween in TBS (TBS-T) before incubating with the specific secondary antibody conjugated with HRP for 1 hour at room temperature on a rocker.

The blots were then washed for 15 minutes in TBS-T followed by 3 further washes for 10 minutes each to remove all unbound antibody. A 1:1 ratio mix of ECL reagents A and B from the ECL kit (GE Healthcare, Amersham, UK) was made and the solution was pipetted directly onto the membrane and left for 2 minutes. Excess ECL reagent was then removed from the blot. Two different methods were used to develop the blots. Firstly, the blot was transferred to an autoradiography cassette and Kodak X-ray film (Wolf Laboratories, York, UK) was used in a dark room with various exposure times to capture the emitted light. The film was developed using a MediPhot 937 film developer (Colenta, Germany) and was digitally scanned to produce an electronic copy. Alternatively, the blot was placed in the Fujifilm LAS 3000 developer (Fujifilm Medical Systems, Stamford, CT, USA) and the image was captured with an appropriate

exposure time. It was also possible to capture an image of a developed X-ray film either through digital scanning or on the Fujifilm LAS 3000 developer to allow quantification.

Target	Species	Details	Dilution	Conditions
pDNA-PK (Ser2056)	Rabbit	Abcam ab18192	1:500	4 °C overnight
pDNA-PK (Thr2609)	Rabbit	Santa Cruz sc-101664	1:500	4 °C overnight
pATM (Ser1981)	Rabbit	R&D Biosciences AF1655	1:500	4 °C overnight
tDNA-PKcs	Mouse	Thermo Shandon MS-370-P	1:100	1 hour room temp.
tATM	Mouse	Abcam ab78	1:1000	1 hour room temp.
Ku70	Mouse	Abcam ab3114	1:2000	4 °C overnight
Ku80	Mouse	Abcam ab3715	1:2000	4 °C overnight
MDR1	Mouse	Santa Cruz sc-13131	1:1000	1 hour room temp.
B-actin	Mouse	Sigma A4700	1:1000	1 hour room temp.
MDM2	Mouse	Calbiochem OP46	1:1000	4 °C overnight
p53	Mouse	Vector VP-P958	1:1000	4 °C overnight
p21	Mouse	Calbiochem OP64	1:200	4 °C overnight
Secondary goat anti-rabbit IgG/HRP	Goat	DAKO P0448	1:1000	1 hour room temp.
Secondary goat anti-mouse IgG/HRP	Goat	DAKO P0447	1:1000	1 hour room temp.

Table 2-2: Antibodies and conditions used in Western blotting. p = phosphorylated, t = total.

2.7.6   *Quantification using Aida Image Analyser*

If quantification of Western blots was required, this was carried out using the Aida Image Analyser version 3.28.001 using the densitometric analysis function. Background measurements were taken and regions of interest were measured with the background subtracted.

2.7.7 Stripping the Western blotting membrane

It was sometimes necessary to strip the bound antibodies from the membrane, allowing the membrane to be re-probed with different antibodies against proteins of a similar molecular weight. To do so, a water bath was set to 55 °C and a box containing 40 ml of stripping buffer (62.5 mM Tris-HCL (pH 6.8), 2 % SDS in water) was pre-warmed in the water bath before the membrane was transferred to the box. β-mercaptoethanol (280 µl) was added in a fume hood and the box was placed in the water bath for 30 minutes. The membrane was removed and washed 3 times for 5 minutes with TBS-T before re-blocking the membrane, as described in Section 2.7.5.2.

2.8 Quantification of single and double-stranded DNA breaks using alkaline Comet assay

2.8.1 Principle

The alkaline Comet assay is a single cell gel electrophoresis technique which allows evaluation of DNA fragmentation associated with DNA damage in cells. The Comet assay measures the ability of cleaved, denatured DNA fragments to migrate out of the nucleus upon the application of an electric field, whereas uncleaved DNA fragments will be trapped within the nucleus. The alkaline Comet assay is sensitive and can be adapted to measure both single and double-stranded DNA breaks along with crosslinks and alkali-labile sites. Following treatment, cells are embedded in agarose gel and lysed, and the DNA is unwound and denatured under alkaline conditions. Low melting point agarose is used which has the optimal pore size to allow solutions to penetrate the agarose gel and reach the cells without disrupting the position of the cells.

The lysed cells are then subjected to an electric current, allowing fragments of DNA to pass out of the nucleus towards the anode, creating a Comet-shaped structure, with undamaged DNA still trapped in the nucleus. The DNA is stained with a fluorescent intercalating dye and the amount of DNA that has passed out of the cell compared to that which is undamaged and still in the nucleus.
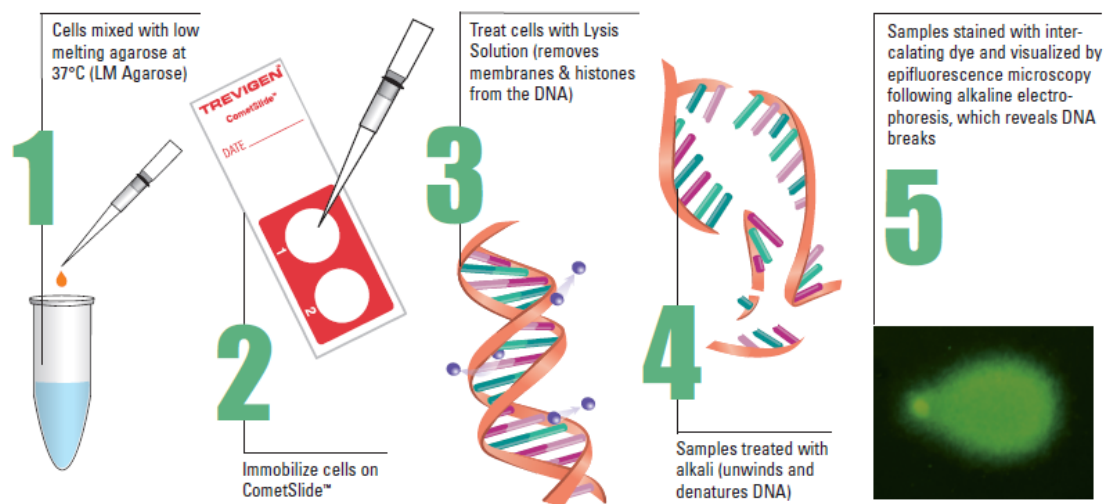
Figure 2-6: Comet assay method

From: www.trevigen.com

2.8.2 Method

Treated cells were harvested, centrifuged and then resuspended in ice-cold PBS at a concentration of 1 x 10^5 cells/ml. Positive control treatments, including mitoxantrone and temozolomide, which are known DNA-damaging agents, were included in each experiment. The reagents for the Comet assay were purchased as a kit from Trevigen (Gaithersberg, MD, USA). The low melting point agarose gel (LM Agarose) was melted in the microwave in 10 second bursts until just melted and then incubated at 37 °C in a water bath. Cells were mixed with the agarose and pipetted onto a Cometslide and then placed at 4 °C for 10 minutes to allow the agarose to gel. Slides were immersed in pre-cooled lysis solution at 4 °C for 30 minutes and then in alkaline unwinding solution (200 mM NaOH, 1 mM EDTA, pH>13) for 30 minutes at room temperature in light-protected conditions. The slides were placed, facing the same direction, in an electrophoresis tank, submersed in alkaline electrophoresis solution (200 mM NaOH, 1 mM EDTA, pH>13) and a current of 300 mA was applied for 40 minutes in light-protected conditions. Slides were washed twice by immersing in dH$_2$O for 5 minutes each and then cells were fixed each time in 70 % (v/v) ethanol for 5 minutes before being left to dry at room temperature overnight. DNA was stained using 100 µl SYBR Green nucleic acid gel stain for 30 minutes at room temperature in light-protected conditions. The excess dye was tapped from the slides and the slides were left to dry at room temperature before microscopic analysis.

2.8.3 Analysis of results by Fluorescence microscopy and quantification of results using Komet 5.5 software

An Olympus BH2-RFCA fluorescence microscope (10x objective) (GX Optical, Suffolk, UK) with Hamamatsu ORCAII BT-1024 cooled CCD camera (Hamamatsu Photonics, Massy, France) were used to view the microscope slides. Image Pro Plus (Media Cybernetics, Bethesda, MD, USA) software was used for image capture. The software package Komet 5.5 (Kinetic Imaging, Nottingham, UK) was used to analyse results. The data were presented using the Olive Tail Moment which takes into account the amount of DNA in the tail (intensity) and the distance of DNA migration (comet tail length).

2.9 mRNA analysis

2.9.1 Principles of quantitative real-time PCR (qRT-PCR)

The polymerase chain reaction (PCR) is designed to quantify mRNA levels and involves converting mRNA into complementary DNA (cDNA). Copies of targeted DNA sections can be synthesised in a three-step procedure of denaturation, primer annealing and elongation in a reaction containing the cDNA, specific primers, deoxyribonucleoside triphosphates (dNTPs) and DNA polymerase. The cDNA is denatured by heating the sample to 95 °C, resulting in single stranded DNA that binds the primers when the sample is cooled to the primer-specific annealing temperature (60 °C for Taqman primers). The primers are designed to bind to sites which flank the target DNA and are complementary to both strands. Once annealed, the primers are then elongated by DNA polymerase and the process repeated for 40 cycles, resulting in amplification of the target sequence.

Quantitative real-time PCR was performed using Taqman gene expression assays (Applied Biosystems, Carlsbad, CA, USA). This assay is a highly quantitative method which relies on an oligonucleotide probe that is bound to the target sequence being cleaved by the 5' endonuclease activity of *Taq* DNA polymerase. The probe consists of a reporter dye, fluorescein (FAM) and a quencher dye (TAMRA). The reporter dye emits fluorescence at a wavelength which is absorbed by the quencher dye until the probe is cleaved by *Taq* DNA polymerase, at which point the reporter dye can emit fluorescence that is detectable upon amplification of the target sequence. Additional

reporter dye molecules are released as the cycles progress and so the fluorescence is proportional to the PCR product.

2.9.2   Preparation of cell extracts

Cells were grown in 6-well plates to 70 % confluency on the day of the experiment. Suspension cells were collected, centrifuged, washed in ice-cold PBS and centrifuged again at 500 x g for 5 minutes in a cooled centrifuge. Adherent cells had the media removed and were washed in ice-cold PBS. Cells were then collected using a cell scraper and centrifuged at 500 x g for 5 minutes in a cooled centrifuge. PBS was removed from cell pellets which were frozen at -20 °C before RNA extraction was carried out the following day.

2.9.3   Extraction of RNA using Qiagen RNeasy Plus Mini Kit

RNA was extracted from the cell pellets using the Qiagen RNeasy Plus Mini kit (Qiagen, West Sussex, UK), as *per* the manufacturer's instructions. Either 350 µl (for adherent cell pellets) or 600 µl (for suspension cell pellets) Buffer RLT Plus was added to the pellet and vortexed for 30 seconds. The suspension was transferred to a gDNA Eliminator spin column placed in a 2 ml collection tube and centrifuged for 1 minute at 8000 x g. The column was discarded and 1 volume (either 350 µl or 600 µl, dependent on the amount of Buffer RLT Plus used) of 70 % (v/v) ethanol was mixed with the flow-through. Up to 700 µl of the flow-through was transferred to a spin column placed in a 2 ml collection tube and centrifuged for 30 seconds at 8000 x g. The flow-through was discarded and 700 µl Buffer RW1 was added to the column which was centrifuged for 30 seconds at 8000 x g. Again the flow-through was discarded and 500 µl Buffer RPE was added to the column which was centrifuged for 30 seconds at 8000 x g. This step was then repeated with centrifugation for 2 minutes at 8000 x g. The spin column was dried by placing it in a new collection tube and centrifugation at full speed for 1 minute. Lastly, the column was placed in a new 1.5 ml collection tube and 30-50 µl RNase-free water was used to elute the RNA by centrifugation for 1 minute at 8000 x g.

2.9.4   RNA concentration and quality determination

The RNA concentration in the samples were determined from 1 µl of sample using the Nanodrop ND-1000 spectrophotometer (Labtech, East Sussex, UK) taking a reading at OD_{260}. The ratio of absorbance at 260 nm and 280 nm assesses the purity of the RNA and it was checked that the ratio was between 1.9 and 2.1 on all occasions.

2.9.5 Reverse transcriptase real time PCR

The reverse transcription (RT) of RNA to cDNA was achieved using the QuantiTect Reverse Transcription Kit (Qiagen, West Sussex, UK). Genomic DNA elimination was the first step and template RNA at a concentration of 1 µg (as calculated from the Nanodrop results) was mixed with 7x gDNA wipeout buffer and made up to 14 µl with RNase-free water. This reaction was incubated at 42 °C for 2 minutes and then placed immediately on ice. The reverse-transcription master mix was prepared amd consisted of 5x Quantiscript RT buffer (containing dNTPs), RT primer mix and (in the positive samples) Quantiscript reverse transcriptase (containing RNase inhibitor). The reaction components were mixed as given in the Table 2-3 below:

Components	Volume *per* reaction
Quantiscript RT buffer, 5x	4 µl
RT primer mix	1 µl
Quantiscript reverse transcriptase	1 µl
Template RNA from genomic DNA elimination reaction	14 µl
Total	20 µl

Table 2-3: Reverse transcription reaction components

A negative control for each sample was also included which consisted of all of the reagents except the reverse transcriptase, in order to detect any contaminations. The reverse transcriptase was replaced with RNase-free water. This reaction mixture was incubated for 30 minutes at 42 °C and then for 3 minutes at 95 °C to inactivate the reverse transcriptase.

2.9.6 Quantitative PCR method

Real-time PCR was carried out on 40 ng cDNA using Taqman gene expression assays for PRKDC (assay ID: Hs00179161_m1), XRCC6 (assay ID: Hs00995282_g1), XRCC5 (assay ID: Hs00221707_m1), ATM (assay ID: Hs00175892_m1), ABCB1 (assay ID: Hs00184500_m1) and β-actin (assay ID: Hs99999903_m1). It was assumed that 1 µg RNA resulted in 1 µg cDNA, and the cDNA was diluted initially 1 in 5 by adding 80 µl water to the 20 µl cDNA from the RT step. A blank control was used containing no cDNA along with a water-only sample. Each PCR well was comprised of the components listed in Table 2-4:

Components	Volume *per* well
Gene expression assay	1 µl
Taqman master mix, 2x	10 µl
RNase free water	5 µl
cDNA (200 ng concentration)	4 µl
Total	**20 µl**

Table 2-4: qRT-PCR reaction components *per* well

Samples were pipetted into a 96-well PCR plate in duplicate (Applied Biosystems, Carlsbad, CA, USA) and the plate was sealed with a plate sealer before being loaded onto the 7500 Fast System (Applied Biosystems, Carlsbad, CA, USA) which employed the following thermal cycler profile: standard 7500 mode, 50 °C – 2 minutes (1 cycle), 95 °C – 10 minutes (1 cycle), then 95°C – 15 seconds and 60 °C – 1 minute (40 cycles). Results were analysed using the 7500 Fast system software and the Δ Δ cycle threshold method (Livak and Schmittgen, 2001) was used to determine gene expression relative to β-actin control. Data were expressed on results graphs as 1/ΔCT.

2.10 Doxorubicin nuclear fluorescence assay

2.10.1 Principle

Dr Chris Hill and Dr David Jamieson in the Newcastle Cancer Centre designed an assay to measure cellular levels of the fluorescent MDR1 substrate doxorubicin (λ_{ex}: 470 nm, λ_{em}: 595 nm) (Hill *et al.*, 2013). The principle behind the assay is that, following treatment, cellular doxorubicin can be visualised using a fluorescent microscope. Cells which overexpress the drug efflux pump, MDR1, will pump out intracellular doxorubicin and therefore will have diminished fluorescence. If MDR1-overexpressing cells are treated with a compound that interferes with drug efflux, effects on cellular doxorubicin can be measured quantitatively by changes in cellular fluorescence.

2.10.2 Method

MDCKII and MDCKII-MDR1 cells were seeded in black, clear-bottomed 96-well plates at a density of 2×10^4 cells *per* well and left to adhere and grow for 3 days. Cells were pre-incubated for 1 hour with varying concentrations of NU7441 (0-10 µM), verapamil (0-10 µM) or cisplatin (10 µM), before a 1-hour incubation with 10 µM

65

doxorubicin. The growth media was removed and the cells were washed twice in PBS before 50 µl of 10% (v/v) formalin in PBS was added for 20 minutes to fix the cells. The formalin was removed and the cells were washed in PBS before 50 µl of 10 µg/ml (v/v) 4',6-diamidino-2-phenylindole (DAPI) and 0.1% (v/v) Triton-X in PBS was added for 20 minutes to permeabilise and stain the cells. The cells were again washed in PBS before a final volume of 200 µl PBS was added to all of the wells and the plates were kept at 4 °C in light-protected conditions until imaged within 24 hours.

2.10.3 Collection and analysis of results

Cells were evaluated for doxorubicin fluorescence using a BD HT Pathway microscope (BD Biosciences, Oxford, UK). Doxorubicin was excited at 488 nm and a 515 nm long-pass filter was used to collect emitted fluorescence greater than 515 nm. The BD HT Pathway software was used to collect arbitrary fluorescence units, using DAPI fluorescence to calculate the area of the cells, from >1000 cells in 3 separate experiments.

2.11   Liquid Chromatography-Mass Spectrometry (LC-MS)

2.11.1 Principle

LC-MS combines two techniques: high-performance liquid chromatography (HPLC) and mass spectrometry (MS) to separate and detect compounds in a sample.

HPLC is a separation technique that permits the resolution of a mixture of analytes and involves passing a sample through an HPLC column that is packed with small particles. The individual components of the sample are introduced to the column by a mobile phase and are separated depending on their chemical interactions with the stationary phase. The elution of the components can be controlled by altering the gradient conditions of the mobile phase. The column used in this study was a reverse phase Phenomenex Luna 3 µm C8 (2), 50 mm x 2 mm, (PNo. 00B-4248-B0, Phenomenex, UK) in which the stationary phase is comprised of silica particles of 3 µm in diameter attached to C8 carbon units.

A mass spectrometer works by analysing the eluent mixture from the HPLC column, after ionisation, to detect the presence of compounds of interest by their mass. On its passage through the instrument molecules are fragmented in a collision cell using

high pressure nitrogen, resulting in the formation of specific fragments of the parent compound which are detected and quantified.

2.11.2 Preparation of cells for LC-MS

CCRF-CEM and CCRF-CEM VCR/R cells were seeded into 6 well plates for 24 hours at a density of 1 x 10^6 cells/ml. The cells were then incubated for 1, 8 or 24 hours in the presence of vincristine at equitoxic GI_{50} concentrations (1 nM for CCRF-CEM cells and 1 µM for CCRF-CEM VCR/R cells) alone or in the presence of 1 µM NU7441, NU7742, DRN1, DRN2 or verapamil. Cells were collected, centrifuged for 5 minutes and washed in PBS twice to remove all trace of media. 400 µl methanol was added to the cells which were then centrifuged at 16,000 x g for 5 minutes to permeabilise the cells and allow the intracellular drug to pass out of the cells into the methanol. The methanol solution was transferred to glass vials and stored at -20 °C until analysed by LC-MS. Vinblastine was used as the internal standard for the assay and was added to the glass vials to give a final concentration of 50 ng/ml.

2.11.3 Method

Samples were analysed using an LC-MS assay validated in-house based on a previously described method (Israels *et al.*, 2010) and fully described in Mould *et al.* (2014). An API4000 LC/MS/MS (Applied Biosystems, USA) was used for analysis, with an LC-200 Micro pump, autosampler and Peltier column oven (Perkin Elmer, UK). The analytical column used was a Phenomenex Luna 3 µm C8 (2) 50 mm x 2 mm column (PNo. 00B-4248-B0, Phenomenex, UK) maintained at 30 °C. Elution of the analytes was performed with mobile phases of 0.02 M ammonium acetate pH 5 (pump A) and 100% methanol (pump B). The analysis was performed using the gradient shown in Table 2-5, at a flow rate of 400 µl/min, and an injection volume of 10 µl.

Step	Total Time (min)	A (%)	B (%)
0	0.0	80	20
1	2.0	80	20
2	7.0	10	90
3	7.5	80	20
4	11.0	80	20

Table 2-5: Gradient conditions of the HPLC mobile phase

Atmospheric pressure chemical ionisation was performed in positive ion mode using nitrogen gas with the following optimum settings: collision gas, 9; curtain gas, 10; ion source gas 1, 21; ion source gas 2, 45 (settings in Table 2-6). The temperature of the heated nebuliser was 450 °C.

Analyte	Retention time (min)	Q1 mass (Da)	Q3 mass (Da)	Declustering potential	Entrance potential	Collision energy	Collision exit potential
Vincristine	6.58	825.4	765.4	101	10	49	26
Vinblastine	6.85	811.4	355.3	161	10	49	10
Verapamil	6.37	455.2	164.7	91	10	41	10
NU7441	7.64	414	247.1	91	10	67	6
NU7742	7.76	412.2	303.2	86	10	59	10

Table 2-6: Mass transitions and optimised MS/MS parameters for vincristine analysis

2.11.4 Analysis of results

Analyst software v1.5 (AB SCIEX, USA) was used for sample analysis, peak integration and analyte quantitation. Additional CCRF-CEM and CCRF-CEM VCR/R cells were collected and counted at the time of collection of the samples. The results were then calculated as vincristine accumulation *per* 1×10^6 cells and then represented on the graphs as the fold change in vincristine concentration measured compared to levels following vincristine treatment alone.

2.12   Confocal Microscopy

2.12.1 Principle

Microscopy was used to examine the intracellular location of a number of proteins and the effects of treatments on their activation and localisation. Confocal microscopy employs laser point scanning and so allows the capture of sharper and clearer images than obtainable with a standard fluorescent microscope.

2.12.2 Preparation of cells

Coverslips (22 mm) (VWR International, Pennsylvania, USA) were immersed in methanol to sterilise them and left for 20 minutes to dry. They were then submerged in

poly L-lysine solution for 10 minutes, washed 3 times in sterile deionised water and left to dry leaning against the sides of petri dishes for 2 hours.

HCT116 cells were grown in 6-well plates on poly L-lysine-coated coverslips at a density of 1.5 x 10^5 *per* well. Cells were left to adhere for 24 hours at 37 °C in a humidified atmosphere of 95 % (v/v) air and 5 % (v/v) CO_2, and then treated with ionising radiation or vincristine and incubated for a further 24 hours.

2.12.3 Fixation and permeabilisation

Cell media was carefully aspirated from the wells and the cells were fixed by adding 4 % (w/v) paraformaldehyde in PBS for 10 minutes on ice. The coverslips were rinsed in PBS and the cells were permeabilised using KCM-T buffer (0.1 % (v/v) Triton X-100 in KCM buffer (120 mM KCl, 20 mM NaCl, 10 mM Tris-HCl, pH 8.0, 1 mM EDTA)).

2.12.4 Staining and immunodetection

The coverslips were carefully removed from the 6-well plates and placed cell-side-up on a strip of parafilm in a large petri dish. The fixed cells were blocked with 400 µl of blocking solution containing 2 % (w/v) bovine serum albumin, 10 % (w/v) dried milk powder in KCM-T buffer for 1-2 hours at room temperature.

The blocking buffer was carefully removed from the coverslips and replaced with 200 µl of primary antibody mix (diluted in blocking buffer). Strips of wet tissue paper were placed in the petri dishes to maintain a humid environment and the petri dishes were stored overnight at 4 ºC.

Immunostaining was performed using the antibodies detailed in Table 2-7 against the following proteins at 4 °C overnight diluted in blocking buffer: phosphorylated DNA-PKcs (pT2609 and pS2056), total DNA-PKcs, PLK1, α-tubulin and γ-tubulin.

Target	Species	Details	Dilution	Conditions
pDNA-PK (Ser2056)	Rabbit	Abcam ab18192	1:100	4 °C overnight
pDNA-PK (Thr2609)	Rabbit	Abcam ab4194	1:100	4 °C overnight
tDNA-PK	Mouse	Thermo Shanden MS-370-P	1:200	4 °C overnight
PLK1	Mouse	Abcam ab17057	1:200	4 °C overnight
α-tubulin	Rabbit	Abcam ab18251	1:200	4 °C overnight
γ-tubulin	Mouse	Abcam ab11316	1:200	4 °C overnight
Secondary Alexa-Fluor 488 goat anti-rabbit IgG	Goat	Life Technologies A11034	1:200	1 hr room temp.
Secondary Alexa-Fluor 594 goat anti-mouse IgG	Goat	Life Technologies A11034	1:200	1 hr room temp.

Table 2-7: Antibodies and conditions used in immunofluorescence throughout this study

The coverslips were then returned to the 6-well plates and washed 3 times in KCM-T buffer and moved to a fresh piece of parafilm before incubation with 200 µl Alexa Fluor 488 goat anti-rabbit antibody and Alexa Fluor 594 goat anti-mouse antibody diluted in blocking buffer for 1 hour in light-protected conditions at room temperature. Excess secondary antibody mix was removed by washing as before in subdued light. Microscope slides (Leica Microsystems, Buckinghamshire, UK) were labelled and 10 µl 4',6-diamidino-2-phenylindole (DAPI) in Vectashield mounting solution (Vector Laboratories Inc, Burlingame, CA, USA) was added to the slides. DAPI produces a blue fluorescence when bound to DNA, with excitation at 360 nm and emission at 460 nm. The coverslip was removed from the KCM-T buffer and excess buffer was removed by dabbing the edges of the coverslips on tissue paper before placing cell-side-down in contact with the DAPI solution. Excess DAPI was blotted from the slides and, once dried, the coverslips were sealed to the slide using clear nail varnish. Slides were kept at 4 °C in light-protected conditions until ready to be viewed.

2.12.5 Detection using Zeiss LSM 700 confocal microscope

Microscope images were obtained on a Zeiss LSM 700 confocal microscope using a 40x objective and higher magnification images were obtained with a 63x objective with oil immersion. The DAPI fluorescence dye was detected at 455 nm (coloured blue in the images), the goat anti-rabbit antibody fluorescence dye was detected at 488 nm

(coloured green in the images) and the goat anti-mouse antibody fluorescence dye was detected at 594 nm (coloured red in the images).

Chapter 3: The effects of the DNA-PK inhibitor NU7441 and the ATM kinase inhibitor KU55933 on the growth inhibitory and cytotoxic activities of microtubule-targeting agents in paired parental and multidrug-resistant cell lines

3.1   Introduction

DNA-PK and ATM are well-characterised DNA double-strand break repair enzymes that play essential roles in non-homologous end-joining (NHEJ) and homologous recombination (HR), respectively. However, DNA-PK and ATM have recently been found to have roles outside of DNA repair that are less well characterised, as discussed in detail in Chapter 1. ATM has been more widely studied and has been found to have roles in mitotic spindle structure and the spindle assembly checkpoint (Oricchio *et al.*, 2006; Palazzo *et al.*, 2014), although DNA-PK has been found to have roles in preventing spindle disruption and mitotic catastrophe, and ensuring chromosomal stability (Shang *et al.*, 2010; Shang *et al.*, 2014). NU7441 and KU55933 are potent, selective and well characterised inhibitors of DNA-PK and ATM, respectively (Hickson *et al.*, 2004; Leahy *et al.*, 2004).

Prior to the commencement of this study, a Masters project was carried out which led to two interesting conclusions (NJ Tan, unpublished results). Firstly, it was noted that CCRF-CEM leukaemia cells could be sensitised not only to DNA-damaging agents by NU7441 and KU55933, but also that small but significant sensitisation was seen with the microtubule-targeting agent vincristine (work carried out by NJ Tan, some of these data are included in Mould *et al.* (2014)). Secondly, the vincristine-resistant CCRF-CEM VCR/R cells, which were resistant to vincristine, doxorubicin and etoposide, were sensitised to these agents to a much greater degree by NU7441 than the parental CCRF-CEM cells. In the current study, the CCRF-CEM and CCRF-CEM VCR/R cell line pair, along with three other paired sensitive and resistant cell lines, were used to investigate whether DNA-PK or ATM inhibition can sensitise parental and multidrug-resistant cells to microtubule-targeting agents, in order to establish the generality of the initial observations in the CCRF-CEM cell line pair.

The multidrug-resistant sublines were all established by exposure of the parental cell line to increasing concentrations of drug over a prolonged period of time, thereby selecting for resistant cells. In relation to vincristine- and paclitaxel-resistant cell lines, there are two main ways that cells can become resistant; the development of tubulin modifications and overexpression of drug efflux transporters, for example MDR1. As the initial experiments were carried out with CCRF-CEM leukaemia cells and the vincristine-resistant CCRF-CEM VCR/R cells, which grow in suspension, further cell lines selected were adherent solid tumour cell lines (ovarian A2780 and SKOV3 cells) and MDR1-mediated resistant paired cell lines generated by exposure to a taxane

(paclitaxel-resistant A2780-TX1000 and SKOV3-TR cells). The bladder cancer KK47 and KK47A cell line pair, although not displaying the same level of MDR1-mediated resistance as seen in the other multidrug-resistant cell lines, were used as a model of resistance developed by exposure to a non-microtubule-targeting cytotoxic agent; in this case doxorubicin (Kimiya *et al.*, 1992).

Phosphorylation of DNA-PK and ATM was used in the studies described in this chapter as a measure of activity in response to both DNA- and non-DNA-damaging agents. Enzyme activation was measured by investigation of autophosphorylation sites on both DNA-PK and ATM, which are known to be activated by DNA-damaging agents and essential for DNA-PK and ATM function in their respective DNA repair pathways.

DNA-PK kinase activity has been demonstrated to be essential for functional NHEJ (Kurimasa *et al.*, 1999). Numerous phosphorylation sites have been identified on DNA-PK and many studies use threonine 2609 phosphorylation as a measure of DNA-PK activity. However, ATM was found to be essential for phosphorylation of the DNA-PK threonine 2609 site (Chen *et al.*, 2007). Autophosphorylation on DNA-PK serine 2056 is essential for DNA double-strand break repair by NHEJ, as demonstrated by S2056A mutation resulting in compromised NHEJ and radiation resistance (Chen *et al.*, 2005). Importantly, phosphorylation at S2056 is ATM-independent (Chen *et al.*, 2005) and no other kinases have been shown to mediate phosphorylation at this site other than DNA-PK itself. Therefore, DNA-PK serine 2056 autophosphorylation was used to measure DNA-PK activation in this study.

There are 5 reported sites of ATM autophosphorylation in response to DNA damage. The most characterised is the serine 1981 site contained within the FRAP-ATM-TRRAP (FAT) domain, and phosphorylation at this site is necessary for the dissociation of the inactive ATM dimer into active monomers (Bakkenist and Kastan, 2003). The serine 1981 site is commonly used as a measure of ATM activity because rapid phosphorylation occurs in response to DNA damage, and therefore this site was investigated in the current study.

3.2   Aims

Following observations that CCRF-CEM and CCRF-CEM VCR/R cells could be sensitised not only to DNA-damaging agents but also to vincristine by the DNA-PK

inhibitor NU7441 and the ATM inhibitor KU55933, and that sensitisation was much greater in the vincristine-resistant CCRF-CEM VCR/R cells, sensitisation and DNA-PK and ATM expression and phosphorylation was examined in other paired cell lines. Four different paired sensitive and multidrug-resistant cell lines were characterised by PCR and Western blotting, and examined using growth inhibition and clonogenic survival assays following treatment with vinca alkaloids or taxanes. Sensitisation was examined using NU7441 and KU55933. NU7441- and KU55933-induced inhibition of DNA-PK and ATM autophosphorylation, respectively, was evaluated by Western blot in response to DNA-damaging ionising radiation, and DNA-PK and ATM phosphorylation in response to vincristine treatment was investigated, in the CCRF-CEM and CCRF-CEM VCR/R cells. The Caspase Glo assay, which measures caspase 3/7 activity, was used to study cell death in response to vincristine, paclitaxel or docetaxel alone or in combination with NU7441. Previous studies have demonstrated that NU7441 and KU55933 cause sensitisation to DNA-damaging agents and studies were performed to measure DNA-strand breaks following vincristine and docetaxel treatment using the COMET assay.

3.3   Results

3.3.1   *Characterisation of the cell lines*

The preliminary data for this project were generated using CCRF-CEM cells and their multidrug-resistant counterpart, CCRF-CEM VCR/R cells. Therefore this cell line was used along with three other paired drug sensitive and multidrug-resistant cell lines (Table 2-1). The cell lines were chosen to represent solid and haematological cancers made resistant to the microtubule-targeting agents vincristine or paclitaxel, or to doxorubicin, through exposure to increasing concentrations of drug. In each case resistance was known to be due to overexpression of the drug-efflux transporter, MDR1.

Initially, cell lines were characterised for basal levels of expression (mRNA and/or protein) of key genes. The CCRF-CEM and CCRF-CEM VCR/R cell lines (Figure 3-1) express autophosphorylated DNA-PK and ATM, as detected by probing the Western blot with antibodies for autophosphorylation sites on these proteins (pDNA-PK (Ser2056) and pATM (Ser1981)). The CCRF-CEM VCR/R cells have higher levels of total and phosphorylated DNA-PKcs and ATM protein, but this higher

expression was not observed at the mRNA level, where the levels were similar for both cell lines (Figure 3-4A). As expected, CCRF-CEM VCR/R cells displayed clear overexpression of MDR1 as detected at the mRNA (p=0.0005) and protein level (Figure 3-1, Figure 3-4).
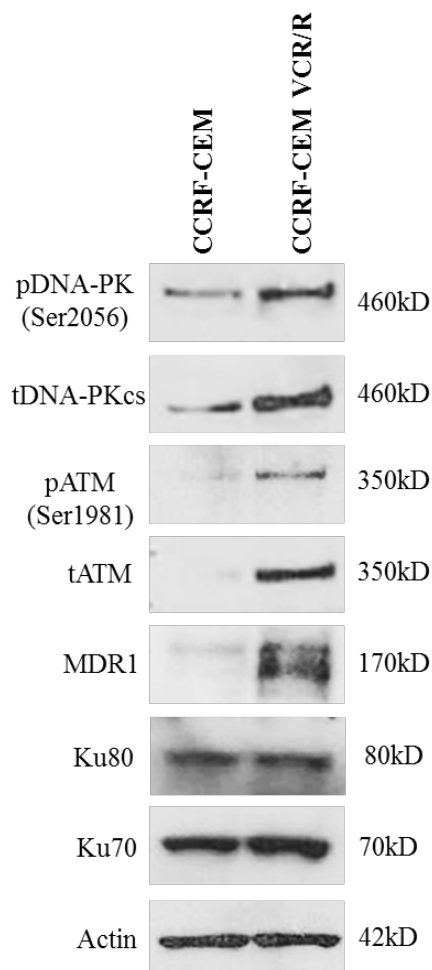
Figure 3-1: Characterisation of CCRF-CEM and CCRF-CEM VCR/R cells by protein expression. CCRF-CEM and CCRF-CEM VCR/R cell lysates were prepared from exponentially-growing cells and phosphorylated DNA-PK (pDNA-PK (Ser2056)), total DNA-PK (tDNA-PKcs), phosphorylated ATM (pATM (Ser1981)), total ATM (tATM), MDR1, Ku80, Ku70 and actin expression was determined by Western blotting using the indicated specific antibodies (Section 2.7.4). Data are representative of 3 independent experiments.

The A2780 and A2780-TX1000 cells express similar levels of DNA-PKcs and ATM mRNA and there is no difference in the protein levels of DNA-PKcs in these cells; a pattern also observed in the paired SKOV3 and SKOV3-TR cells (Figure 3-2, Figure 3-4B and C). Again as expected, both the A2780-TX1000 cells and the SKOV3-TR cells overexpress MDR1 at both the mRNA and the protein levels. KK47A have

previously been shown to overexpress MDR1 (Hasegawa *et al.*, 1995) and there was no difference in total DNA-PKcs levels between the KK47 and the KK47A cells (Figure 3-3).
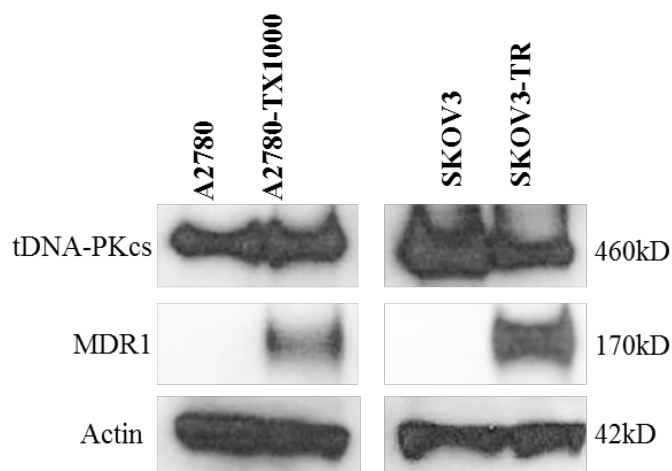
Figure 3-2: Characterisation of A2780 and A2780-TX1000 cells and SKOV3 and SKOV3-TR cells by protein expression. A2780 and A2780-TX1000 and SKOV3 and SKOV3-TR cell lysates were prepared from exponentially-growing cells and total DNA-PK (tDNA-PKcs), MDR1 and actin expression was determined by Western blotting using the indicated specific antibodies (Section 2.7.4). Data are representative of 3 independent experiments.
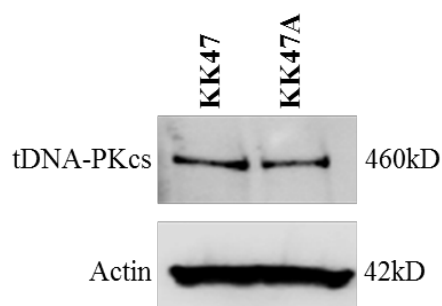
Figure 3-3: Characterisation of KK47 and KK47A cells by protein expression. KK47 and KK47A cell lysates were prepared from exponentially-growing cells and total DNA-PK (tDNA-PKcs) and actin expression was determined by Western blotting using the indicated specific antibodies (Section 2.7.4). Data are representative of 3 independent experiments. KK47 cell work carried out during EM MRes project.
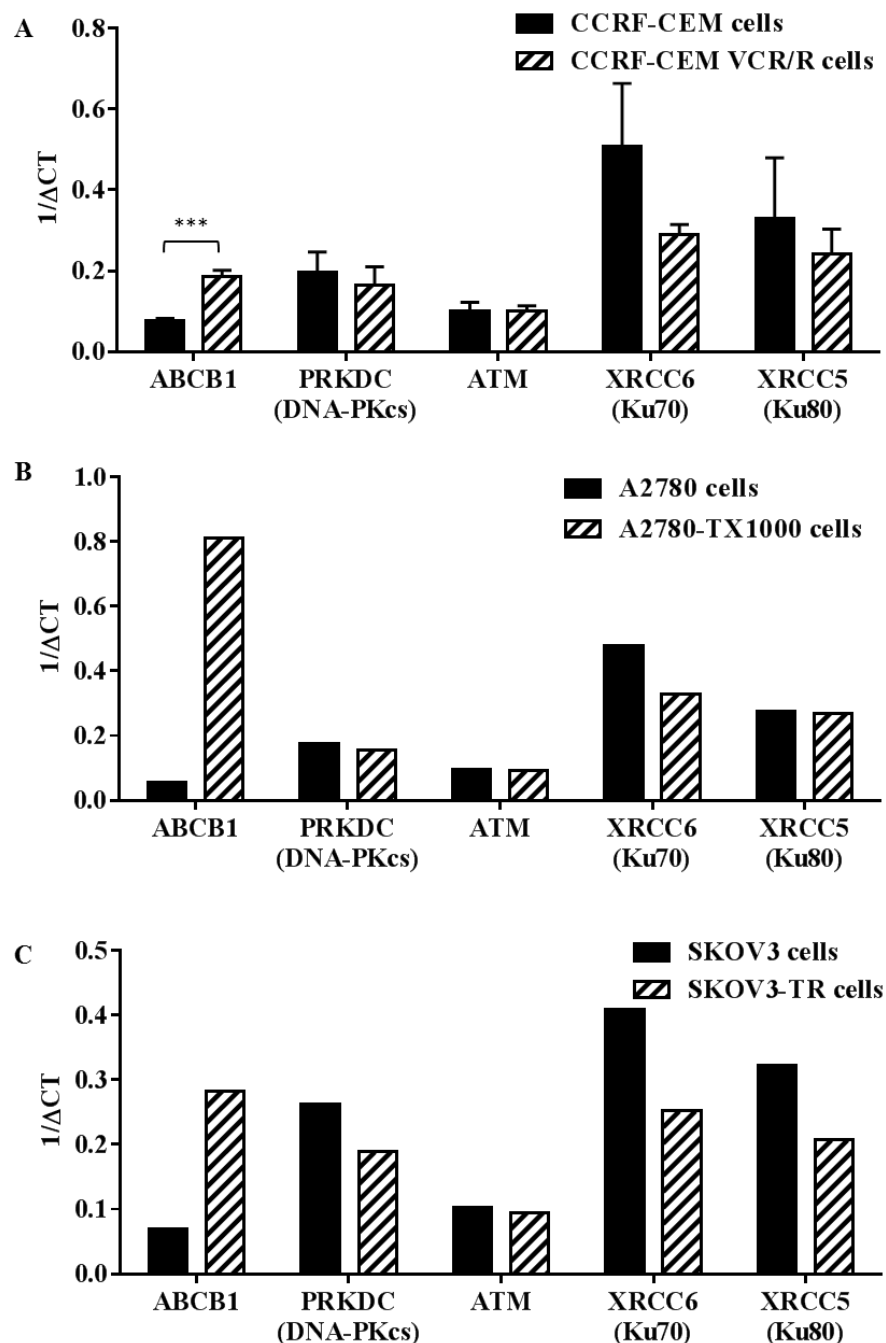
Figure 3-4: Characterisation of (A) CCRF-CEM and CCRF-CEM VCR/R cells, (B) A2780 and A2780-TX1000 cells and (C) SKOV3 and SKOV3-TR cells by mRNA expression. Cell pellets were prepared from exponentially-growing cells and ABCB1, PRKDC, ATM, XRCC6, XRCC5 and β-actin mRNA expression was determined by real-time quantitative PCR using the indicated gene expression assays (Section 2.9.5). The cycle threshold (CT) value was determined by 7500 Fast RT PCR system and data are presented as $1/\Delta CT$ relative to β-actin. Results for CCRF-CEM and CCRF-CEM VCR/R cells are mean ± standard error of three independent experiments, each using duplicate samples. Significant differences between CCRF-CEM and CCRF-CEM VCR/R cells were evaluated using an unpaired *t*-test. Asterisk indicates a statistically significant difference (* *p<0.05*, ** *p<0.01*, *** *p<0.001*). Results for A2780 and A2780-TX1000 cells and SKOV3 and SKOV3-TR cells are mean results of duplicates in 1 experiment.

The p53 status of the parental and multidrug-resistant cell lines was established because cells that become resistant to drug treatment can develop p53 mutations. The parental SKOV3 cells are known to have a *TP53* homozygous mutation (COSMIC, 2014) and the KK47 and KK47A cells both have wild-type functional p53, as previously demonstrated by Shirakawa *et al.* (2001).

SJSA1 osteosarcoma cells were used as a positive control as it is known that they have wild type p53, overexpress MDM2 and display a p53 wild-type response to the MDM2-inhibitor Nutlin-3 (Arva *et al.*, 2008). P53 promotes MDM2 transcription and MDM2 acts as an inhibitor of p53 stability and function, and Nutlin-3 inhibits the interaction between p53 and MDM2 by binding to MDM2 in the p53 binding pocket, therefore enhancing and prolonging p53 transcriptional activity. Cells were therefore treated with 0, 1 and 10 µM Nutlin-3 to examine whether they exhibit a wild-type p53 response.

For SJSA1 cells, as shown in Figure 3-5, only 10 µg of protein was loaded onto the gel because this cell line overexpresses MDM2. In SJSA1 cells p53 induction was observed in response to Nutlin-3 treatment and, as expected, MDM2 expression also increased, along with p21, which is a downstream marker of p53 function.

However, in the CCRF-CEM and CCRF-CEM VCR/R cells, there were very high, constant levels of p53 protein detected, even in untreated cells, but no MDM2 or p21 expression, indicating that p53 is non-functional in this cell line. This result is consistent with the mutation data for the CCRF-CEM cell line in the COSMIC database which lists two heterozygous mutations in the *TP53* gene (COSMIC, 2014).

In contrast to CCRF-CEM cells, A2780 cells have no *TP53* mutations listed in the COSMIC database and a Nutlin-3 concentration-dependent induction of p53, MDM2 and p21 expression was seen; similar to that observed in the SJSA1 cells (Figure 3-6). However, untreated A2780-TX1000 cells had higher levels of p53 when compared with A2780 cells, and there was no induction of p53, MDM2 or p21 observed in this cell line following Nutlin-3 treatment, suggesting that A2780-TX1000 cells may have aquired a p53 mutation. To confirm this suggestion, the A2780-TX1000 cells were submitted for *TP53* next generation sequencing (NewGene, Newcastle upon Tyne, UK) and it was confirmed that this cell line was *TP53* mutant with a deletion in exon 4 (delATGGATG).
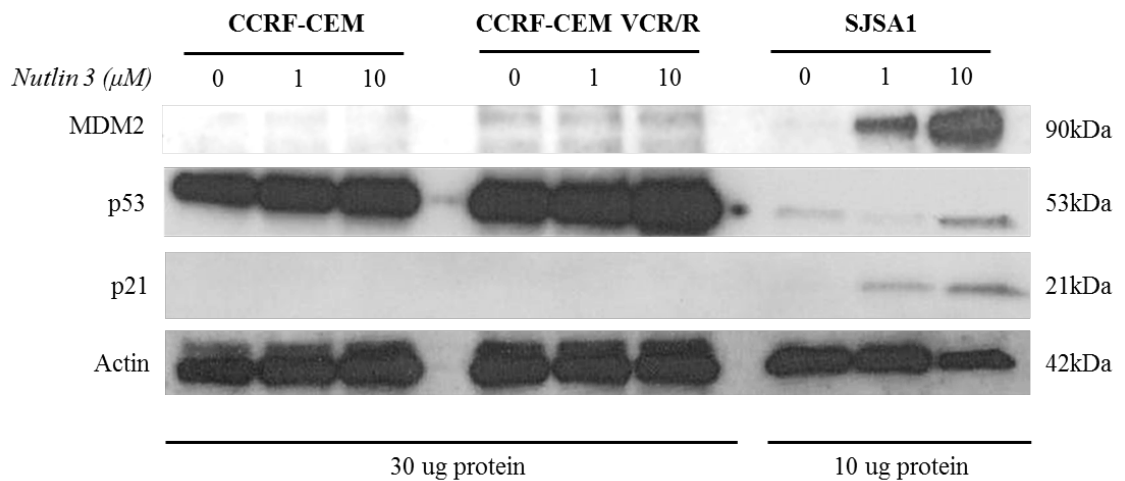
Figure 3-5: CCRF-CEM and CCRF-CEM VCR/R cells have non-functional p53.
CCRF-CEM and CCRF-CEM VCR/R cells were treated with 0, 1 or 10 µM Nutlin-3 for 8 hours. SJSA1 cells were used as a p53 wild-type positive control cell line (10 µg protein loaded). Cell lysates were prepared, 30 µg protein loaded onto the gel and MDM2, p53, p21 and actin expression was determined by Western blotting using the indicated specific antibodies (Section 2.7.4). X-ray film exposure time varied depending on the intensity of signal. Data are representative of 3 independent experiments.
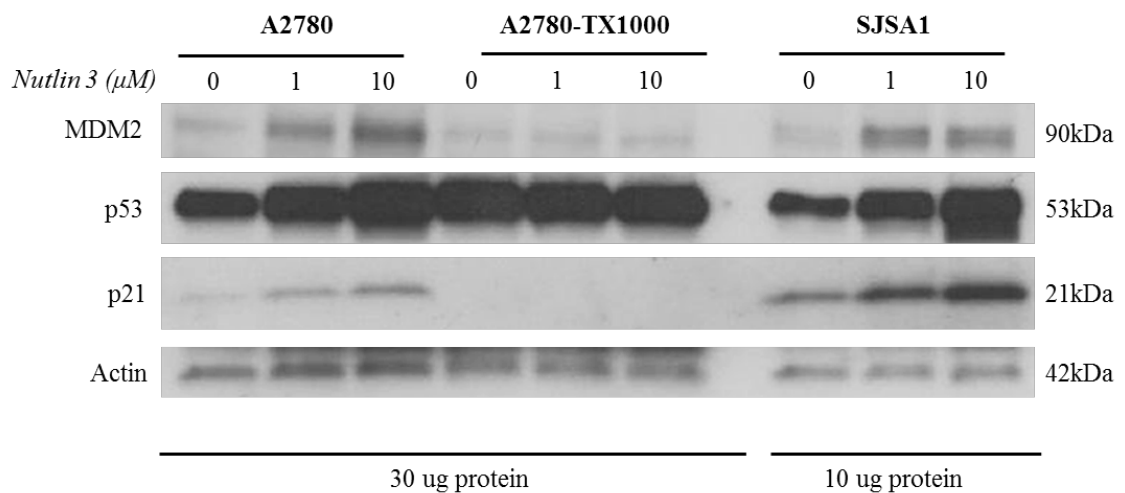
Figure 3-6: A2780 cells have functional p53 but A2780-TX1000 cells have non-functional p53. A2780 and A2780-TX1000 cells were treated with 0, 1 or 10 µM Nutlin-3 for 8 hours. SJSA1 cells were used as a p53 wild-type positive control cell line (10 µg protein loaded). Cell lysates were prepared, 30 µg protein loaded onto the gel and MDM2, p53, p21 and actin expression was determined by Western blotting using the indicated specific antibodies (Section 2.7.4). X-ray film exposure time varied depending on the intensity of signal. Data are representative of 3 independent experiments.

80

3.3.2 *Inhibition of DNA-PK and ATM by NU7441 and KU55933, respectively, in CCRF-CEM cell lines*

The inhibitory activity of NU7441 and KU55933 against their target enzymes was investigated in the CCRF-CEM and CCRF-CEM VCR/R cell lines. DNA damage was induced using 10 Gy of ionising radiation and inhibition of autophosphorylation at DNA-PK serine 2056 or ATM serine 1981, following pretreatment with increasing concentrations of NU7441 or KU55933, respectively, was investigated.

Figure 3-7 shows DNA-PK inhibition induced by NU7441 in both the CCRF-CEM and CCRF-CEM VCR/R cells. The Western blot reveals higher basal levels of phosphorylated DNA-PK (Ser2056) in the CCRF-CEM VCR/R cells, as observed previously (Figure 3-1). DNA-PK was autophosphorylated in response to 10 Gy ionising radiation in both cell lines and a concentration-dependent inhibition of autophosphorylation was observed with NU7441. The graphs were generated by densitometry quantification of 3 independent Western blots, with the phosphorylated DNA-PK normalised to actin in each sample, and then plotted as % inhibition of phosphorylated DNA-PK compared to that observed with 10 Gy IR alone. The concentration that caused 50 % phosphorylated DNA-PK inhibition (IC_{50}) is displayed on the graphs for each cell line, and IC_{50} values in both cell lines are similar (0.25 µM in CCRF-CEM cells (Figure 3-7B), 0.46 µM in CCRF-CEM VCR/R cells (Figure 3-7C)). These IC_{50} values are similar to the value of 0.3 µM NU7441 previously determined in K562 cells (Tavecchio *et al.*, 2012). NU7441 was used at 1 µM in subsequent experiments as this concentration is greater than the IC_{50} of both CCRF-CEM and CCRF-CEM VCR/R cells, and 1 µM has previously been shown to be the optimal concentration for DNA-PK inhibition without NU7441 causing cellular toxicity (Zhao *et al.*, 2006; Tavecchio *et al.*, 2012).
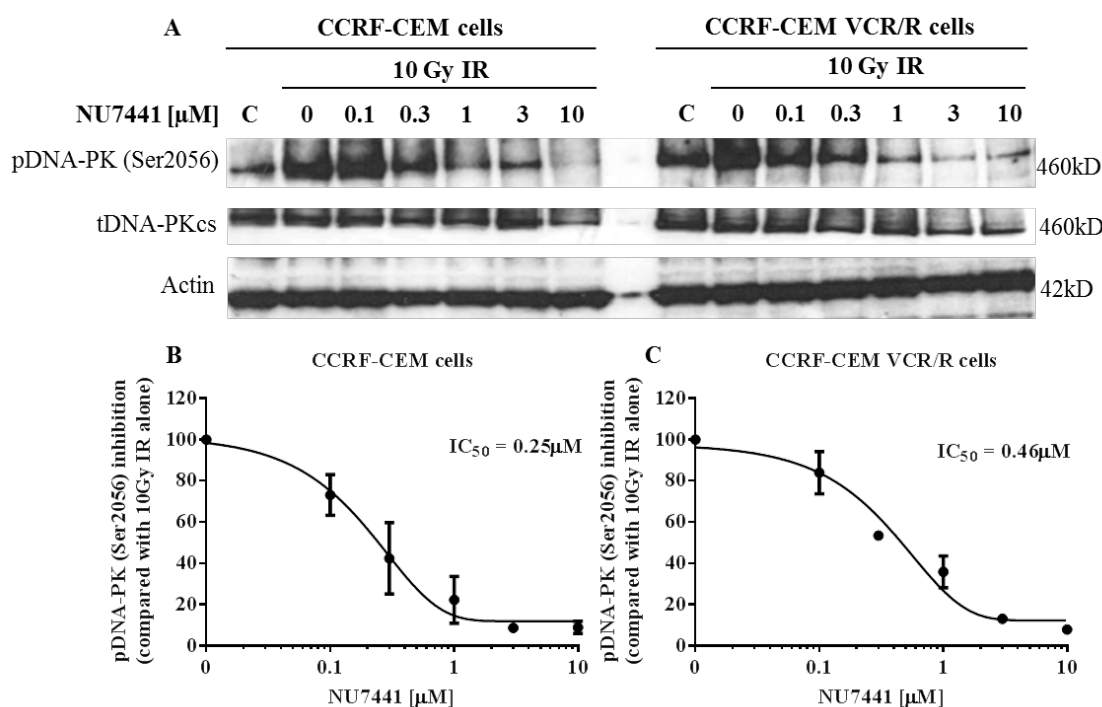
Figure 3-7: NU7441 is a potent inhibitor of IR-activated DNA-PK phosphorylation in CCRF-CEM and CCRF-CEM VCR/R cells. CCRF-CEM and CCRF-CEM VCR/R cells were pretreated for 1 hour with NU7441 (0-10 μM) before cells were irradiated with 10 Gy IR, and cell lysates were collected after a further 30 minutes. (**A**) DNA-PK levels and phosphorylation, and actin expression, were determined by Western blotting using the indicated specific antibodies (Section 2.7.4). Data represents findings of 3 independent experiments. (**B**) and (**C**) Mean ± SEM pDNA-PK inhibition following quantification of results from 3 independent Western blots. The lines were fitted using non-linear regression analysis.

The experiment was repeated in the presence of increasing concentrations of KU55933 in place of NU7441 and the results are shown in Figure 3-8. Higher basal ATM phosphorylation at serine 1981 was observed in the CCRF-CEM VCR/R cells compared with the parental cells before treatment, and ATM phosphorylation was increased after treatment with 10 Gy IR in both cell lines but, more clearly in the CCRF-CEM VCR/R cells compared with the CCRF-CEM cells. ATM phosphorylation was inhibited by KU55933 in both cell lines with IC_{50} values of 6.1 μM in CCRF-CEM cells (Figure 3-8B) and 3.6 μM in CCRF-CEM VCR/R cells (Figure 3-8C). KU55933 was used at 10 μM in subsequent experiments as this concentration is higher than the IC_{50} values in both CCRF-CEM and CCRF-CEM VCR/R cells, and this concentration has been previously be demonstrated to maximally potentiate ionising radiation-induced cell killing (Hickson *et al.*, 2004).
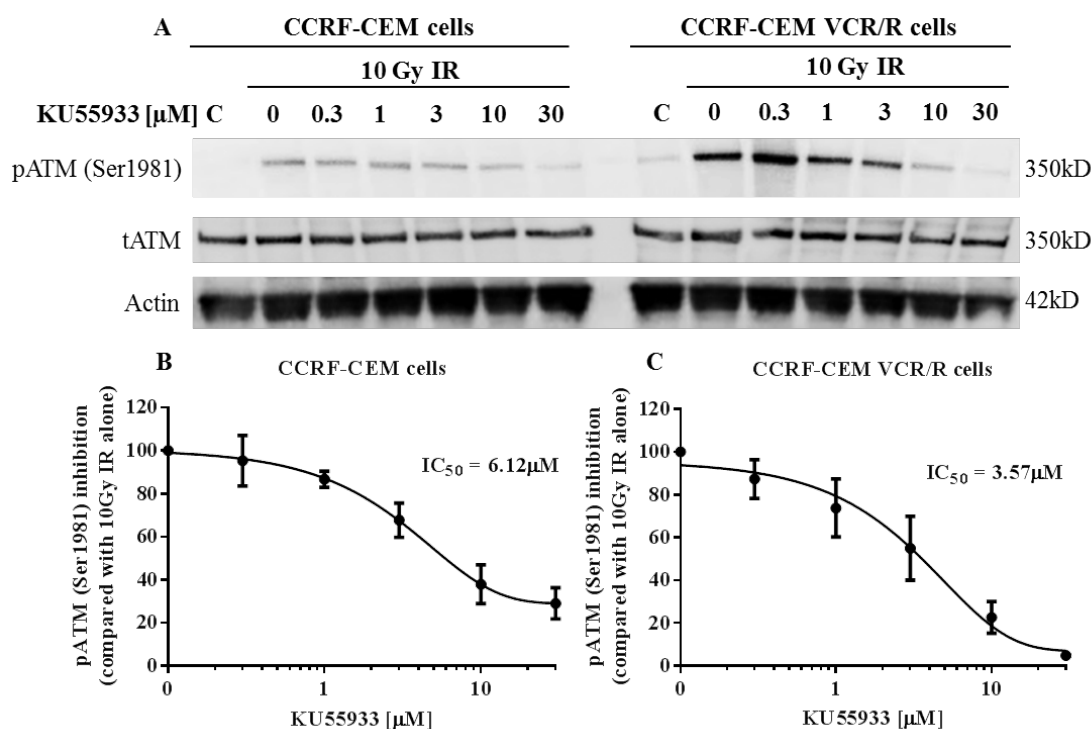
Figure 3-8: KU55933 is a potent inhibitor of IR-activated ATM phosphorylation in CCRF-CEM and CCRF-CEM VCR/R cells. CCRF-CEM and CCRF-CEM VCR/R cells were pretreated for 1 hour with varying concentrations of KU55933 (0-30 μM) before cells were irradiated with 10 Gy IR, and cell lysates were collected after a further 30 minutes. (**A**) ATM levels and phosphorylation, and actin expression, were determined by Western blotting using the indicated specific antibodies (Section 2.7.4). Data represents findings of 3 independent experiments. (**B**) and (**C**) Mean ± SEM pATM inhibition following quantification of results from 3 independent Western blots. The lines were fitted using non-linear regression analysis. Stephanie Burnell (SB) carried out two of the independent experiments.

3.3.3 NU7441 and KU55933 caused greater sensitisation in multidrug-resistant cells compared with parental cells

Having characterised the cell lines and the inhibitors, the sensitivity of the 4 different paired parental and multidrug-resistant cell lines to vincristine, docetaxel or paclitaxel alone or in the presence of NU7441 (1 μM) or KU55933 (10 μM) was examined using the XTT assay (Section 2.3).

For each data set, the bar charts show the 50 % growth inhibitory concentrations calculated from the line graphs with statistical analyses using an unpaired *t*-test. The GI_{50} data for all of the cell lines are displayed in Table 3-1.

CCRF-CEM cells were sensitised 1.5-fold (p=0.02) and 6-fold (p=0.0006) to vincristine by 1 µM NU7441 and 10 µM KU55933, respectively, but were not sensitised to docetaxel (Figure 3-9). CCRF-CEM VCR/R cells, developed by exposure to increasing concentrations of vincristine, were 3200-fold resistant to vincristine (p=0.02) and 105-fold (p=0.006) cross-resistant to docetaxel. The CCRF-CEM VCR/R cells were sensitised by NU7441 (1 µM) and KU55933 (10 µM) to both vincristine (7-fold (p=0.01) and 48-fold (p=0.006), respectively) and docetaxel (7-fold (p=0.003) and 53-fold (p=0.002), respectively), i.e. to a much greater degree than the parental CCRF-CEM cells.

A2780 cells were sensitised 20-fold (p<0.0001) to paclitaxel at the GI_{50} concentration by 10 µM KU55933 (Figure 3-10). However, KU55933 did not sensitise A2780 cells to vincristine, and NU7441 did not sensitise the A2780 cells to either vincristine or paclitaxel at the GI_{50} concentration. A2780-TX1000 cells, generated by exposure to increasing concentrations of paclitaxel, were 8800-fold resistant (p=0.0002) to paclitaxel and 5100-fold cross-resistant (p=0.003) to vincristine, when compared with the parental A2780 cells. The large resistance to paclitaxel and cross-resistance to vincristine is in agreement with the relatively high *ABCB1* mRNA levels found in this cell line (Figure 3-4). The A2780-TX1000 cells were sensitised to paclitaxel 3.5-fold (p=0.002) and 17-fold (p=0.0003), and to vincristine 5.7-fold (p=0.007) and 24-fold (p=0.01), by 1 µM NU7441 and 10 µM KU55933, respectively.

The parental SKOV3 cell line was not sensitised by either NU7441 (1 µM) or KU55933 (10 µM) to vincristine or paclitaxel (Figure 3-11). The SKOV3-TR cell line, generated by exposure to increasing concentrations of paclitaxel, was 355-fold (p=0.0008) resistant to paclitaxel and 340-fold (p=0.01) resistant to vincristine, and was sensitised 7.6-fold (p=0.002) and 27-fold (p=0.0009) to paclitaxel, and 17-fold (p=0.01) and 11-fold (p=0.02) to vincristine, by 1 µM NU7441 and 10 µM KU55933, respectively.

The parental KK47 cells were not sensitised to docetaxel or vincristine by NU7441 (1 µM) (Figure 3-12). The KK47A cell line was developed in the same way as the A2780-TX1000 and SKOV3-TR cell lines but with exposure to doxorubicin rather than an antimitotic agent. The KK47A cells were 3.2-fold (p=0.03) resistant to vincristine but not significantly resistant to docetaxel. In contrast to KK47 cells, KK47A cells were significantly sensitised to both vincristine and docetaxel by 1 µM NU7441 (3.4-fold (p=0.02) and 2.5-fold (p=0.04), respectively).

KU55933 (10 µM) consistently caused a greater sensitisation to the cytotoxic drugs than 1 µM NU7441 in all of the parental cell lines. Also, the sensitisation effects were greater when the inhibitors were used in combination with vincristine, as opposed to a taxane (docetaxel or paclitaxel) in all of parental and multidrug-resistant cell lines, except the KK47A cell line.
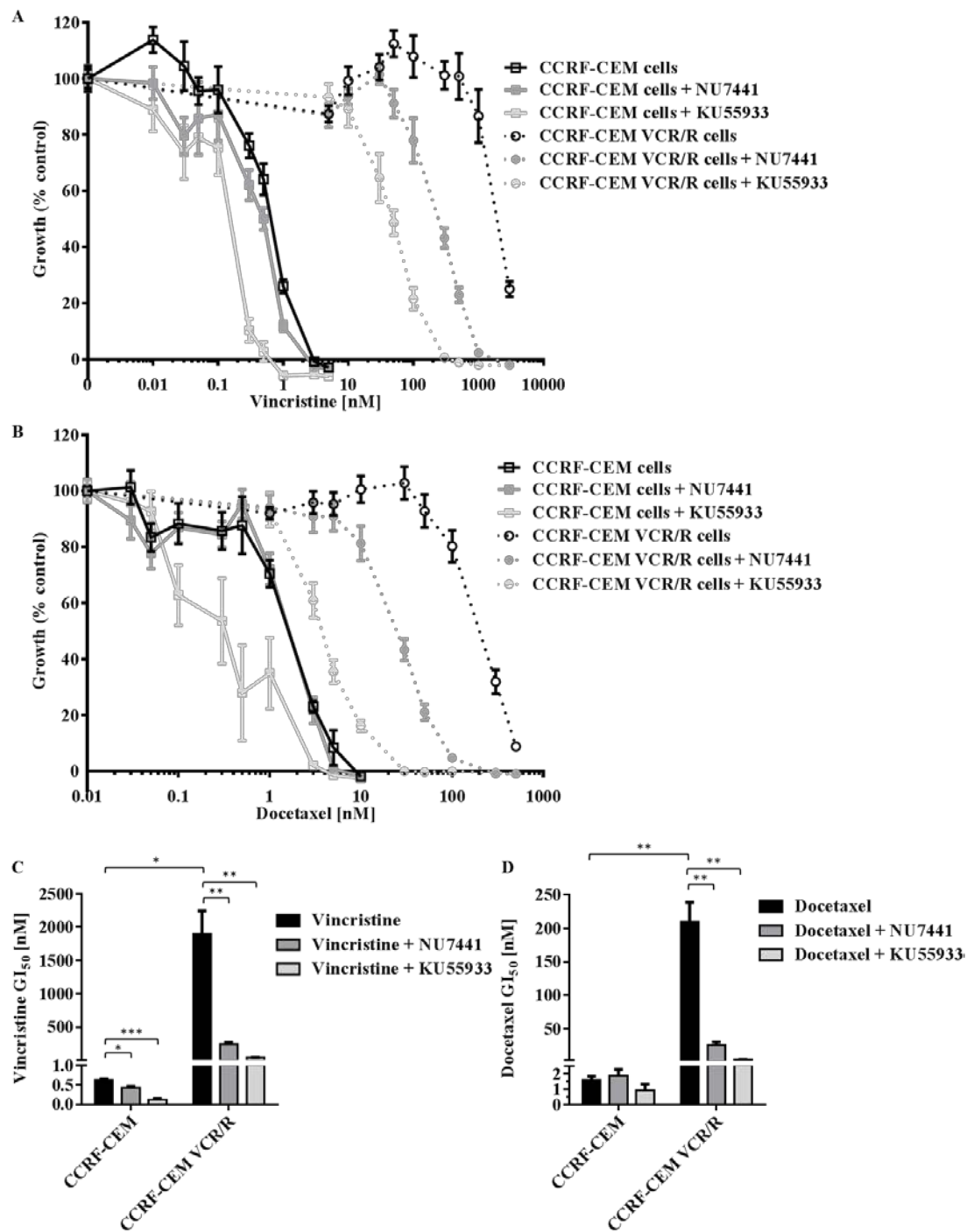
Figure 3-9: CCRF-CEM cells are sensitised to vincristine and docetaxel by KU55933 and CCRF-CEM VCR/R cells are sensitised to vincristine and docetaxel by both NU7441 and KU55933. CCRF-CEM and CCRF-CEM VCR/R cells were treated with (**A** and **C**) vincristine or (**B** and **D**) docetaxel alone or in combination with 1 μM NU7441 or 10 μM KU55933 for 72 hours and % growth was analysed by XTT assay (Section 2.3). (**A**) and (**B**) data are presented as a percentage of vehicle control cells. Points represent the mean of ≥3 independent experiments, each in triplicate, ± standard error. (**C**) Vincristine and (**D**) docetaxel GI_{50} data are presented as the GI_{50} means ± standard error. Asterisk indicates a statistically significant difference using the Student's unpaired *t*-test when compared with the GI_{50} for drug alone (* *p<0.05*, ** *p<0.01*, *** *p<0.001*).
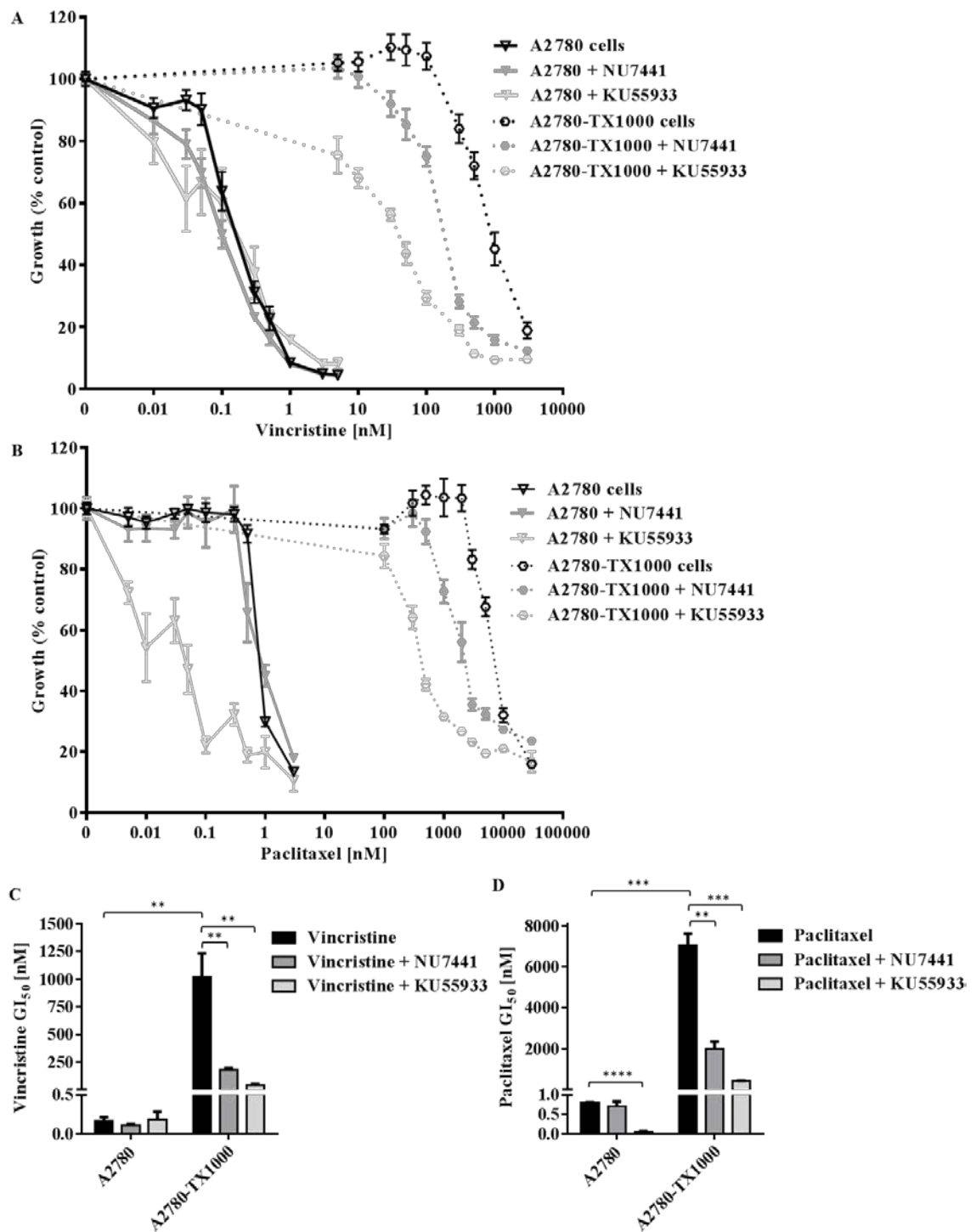
Figure 3-10: A2780 cells are sensitised to paclitaxel by KU55933 and A2780-TX1000 cells are sensitised to vincristine and paclitaxel by both NU7441 and KU55933. A2780 and A2780-TX1000 cells were treated with (**A** and **C**) vincristine or (**B** and **D**) paclitaxel alone or in combination with 1 µM NU7441 or 10 µM KU55933 for 72 hours and % growth was analysed by XTT assay (Section 2.3). (**A**) and (**B**) data are presented as a percentage of vehicle control cells. Points represent the mean of ≥3 independent experiments, each in triplicate, ± standard error. (**C**) Vincristine and (**D**) paclitaxel GI_{50} data are presented as the GI_{50} means ± standard error. Asterisk indicates a statistically significant difference using the Student's unpaired *t*-test when compared with the GI_{50} for drug alone (* *p<0.05*, ** *p<0.01*, *** *p<0.001*, **** *p<0.0001*).
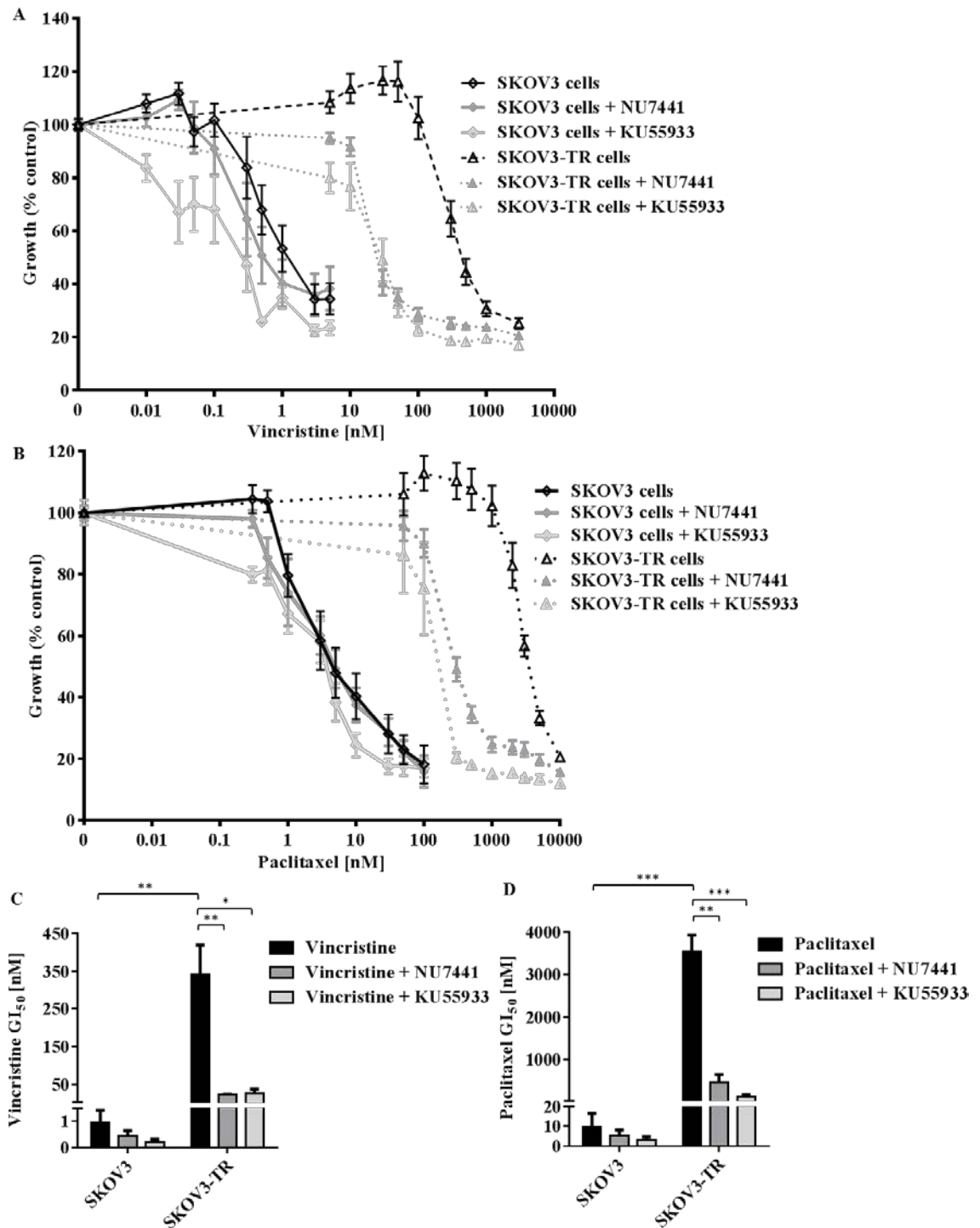
Figure 3-11: SKOV3 cells are sensitised to vincristine by KU55933 and SKOV3-TR cells are sensitised to vincristine and paclitaxel by both NU7441 and KU55933. SKOV3 and SKOV3-TR cells were treated with (**A** and **C**) vincristine or (**B** and **D**) paclitaxel alone or in combination with 1 µM NU7441 or 10 µM KU55933 for 72 hours and % growth was analysed by XTT assay (Section 2.3). (**A**) and (**B**) data are presented as a percentage of vehicle control cells. Points represent the mean of ≥ 3 independent experiments, each in triplicate, $\pm$ standard error. (**C**) Vincristine and (**D**) paclitaxel GI_{50} data are presented as the GI_{50} means $\pm$ standard error. Asterisk indicates a statistically significant difference using the Student's unpaired t-test when compared with the GI_{50} for drug alone (* $p<0.05$, ** $p<0.01$, *** $p<0.001$).

Figure 3-12: KK47A cells are more resistant to vincristine and docetaxel than the parental KK47 cells and are sensitised to vincristine and docetaxel by NU7441. KK47 and KK47A cells were treated with (**A, C, E, G**) vincristine or (**B, D, F, H**) docetaxel alone or in combination with 1 µM NU7441 for 72 hours and % growth was analysed by XTT assay (Section 2.3). (**A-F**) Data are presented as a percentage of vehicle control cells. Points represent the mean of ≥3 independent experiments, each in triplicate, ± standard error. (**G**) Vincristine and (**H**) docetaxel GI_{50} data are presented as the GI_{50} means ± standard error. Asterisk indicates a statistically significant difference using the Student's unpaired *t*-test when compared with the GI_{50} for drug alone (* *p<0.05)*. KK47 cell work carried out during EM MRes project.

GI$_{50}$ drug (nM)	CCRF-CEM cells				CCRF-CEM VCR/R cells		
	Drug	Drug + NU7441	Drug + KU55933		Drug	Drug + NU7441	Drug + KU55933
Vincristine	0.6 ± 0.04	$0.4 \pm 0.04^{p=0.02}$	$0.1 \pm 0.04^{p=0.0006}$		$1900 \pm 340_{p=0.02}$	$250 \pm 30^{p=0.01}$	$40 \pm 10^{p=0.006}$
Docetaxel	2.0 ± 0.2	2.0 ± 0.4^{ns}	1.0 ± 0.5^{ns}		$210 \pm 30_{p=0.006}$	$30 \pm 4.0^{p=0.003}$	$4.0 \pm 1.0^{p=0.002}$

GI$_{50}$ drug (nM)	A2780 cells				A2780-TX1000 cells		
	Drug	Drug + NU7441	Drug + KU55933		Drug	Drug + NU7441	Drug + KU55933
Vincristine	0.2 ± 0.05	0.1 ± 0.02^{ns}	0.2 ± 0.1^{ns}		$1020 \pm 210_{p=0.003}$	$180 \pm 20^{p=0.007}$	$43 \pm 9^{p=0.01}$
Paclitaxel	0.8 ± 0.02	0.7 ± 0.1^{ns}	$0.04 \pm 0.02^{p<0.0001}$		$7050 \pm 550_{p=0.0002}$	$2020 \pm 340^{p=0.002}$	$410 \pm 35^{p=0.0003}$

GI$_{50}$ drug (nM)	SKOV3 cells				SKOV3-TR cells		
	Drug	Drug + NU7441	Drug + KU55933		Drug	Drug + NU7441	Drug + KU55933
Vincristine	1 ± 0.5	0.4 ± 0.2^{ns}	0.2 ± 0.1^{ns}		$340 \pm 80_{p=0.01}$	$20 \pm 2^{p=0.01}$	$30 \pm 10^{p=0.02}$
Paclitaxel	10 ± 7	6 ± 3^{ns}	3 ± 1^{ns}		$3550 \pm 380_{p=0.0008}$	$470 \pm 180^{p=0.002}$	$130 \pm 50^{p=0.0009}$

GI$_{50}$ drug (nM)	KK47 cells				KK47A cells		
	Drug	Drug + NU7441	-		Drug	Drug + NU7441	-
Vincristine	1.8 ± 0.5	1.1 ± 0.1^{ns}	-		$5.8 \pm 1.1_{p=0.03}$	$1.7 \pm 0.3^{p=0.02}$	-
Docetaxel	1.3 ± 0.4	0.5 ± 0.06^{ns}	-		$2.0 \pm 0.34_{ns}$	$0.8 \pm 0.22^{p=0.04}$	-

Table 3-1: GI$_{50}$ concentrations of drug alone or in the presence of the NU7441 or KU55933 in four paired sensitive and multidrug-resistant cell lines. Cells were treated with vincristine, docetaxel or paclitaxel alone or in combination with 1 µM NU7441 or 10 µM KU55933 for 72 hours and % growth was analysed by XTT assay (Section 2.3). The data are presented as the GI$_{50}$ mean (nM) of ≥ 3 independent experiments, each in triplicate, $\pm$ standard error. Significant differences between parental and multidrug-resistant cells treated with drug alone were calculated using an unpaired *t*-test and results are shown as a subscript. Significant differences between cells treated with drug alone and cells treated with drug + inhibitor were calculated using an unpaired *t*-test and results are shown as a superscript. ns = not-significant. KK47 cell work carried out during EM MRes project.

3.3.4 *KU55933 significantly sensitised cells to vincristine and paclitaxel*

To determine whether sensitisation to microtubule-targeting agent-induced growth inhibition by NU7441 and KU55933 in the 4 paired cell lines reflected increased cytotoxicity, cell survival assays were performed.

Survival assays on the suspension CCRF-CEM and CCRF-CEM VCR/R cell lines were performed using an enriched semi-solid methylcellulose medium, Methocult. The plating efficiency of suspension cell lines in sloppy agar, which is a commonly-used method, is often quite poor but the plating efficiency in methylcellulose for these cell lines was between 35-40 %.

CCRF-CEM and CCRF-CEM VCR/R cells were treated with vincristine alone or in combination with NU7441 (1 µM) or KU55933 (10 µM) for 24 hours before the drugs were washed off and cells were plated out and left for colonies to establish for 14 days (Section 2.5). It was not possible to obtain 90 % lethal concentrations (LC_{90}) for the CCRF-CEM VCR/R cells as they did not reach 10 % survival at the highest vincristine concentration used (10 µM). However, there was a 13-fold increase in cytotoxicity in response to 10 µM vincristine in combination with KU55933 (10 µM). NU7441 (1 µM) had no effect on cell survival in the CCRF-CEM VCR/R cell line. In the parental CCRF-CEM cell line, 10 µM KU55933 sensitised CCRF-CEM cells to vincristine at concentrations of 0.3 nM and above. However, NU7441 (1 µM) did not show any marked sensitisation effects until the higher concentrations of vincristine were tested (3-30 nM).
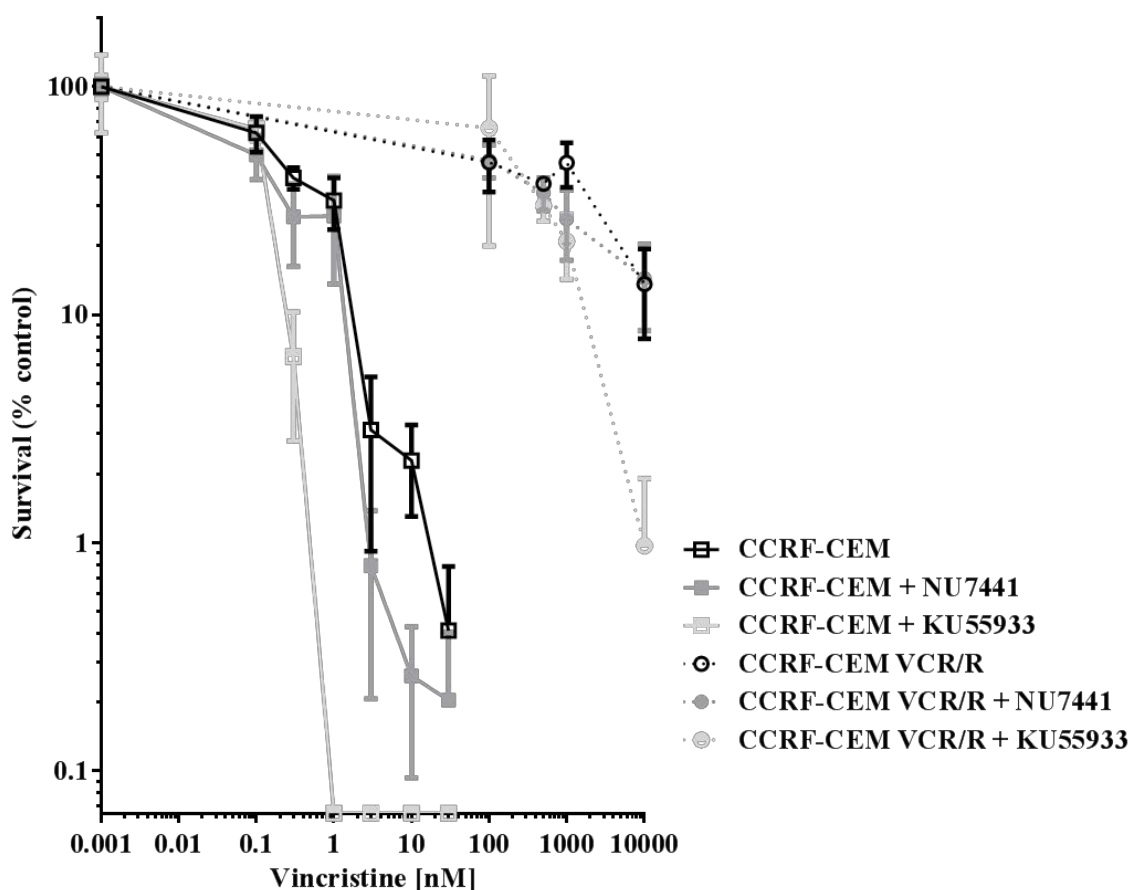
Figure 3-13: CCRF-CEM and CCRF-CEM VCR/R cells are not markedly sensitised to vincristine cytotoxicity by NU7441 or KU55933. CCRF-CEM and CCRF-CEM VCR/R cells were treated with vincristine alone or in combination with 1 µM NU7441 or 10 µM KU55933 for 24 hours. Survival was analysed by methylcellulose clonogenic assay (Section 2.5). Data are presented as a percentage of vehicle or inhibitor alone control cells. Vincristine alone and vincristine plus NU7441 points represent the mean of 3 independent experiments, vincristine plus KU55933 points represent the mean of 2 independent experiments, each in triplicate, ± standard error. SB carried out one of the independent experiments with KU55933.

Cell survival was also investigated in the A2780 and A2780-TX1000 solid-tumour cell lines following treatment with paclitaxel alone or in combination with NU7441 (1 µM) or KU55933 (10 µM). It was not possible to obtain 90 % lethal concentrations (LC_{90}) for the A2780 or A2780-TX1000 cells as they did not reach 10 % survival at the highest paclitaxel concentration used (10 µM). In the A2780 cell line, 1 µM NU7441 did not reduce the cell survival in combination with paclitaxel when compared with paclitaxel alone. However, 10 µM KU55933 caused a 19.1-fold sensitisation in A2780 cells to 1 nM paclitaxel. The A2780-TX1000 cells were highly

resistant to paclitaxel in comparison to the parental A2780 cell line, and the data for the A2780-TX1000 cell line suggests sensitisation to paclitaxel by NU7441 and KU55933 may be obtained, but higher concentrations of paclitaxel would need to be tested.
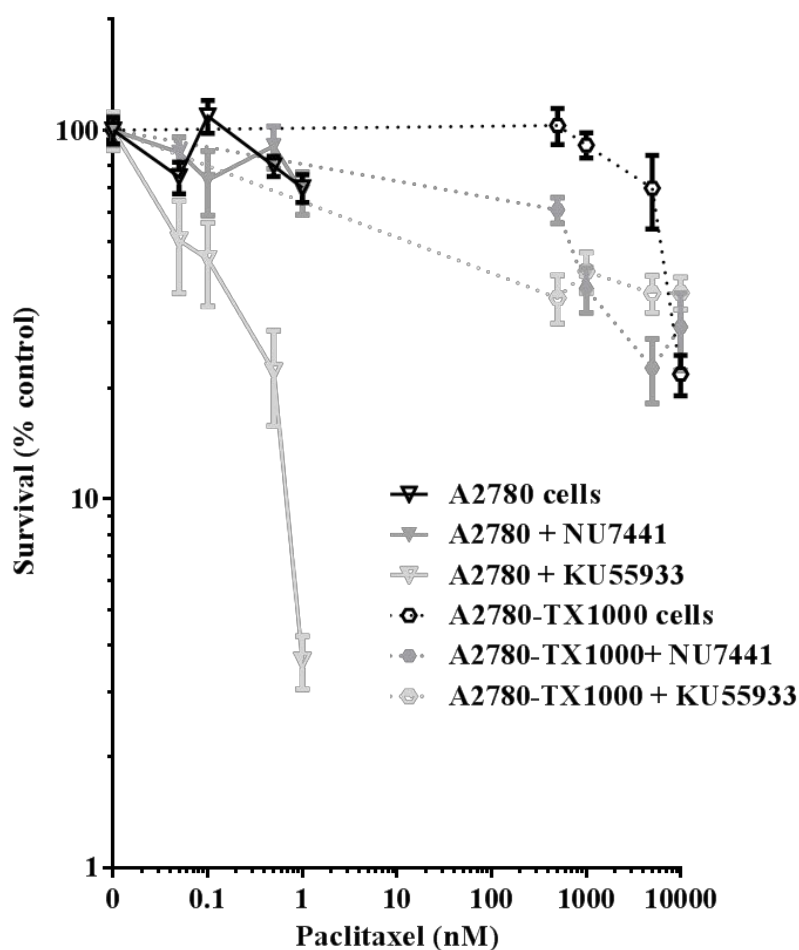
Figure 3-14: A2780 cells are sensitised by KU55933 and A2780-TX1000 cells are sensitised by both NU7441 and KU55933 to paclitaxel cytotoxicity. A2780 and A2780-TX1000 cells were treated with paclitaxel alone or in combination with 1 μM NU7441 or 10 μM KU55933 for 24 hours. Survival was analysed by clonogenic assay (Section 2.4). Data are presented as a percentage of vehicle or inhibitor alone control cells. Points represent the mean of 3 independent experiments, each in triplicate, ± standard error.

3.3.5 DNA-PK underwent autophosphorylation, but ATM did not, in response to vincristine in CCRF-CEM and CCRF-CEM VCR/R cell lines

Phosphorylation of DNA-PK and ATM were investigated in CCRF-CEM and CCRF-CEM VCR/R cells following treatment with vincristine. Cells were treated with concentrations of vincristine that included the GI_{50} concentrations determined for each cell line (Figure 3-9); however, because the cells for these Western blotting experiments were only treated for 24 hours, higher concentrations of vincristine were also included. Following vincristine treatment, DNA-PK was phosphorylated at serine 2056 in a concentration-dependent manner (Figure 3-15). Unexpectedly, the total DNA-PKcs protein levels decreased in a concentration-dependent manner. This result could not be a cross-antibody or a membrane stripping effect as separate Western blots were performed, one being probed for phosphorylated DNA-PK and one for total DNA-PK.
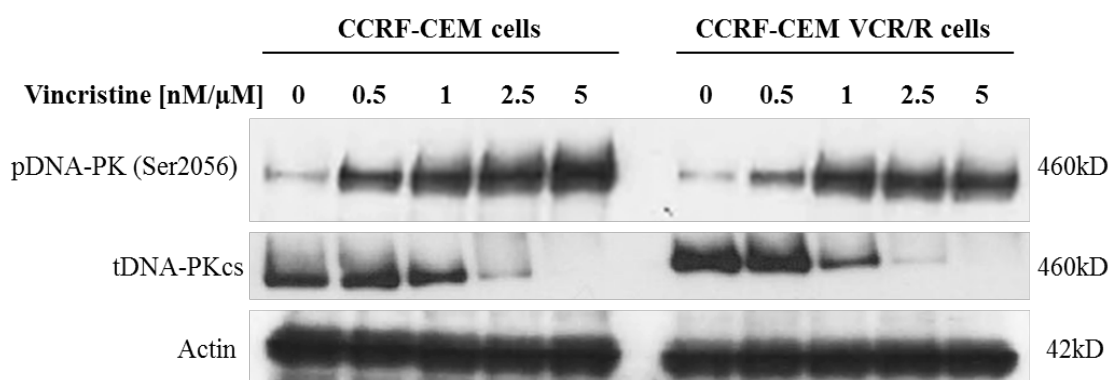
Figure 3-15: Concentration-dependent DNA-PK phosphorylation in response to vincristine. CCRF-CEM and CCRF-CEM VCR/R cells were treated with varying concentrations of vincristine (0-5 nM and 0-5 µM, respectively) for 24 hours. Cell lysates were prepared and DNA-PK levels and phosphorylation, and actin expression, were determined by Western blotting using the indicated specific antibodies (Section 2.7.4). Data are representative of 3 independent experiments.

An additional experiment using the same treatment conditions was performed, and the membranes were probed for total ATM and ATM serine 1981 phosphorylation. A positive control was also included, namely MDA-MB-231 cells which are known to phosphorylate ATM at serine 1981 in response to ionising radiation (Toulany *et al.*, 2006) (Figure 3-16).

There was no ATM phosphorylation in the CCRF-CEM cell lines in response to vincristine as measured by the serine 1981 phosphorylation site, and the total ATM protein level was constant.
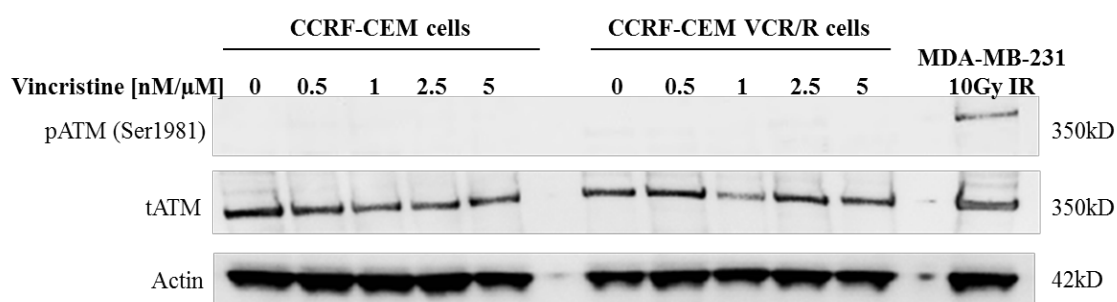
Figure 3-16: ATM is not phosphorylated in response to vincristine. CCRF-CEM and CCRF-CEM VCR/R cells were treated with varying concentrations of vincristine (0-5 nM and 0-5 µM, respectively) for 24 hours. Irradiated MDA-MB-231 cells were included as a positive control for ATM serine 1981 phosphorylation. Cell lysates were prepared and ATM levels and phosphorylation, and actin expression, were determined by Western blotting using the indicated specific antibodies (Section 2.7.4). Data are representative of 3 independent experiments. SB carried out two of the independent experiments.

To confirm that the DNA-PK phosphorylation observed (Figure 3-15) was due to DNA-PK activation, the inhibitory effect of 1 μM NU7441 on phosphorylation was examined. Cells were treated with their respective vincristine GI$_{50}$ concentrations alone or in combination with 1 μM NU7441. Induction of DNA-PK phosphorylation was observed in response to vincristine, and this phosphorylation was inhibited by NU7441 (1 μM) in both cell lines (Figure 3-17).
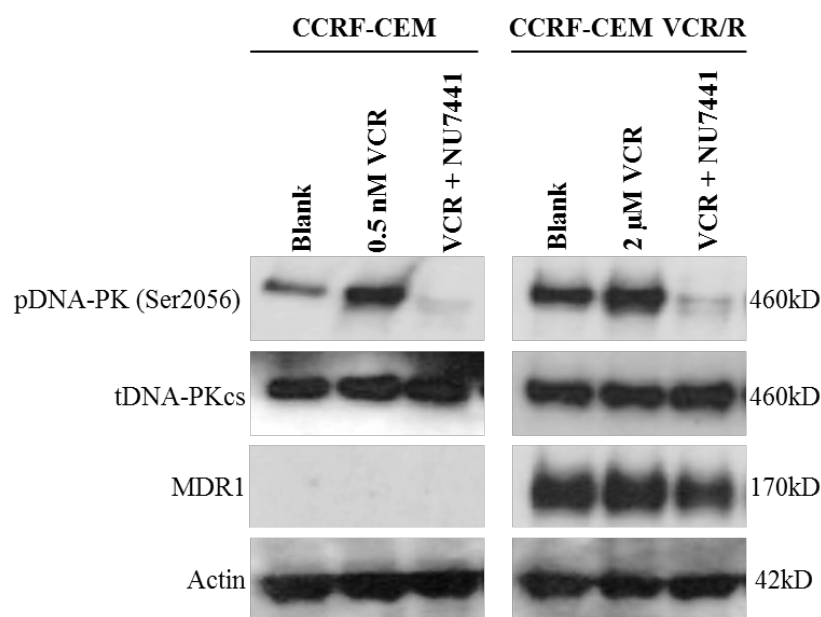
Figure 3-17: Vincristine-induced DNA-PK phosphorylation is inhibited by NU7441. CCRF-CEM and CCRF-CEM VCR/R cells were treated with vincristine (0.5 nM and 2 μM, respectively) alone or in the presence of NU7441 (1 μM) for 24 hours. Cell lysates were prepared and DNA-PK levels and phosphorylation, MDR1 and actin expression were determined by Western blotting using the indicated specific antibodies (Section 2.7.4). Data are representative of 3 independent experiments.

These experiments demonstrated that DNA-PK is phosphorylated at serine 2056 in a concentration-dependent response to vincristine, and that phosphorylation is inhibited by 1 μM NU7441. In contrast, ATM autophosphorylation at serine 1981 was not observed, although this site is a known site of autophosphorylation in response to DNA-damaging agents as shown in Figure 3-8 with ionising radiation in these cell lines.

3.3.6 Vincristine, paclitaxel and docetaxel induce caspase 3/7 activation in parental and multidrug-resistant tumour cell lines

NU7441 and KU55933 were shown to sensitise cells to microtubule-targeting agents (Sections 3.3.3 and 3.3.4) and the mechanism of cell death involved was investigated using the caspase 3/7 assay to evaluate the role of apoptosis.

KU55933 was found to interfere with the Caspase-Glo assay, i.e. the inhibitor alone with no cells present gave a high luminescence reading, and so it was not possible to measure caspase 3/7 activity in cells treated with KU55933 using this assay. However, the other cytotoxic drugs and NU7441 did not interfere with the Caspase-Glo assay.

CCRF-CEM and CCRF-CEM VCR/R cells were treated with a GI_{50} vincristine concentration either alone or in combination with 1 µM NU7441, or with the GI_{50} concentration of mitoxantrone for 6 hours (a positive control treatment based on unpublished data obtained by NJ Tan). Six hours was chosen as the time point for caspase activity to be measured as this is long enough for the compounds to have entered the cells and caused an induction of caspase 3/7 activity, but before cells have undergone cell death, when the signal is lost.

Vincristine increased caspase 3/7 activity to a level similar to or higher than the positive control mitoxantrone, in both the CCRF-CEM and CCRF-CEM VCR/R cells (Figure 3-18). In CCRF-CEM cells, NU7441 increased vincristine-induced caspase 3/7 activity by 21 % and by 187 % in CCRF-CEM VCR/R cells, although this was not statistically significant. There were much higher levels of caspase 3/7 activity detected in the CCRF-CEM VCR/R cells compared with the parental CCRF-CEM cells in response to GI_{50} drug concentrations (>100 % increase in caspase 3/7 activity compared with >35 % increase, respectively), indicating that caspase activation is much greater in the multidrug-resistant cells at the equitoxic vincristine and mitoxantrone concentrations.
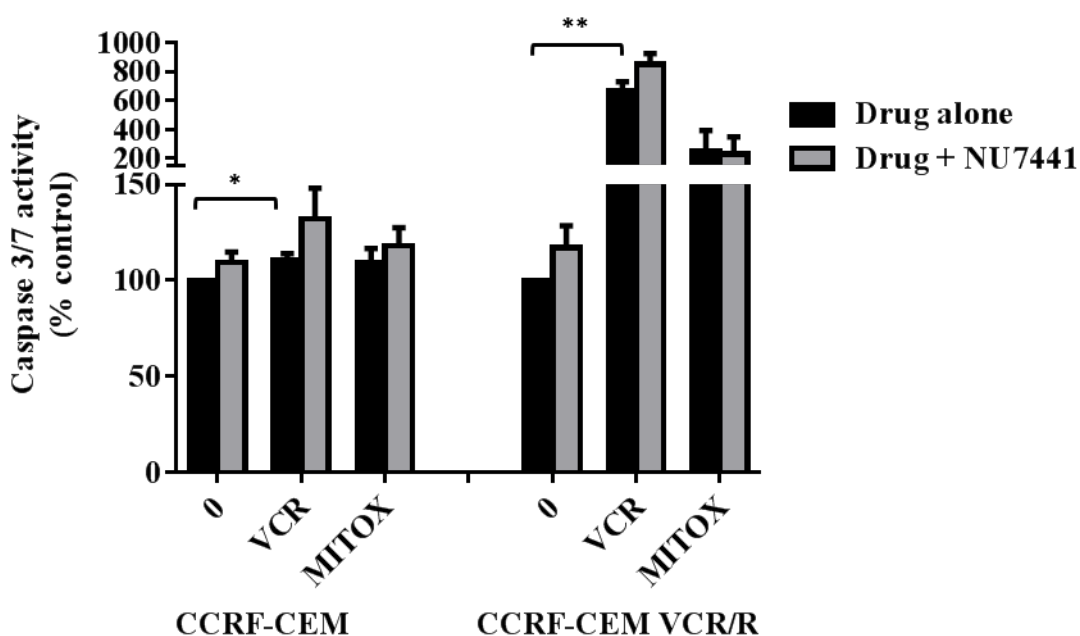
Figure 3-18: Vincristine increases caspase 3/7 activity in CCRF-CEM and CCRF-CEM VCR/R cells but there is no additional increase in caspase activity with NU7441. CCRF-CEM and CCRF-CEM VCR/R cells were treated with vincristine (0.5 nM and 2.5 µM, respectively) or mitoxantrone (10 nM and 1 µM, respectively) alone or in the presence of NU7441 (1 µM) for 6 hours. Caspase 3/7 activity was determined by Caspase-Glo assay (Section 2.6). Bars represent the mean of ≥3 independent experiments, each in triplicate, ± standard error. Significant differences between untreated cells and cells treated with drug and between cells treated with drug alone and drug + NU7441 were evaluated using an unpaired *t*-test. Asterisk indicates a statistically significant difference (* *p<0.05, ** p<0.01).

Caspase 3/7 activation was also studied in A2780 and A2780-TX1000 cells using both GI_{50} and 5 x GI_{50} concentrations of paclitaxel, alone or in combination with 1 µM

NU7441. There was no induction of apoptosis with 1 μM NU7441 treatment alone, in agreement with the growth inhibition and survival data showing that 1 μM NU7441 alone was not toxic (Figure 3-19). Paclitaxel caused an increase in caspase 3/7 activity, up to a 255 % increase in A2780 cells and a 177 % increase in A2780-TX1000 cells, indicating paclitaxel causes cell death *via* apoptosis. There was no further increase in caspase 3/7 activity in the A2780 cells with the addition of NU7441 (1 μM), which is in agreement with the lack of sensitisation seen in the growth inhibition and clonogenic survival experiments. However, in the A2780-TX1000 cells there was a marked 173 % increase in caspase 3/7 activity with the addition of NU7441 (1 μM) at a paclitaxel concentration of 5 μM.
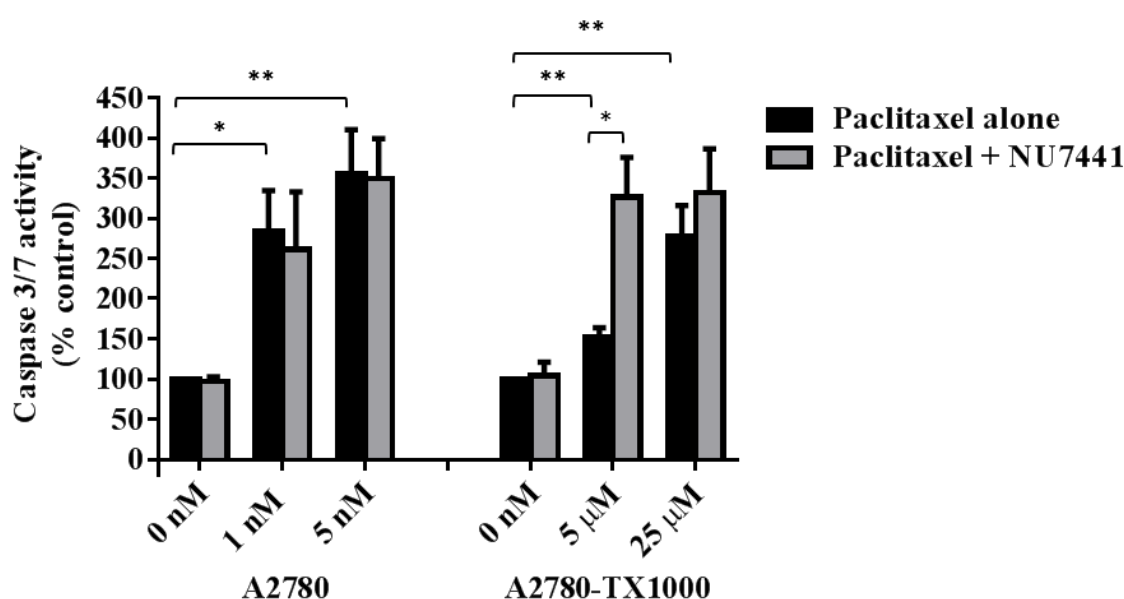
Figure 3-19: Paclitaxel increases caspase 3/7 activity in A2780 and A2780-TX1000 cells and there is an increase in caspase activity with NU7441 in A2780-TX1000 cells. A2780 and A2780-TX1000 cells were treated with paclitaxel (0, 1, 5 nM and 0, 5, 25 μM, respectively) alone or in the presence of NU7441 (1 μM) for 6 hours. Caspase 3/7 activity was determined by Caspase-Glo assay (Section 2.6). Bars represent the mean of ≥3 independent experiments, each in triplicate, ± standard error. Significant differences between untreated cells and cells treated with drug, and between cells treated with drug alone and drug + NU7441, were evaluated using an unpaired *t*-test. Asterisk indicates a statistically significant difference (* *p<0.05*, ** *p<0.01*).

KK47 and KK47A cells were also investigated for caspase 3/7 activation, in response to a range of docetaxel concentrations. Docetaxel caused a concentration-dependent increase in caspase 3/7 activity in both cell lines, up to a 143 % increase in the KK47 cells and a 185 % increase in the KK47A cells (Figure 3-20). Although only

statistically significant at 20 nM docetaxel in KK47 cells, due to experimental variation, NU7441 increased apoptosis at all concentrations of docetaxel.
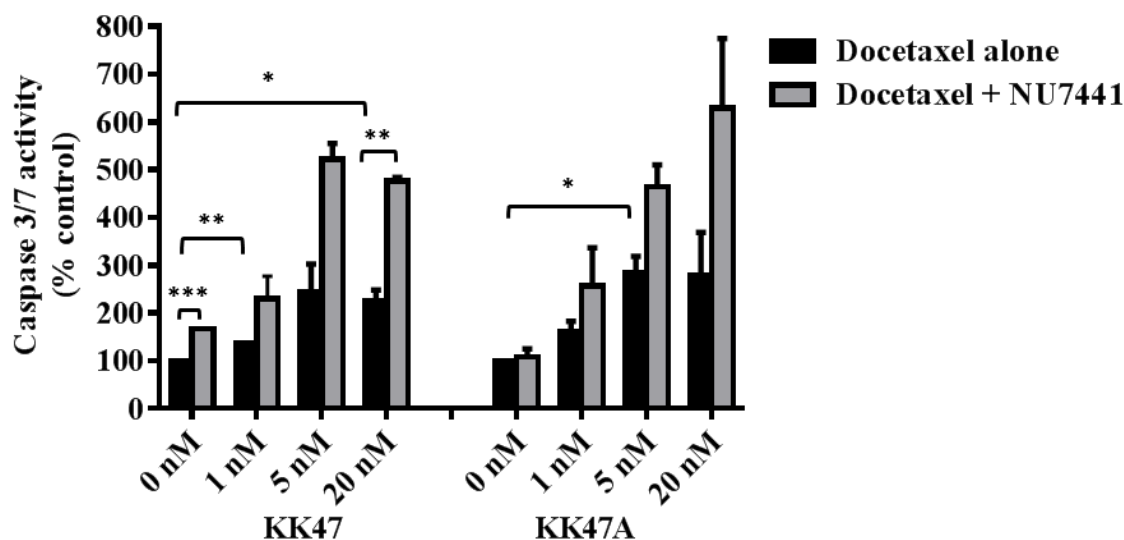
Figure 3-20: Docetaxel increases caspase 3/7 activity in a concentration-dependent manner in KK47 and KK47A cells which is enhanced by NU7441 in KK47 cells. KK47 and KK47A cells were treated with docetaxel (0, 1, 5, 20 nM and 0, 1, 5, 20 µM, respectively) alone or in the presence of NU7441 (1 µM) for 6 hours. Caspase 3/7 activity was determined by Caspase-Glo assay (Section 2.6). Bars represent the mean of 2 independent experiments, each in triplicate, ± standard error. Significant differences between untreated cells and cells treated with drug, and between cells treated with drug alone and drug + NU7441, were evaluated using an unpaired *t*-test. Asterisk indicates a statistically significant difference (* *p<0.05, ** p<0.01, *** p<0.001*). KK47 cell work carried out during EM MRes project.

The caspase 3/7 activity results show that vincristine, docetaxel and paclitaxel all cause cell death, at least in part *via* the caspase-dependent apoptosis pathway, and that 1 µM NU7441 can increase drug-induced apoptosis.

3.3.7 *The microtubule-targeting agents vincristine and docetaxel did not cause DNA strand breaks*

DNA-PK activation, measured by autophosphorylation of DNA-PK, is conventionally associated with DNA repair following treatment with a DNA-damaging agent, and caspase 3/7-dependent apoptosis is commonly associated with cell death following DNA damage. Although the mechanism of action of the vinca alkaloids and the taxanes is known to involve interaction with the microtubules and not DNA, clear evidence of DNA-PK phosphorylation following vincristine treatment is presented here

(Section 3.3.5). Experiments were therefore performed to determine whether vincristine and docetaxel were in fact causing DNA strand breaks.

The alkaline COMET technique allows DNA fragmentation to be examined in a single cell gel electrophoresis assay. Experiments were carried out with both KK47 cells and CCRF-CEM cells following docetaxel or vincristine treatment. Mitoxantrone and temozolomide were used as positive control agents, which are known to induce DNA damage.

DNA damage was assessed by microscopy using the DNA-intercalating dye, SYBR green and quantified using KOMET software. In cells without DNA-damage, the DNA remains intact and does not pass out of the nucleus following application of an electrical current. However, if the DNA is damaged small DNA fragments will pass out of the nucleus under an electrical current and will form a "tail" behind the nucleus (the "head" of the COMET), with smaller DNA fragments travelling further.

Untreated KK47 and CCRF-CEM cells showed no DNA damage, i.e. the cells have round, intact nuclei (Figure 3-21A and G) and a very low olive tail moment (which reflects the size of tail and intensity of DNA fragments in tail) (Figure 3-22). The positive control compounds mitoxantrone (Figure 3-21B and I) and temozolomide (Figure 3-21C) induced high levels of DNA damage as shown by the presence of an intense comet tail and a high olive tail moment. The temozolomide-treated cells had so much DNA damage that the KOMET software could not reproducibly detect the heads of the comet which is required for calculation for the olive tail moment, hence the temozolomide data are not presented in the olive tail moment graphs (Figure 3-22). In contrast to the DNA damage seen with mitoxantrone and temozolomide, there was no DNA damage observed following treatment with cytotoxic concentrations of docetaxel or vincristine, in either KK47 or CCRF-CEM cells (Figure 3-21E, F and H, Figure 3-22). The alkaline COMET assay detects both single and double-strand DNA breaks, alkali-labile sites and DNA crosslinks, and these results demonstrate that vincristine and docetaxel do not cause DNA lesions of the type conventionally associated with DNA-PK activation.
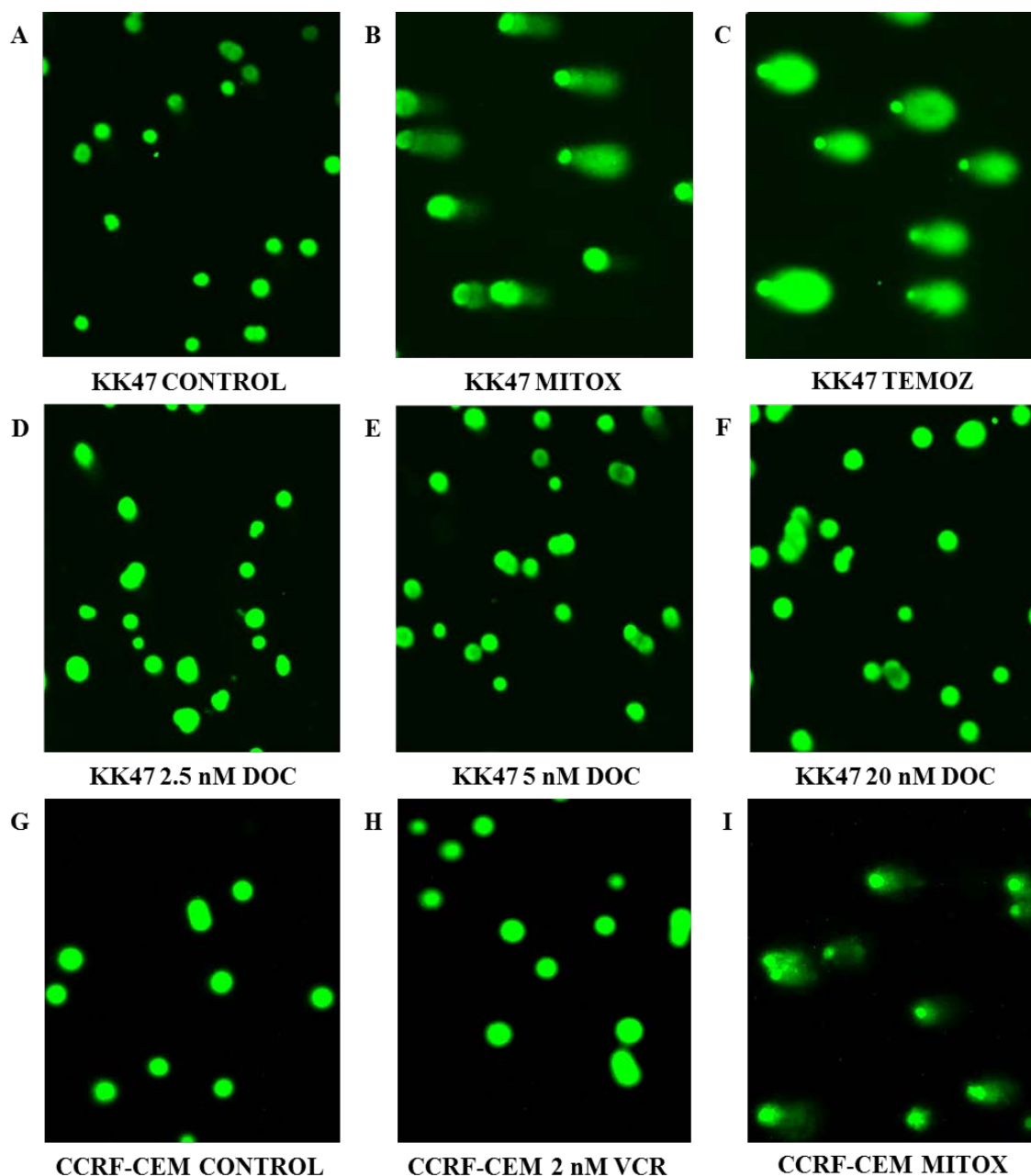
Figure 3-21: Docetaxel and vincristine do not cause DNA strand breaks. (**A**) Untreated KK47 cells. KK47 cells treated with (**B**) 0.5 µM mitoxantrone (MITOX) (positive control), (**C**) 1 mM temozolomide (TEMOZ) (positive control) or (**D-F**) 2.5, 5 or 20 nM docetaxel (DOC) for 24 hours. (**G**) Untreated CCRF-CEM cells. CCRF-CEM cells treated with (**H**) 2 nM vincristine (VCR) or (**I**) 10 nM MITOX for 24 hours. DNA strand breaks were determined using the COMET assay (Section 2.8) and representative images chosen from images from duplicate slides in 1 experiment for each cell line. KK47 cell work carried out during EM MRes project. SB and EM jointly carried out the COMET assay on CCRF-CEM cells.
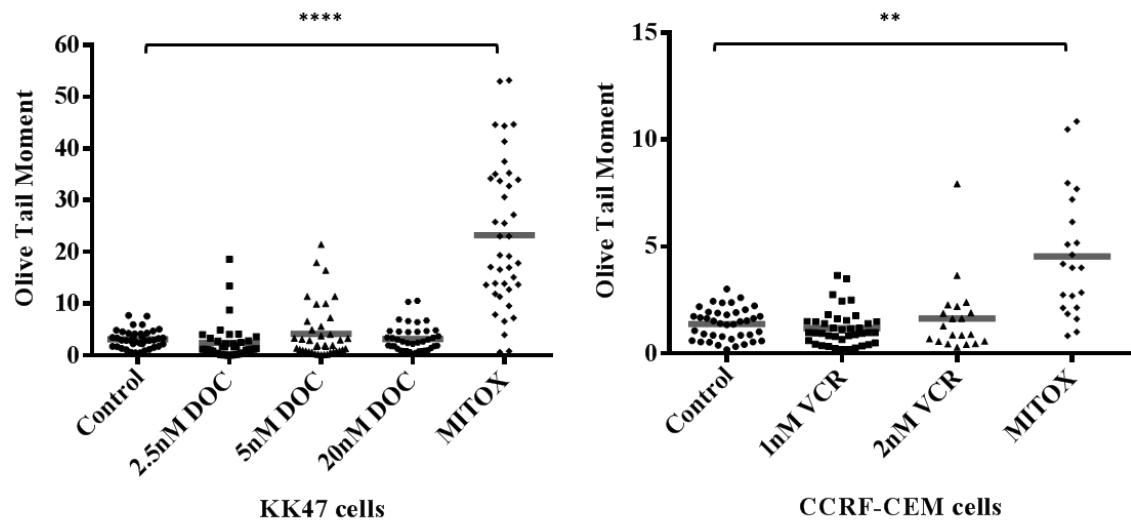
Figure 3-22: There is no significant DNA damage after docetaxel or vincristine treatment, as measured by the Olive Tail Moment. KK47 cells were treated with 0.5 µM mitoxantrone (MITOX) (positive control) or 2.5, 5 or 20 nM docetaxel (DOC) for 24 hours. CCRF-CEM cells were treated with 1 or 2 nM vincristine (VCR) or 10 nM MITOX for 24 hours. DNA strand breaks were determined using the COMET assay (Section 2.8). Analysis of the COMET assay results using Komet 5.5 software showing the Olive Tail Moment (OTM) ([(tail mean – head mean) * tail % DNA] / 100) for at least 20 cells in each treatment category. Horizontal lines indicate the mean OTM for each treatment. Data are the results of duplicates in 1 experiment. Asterisk indicates a statistically significant difference using an unpaired *t*-test when compared with control cells (** *p<0.01*, **** *p<0.0001*). KK47 cell work carried out during EM MRes project. SB and EM jointly carried out the COMET assay on CCRF-CEM cells.

3.4 Discussion and future work

The studies described in this chapter evaluated the roles of DNA-PK and ATM in the sensitivity of tumour cells to microtubule-targeting agents, using the specific inhibitors NU7441 and KU55933, respectively, and were stimulated by reports that DNA-PK and ATM may play a role in mitotic spindle assembly and the spindle assembly checkpoint (Oricchio *et al.*, 2006; Shang *et al.*, 2010).

CCRF-CEM acute lymphoblastic leukaemia cells were used initially in this study, along with their vincristine-resistant counterpart, CCRF-CEM VCR/R cells, and this pair of cell lines has been extensively investigated previously. The parental CCRF-CEM cells are an unstable cell line with respect to ploidy, and polyploidy has previously been associated with loss of at least two of the four chromosome 8 copies (Pittman *et al.*, 1993). However, in the karyotypic analysis carried out by Pittman *et al.* (1993), the CCRF-CEM VCR/R cell lines displayed neither polyploid clones nor loss of chromosome 8. The authors therefore suggested that loss of genes on chromosome 8 (e.g. *c-myc*) may facilitate ploidy changes or provide a selective advantage, as near- or pseudo-tetraploid parental cells without loss of chromosome 8 were not observed, and pseudo-tetraploid cells were not observed in CCRF-CEM VCR/R cells with a normal chromosome 8 and a deleted chromosome 8.

However, the COSMIC cell line database does state that the parental CCRF-CEM cells have microsatellite instability (D17S250), 3 mutations on chromosome 8 (WHSC1L1, PCM1 and UBR5) and a small section of chromosome 8 with a copy number gain at 130 Mb, indicating that the cell line tested in the COSMIC database does not have the chromosome 8 abnormalities indicated in previous papers (COSMIC, 2014).

DNA-PK is located on chromosome 8 and the CCRF-CEM cells used in this study have a functional DNA-PK response. The CCRF-CEM VCR/R cells have greater levels of DNA-PKcs protein present but similar levels of *PRKDC* mRNA, so the higher levels of DNA-PKcs protein are unlikely to be due to additional copies of chromosome 8. Also, DNA-PK is located at around 48 Mb on chromosome 8, which is not near the area of copy number variation described on the COSMIC database. However, using fluorescent *in-situ* hybridisation it would be interesting to compare chromosomal abnormalities in the cell line pair used in these studies.

The higher levels of DNA-PKcs and ATM protein detected in the resistant CCRF-CEM VCR/R cell line (Figure 3-1) could indicate that this multidrug-resistant

cell line has acquired higher levels of DNA double-strand break repair capacity. However, the A2780-TX1000 and SKOV3-TR cells did not display higher levels of DNA-PK than their respective parental cell lines, and hence increased DNA-PK appears to be CCRF-CEM VCR/R cell line-specific.

The A2780-TX1000 cells and the SKOV3-TR cells were cultured in the presence of paclitaxel to maintain their multidrug-resistance status, although the cells were cultured in drug-free medium for at least 3 days before experiments were carried out. In contrast, CCRF-CEM VCR/R cells overexpress MDR1 and display resistance properties without the need for the presence of vincristine in their growth medium, indicating a stable change in copy number of *ABCB1*.

The p53 status of the cell lines and their resistant counterparts was determined either from functional studies or published genotypes. The CCRF-CEM cell line pair was p53 non-functional (Figure 3-5), the A2780 cells were p53 wild-type and the A2780-TX1000 cells were p53 non-functional (Figure 3-6), the SKOV3 cell line pair were p53 mutant (COSMIC, 2014) and the KK47 cell line pair were p53 wild-type (Shirakawa *et al.*, 2001). It was important to understand the p53 status of the cells, as p53 is an important protein in cellular responses to anti-cancer agents and the *TP53* gene is commonly mutated in cancer.

However, despite the different p53 status of the cell lines and their drug resistant counterparts, the same pattern of sensitisation to microtubule-targeting agents by 1 µM NU7441 and 10 µM KU55933 was observed throughout. These findings are in line with previous studies demonstrating that cell death caused by tubulin-binding agents can occur through both p53-dependent and p53-independent apoptosis pathways (Woods *et al.*, 1995). Whether NU7441 and KU55933 interact with MDR1, resulting in greater sensitisation in the resistant cell lines, is the focus of investigations described in Chapter 4.

In growth inhibition studies in the parental cell lines, significant vincristine sensitisation by 1 µM NU7441 was only observed in the CCRF-CEM cells. Sensitisation by 10 µM KU55933 in parental cells was observed in the CCRF-CEM cells in response to vincristine, and in the A2780 cells in response to paclitaxel.

The sensitisation caused by 1 µM NU7441 in the CCRF-CEM VCR/R cells was observed with both vincristine and docetaxel. However, the effect of 10 µM KU55933 differed depending on both the microtubule-targeting agent and the cell line. In the CCRF-CEM and CCRF-CEM VCR/R cells, KU55933 (10 µM) sensitised to a greater degree than NU7441 (1 µM) in response to both vincristine and docetaxel. In the A2780

and A2780-TX1000 cells, there was greater sensitisation with KU55933 (10 µM) observed in all combinations apart from A2780 cells treated with vincristine, where no sensitisation was observed with KU55933. Conversely, in the SKOV3 and SKOV3-TR cell line, KU55933 (10 µM) caused similar sensitisation to NU7441 (1 µM) although there was no sensitisation in the SKOV3 cells treated with paclitaxel. Therefore the sensitisation effect with KU55933 is not microtubule-targeting agent-dependent, i.e. it is seen with both a vinca alkaloid and a taxane. The A2780 cells are p53 functional whereas the SKOV3 and CCRF-CEM cells are p53 non-functional. Nevertheless, all the cell types were sensitised to both vincristine and docetaxel by KU55933, indicating that sensitisation is not p53 dependent. According to the COSMIC database (COSMIC, 2014), SKOV3 cells have heterozygous mutations in a number of DNA repair proteins, including ATM, BUB1B, Chk2 and PI3KA, and these mutations could explain the reduced KU55933 effect compared with the other cell lines. For example, if ATM is mutant and non-functional in SKOV3 cells then sensitisation by KU55933 might not be expected.

In the methylcellulose cytotoxicity assay, KU55933 caused sensitisation in CCRF-CEM and CCRF-CEM VCR/R cells in response to vincristine at higher concentrations (Figure 3-13). Sensitisation of A2780 cells with KU55933 was observed with paclitaxel (Figure 3-14), and these results are consistent with the growth-inhibition experiments with KU55933.

DNA-PK autophosphorylation was observed in response to vincristine in a concentration-dependent manner (Figure 3-15). In the Western blotting experiments, cells were treated for 24 hours with vincristine before cell lysates were prepared. Phosphorylation was observed even at concentrations of vincristine below the GI_{50} value (which was calculated after drug treatment for 72 hours) and so the effect is unlikely to be secondary to cytotoxicity and suggests that DNA-PK plays a role in the response of cells to the microtubule-targeting agents.

The observation that total DNA-PKcs decreased in a concentration-dependent manner in response to vincristine treatment in CCRF-CEM cells was not expected (Figure 3-15). Two separate membranes were probed for total and phosphorylated DNA-PK and therefore this result was not a membrane-stripping artefact. The total DNA-PKcs antibody (MS-370-P) used was supplied by Thermo Scientific and is a monoclonal antibody that reacts with an epitope at aa 3198-4127, and only binds to intact DNA-PKcs protein and not its degradation products (Fisher Scientific, 2014). There are two possibilities for the apparent loss of DNA-PK following vincristine

treatment. One possibility is that DNA-PK phosphorylation at serine 2056 prevents MS-370-P antibody binding and this could be investigated using a different total DNA-PKcs antibody. The second possibility is that the DNA-PKcs protein is targeted for degradation in response to vincristine. The apparent molecular weight of the DNA-PKcs was not altered by vincristine treatment and so it is unlikely that extensive ubiquitination was induced; however, ubiquitinated DNA-PKcs might not be detected by the antibody used. Immunoprecipitation of total DNA-PKcs using a number of antibodies followed by Western blotting using a ubiquitin antibody after treatment might elucidate whether DNA-PKcs is being targeted for ubiquitin degradation.

Growth inhibition and clonogenic assay data demonstrated that KU55933 sensitised parental and multidrug-resistant cells to vincristine and docetaxel, suggesting that ATM plays a role in the cellular response to these agents, and hence autophosphorylation of ATM was examined. ATM phosphorylation was investigated by Western blotting for serine 1981 phosphorylation, a site modified in response to DNA damaging agents. Although autophosphorylation of ATM at serine 1981 in response to vincristine was not observed, this does not prove that ATM is not activated and phosphorylation at a different site cannot be excluded.

A publication by Yang *et al.* (2011) investigated the role of ATM in mitosis and identified a new phosphorylation site on ATM that is modified during mitosis in the absence of DNA damage. These authors demonstrated weak ATM serine 1981 phosphorylation in mitotic cells in the absence of DNA damage, and Aurora-B kinase was identified as being activated in mitosis and required for mitotic ATM activation. Yang *et al.* (2011) also demonstrated that Aurora-B kinase phosphorylates ATM on serine 1403, which was required for mitotic ATM activation and the spindle checkpoint. Based on these findings it is possible that vincristine treatment, which interferes with the mitotic spindle and mitotic progression, may be activating ATM at the serine 1403 phosphorylation site, independent of serine 1981 phosphorylation. Unfortunately, there are no commercially-available phospho-specific antibodies to the serine 1403 site on ATM, so ATM activation at this site could not be investigated. Knockdown of Aurora-B kinase could be achieved using siRNA followed by vincristine treatment alone or in the presence of KU55933, to investigate whether vincristine-induced growth inhibition of cells is altered, and whether the sensitisation effects of KU55933 involve Aurora-B kinase-dependent mitotic ATM activity. In this context, studies with Aurora-B kinase inhibitors could also be performed.

The Caspase Glo assay was used in this study to investigate caspase 3/7-mediated programmed cell death in response to microtubule-targeting agents alone and in combination with NU7441 or KU55933. Vincristine, paclitaxel and docetaxel increased caspase 3/7-mediated apoptosis in both sensitive and multidrug-resistant cells, indicating that caspase 3/7-mediated cell death is a mechanism activated in response to these agents. However, NU7441 (1 µM) co-treatment did not increase caspase 3/7-mediated apoptosis to a degree that corresponded to the level of sensitisation observed in the growth inhibition assays. Interestingly, in the CCRF-CEM cells, a greater relative increase in the vincristine-induced caspase 3/7 activation was observed with 1 µM NU7441 than in the CCRF-CEM VCR/R cells, whereas in the growth inhibition experiments the impact of NU7441 was greater in the resistant cell line.

KU55933 was found to interfere with the Caspase-Glo assay and produce a luminescent signal when no cells were present and so caspase 3/7 activation would need to be investigated using a different technique, for example, Western blotting using caspase 3 and caspase 7 antibodies. Alternatively, apoptosis could be studied by Annexin V staining, PARP cleavage or flow cytometric measurement of the sub-G1 population.

Although vinca alkaloids and taxanes have previously been reported to induce apoptosis *via* caspase 3/7-mediated apoptosis, other mechanisms of cell death in response to microtubule-targeting agents have been demonstrated that are caspase-independent, including lysosomal cathepsin B-mediated cell death or mitotic catastrophe (Broker *et al.*, 2004; Morse *et al.*, 2005). The mechanisms were not studied here but cathepsin B activity could be measured using a commercially available fluorometric kit in which the synthetic substrate RR-AFC (amino-4-trifluoromethyl coumarin) is cleaved to AFC by cathepsin B, and AFC quantified using a fluorescent plate reader (Abcam Cathepsin B Activity Assay Kit).

The COMET assay results demonstrated that as expected the microtubule-targeting agents, vincristine and docetaxel, were not causing any DNA damage breaks, and therefore the mechanism of cell death may be distinct from a DNA-damage-induced mechanism.

Mitotic catastrophe is a complex process and not easily measured. Mitotic catastrophe is defined as abnormal mitosis characterised by micronucleated cells that continue with mitosis and generate aneuploidy that leads to cell death, *via* necrosis or apoptosis, or permanent growth arrest (reviewed in Al-Ejeh *et al.* (2010)). Methods to measure mitotic catastrophe involve the morphological evaluation of cells by

microscopy which are defined as being normal mitotic, aberrant mitotic or as having micronuclei (Morse *et al.*, 2005). Alternatively, time-lapse microscopy can be used, as described by Shang *et al.* (2010), who demonstrated that inactivation of DNA-PK caused mitotic catastrophe in response to DNA damage. This latter study highlights the role of DNA-PK in preventing mitotic catastrophe and the investigation of mitotic catastrophe would be a relevant extension of the studies described here. In this regard, cellular morphology was examined by confocal microscopy in the HCT116 cell line after treatment with ionising radiation and vincristine as described in Chapter 7.

Cancers that are resistant to apoptosis due to, for example, therapy-induced changes in Bcl-2 or p53 function, may benefit from treatments that promote other mechanisms of cell death, such as mitotic catastrophe (Gewirtz, 2000; Al-Ejeh *et al.*, 2010). Three human breast cancer cell lines with varying levels of Bcl-2 or p53 expression underwent mitotic catastrophe following docetaxel treatment, and it was suggested that targeting the mitotic spindle assembly may be an effective approach to killing apoptosis-resistant cells (Morse *et al.*, 2005). If DNA-PK and ATM are found to play a role in the mitotic spindle, and that inhibition leads to mitotic catastrophe, the therapeutic potential of inhibition of DNA repair proteins could be extended to the treatment of apoptosis-resistant cancers, and could be an additional mechanism for the sensitisation of cells to microtubule-targeting agents.

Although the growth inhibition and cytotoxicity data demonstrated the significant effects of NU7441 and KU55933 in enhancing the activity of microtubule-targeting agents *in vitro*, sensitisation should be confirmed in an *in vivo* setting.

An *in vivo* study design could involve wild-type and multidrug-resistant cells such as the ovarian A2780 and A2780-TX1000 implanted to create xenografts followed by treatment with paclitaxel and inhibitors of DNA-PK and ATM. Mice would be treated with either inhibitor alone, paclitaxel alone or a combination of DNA-PK or ATM inhibitors and paclitaxel. Tumour growth would be recorded and also *ex vivo* pharmacodynamic studies of phosphorylated DNA-PK and phosphorylated ATM performed in tumour samples and normal tissue, as well as the evaluation of markers of proliferation and apoptosis. Furthermore, the pharmacokinetics and toxicity of paclitaxel given in combination with these inhibitors should be investigated because, as described in Chapter 4, these inhibitors affect drug efflux *via* the drug efflux pump MDR1 and therefore toxicity may be enhanced in normal MDR1-expressing cells, such as the gastrointestinal tract.

3.5   Summary

The DNA-PK inhibitor, NU7441 (1 µM), and the ATM inhibitor, KU55933 (10 µM), were tested in combination with microtubule-targeting agents in a panel of sensitive and multidrug-resistant cell lines. KU55933 (10 µM) caused greater sensitisation than NU7441 (1 µM) in parental and multidrug-resistant cells. The sensitisation effects demonstrated in the multidrug-resistant cell lines by both inhibitors was greater than the sensitisation seen in the parental cells. DNA-PK was phosphorylated at an autophosphorylation site following vincristine treatment in a concentration-dependent manner, and phosphorylation was inhibited by NU7441. The microtubule-targeting agents caused an increase in caspase 3/7 activity, and vincristine and docetaxel did not cause DNA damage, as measured by the COMET assay. These findings highlight possible roles for DNA-PK and ATM in the response of cells to microtubule-targeting agents, which will be investigated further in the following chapters.

Chapter 4: Identification of dual DNA-PK and MDR1 inhibitors, and ATM kinase and MDR1 inhibitors, for the potentiation of cytotoxic drug activity

4.1 Introduction

The results in Chapter 3 demonstrated that the small molecule inhibitors NU7441 and KU55933 caused greater sensitisation to vincristine, docetaxel and paclitaxel in three different multidrug-resistant cell lines compared with their parental cell lines. The multidrug-resistant cells are resistant through the overexpression of the efflux protein MDR1 (Figure 3-1, Figure 3-2) and the microtubule-targeting agents are known to be subject to efflux by MDR1. Therefore the studies described in this chapter tested the hypothesis that NU7441 and KU55933 may be interfering with drug efflux *via* MDR1 in the multidrug-resistant cells.

MDR1/P-glycoprotein (the product of the *ABCB1/MDR1* gene) was the first member of the (ATP)-binding cassette (ABC) superfamily of transmembrane transporters to be cloned, and is known to play a significant role in the multidrug-resistance (MDR) phenotype in cancer cells (Chen *et al.*, 1986). MDR1 is a 170 kDa protein located in the apical membrane of many cell types which acts as a drug efflux transporter in the liver, kidneys, gastrointestinal tract, and multiple blood barriers including the blood-brain and the blood-placental barriers (Sikic *et al.*, 1997; Gottesman *et al.*, 2002). MDR1 is known to confer resistance to a number of anticancer agents, including the vinca alkaloids, taxanes and anthracyclines (Allen *et al.*, 2000).

Verapamil, a calcium channel blocker used clinically as a coronary vasodilator, was amongst the first compounds identified that could reverse MDR and potentiate the effects of MDR1 substrates such as vincristine (Tsuruo *et al.*, 1981; Tsuruo *et al.*, 1983). Verapamil, along with a number of other MDR1 blockers, have proved largely unsuccessful in clinical trials due to toxicity or side effects (Szakacs *et al.*, 2006). In the current chapter, verapamil was used as a positive control as it is known to interfere with drug efflux *via* MDR1.

NU7441 is a potent ATP-competitive DNA-PK inhibitor (IC_{50} = 14 nM) (Leahy *et al.*, 2004). NDD0004 (DNA-PK IC_{50} = 10 nM) is a more potent, selective and soluble version of NU7441 (unpublished results). In order to allow investigation into structural properties and DNA-PK inhibitory effects that may affect any interaction with MDR1, it was possible to obtain three NU7441 derivatives, described in detail in Chapter 1. Briefly, NU7742 is an inactive derivative of NU7441 (IC_{50} > 10 µM) in which the morpholine oxygen has been replaced with a methylene group and the atropisomers DRN1 (DNA-PK IC_{50} = 2 nM) and DRN2 (DNA-PK IC_{50} = 7 µM) have a methyl substituent at the 7-position of the chromen-4-one ring and DNA-PK inhibitory activity

resides exclusively in the laevorotatory enantiomer DRN1 (Clapham *et al.*, 2012). KU55933 is an ATP-competitive, potent inhibitor of ATM kinase (IC_{50} = 13 nM) (Hickson *et al.*, 2004).

Neither NU7441 nor KU55933 have previously been investigated in relation to transporters and drug efflux. However, there have recently been a number of publications reporting that targeted anticancer therapies can reverse MDR by inhibiting the efflux functions of the ABC family of transporters, including ABCB1 (MDR1). Thus the kinase inhibitors imatinib and nilotinib (BCR-Abl inhibitors) (Hegedus *et al.*, 2009), gefitinib and erlotinib (EGFR inhibitors) (Kitazaki, 2005; Shi *et al.*, 2007), lapatinib (Her-2 inhibitor) (Dai *et al.*, 2008), apatinib (VEGFR2 inhibitor) (Mi *et al.*, 2010), and sorafenib (multi-tyrosine and Raf kinases inhibitor) (Eum *et al.*, 2013) have all been shown to be potent inhibitors of ABCB1.

4.2   Aims

Following observations that the DNA-PK inhibitor NU7441 and the ATM inhibitor KU55933 caused greater sensitisation to cytotoxic agents in MDR1-overexpressing *versus* non-overexpressing cells (Chapter 3), this study aimed to investigate whether NU7441 or KU55933 were enhancing activity by interacting with MDR1. In order to test this hypothesis, doxorubicin accumulation in combination with NU7441, NDD0004 or the positive control verapamil was measured using the MDCKII and the MDR1-overexpressing MDCKII-MDR1 cells. The growth-inhibitory and activation-inhibitory status of the different compounds was investigated in the CCRF-CEM and CCRF-CEM VCR/R cells. Intracellular vincristine, NU7441, NU7441 analogues and KU55933 drug concentrations were measured quantitatively by LC-MS.

4.3   Results

4.3.1   NU7441 and KU55933 alone are not substrates for MDR1

The growth inhibitory activity of NU7441, KU55933 and verapamil alone in CCRF-CEM parental cells and the paired multidrug-resistant CCRF-CEM VCR/R cells was determined by XTT growth inhibition assay, to determine whether NU7441 and KU55933 were substrates for MDR1. If these compounds were MDR1 substrates, it would be expected that the multidrug-resistant cells would be resistant to NU7441 and KU55933. Thus the compounds would be actively transported out of the cells and intracellular drug concentrations would be lower, resulting in reduced growth inhibition. However, Figure 4-1 demonstrates that there was no difference in the growth inhibitory effects of NU7441 or KU55933 in the parental and multidrug-resistant cells (NU7441 GI_{50} 4.0 µM and 3.7 µM, respectively) (KU55933 GI_{50} 17.9 µM and 17.0 µM, respectively), suggesting that these compounds are not substrates of MDR1. Verapamil was included as a positive control as it is known to be a competitive substrate of MDR1; however it was not possible to compare the growth inhibitory effects of verapamil as there was no effect on either cell line up to 50 µM.
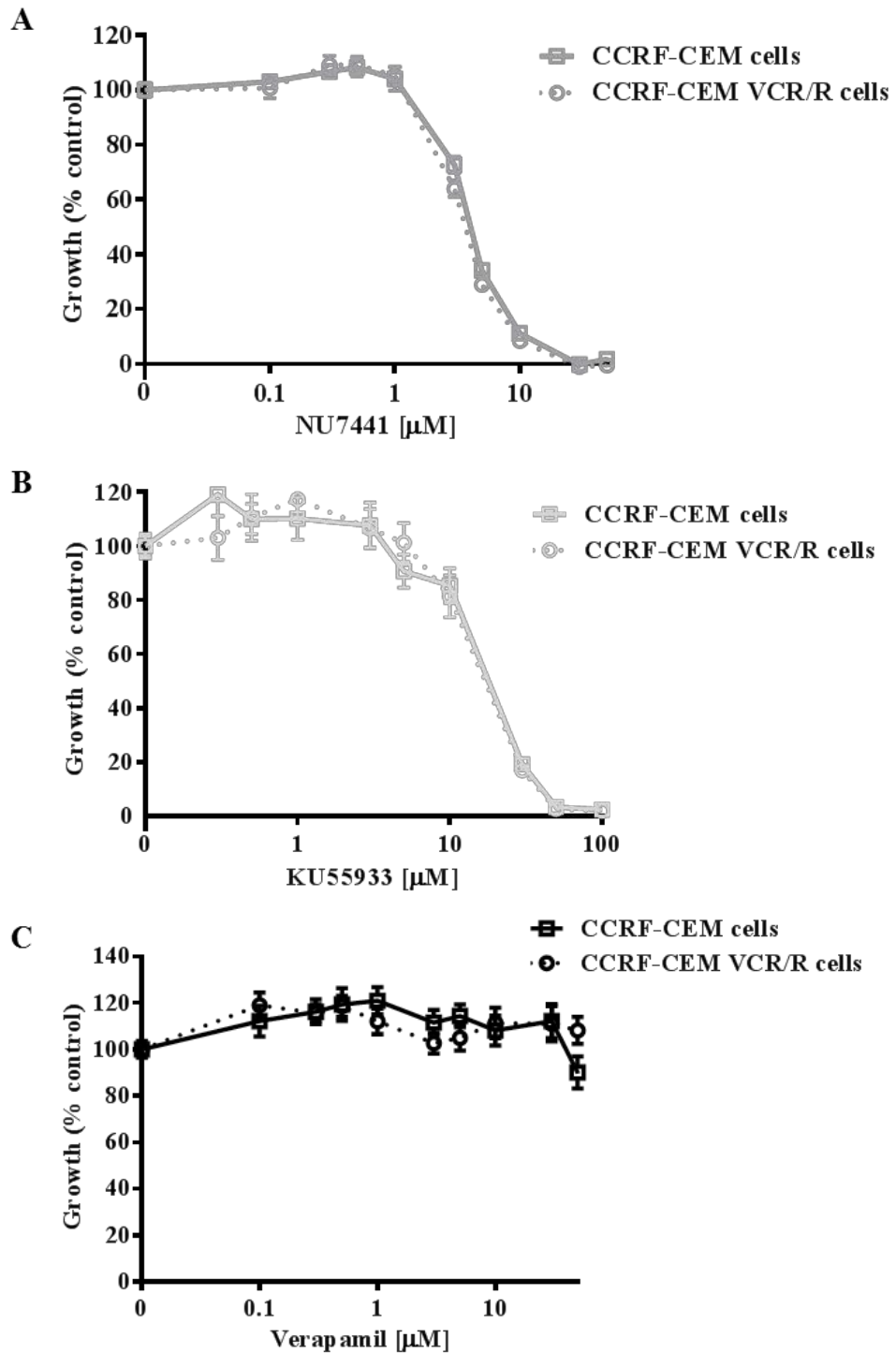
Figure 4-1: NU7441 and KU55933 are not substrates of MDR1. CCRF-CEM (square points) and CCRF-CEM VCR/R (round points) cells were treated with (**A**) NU7441, (**B**) KU55933 and (**C**) verapamil at the indicated concentrations for 72 hours and % growth was analysed by XTT assay (Section 2.3). The data are presented as a percentage of vehicle control cells. Points represent the mean of ≥3 independent experiments, each in triplicate ± standard error.

4.3.2 The DNA-PK inhibitors NU7441 and NDD0004 interact with MDR1 to increase nuclear doxorubicin accumulation in MDR1-overexpressing MDCKII-MDR1 cells

To investigate the interaction of NU7441 with MDR1, a doxorubicin (DOX) fluorescence assay was performed. Doxorubicin is a fluorescent cytotoxic MDR1 substrate and this assay measured doxorubicin fluorescence levels in the nucleus using an MDR1-overexpressing cell line paired with its parental counterpart.

The MDCKII and MDCKII-MDR1 cells were obtained from Alfred Schinkel (Netherlands Cancer Institute). These cells are a Madin-Darby canine kidney strain II cell line, and the MDCKII-MDR1 subline overexpresses the human *MDR1* gene due to transfection (Evers *et al.*, 1998). This MDR1-overexpressing cell line is a useful model as it means any effects seen, by comparison with the parental cells, be attributed to MDR1 alone. The cells were characterised by demonstrating human MDR1 protein overexpression (Figure 4-2) and human *ABCB1* mRNA expression (Table 4-1) in the MDCKII-MDR1 cells.
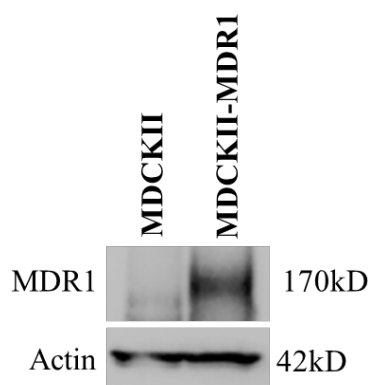
Figure 4-2: Human MDR1 protein is overexpressed in MDCKII-MDR1 cells.
MDCKII and MDCKII-MDR1 cell lysates were prepared from exponentially-growing cells and MDR1 expression was determined by Western blotting using the indicated specific antibodies (Section 2.7.4). Data represents findings of 3 independent experiments.

The mRNA data in Table 4-1 cannot be displayed as relative to the control cells because the primers for the β-actin housekeeping gene only recognise human β-actin and not canine. There was no human *ABCB1* mRNA detected in the parental MDCKII cells up to the end of the 40 cycles of the PCR, whereas it was detectable after 20 cycles in the MDCKII-MDR1 cells.

Cell line	Gene	Cycle threshold value
MDCKII	*ABCB1*	>40
MDCKII-MDR1	*ABCB1*	20

Table 4-1: Cycle threshold value of human *ABCB1* in MDCKII and MDCKII-MDR1 cells. Taqman real-time PCR of MDCKII and MDCKII-MDR1 examining human *ABCB1* mRNA expression (Section 2.9.5). The cycle threshold value was determined by 7500 Fast RT PCR system.

The effect of NU7441 on nuclear doxorubicin accumulation was examined using the nuclear doxorubicin fluorescence assay. Nuclei were stained with DAPI (blue) and doxorubicin naturally fluoresces red. Verapamil was used as a positive control compound as it is known to interact with MDR1 and cause intracellular accumulation of MDR1 substrates (including doxorubicin) (Tsuruo *et al.*, 1983).

NDD0004 (synthesised in the chemistry department of the Newcastle Cancer Centre) is a DNA-PK inhibitor based on NU7441 but with a HAT morpholine structure and a water-solubilising group which increases potency, selectivity and solubility. NDD0004 was included in this experiment as this compound has subsequently been used by others in Newcastle Cancer Centre and it was necessary to determine if there was any interaction with MDR1, but its use was not continued in this PhD work as extensive work had already been carried out with NU7441.

There was less doxorubicin detectable in the MDCKII-MDR1 cells compared with the MDCKII cells, reflecting the greater efflux of doxorubicin by MDR1 (see images for cells treated with DOX alone in Figure 4-3 and Figure 4-4). There was a concentration-dependent increase in doxorubicin fluorescence in the MDCKII-MDR1 cells with the addition of the competitive MDR1 substrate, verapamil; a 1.6-fold (p=0.01) increase at 10 µM (Figure 4-4). There was also a concentration-dependent increase in nuclear doxorubicin accumulation, consistent with inhibition of efflux, following the addition of NU7441 and NDD0004 (Figure 4-4). Thus there was a significant 1.2-fold (p=0.02) increase in doxorubicin fluorescence at 1 µM NU7441, which is the concentration previously shown to be optimal for DNA-PK inhibition with no cellular toxicity (Zhao *et al.*, 2006). There was a 1.4-fold (p=0.04) increase in doxorubicin fluorescence in the presence of 1 µM NDD0004; however, in contrast to the MDCKII-MDR1 cells there was no significant change in doxorubicin fluorescence with either verapamil or NU7441 in the MDCKII cells (Figure 4-3), consistent with the

effect seen in the MDCKII-MDR1 cells being due to NU7441 interacting with MDR1 and the blockade of doxorubicin efflux from these cells.
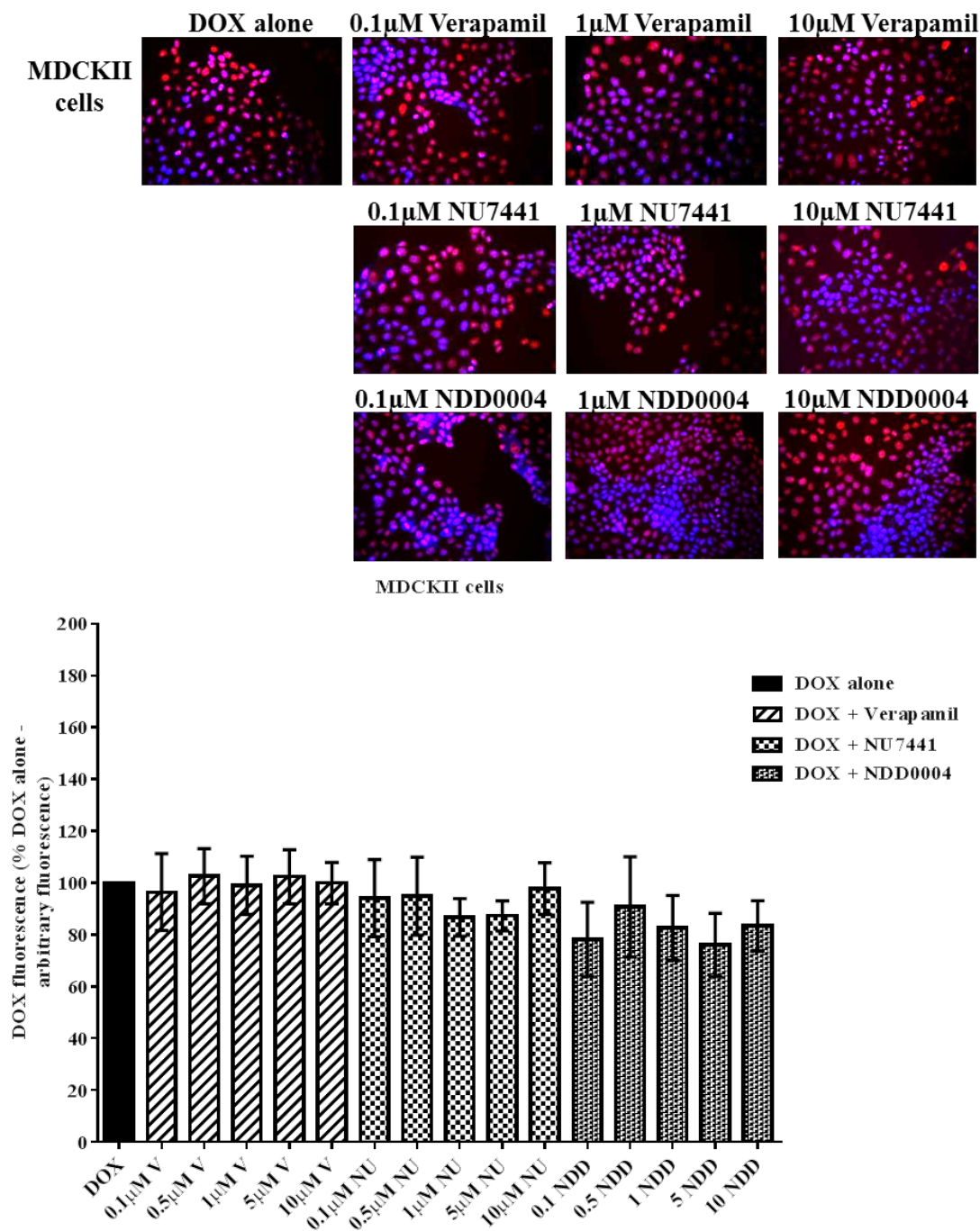
Figure 4-3: Verapamil, NU7441 and NDD0004 have no effect on doxorubicin fluorescence in MDCKII cells. MDCKII cells were treated with 0.1, 0.5, 1, 5, 10 µM verapamil (striped bars), NU7441 (hatched bars) or NDD0004 (spotted bars) for 1 hour followed by 10 µM doxorubicin (DOX) for 1 hour. Cells were fixed and stained with DAPI and DOX nuclear fluorescence was detected on a BD pathway HT microscope (Section 2.10). Representative images show DAPI (blue) and doxorubicin (red) fluorescence. Results are mean ± standard error of three independent experiments.
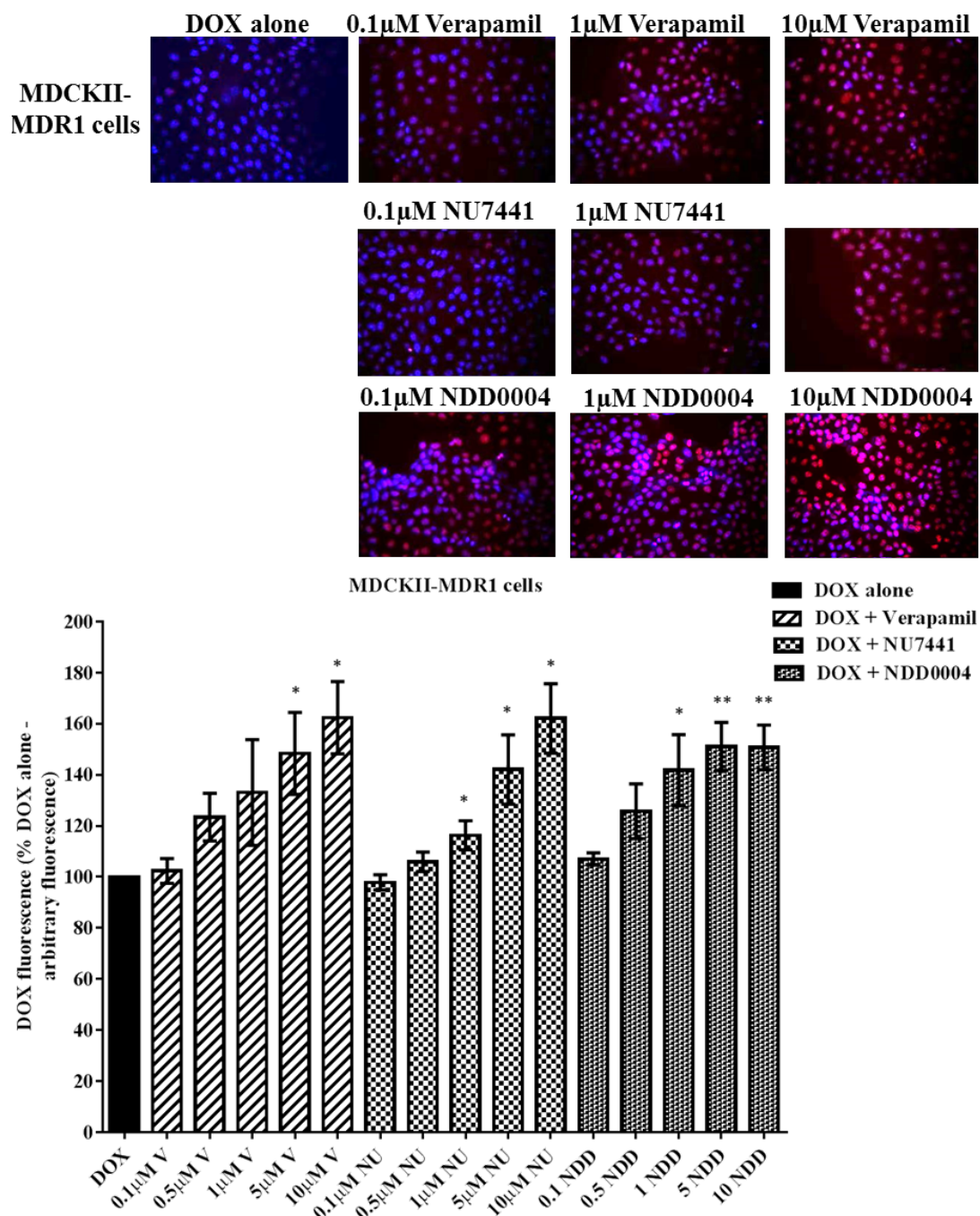
Figure 4-4: Verapamil, NU7441 and NDD0004 cause a concentration-dependent increase in doxorubicin fluorescence in MDCKII-MDR1 cells. MDCKII-MDR1 cells were treated with 0.1, 0.5, 1, 5, 10 µM verapamil (striped bars), NU7441 (hatched bars) or NDD0004 (spotted bars) for 1 hour followed by 10 µM doxorubicin (DOX) for 1 hour. Cells were fixed and stained with DAPI and DOX nuclear fluorescence was detected on a BD pathway HT microscope (Section 2.10). Representative images show DAPI (blue) and doxorubicin (red) fluorescence. Results are mean ± standard error of three independent experiments. Asterisk indicates a statistically significant difference (* $p<0.05$, ** $p<0.01$).

4.3.3 The effect of DNA-PK inhibitory and non-inhibitory compounds on DNA-PK activation and cell growth alone and in combination with vincristine or docetaxel in CCRF-CEM and CCRF-CEM VCR/R cells

Following the observation that NU7441 was interacting with MDR1 to increase doxorubicin nuclear accumulation, it was necessary to determine if the effect of NU7441 was direct or mediated indirectly following DNA-PK inhibition. To do so a panel of NU7441 derivatives with different DNA-PK inhibitory properties was used. It is known that the morpholine group is necessary for the DNA-PK inhibitory activity of NU7441 (DNA-PK IC_{50} = 14 nM) (Hardcastle *et al.*, 2005), as replacement of the morpholine oxygen with a methylene group results in loss of activity as seen with NU7742 (DNA-PK IC_{50} > 10 µM). Two atropisomeric derivatives of NU7441, DRN1 and DRN2, were used in these studies (Clapham *et al.*, 2012). Introduction of a methyl substituent at the 7-position of the chromen-4-one ring restricts rotation between the dibenzothiophene and the chromenone rings causing atropisomerism. DRN1 is the laevorotatory enantiomer, showing high potency against DNA-PK (IC_{50} = 2 nM), whereas the dextrorotatory enantiomer, DRN2, has markedly reduced inhibitory activity (IC_{50} = 7 µM). The ATM inhibitor, KU55933 is in general terms structurally similar to NU7441 and its derivatives.

The DNA-PK inhibitory properties of the NU7441 derivatives in the CCRF-CEM and CCRF-CEM VCR/R cells were determined by Western blotting. DNA-PK was activated by doxorubicin, a known DNA-PK-activating agent (Shaheen *et al.*, 2011), and the drug that was used in the fluorescence microscopy. Vincristine was also used as a positive control as results in Chapter 3 demonstrated that vincristine activates DNA-PK. Vincristine was used in the LC-MS experiments described below. Both CCRF-CEM and CCRF-CEM VCR/R cell lines have basal DNA-PK activity as demonstrated by detection of DNA-PK phosphorylated at serine 2056, a site of DNA-PK autophosphorylation. Cells were treated with GI_{50} doxorubicin (40 nM in CCRF-CEM cells, 2 µM in CCRF-CEM VCR/R cells) or vincristine concentrations (0.5 nM in CCRF-CEM cells, 2 µM in CCRF-CEM VCR/R cells) both alone and in combination with 1 µM NU7441, NU7742, DRN1, DRN2 or verapamil. NU7441 and DRN1 significantly inhibited DNA-PK activity in both cell lines, whereas NU7742, DRN2 and verapamil had no effect on DNA-PK phosphorylation (Figure 4-5).
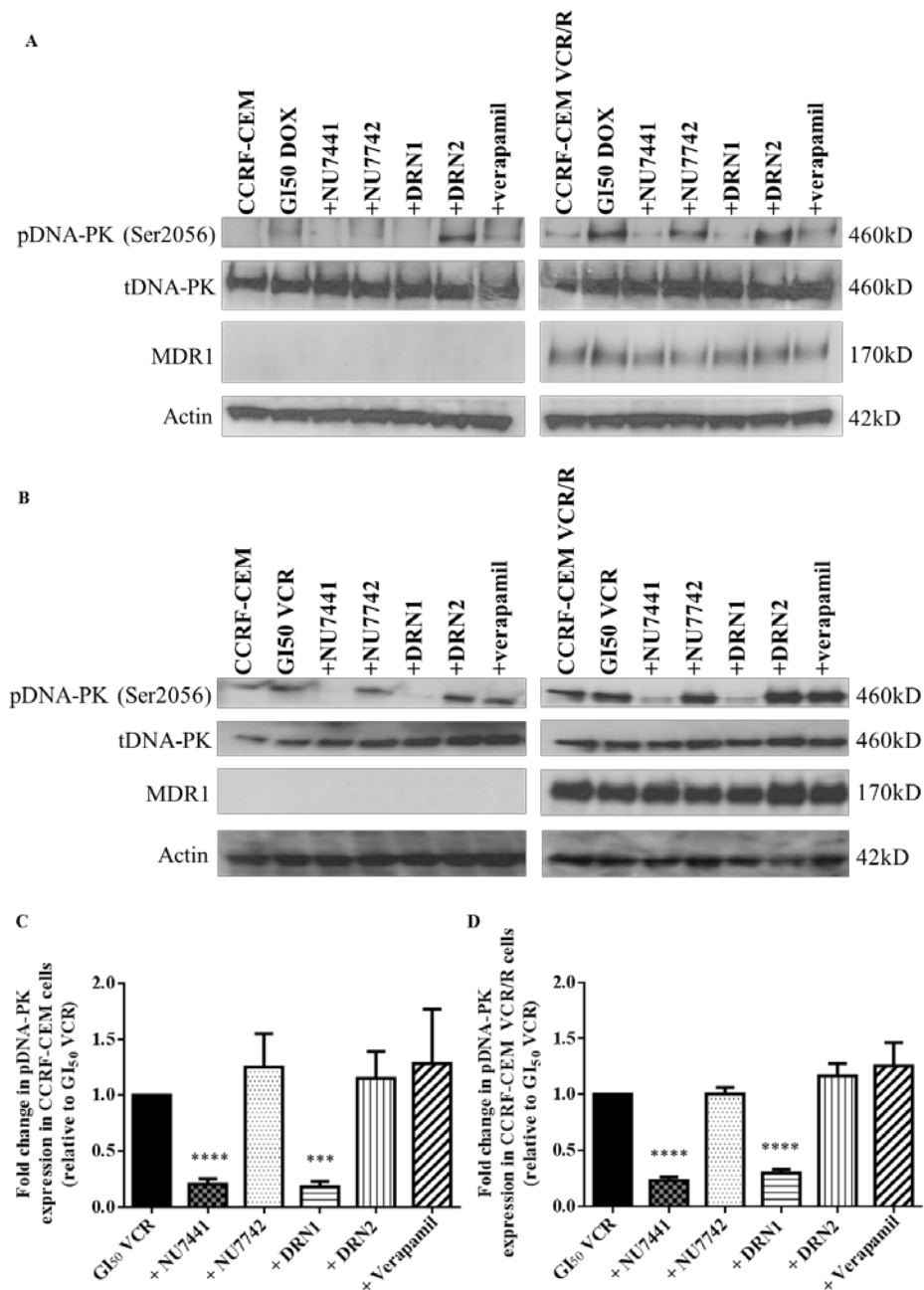
Figure 4-5: Effect of NU7441, NU7742, DRN1 and DRN2 on drug-induced DNA-PK activation. CCRF-CEM and CCRF-CEM VCR/R cells were treated for 8 hours with GI_{50} concentrations of (**A**) doxorubicin (DOX) or (**B**) vincristine (VCR) alone or in combination with 1 μM NU7441, NU7742, DRN1, DRN2 or verapamil. Cell lysates were prepared and DNA-PK activity and expression, and MDR1 expression, were determined by Western blotting using the indicated antibodies (Section 2.7.4). Each blot represents findings of 3 independent experiments. (**C**) and (**D**) Quantification by densitometry of 3 independent Western blots for GI_{50} VCR, + NU7441 and + NU7742 and 2 independent experiments for + DRN1, + DRN2 and + verapamil displayed as the fold change in pDNA-PK level relative to the level in cells treated with GI_{50} VCR alone. Asterisk indicates a statistically significant difference using the Student's unpaired t-test when compared with the data for GI_{50} VCR alone (*** $p<0.001$, **** $p<0.0001$).

121

The growth inhibitory properties of the inhibitors were then examined in combination with vincristine or docetaxel in CCRF-CEM and CCRF-CEM VCR/R cells shown in Figure 4-6 to Figure 4-9, and the data are summarised in Figure 4-10 and presented in a tabular format (Table 4-2).

In the following graphs, 1 µM NU7441 and 10 µM KU55933 are displayed as solid lines with the other inhibitors and/or concentrations appearing as dashed lines (Figure 4-6 to Figure 4-9). Fold sensitisation was calculated from the 50 % growth-inhibitory concentration and the *p*-value is calculated using an unpaired Student's *t*-test (Figure 4-10, Table 4-2).

None of the inhibitors were growth inhibitory when used alone in CCRF-CEM or CCRF-CEM VCR/R cells alone. In the CCRF-CEM cells, there was a significant 1.4-fold (p=0.02) sensitisation in vincristine GI_{50} with NU7441 (Figure 4-6). 1 µM KU55933 was included for comparison with the LC-MS data (Section 4.3.4), and this concentration did not sensitise CCRF-CEM cells; however, 10 µM KU55933 did cause a 5.2-fold (p=0.0006) sensitisation to vincristine in CCRF-CEM cells.
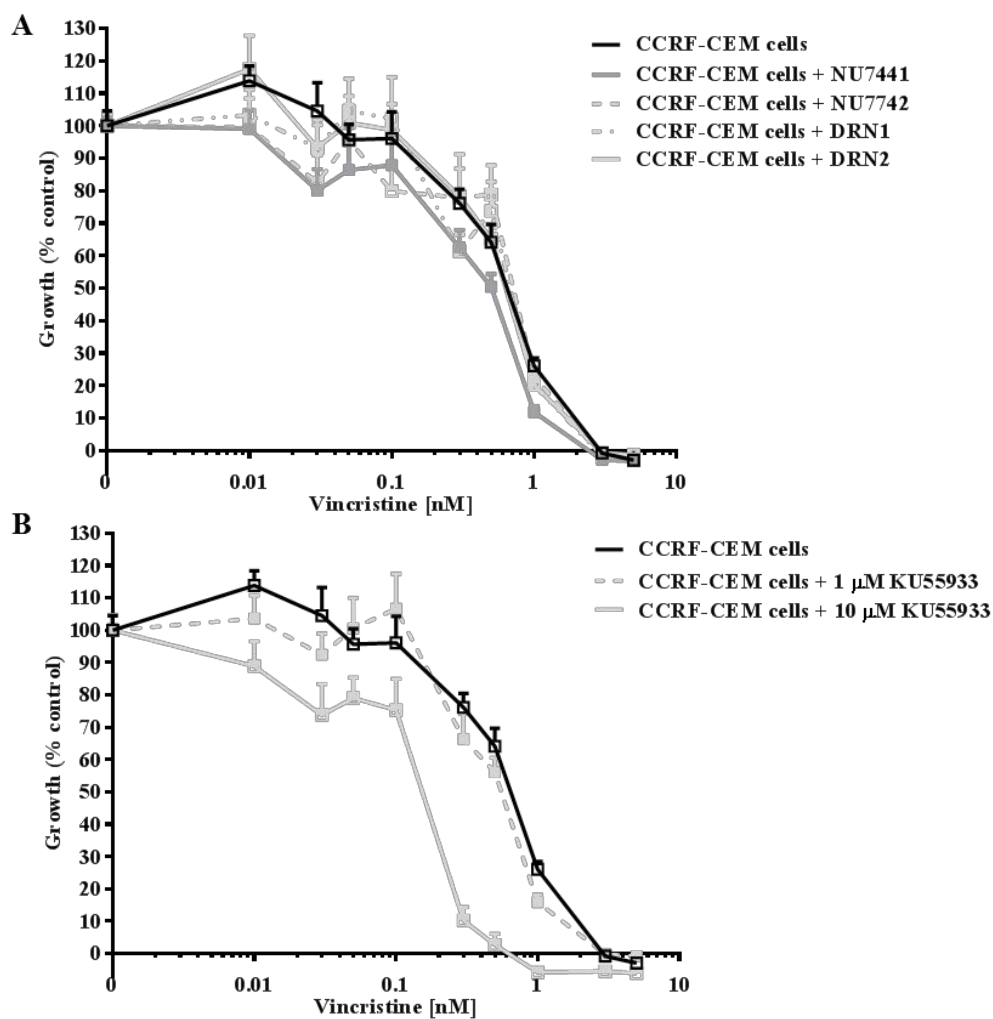
Figure 4-6: CCRF-CEM cells are significantly sensitised to vincristine by 1 μM NU7441 and 10 μM KU55933. CCRF-CEM cells were treated with vincristine alone or in combination with (**A**) 1 μM NU7441, NU7742, DRN1, DRN2 or (**B**) 1 μM or 10 μM KU55933 for 72 hours and % growth was analysed by XTT assay (Section 2.3). The data are presented as a percentage of vehicle control cells. Points represent the mean of ≥3 independent experiments, each in triplicate, ± standard error.

As previously discussed in Chapter 3, the CCRF-CEM VCR/R cells were approximately 3000-fold (p=0.02) resistant to vincristine compared with the parental CCRF-CEM cells (Figure 4-7). There was significant sensitisation at the GI_{50} concentration to vincristine by NU7441 (7.7-fold, p=0.01), NU7742 (3.3-fold, p=0.02), DRN1 (2.6-fold, p=0.04) and 10 µM KU55933 (49-fold, p=0.006), which contrasts with data for the parental cell line (Figure 4-6) where only1 µM NU7441 and 10 µM KU55933 caused sensitisation.
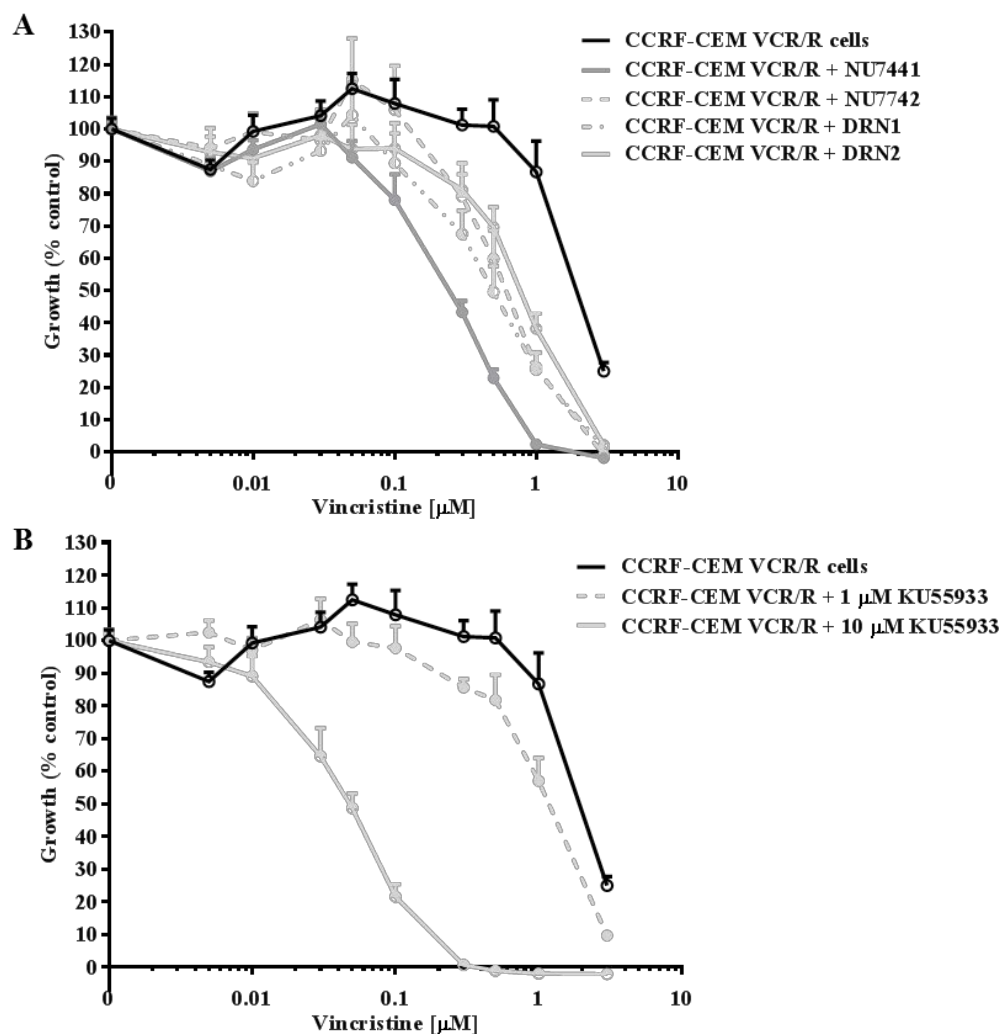
Figure 4-7: CCRF-CEM VCR/R cells are sensitised to vincristine by DNA-PK and ATM inhibitors. CCRF-CEM VCR/R cells were treated with vincristine alone or in combination with (**A**) 1 µM NU7441, NU7742, DRN1, DRN2 or (**B**) 1 µM or 10 µM KU55933 for 72 hours and % growth was analysed by XTT assay (Section 2.3). The data are presented as a percentage of vehicle control cells. Points represent the mean of ≥3 independent experiments, each in triplicate, ± standard error.

Growth inhibition was also examined with the inhibitors in combination with a second microtubule-targeting agent, docetaxel. None of the DNA-PK or ATM inhibitors had a significant effect on the GI_{50} value for docetaxel of the parental CCRF-CEM cell line (Figure 4-8).
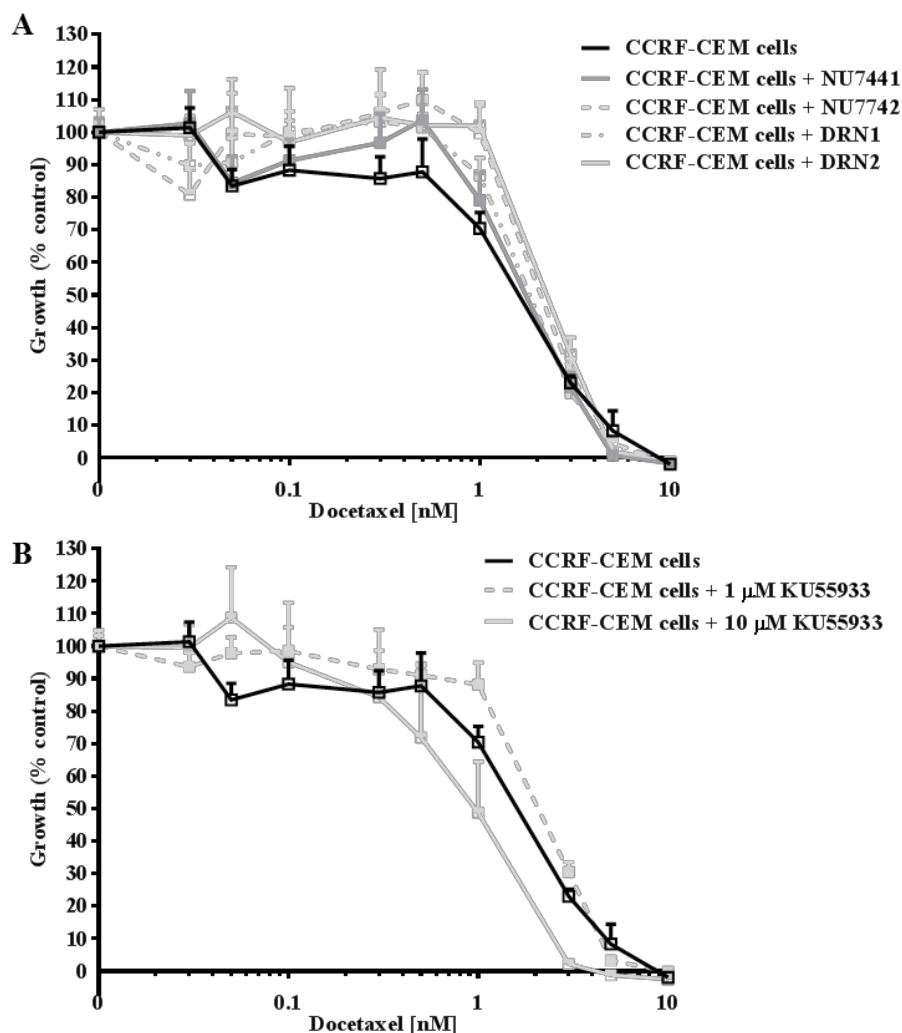
Figure 4-8: CCRF-CEM cells are not sensitised to docetaxel by DNA-PK and ATM inhibitors. CCRF-CEM cells were treated with docetaxel alone or in combination with (**A**) 1 µM NU7441, NU7742, DRN1, DRN2 or (**B**) 1 µM or 10 µM KU55933 for 72 hours and % growth was analysed by XTT assay (Section 2.3). The data are presented as a percentage of vehicle control cells. Points represent the mean of $\geq$3 independent experiments, each in triplicate, $\pm$ standard error.

The CCRF-CEM VCR/R cells were 133-fold (p=0.006) resistant to docetaxel compared with the parental CCRF-CEM cell line. Sensitivity to docetaxel was greater in combination with NU7441 (8.1-fold, p=0.003), NU7742 (3.1-fold, p=0.01), DRN2 (1.8-fold, p=0.048) and 10 µM KU55933 (58-fold, p=0.002) (Figure 4-9).
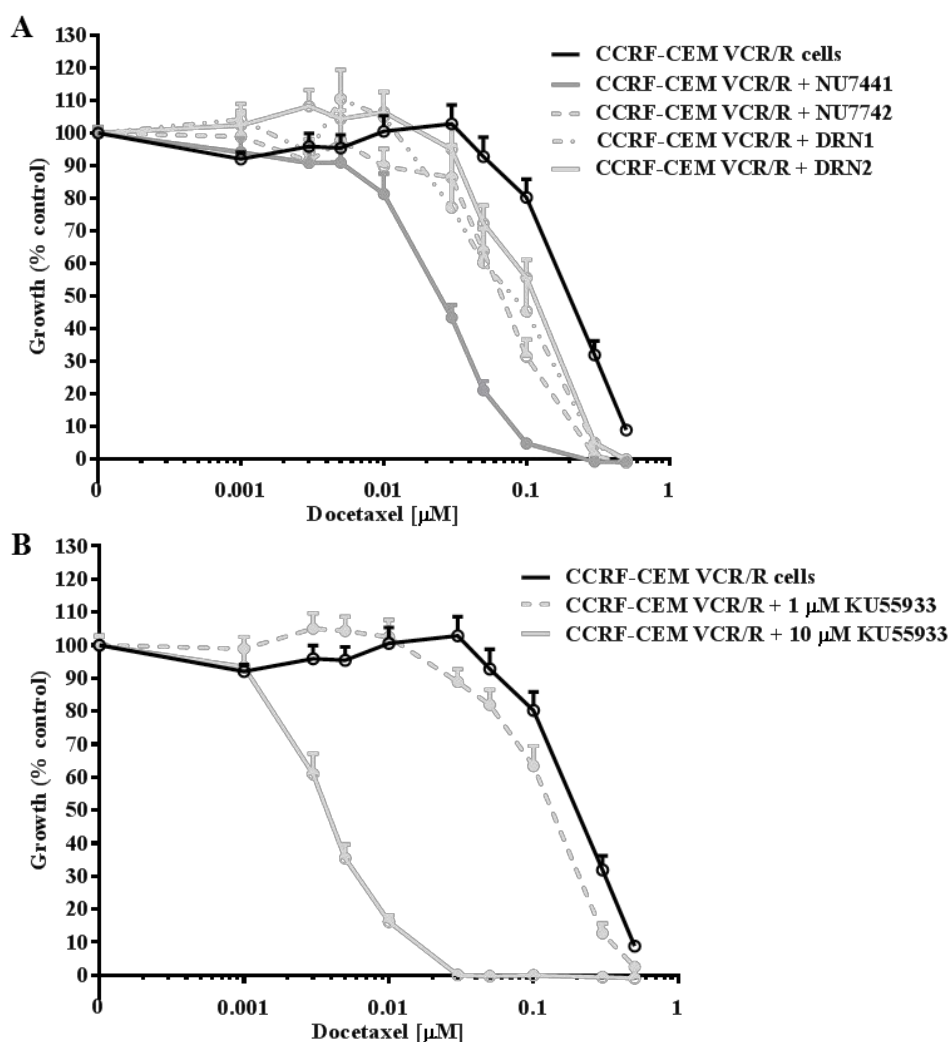
Figure 4-9: CCRF-CEM VCR/R cells are sensitised to docetaxel by DNA-PK and ATM inhibitors. CCRF-CEM VCR/R cells were treated with docetaxel alone or in combination with (**A**) 1 µM NU7441, NU7742, DRN1, DRN2 or (**B**) 1 µM or 10 µM KU55933 for 72 hours and % growth was analysed by XTT assay (Section 2.3). The data are presented as a percentage of vehicle control cells. Points represent the mean of ≥3 independent experiments, each in triplicate, ± standard error.

The GI_{50} concentrations for vincristine or docetaxel alone and in combination with DNA-PK and ATM inhibitors in both cell lines with all of the different treatments are displayed graphically in Figure 4-10 and values given in Table 4-2. Sensitisation effects in the CCRF-CEM VCR/R cells with the inhibitors in combination for both vincristine and docetaxel was much greater than in the CCRF-CEM cells, with 1 µM

NU7441 and 10 µM KU55933 inducing the greatest sensitisation. There is a noticeable difference between the effects of the DNA-PK-inhibitory NU7441 and DNA-PK non-inhibitory NU7742 compounds, which suggests a role of DNA-PK in the sensitisation observed in these cell lines. However, there were no observable differences between the DNA-PK inhibitory DRN1 and non-inhibitory DRN2 compounds.
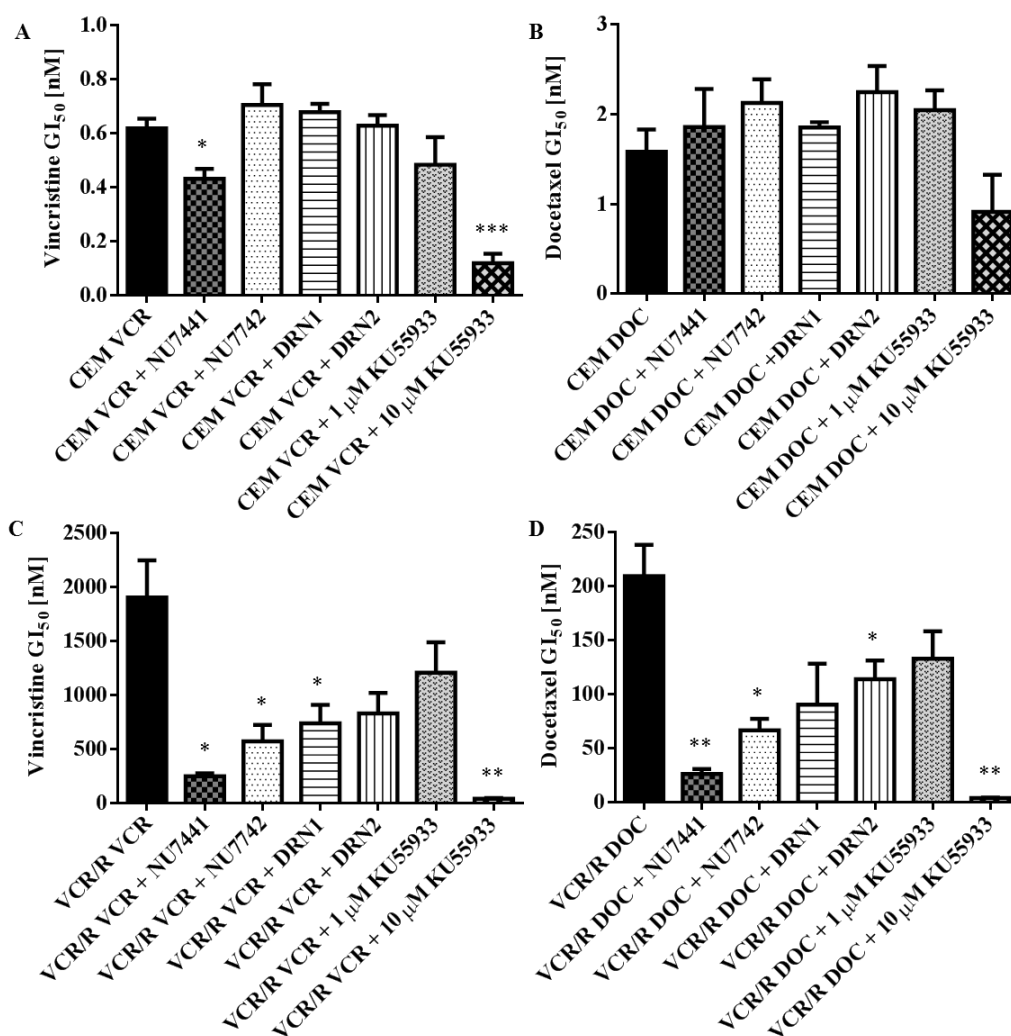
Figure 4-10: GI_{50} concentrations of vincristine or docetaxel alone or in the presence of the DNA-PK and ATM inhibitors. (**A**) and (**B**) CCRF-CEM and (**C**) and (**D**) CCRF-CEM VCR/R cells were treated with vincristine or docetaxel alone or in combination with 1 µM NU7441, NU7742, DRN1, DRN2, 1 µM or 10 µM KU55933 for 72 hours and % growth was analysed by XTT assay (Section 2.3). The data are presented as the GI_{50} mean of ≥ 3 independent experiments, each in triplicate, $\pm$ standard error. Asterisk indicates a statistically significant difference using the Student's unpaired t-test when compared with the GI_{50} for drug alone (* $p<0.05$, ** $p<0.01$, *** $p<0.001$).

	CCRF-CEM cells						
	Drug [nM]	Drug + NU7441 [nM] (PF_{50})	Drug + NU7742 [nM] (PF_{50})	Drug + DRN1 [nM] (PF_{50})	Drug + DRN2 [nM] (PF_{50})	Drug + 1 µM KU55933 [nM] (PF_{50})	Drug + 10 µM KU55933 [nM] (PF_{50})
Vincristine GI_{50}	0.6 ± 0.04	$0.4 \pm 0.04^{p=0.02}$ (1.4)	0.7 ± 0.08^{ns} (0.9)	0.7 ± 0.03^{ns} (0.9)	0.6 ± 0.04^{ns} (1)	0.5 ± 0.1^{ns} (1.3)	$0.1 \pm 0.04^{p=0.0006}$ (5.2)
Docetaxel GI_{50}	1.6 ± 0.3	1.9 ± 0.4^{ns} (0.9)	2.1 ± 0.3^{ns} (0.7)	1.9 ± 0.06^{ns} (0.9)	2.3 ± 0.3^{ns} (0.7)	1.9 ± 0.4^{ns} (0.9)	0.9 ± 0.4^{ns} (1.7)
	CCRF-CEM VCR/R cells						
	Drug [nM] (RF_{50})	Drug + NU7441 [nM] (PF_{50})	Drug + NU7742 [nM] (PF_{50})	Drug + DRN1 [nM] (PF_{50})	Drug + DRN2 [nM] (PF_{50})	Drug + 1 µM KU55933 [nM] (PF_{50})	Drug + 10 µM KU55933 [nM] (PF_{50})
Vincristine GI_{50}	$1900 \pm 344_{p=0.02}$ (3060)	$246 \pm 28^{p=0.01}$ (7.7)	$572 \pm 153^{p=0.02}$ (3.3)	$739 \pm 170^{p=0.04}$ (2.6)	831 ± 188^{ns} (2.3)	1200 ± 281^{ns} (1.6)	$39 \pm 7.2^{p=0.006}$ (49)
Docetaxel GI_{50}	$210 \pm 29_{p=0.006}$ (133)	$26 \pm 4^{p=0.003}$ (8.1)	$67 \pm 11^{p=0.01}$ (3.2)	$90 \pm 38^{ns} (2.3)$	$114 \pm 17^{p=0.048}$ (1.8)	133 ± 25^{ns} (1.6)	$3.6 \pm 0.5^{p=0.002}$ (58)

Table 4-2: GI_{50} concentrations of vincristine or docetaxel alone or in the presence of the DNA-PK and ATM inhibitors. CCRF-CEM and CCRF-CEM VCR/R cells were treated with vincristine or docetaxel alone or in combination with 1 µM NU7441, NU7742, DRN1, DRN2, 1 µM or 10 µM KU55933 for 72 hours and % growth was analysed by XTT assay (Section 2.3). The data are presented as the GI_{50} mean of ≥ 3 independent experiments, each in triplicate, ± standard error. Significant differences between CCRF-CEM and CCRF-CEM VCR/R cells treated with drug alone were calculated using an unpaired t-test shown as subscript. Significant differences between cells treated with drug alone and cells treated with drug + inhibitor were calculated using an unpaired t-test shown as superscript. ns = non-significant. PF_{50} = potentiation factor of inhibitor compared with drug alone. RF_{50} = resistance factor to drugs in CCRF-CEM VCR/R cells compared with CCRF-CEM cells.

4.3.4 Both DNA-PK inhibitory and non-inhibitory NU7441 derivatives, and KU55933, increase intracellular vincristine levels in MDR cells

Following the observation that NU7441 interacts with MDR1, as shown by the doxorubicin efflux fluorescence microscopy data in the MDCKII-MDR1 cells (Figure 4-4), this effect was further investigated using a more quantitative approach and the microtubule-targeting agent, vincristine.

CCRF-CEM and CCRF-CEM VCR/R cells were treated with GI_{50} (0.5 nM and 2 μM, respectively) and 5 x GI_{50} (2.5 nM and 10 μM, respectively) concentrations of the MDR1 substrate vincristine, either alone or in combination with 1 μM NU7441, NU7742, DRN1, DRN2, verapamil, 1 μM or 10 μM KU55933. Although the cellular concentration data following exposure to GI_{50} and 5 x GI_{50} vincristine demonstrated the same trends in accumulation in the presence of the inhibitors, the error bars on the 5 x GI_{50} data were larger and cellular toxicity, particularly after 8 hours, was potentially responsible for the greater variation. Therefore data generated following exposure to the GI_{50} vincristine concentration were deemed to be more accurate and these data were used in statistical analyses, although the 5 x GI_{50} data are included in Figure 4-12 for comparison.

None of the compounds altered vincristine concentrations in the CCRF-CEM cells after 1 or 8 hours treatment at the GI_{50} concentration (Figure 4-11A) or 5 x GI_{50} concentration (Figure 4-12A). In contrast, in the CCRF-CEM VCR/R cells, all of the compounds tested increased the intracellular vincristine level when compared with vincristine alone at both 1 and 8 hours, and at both vincristine concentrations, consistent with an inhibition of vincristine efflux (Figure 4-11B, Figure 4-12B). At the concentration tested (1 μM), NU7441 induced the highest vincristine accumulation of all the DNA-PK-inhibitory and non-inhibitory compounds at both 1 hour (1.3-fold; p=0.01) and 8 hours (2.1-fold; p=0.04), i.e. to a level similar to that induced by 1 μM verapamil (Figure 4-11B). NU7742 did not increase intracellular vincristine to the same degree as NU7441 (1.5-fold at 8 hours), suggesting that the morpholine group may play a role in the interaction between NU7441 and MDR1 or that the DNA-PK inhibitory activity of NU7441 may play a role. Both DRN1 and DRN2 increased intracellular vincristine levels to the same degree (1.4-fold) after 8 hours, although not to the same degree as NU7441, which suggests that DNA-PK activity is not a contributory factor in modulating MDR1 function. KU55933 (1 μM) was included in this experiment to allow a direct comparison with NU7441 and its derivatives, as well as 10 μM KU55933, the concentration used in all other *in vitro* experiments with this inhibitor. Both 1 and 10

µM KU55933 increased intracellular vincristine concentration at 1 and 8 hours; however, due to time constraints, it was only possible to carry out two LC-MS experiments with 1 µM KU55933 and one experiment with 10 µM KU55933.
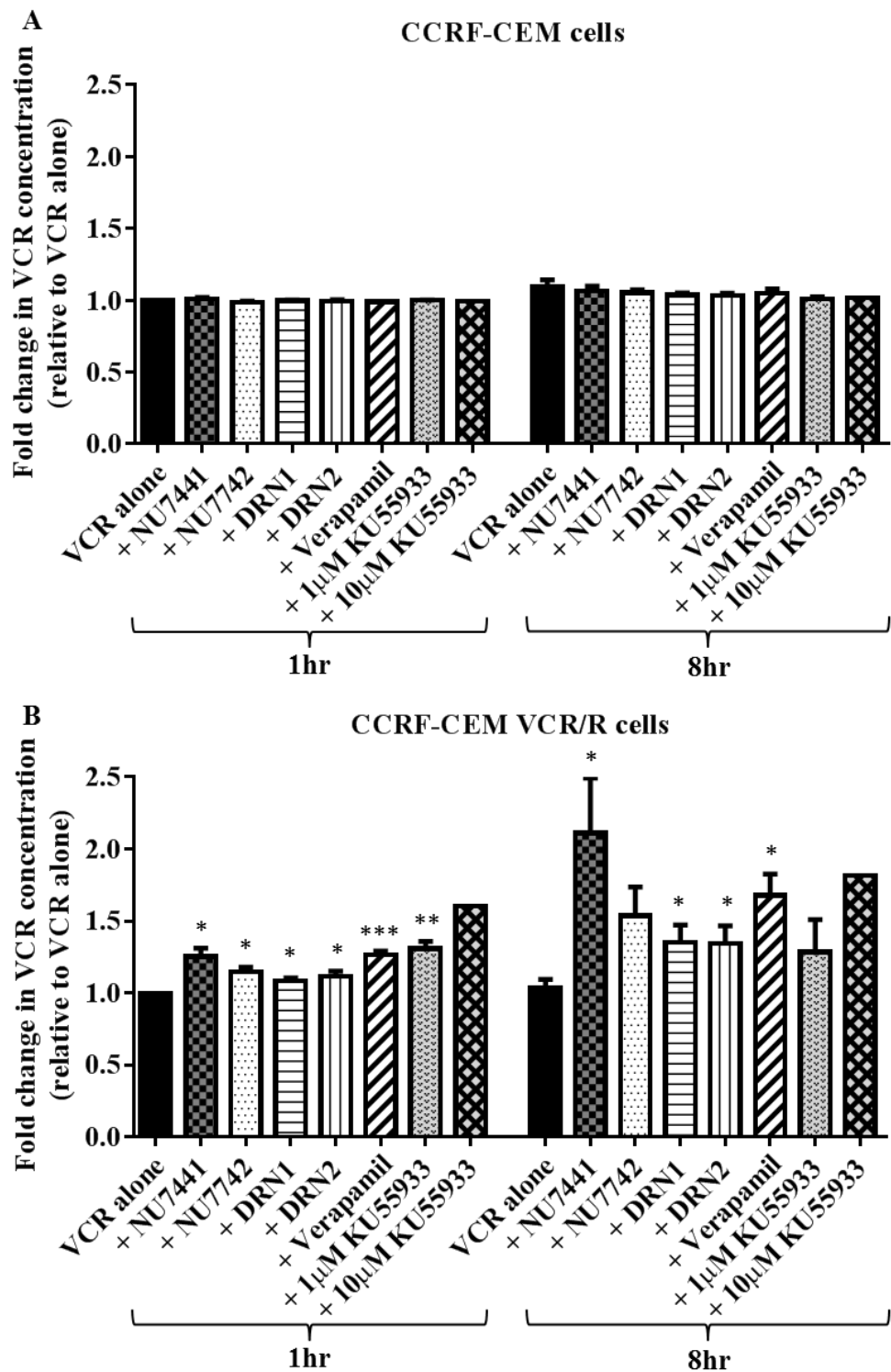
Figure 4-11: Both DNA-PK inhibitory and non-inhibitory NU7441 derivatives increase intracellular vincristine levels in CCRF-CEM VCR/R cells treated with GI$_{50}$ vincristine. (**A**) CCRF-CEM and (**B**) CCRF-CEM VCR/R cells were treated for 1 or 8 hrs with GI$_{50}$ concentrations of vincristine (VCR) alone or in combination with 1 μM NU7441, NU7742, DRN1, DRN2, verapamil, 1 or 10 μM KU55933. Intracellular vincristine levels were measured using LC–MS (Section 2.11). Bars are mean of ≥ 3 independent experiments ± standard error. Asterisk indicates a statistically significant difference in fold change in VCR using the Student's unpaired *t*-test when compared with 1 hr VCR treatment alone (* *p<0.05,* ** *p<0.01,* *** *p<0.001*).
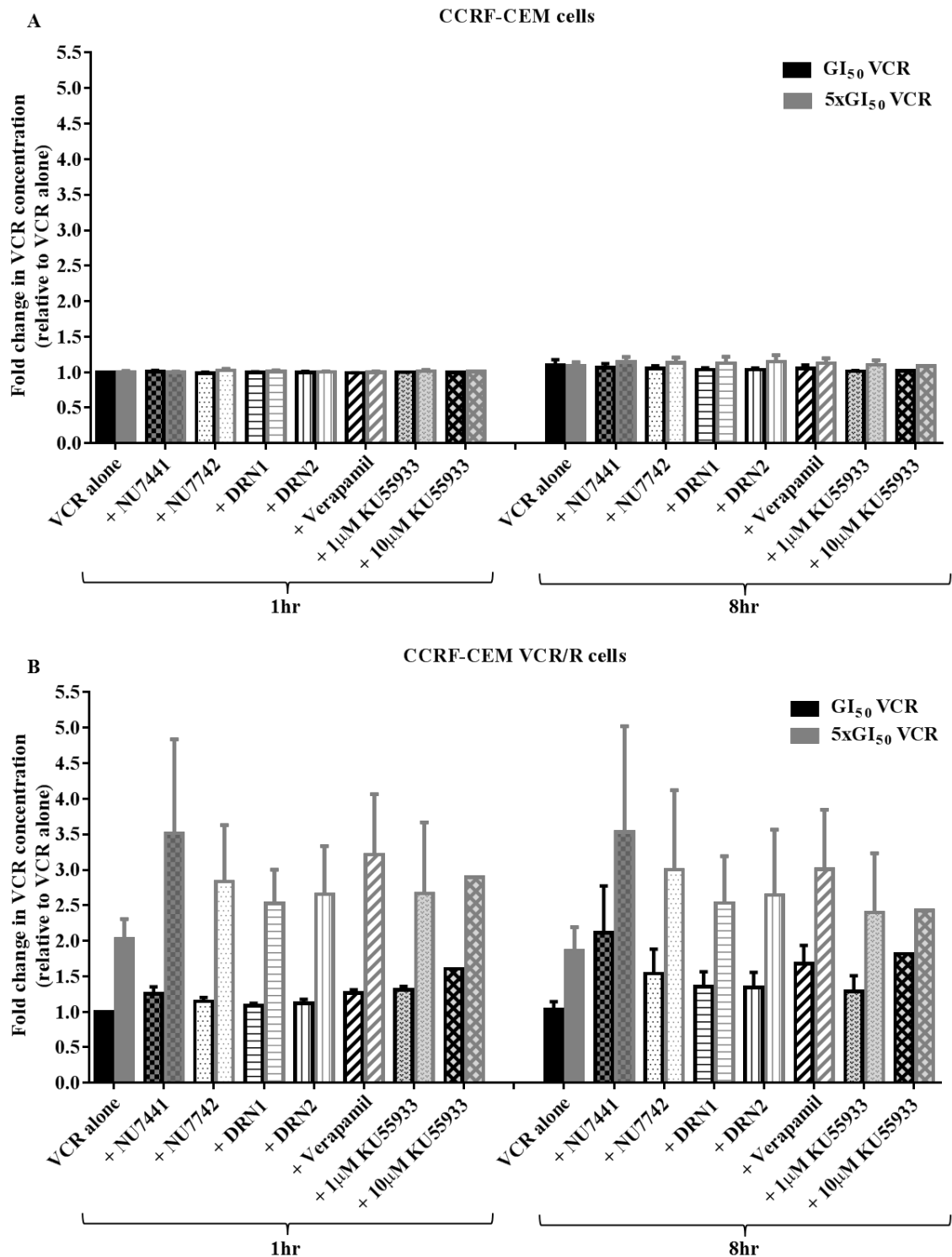
Figure 4-12: Both DNA-PK inhibitory and non-inhibitory NU7441 derivatives increase intracellular vincristine levels in CCRF-CEM VCR/R cells after treatment with 1 or 5 x GI$_{50}$ VCR. (**A**) CCRF-CEM and (**B**) CCRF-CEM VCR/R cells were treated for 1 or 8 hrs with GI$_{50}$ (black) or 5 x GI$_{50}$ (grey) concentrations of vincristine (VCR) alone or in combination with 1 μM NU7441, NU7742, DRN1, DRN2, verapamil, 1 or 10 μM KU55933. Intracellular vincristine levels were measured using LC–MS (Section 2.11). Bars are mean of ≥3 independent experiments ± standard error.

It was also possible to measure the intracellular levels of the inhibitors NU7441, NU7742, verapamil and KU55933 in the same samples of the CCRF-CEM and CCRF-CEM VCR/R cells using the same LC-MS method. Standard curves were produced for each inhibitor to validate their detection using this method. DRN1 and DRN2 were not independently detectable using the LC-MS as they are the same molecular weight and structure with only the direction of the methyl group differing between the two compounds. Therefore, during LC-MS analysis, the two compounds fragment in the same way and are not be distinguishable from each other.

There was no change between 1 and 8 hours in the levels of the compounds in the CCRF-CEM cells, apart from a significant 1.2-fold (p=0.04) decrease in intracellular verapamil after 8 hours (Figure 4-13A, C and E). In the CCRF-CEM VCR/R cells, the intracellular verapamil concentrations were the same after 1 and 8 hours (Figure 4-13F). There was however a significant 1.4-fold (p=0.03) increase in intracellular NU7441 levels at 8 hours, suggesting accumulation (Figure 4-13B). There were no changes between 1 and 8 hours in the levels of NU7742 in either cell line. There was also no change in KU55933 levels following exposure to 1 µM compound in either cell line and it was not possible to carry out statistical analysis on the 10 µM KU55933 treatment due to the experiment being carried out only once.
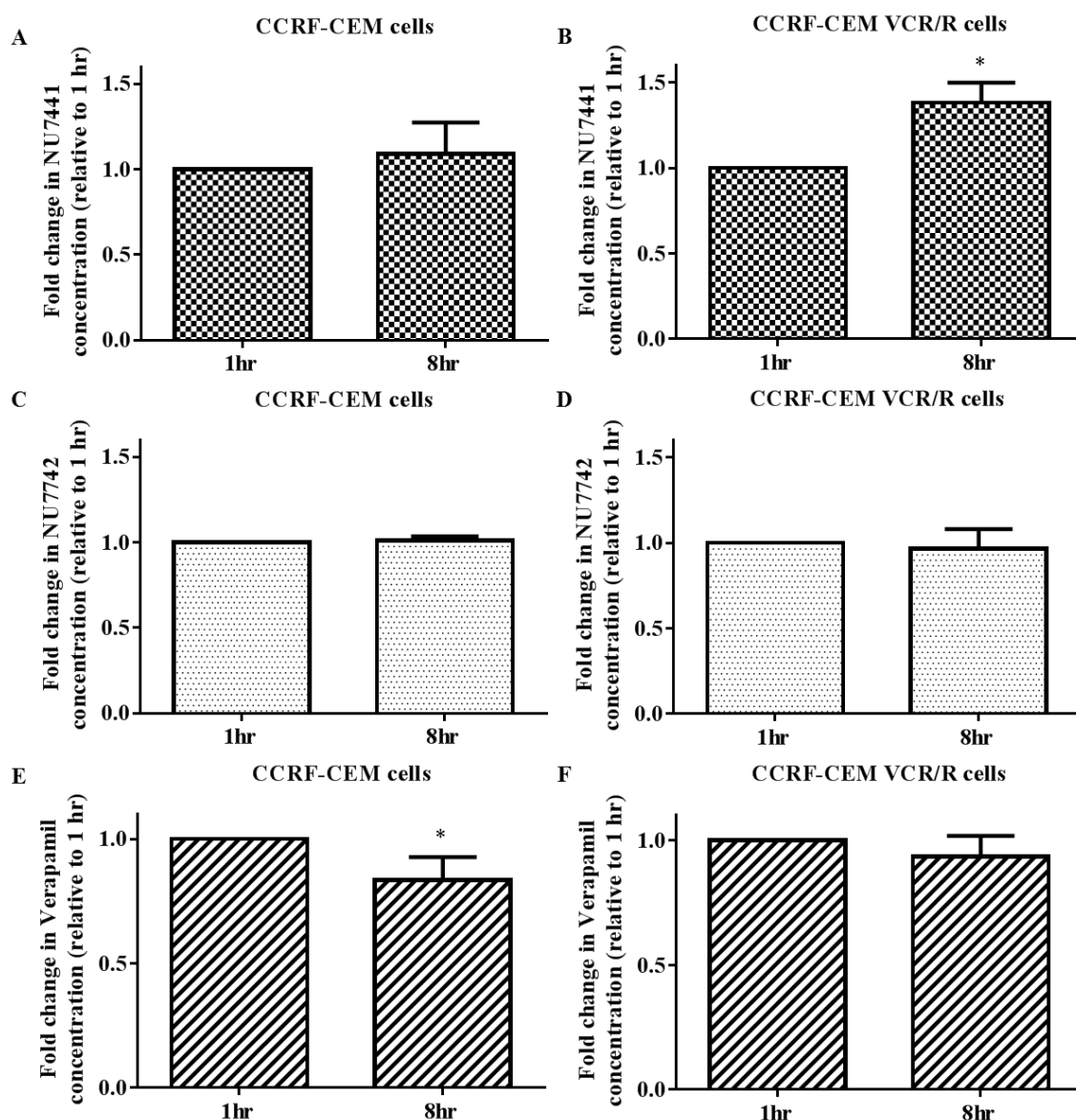
Figure 4-13: NU7441, NU7742 and verapamil intracellular levels in the CCRF-CEM and CCRF-CEM VCR/R cells after 1 and 8 hour treatment. CCRF-CEM and CCRF-CEM VCR/R cells were treated for 1 or 8 hrs with GI_{50} or 5 x GI_{50} concentrations of vincristine in combination with 1 μM NU7441, NU7742 or verapamil. Intracellular NU7441 (hatched bars), NU7742 (dotted bars) and verapamil (striped bars) levels were measured using LC–MS after exposure (Section 2.11). Bars are mean of ≥ 3 independent experiments ± standard error. Asterisk indicates a statistically significant difference in the fold change in intracellular NU7441, NU7742 and verapamil using the Student's unpaired *t*-test when compared with 1 hr NU7441, NU7742 and verapamil treatment (* *p<0.05*).
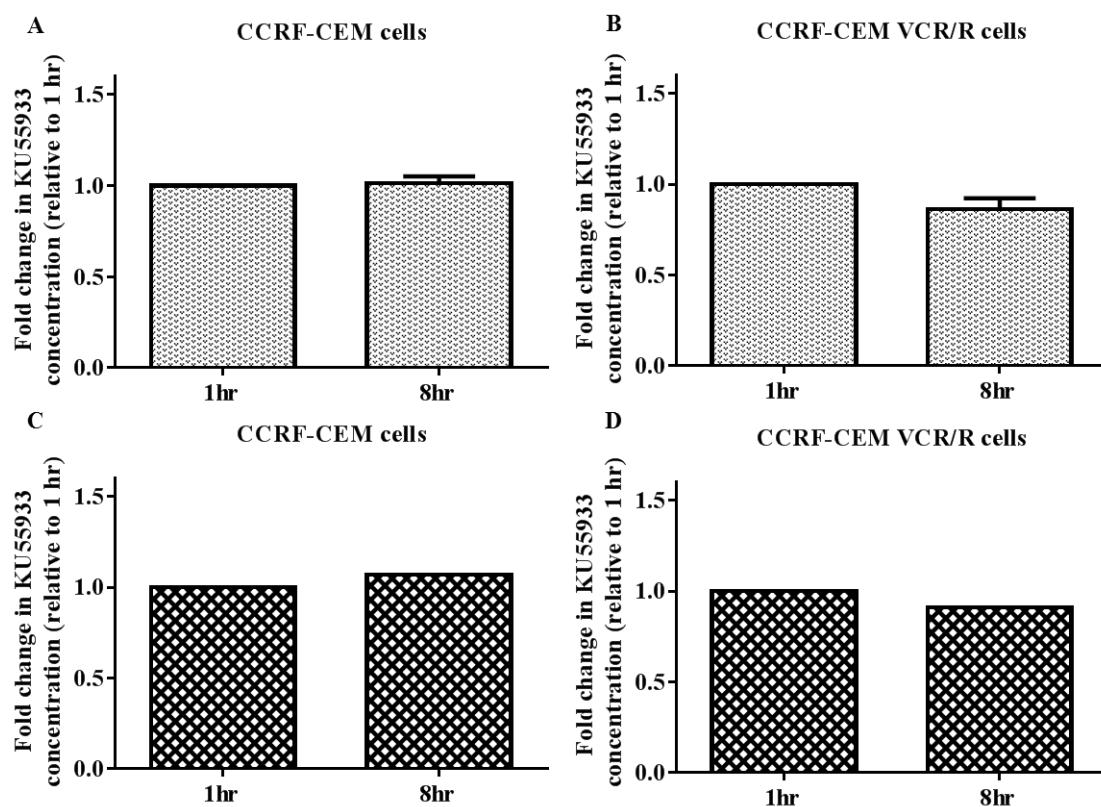
Figure 4-14: KU55933 intracellular levels after 1 and 8 hours in either the CCRF-CEM or CCRF-CEM VCR/R cells. CCRF-CEM and CCRF-CEM VCR/R cells were treated for 1 or 8 hrs with GI_{50} or 5 x GI_{50} concentrations of vincristine in combination with 1 or 10 µM KU55933. Intracellular 1 µM KU55933 (dotted bars) and 10 µM KU55933 (gridded bars) levels were measured using LC–MS after exposure (Section 2.11). 1 µM KU55933 bars are mean of 2 independent experiments ± standard error. 10 µM KU55933 bars represent 1 experiment.

4.3.5   Cell diameter and volume determination

Due to the differences in intracellular vincristine accumulation between the CCRF-CEM and CCRF-CEM VCR/R cells, experiments were performed to determine whether the size of the cells may have had an impact on intracellular drug accumulation.

Two different passages of both CCRF-CEM and CCRF-CEM VCR/R cells were collected and cell diameter and volume was measured using an Imagestream (Amnis, Seattle, USA), which is an imaging flow cytometer that takes images of individual cells and the Ideas Software calculates the diameter of individual cells in a population of at least 4600 cells. The diameter of the CCRF-CEM cells was 13.3-13.5 µm whereas the diameter of the CCRF-CEM VCR/R cells was 13.7 µm (Figure 4-15, Table 4-3). This difference is statistically significant ($p<0.0001$); however, the magnitude of this difference (maximum 3 %) would not have a major impact on apparent intracellular levels.
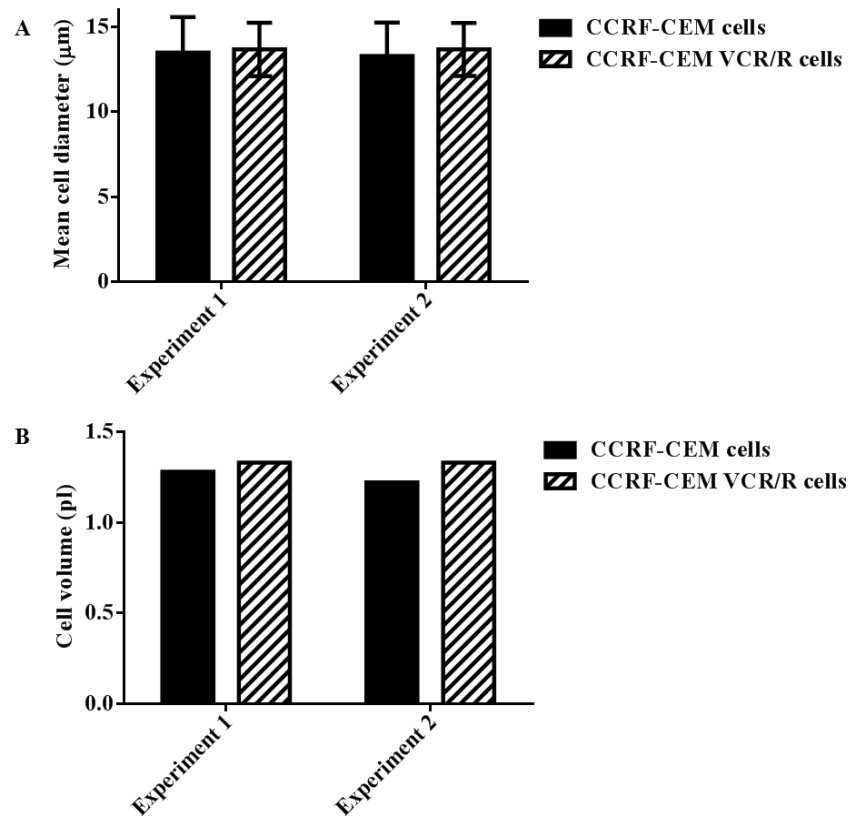
Figure 4-15: Mean cell diameter and cell volume of two different samples of CCRF-CEM and CCRF-CEM VCR/R cells. 1.5 ml of two different passages of exponentially growing CCRF-CEM and CCRF-CEM VCR/R cells were collected in PBS, counted and imaged using the Imagestream flow cytometer and individual cell diameter was calculated using masks set by the Ideas Software. The volume was calculated using the equation ($\pi d^3/6$) where d=diameter.

	Experiment 1		Experiment 2	
	CCRF-CEM cells	**CCRF-CEM VCR/R cells**	**CCRF-CEM cells**	**CCRF-CEM VCR/R cells**
Mean diameter (μm)	13.5	13.7	13.3	13.7
SD (μm)	2.1	1.6	2	1.6
Count	4607	6593	4649	6639
Volume (pl)	1.3	1.3	1.2	1.3

Table 4-3: Cell diameter measurements and calculated volumes of CCRF-CEM and CCRF-CEM VCR/R cells by the Imagestream. 1.5 ml of two different passages of exponentially growing CCRF-CEM and CCRF-CEM VCR/R cells were collected in PBS, counted and imaged using the Imagestream flow cytometer and individual cell diameter was calculated using masks set by the Ideas Software. The volume was calculated using the equation ($\pi d^3/6$) where d=diameter.

4.4   Discussion and future work

It is known that many conventional cytotoxic anticancer drugs are transported out of the cell by MDR1, and that MDR1 affects both the intracellular accumulation and intra-tumour distribution of compounds (Martin *et al.*, 2003). The importance of the ABC transporter family has been somewhat overlooked in the development of more targeted therapies but a number of recent publications have demonstrated that targeted therapies can also interact with this family of transporters (Kitazaki, 2005; Shi *et al.*, 2007; Dai *et al.*, 2008; Hegedus *et al.*, 2009; Mi *et al.*, 2010; Shi *et al.*, 2011; Eum *et al.*, 2013). Understanding the role of drug efflux transporters is therefore key when investigating combinations of targeted therapies with drugs that are MDR1 substrates.

NU7441 and KU55933 are potent inhibitors of DNA-PK and ATM, respectively. During investigations into the effect of these inhibitors on the activity of a range of chemotherapeutic agents in both parental and multidrug-resistant cells, it was noted that NU7441 and KU55933 sensitised multidrug-resistant cells to vincristine, docetaxel and paclitaxel, and to a greater degree than in parental cells. The multidrug-resistant cells are resistant *via* overexpression of the efflux transporter MDR1 and have been generated by stepwise treatment with increasing concentrations of drug. Therefore, it was hypothesised that there were potential interactions between NU7441 and MDR1, and KU55933 and MDR1.

Initially, the doxorubicin fluorescence assay demonstrated that NU7441 increases doxorubicin accumulation in a concentration-dependent manner in paired wild-type and MDR1-overexpressing MDCKII cells. The kinase inhibitor sorafenib is used to treat advanced renal cell carcinoma (Kane *et al.*, 2006) and hepatocellular carcinoma (Lang, 2008), and MDR1 has been shown to play a major role in the acquired resistance phenotype in hepatocellular carcinoma (Meena *et al.*, 2013). Furthermore sorafenib has been shown to reverse paclitaxel resistance in MDR cells and cause a concentration-dependent increase in the uptake and retention of rhodamine 123; suggesting that sorafenib inhibits MDR1 (Eum *et al.*, 2013). The data presented here with NU7441 are consistent with the findings for sorafenib and suggest that NU7441 inhibits MDR1. There are various techniques that have been used to investigate transporter interactions with small molecule inhibitors. Intracellular drug levels have previously been measured by radiolabelling of drugs, with intracellular accumulation determined by measuring the radioactivity (Shi *et al.*, 2007; Dai *et al.*, 2008). Alternatively, intracellular doxorubicin transport has been measured by flow cytometric analysis by exploring the inherent

137

fluorescence of the molecule (Mi *et al.*, 2010). Doxorubicin has also been used previously in a fluorescence competition assay to investigate competitive MDR1-mediated efflux, with increased doxorubicin fluorescence demonstrated following pre-treatment with the anti-tumour antibiotic, actinomycin D (Hill *et al.*, 2013). This approach was the basis for the methodology used in this study.

To investigate whether drug accumulation induced by NU7441 or KU55933 was linked to DNA-PK or ATM inhibition, respectively, a range of NU7441 derivatives with different DNA-PK inhibitory properties and KU55933 were studied. There was no difference in vincristine-induced growth inhibition in the parental CCRF-CEM cells when vincristine was used in combination with NU7441 or its derivatives. However, in the CCRF-CEM VCR/R cells, NU7441 sensitised cells to a greater degree than NU7742, which suggests that DNA-PK inhibition is a contributory factor. Conversely, there was no difference in sensitisation induced by the DNA-PK inhibitory compound DRN1 and the DNA-PK non-inhibitory compound DRN2. However, this is the first study to treat cells with DRN1 and DRN2 *in vitro* and therefore little is known about their pharmacological properties of DRN1 and DRN2, making it difficult to draw any conclusions from the findings with these compounds. KU55933 at 10 µM sensitised both the sensitive and multidrug-resistant cells to vincristine and docetaxel to a greater degree than NU7441 and its derivatives at 1 µM.

LC-MS is a direct, highly sensitive and quantitative method which can be used to measure the intracellular accumulation of compounds. Quantitative determination of intracellular concentrations of tyrosine kinase inhibitors have previously been successfully measured by LC-MS (Hegedus *et al.*, 2009). All of the compounds investigated here increased intracellular vincristine concentration, as shown by LC-MS, in the MDR1-overexpressing CCRF-CEM VCR/R cells regardless of their DNA-PK or ATM-inhibitory activity.

Compounds that interact with MDR1 can do so by different mechanisms. Verapamil is known to modulate drug resistance by acting as a competitive MDR1 substrate (Cano-Gauci and Riordan, 1987). It was observed that the levels of verapamil decreased over time, which is consistent with a competitive substrate. Interestingly, NU7441 has similar growth inhibitory activity alone in the sensitive and resistant cells and there was no observed reduction in intracellular levels of NU7441 over time (Figure 4-1 and Figure 4-13A and B). This result suggests that NU7441 may not act as a competitive substrate but rather as an inhibitor of MDR1. However, further investigations would be necessary to explore this interesting possibility. The levels of

NU7742 did not change between 1 and 8 hours and, although there is not enough data to carry out statistical analysis, there is no apparent difference in KU55933 levels in the parental and multidrug-resistant cells. Inhibitors can have different mechanisms of MDR1 modulation and a more specific method is required to elucidate the mechanisms and transport of the inhibitors.

It would be interesting to confirm the preliminary LC-MS data with KU55933 (ATM IC_{50} = 13 nM) and to include the inactive KU55933 derivative, KU58050, which has a piperidine instead of a morpholine moiety resulting in a marked decrease in ATM-inhibitory activity (ATM IC_{50} = 2.96 µM) (Hickson *et al.*, 2004). Replacement of the morpholine group in KU55933 with a piperidine group is the same modification introduction in NU7742, which proved to be a useful control compound in the studies described here.

The photoaffinity analogue of prazosin, [125I]-iodoarylazidoprazosin (IAAP) has been used widely to investigate ABCB1 and ABCG2 substrate and inhibitor interactions in crude membrane preparation from cells or tissues expressing these transporter proteins (Sauna and Ambudkar, 2000). If an inhibitor interacts at the prazosin-binding site of ABCB1 or ABCG2, [125I]-IAAP photolabelling is inhibited. This assay is often carried out in parallel with an ATPase activity assay as drug-stimulated ATPase activity is a measure of substrate interaction at the drug-binding sites of transporters (Shi *et al.*, 2007; Dai *et al.*, 2008; Dohse *et al.*, 2010; Mi *et al.*, 2010; Shi *et al.*, 2011; Sen *et al.*, 2012). Experiments using this technique to investigate inhibitor interactions with not only MDR1/ABCB1 but also other members of the ABC family of transporters, e.g. ABCG2/BCRP would be useful.

Although the clinical relevance of MDR1 expression in solid tumours remains controversial, MDR1 has been shown to be relevant to acquired drug resistance in haematological cancers (de Grouw *et al.*, 2006). MDR is a biomarker for poor prognosis in patients with haematological cancers who can be cross-resistant to standard chemotherapeutic agents that are MDR1 substrates. The MDR substrates doxorubicin, etoposide and vincristine are used clinically in the treatment of haematological malignancies, for example acute myeloid leukaemia (AML) and acute lymphoblastic leukaemia (ALL) (Mathe *et al.*, 1974; Freireich *et al.*, 1976; Pizzo *et al.*, 1976) and docetaxel is used in the treatment of solid cancers, such as prostate and breast cancer (Crown *et al.*, 2004; Hotte and Saad, 2010). NU7441 has been shown to sensitise cells to mitoxantrone, doxorubicin (*in vitro*) and etoposide (*in vitro* and *in vivo*) (Zhao *et al.*, 2006; Willmore *et al.*, 2008), and this study has demonstrated that NU7441 can

sensitise CCRF-CEM cells to vincristine. KU55933 has been shown to sensitise cells to the topoisomerase II poisons, doxorubicin, etoposide and the topoisomerase I inhibitor camptothecin (Hickson *et al.*, 2004), and this study has demonstrated that KU55933 can sensitise cells to vincristine and docetaxel.

In a clinical setting, the contribution of drug efflux transporters in the resistance to cancer therapeutics is a hotly debated topic. Nevertheless, MDR1 overexpression has been linked with resistance to a number of agents, including the vinca alkaloids and taxanes used in this study (Allen *et al.*, 2000). In theory, the idea of a compound that can increase intracellular drug concentrations in MDR1-overexpressing drug-resistant cancer cells is attractive but many of the compounds designed to interact with MDR1 have proved largely unsuccessful due to toxicity or adverse side effects, mainly involving normal tissue sites that also overexpress drug efflux transporters e.g. gastrointestinal tract (Szakacs *et al.*, 2006). A number of clinical trials also reported adverse pharmacokinetic interactions with MDR1 inhibitor and cytotoxic drug co-administration. For example, increased area under the curve, lower maximal tolerated doses and reduced drug clearance of paclitaxel and vinblastine were all observed in clinical trials and suggest prolonged drug elimination with MDR1 inhibition (Bates *et al.*, 2001; Chico *et al.*, 2001; Modok *et al.*, 2006). However, if MDR1 interaction was an additional effect of a targeted compound and could increase the intracellular concentration of chemotherapeutic agents, as well as enhancing the effect of the DNA-damaging or microtubule-targeting agents, this could potentially be an interesting prospect; especially due to the large sensitisation seen in the multidrug-resistant cells compared with the parental cells, suggesting a therapeutic window opportunity.

From a targeted cancer drug discovery viewpoint, the ideal candidate compound has only one target and will not interact with any other signalling pathways or cellular processes, thereby ensuring that effects observed are directly and solely related to the target. Nevertheless, most of the targeted compounds in development will have off-target effects, be this due to interactions with other members of the target protein family or other signalling pathways. However, a compound such as NU7441 or KU55933 that interacts with both a signalling pathway and a drug efflux process is a novel and interesting prospect, provided the two effects are sufficiently understood.

Oral bioavailability and brain penetration can limit the therapeutic efficacy of compounds and are controlled by the expression of transporters in the apical membranes of cells in the small intestine or blood brain barrier, respectively. Many commonly-used chemotherapeutics and novel small-molecule inhibitors have been found to be

transported by MDR1 and/or other transporters from the ABC-family. For example, vemurafenib is a B-Raf^{V600E} inhibitor developed to inhibit the V600E mutant form of B-Raf present in over 60% of malignant melanomas and, although it has proven promising in clinical trials, brain metastases is one of the most common causes of death in melanoma patients (Sampson *et al.*, 1998; Davies *et al.*, 2002). Therefore, interactions with the ABC-transporters were investigated to try to enhance brain penetration. Using *in vitro* transwell assays to examine transport across an intact membrane, and *in vivo* mouse models with differential expression of transporters (e.g. *Abcb1a/1b$^{-/-}$ and Abcg2$^{-/-}$* mice), it was demonstrated that oral bioavailability and brain penetration were restricted by these transporters, which could be enhanced by the dual ABCB1/ABCG2 inhibitor, elacridar (Durmus *et al.*, 2012). The role of transporters in oral bioavailability and brain penetration has also been demonstrated with the PARP inhibitor rucaparib (Durmus *et al.*, 2014).

It would be interesting to study NU7441 and KU55933 further using some of these additional techniques. For example, the transwell assay for examining drug transport across an intact membrane in MDCKII cells with differential expressions of human transporters could be used to determine interactions with transporters other than MDR1 and would confirm whether NU7441 and KU55933 are competitive substrates or blockers of these transporters. This assay could also be used to examine the enhancement of transport of ABC-transporter substrates, such as vincristine and docetaxel, across the membrane. *In vivo* models with differential expression of transporters could confirm the *in vitro* findings and examine whether NU7441 and KU55933 would increase the oral bioavailability and brain penetration of MDR1 substrate drugs. If NU7441 and KU55933 were given in combination with MDR1 substrates, the MDR1-blocking effect, alongside the inhibition of DNA repair and effects on mitosis, could increase the efficacy of both DNA-damaging and anti-mitotic compounds. It would be possible to go on to examine the dual effects of these inhibitors using mouse models with different DNA-PK or ATM expression levels alongside transporter expression levels.

4.5   Summary

A panel of inhibitors with different structures and inhibitory properties were investigated for their effects on doxorubicin, vincristine and docetaxel growth inhibition

and/or accumulation in cell line models of multidrug resistance. NU7441 increased intranuclear doxorubicin accumulation in MDR1-overexpressing cells in a concentration-dependent manner. All of the inhibitors tested caused an increase in intracellular vincristine but 1 µM NU7441 and 10 µM KU55933 caused the greatest intracellular vincristine accumulation compared with the NU7441 derivatives. Using paired MDR1 wild-type and overexpressing CCRF-CEM cells, there was no difference in growth inhibition or intracellular accumulation of NU7441 and KU55933 when studied alone, indicating these inhibitors may act as inhibitors of MDR1 and not competitive substrates.

In conclusion, this study highlights the role of NU7441 as a dual DNA-PK and MDR1 inhibitor, and KU55933 as a dual ATM and MDR1 inhibitor, and this extends the therapeutic potential of these compounds when used in combination with MDR substrates to sensitise both wild-type and MDR phenotypes.

Chapter 5: Investigation into the response of paired parental and multidrug-resistant cells to ionising radiation alone and in combination with NU7441 or KU55933

5.1 Introduction

The majority of cancer patients are treated with a combination of radiation therapy and chemotherapy. Radiation therapy damages DNA both directly (by ionising atoms in DNA) or indirectly (hydroxyl radicals from ionised water molecules attack the DNA), inducing many forms of DNA damage, including DNA single-strand and double-strand breaks (Mahaney *et al.*, 2009). Double-strand breaks in response to ionising radiation occur when two single-strand breaks occur within 10-20 base pairs and, therefore, IR-induced DNA double-strand breaks commonly contain overhanging ends, which must be repaired correctly to prevent chromosomal translocations, genomic instability and cell death (Povirk, 2006; Mahaney *et al.*, 2009).

There are two main mammalian DNA double-strand break repair pathways as discussed in Chapter 1: homologous recombination (HR) and non-homologous end joining (NHEJ). In mammalian cells, NHEJ is the dominant pathway for ionising radiation-induced double-strand breaks (Bolderson *et al.*, 2009). NHEJ repairs strand breaks by ligating the two broken ends in a sequence-independent manner, and since ionising radiation-induced double-strand breaks contain overhanging ends, this can result in a loss of DNA at the repair site, resulting in inaccurate repair. Homologous recombination can only occur in late S and G2 phases after DNA replication has taken place, allowing a sister chromatid to be used as a homologous template for accurate repair.

Targeting repair pathways that are essential for cancer cell survival in response to radio- or chemotherapy is an active research area and many small molecule inhibitors of essential components of repair pathways are currently being investigated. A number of non-specific PIKK inhibitors, such as caffeine and LY294002, have been shown to increase sensitivity to radiation and chemotherapeutic agents (Vlahos *et al.*, 1994; Sarkaria *et al.*, 1999; Gharbi *et al.*, 2007), highlighting the importance of this family of enzymes in the response of cells to ionising radiation.

The PIKK ATM was identified as an attractive kinase for targeted inhibition after it was discovered that patients with ataxia telangiectasia, resulting from an ATM mutation, were highly sensitive to radiation (Savitsky *et al.*, 1995). The selective ATM kinase inhibitor, KU55933, discovered by drug library screening for compounds based on LY294002, has been shown to cause cellular radio-sensitisation and inhibition of ionising radiation-induced ATM-dependent phosphorylation events (Hickson *et al.*, 2004). A more selective ATM inhibitor, KU60019 has been found to be a radio-

sensitiser for glioma cells *in vitro* (Golding *et al.*, 2009), and a preliminary *in vivo* study demonstrated delayed tumour progression and increased survival in mice with paediatric gliomas treated with KU60019 plus irradiation compared with control irradiated mice (Vecchio *et al.*, 2014).

Targeting the NHEJ pathway has also been shown to be effective in producing radiosensitisation. Cells that are deficient in the catalytic subunit of DNA-PK or in Ku subunits are more radio- and chemosensitive than proficient cells, indicating a role for DNA-PK in responding to DNA double-strand break-inducing treatments (Lees-Miller *et al.*, 1995; Ouyang *et al.*, 1997). The selective DNA-PK inhibitor, NU7441, has been shown to sensitise cells to ionising radiation but limited solubility has restricted *in vivo* experiments with this inhibitor (Zhao *et al.*, 2006).

Along with DNA-PK and ATM inhibitors, a number of other small molecule inhibitors or peptides that target a range of proteins involved in DNA repair, for example Chk1 and Chk2, the Mre11-Rad50-Nbs1 complex, Rad51 and PARP1, have been shown to be radiosensitisers (reviewed in (Bolderson *et al.*, 2009)).

5.2   Aims

The aim of this study was to investigate the radiosensitivity of paired sensitive and multidrug-resistant cell lines and the effect of DNA-PK and ATM inhibition on sensitivity. Three paired cell lines: CCRF-CEM and CCRF-CEM VCR/R cells, A2780 and A2780-TX1000 cells and SKOV3 and SKOV3-TR cells, were treated with increasing doses of ionising radiation and the growth inhibition was determined by XTT assay. The cytotoxicity in CCRF-CEM and CCRF-CEM VCR/R cells was then be investigated by methylcellulose clonogenic assay, and the cytotoxicity in A2780 and A2780-TX1000 cells was investigated by clonogenic survival assay, to determine if the observed growth-inhibitory effects were due to cytotoxicity.

5.3 Results

5.3.1 *Increased resistance to ionising radiation in multidrug-resistant cell lines*

Previously, in Chapter 3, three paired sensitive and microtubule-targeting agent-resistant cell lines were characterised and their multidrug-resistant phenotype was attributed to an overexpression of the drug efflux transporter, MDR1. Sensitisation to different microtubule-targeting agents by the DNA-PK inhibitor, NU7441 and the ATM inhibitor, KU55933 was greater in multidrug-resistant cells and studies described in Chapter 4 demonstrated that this effect was largely due to NU7441 and KU55933 interfering with drug efflux *via* MDR1. During this work, ionising radiation was used as a control cytotoxic treatment and the radiation response was expected to be independent of MDR1 status. Accordingly, it was hypothesised that the sensitive and multidrug-resistant cells would display the same sensitivity to ionising radiation and the same level of radiosensitisation with NU7441 and KU55933.

Interestingly, the hypothesised pattern of sensitivity was not observed in the paired sensitive and resistant cell lines. The CCRF-CEM and CCRF-CEM VCR/R cell line pair was primarily investigated for their sensitivity to ionising radiation and sensitisation caused by NU7441 and KU55933. Unexpectedly, CCRF-CEM cells were found to be 6.4-fold (p=0.005) more sensitive to ionising radiation than the multidrug-resistant CCRF-CEM VCR/R cells (Figure 5-1). There was no significant sensitisation with either NU7441 or KU55933 in either cell line.
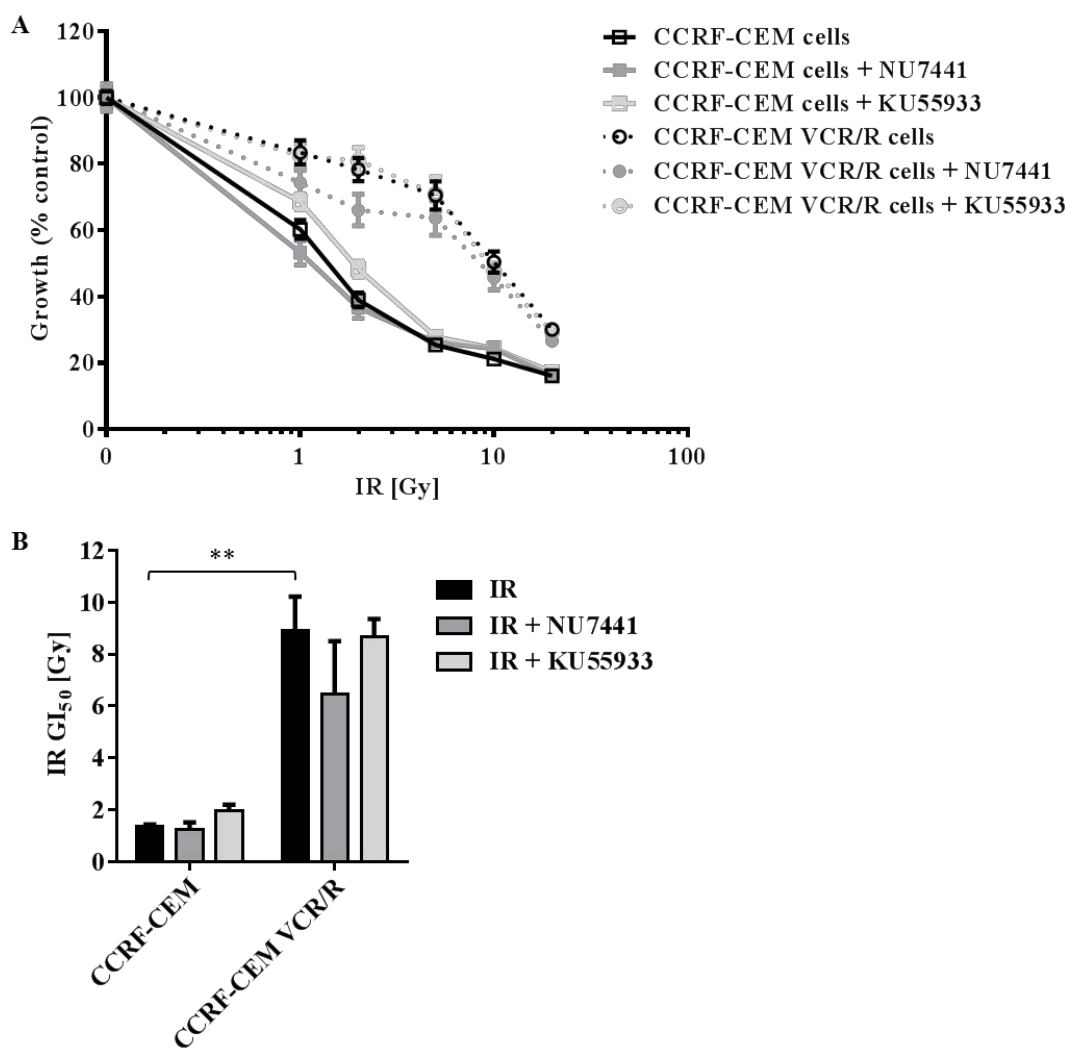
Figure 5-1: CCRF-CEM cells are more sensitive to ionising radiation than the CCRF-CEM VCR/R cells. CCRF-CEM and CCRF-CEM VCR/R cells were treated with ionising radiation (IR) (0-20 Gy) alone or in combination with 1 μM NU7441 or 10 μM KU55933 for 72 hours and % growth was analysed by XTT assay (Section 2.3). (**A**) Data are presented as a percentage of vehicle control cells. Points represent the mean of $\geq$3 independent experiments, each in triplicate, $\pm$ standard error. (**B**) GI$_{50}$ data are presented as the GI$_{50}$ means $\pm$ standard error. Asterisk indicates a statistically significant difference using the Student's unpaired *t*-test when compared with the GI$_{50}$ for IR alone (** *p<0.01*).

Following these interesting observations in the CCRF-CEM and CCRF-CEM VCR/R cell line pair, the radiosensitivity of another paired cell line, A2780 and A2780-TX1000 cells, was investigated to see if multidrug-resistant cells were radio-resistant in a solid ovarian cancer model, or if radiation resistance in multidrug-resistant cells is cell-line dependent.

The A2780 cells were more sensitive to ionising radiation than the A2780-TX1000 cells. It was not possible to obtain GI$_{50}$ concentrations for the A2780-TX1000

cells because they were so radioresistant. In contrast to CCRF-CEM cells, A2780 cells were significantly sensitised 3.2-fold by NU7441 at the GI_{50} dose of ionising radiation, but otherwise NU7441 or KU55933 did not cause radiosensitisation.
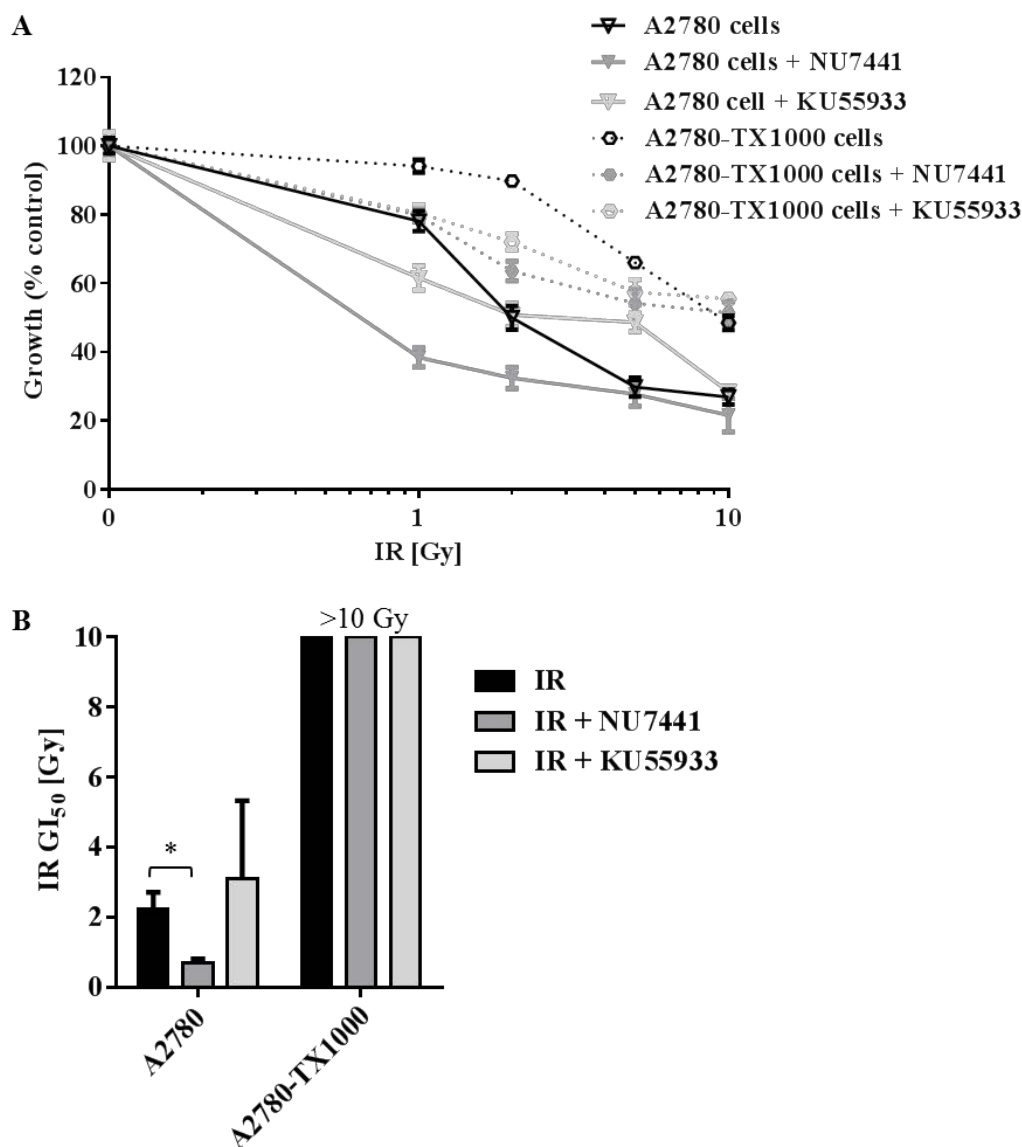
Figure 5-2: A2780 cells are significantly more sensitive to ionising radiation than the A2780-TX1000 cells. A2780 and A2780-TX1000 cells were treated with ionising radiation (IR) alone (0-10 Gy) or in combination with 1 μM NU7441 or 10 μM KU55933 for 72 hours and % growth was analysed by XTT assay (Section 2.3). (**A**) Data are presented as a percentage of vehicle control cells. Points represent the mean of ≥3 independent experiments, each in triplicate, ± standard error. (**B**) GI_{50} data are presented as the GI_{50} means ± standard error. Asterisk indicates a statistically significant difference using the Student's unpaired t-test when compared with the GI_{50} for IR alone (* $p<0.05$).

The final cell line pair to be investigated was the SKOV3 and SKOV3-TR cells. Both of these cell lines were radio-resistant relative to the A2780 and CCRF-CEM cell line pairs. SKOV3-TR cells were in fact so radio-resistant that GI_{50} values for ionising radiation were > 20 Gy in this cell line for ionising radiation alone or in combination with 1 µM NU7441 or 10 µM KU55933. NU7441 and KU55933 appeared to have greater sensitisation effects in the parental SKOV3 cells compared with SKOV3-TR cells, with NU7441 significantly sensitising the SKOV3 cells 3-fold (p=0.003) to ionising radiation at the GI_{50} dose.
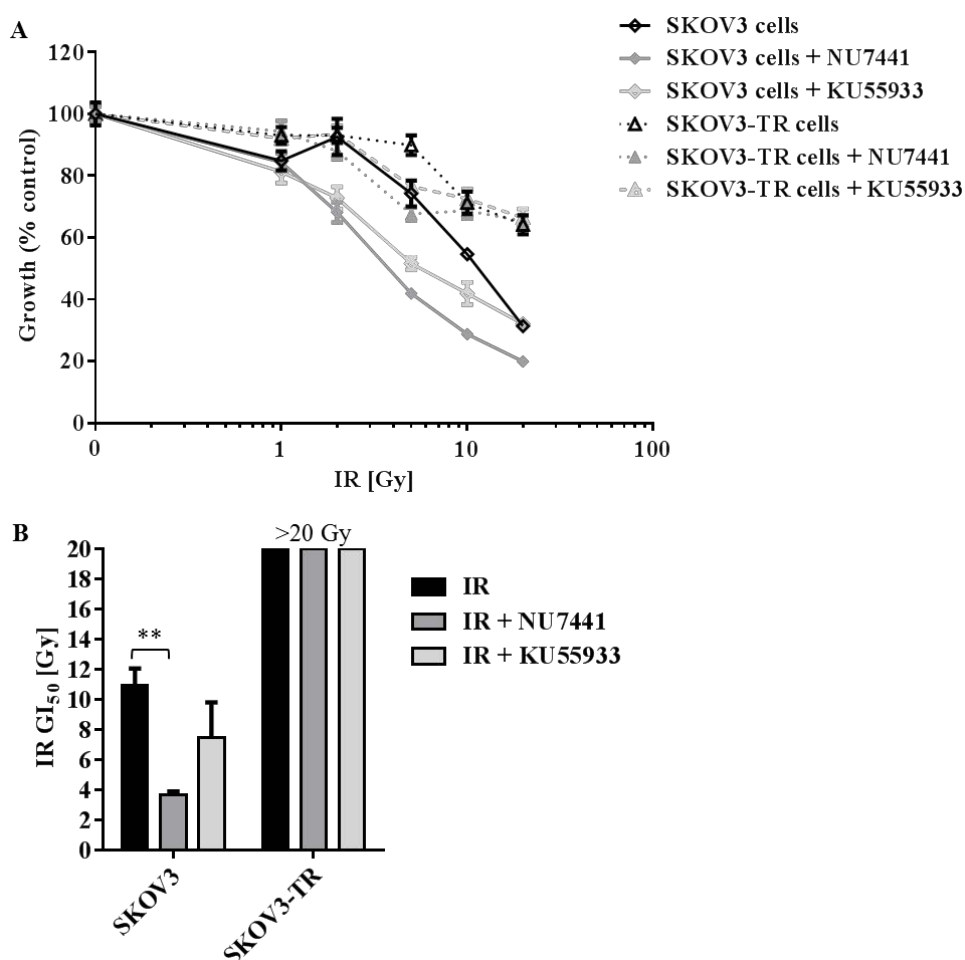
Figure 5-3: SKOV3 cells are significantly more sensitive to ionising radiation than the SKOV3-TR cells. SKOV3 and SKOV3-TR cells were treated with ionising radiation (IR) (0-20 Gy) alone or in combination with 1 µM NU7441 or 10 µM KU55933 for 72 hours and % growth was analysed by XTT assay (Section 2.3). (**A**) Data are presented as a percentage of vehicle control cells. Points represent the mean of ≥3 independent experiments, each in triplicate, ± standard error. (**B**) GI_{50} data are presented as the GI_{50} means ± standard error. Asterisk indicates a statistically significant difference using the Student's unpaired *t*-test when compared with the GI_{50} for IR alone (** *p<0.01*).

The results in Figure 5-1 to Figure 5-3 demonstrated that cells made resistant to microtubule-targeting agents, and displaying classical drug resistance through MDR1 overexpression, were more resistant to ionising radiation as measured by an XTT growth inhibition assay. Additionally, in these three cell lines, there is no consistent sensitisation to ionising radiation by DNA-PK or ATM inhibition.

Experiments were then performed to investigate the cytotoxic effects of ionising radiation on two of the paired sensitive and resistant cell lines. In CCRF-CEM and CCRF-CEM VCR/R cells, investigated using the methylcellulose cell survival assay, a similar pattern was observed as in the growth inhibition experiments. The CCRF-CEM cells were 2.7-fold (p=0.002) more sensitive to ionising radiation than the multidrug-resistant CCRF-CEM VCR/R cells (Figure 5-4). NU7441 sensitised A2780 cells and KU55933 sensitised both A2780 and A2780-TX1000 cells to ionising radiation.
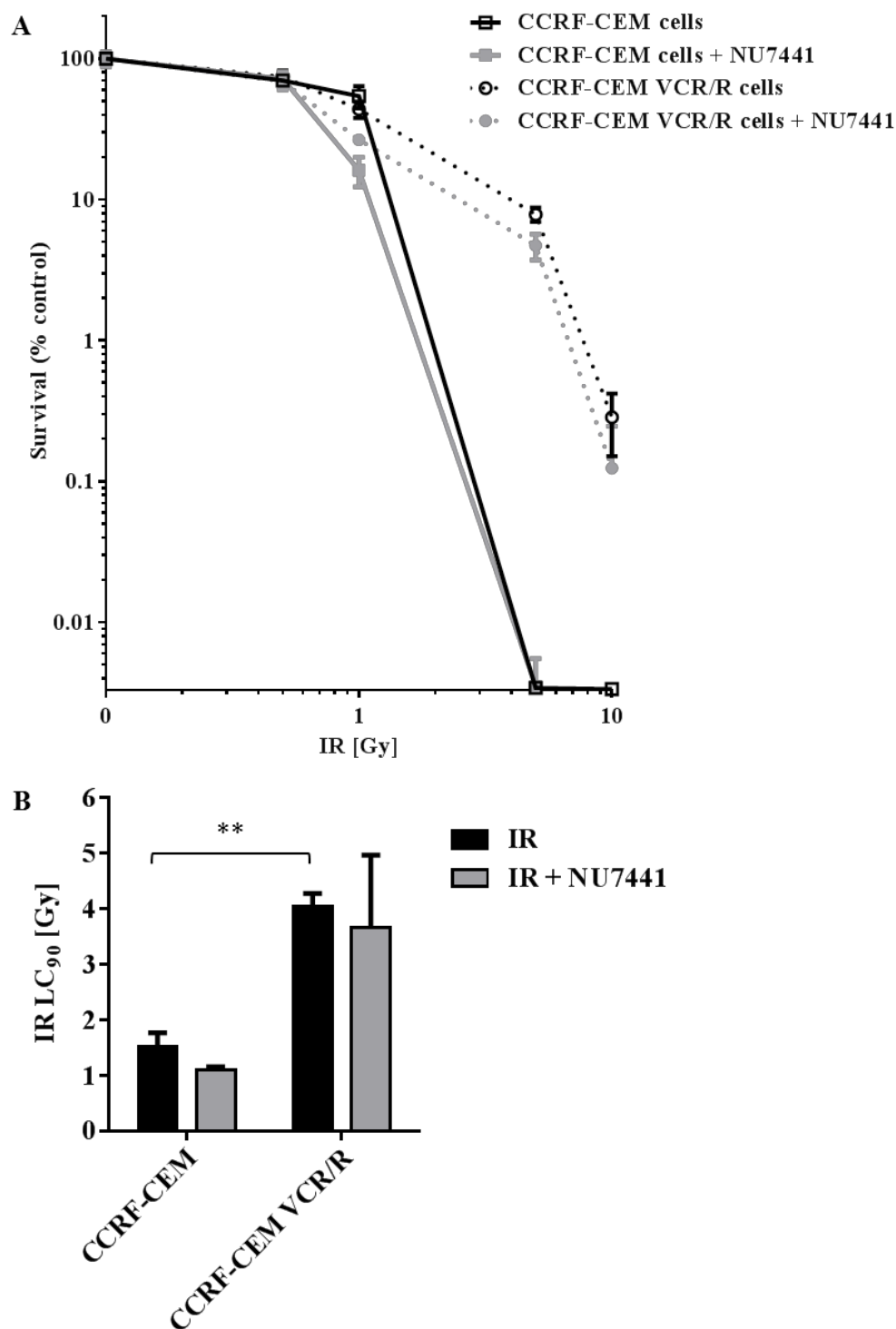
Figure 5-4: CCRF-CEM cells are more sensitive to ionising radiation than CCRF-CEM VCR/R cells, as demonstrated by cytotoxicity assay. CCRF-CEM and CCRF-CEM VCR/R cells were treated with ionising radiation (IR) alone or in combination with 1 µM NU7441 for 24 hours. % Survival was analysed by methylcellulose assay (Section 2.5). (**A**) Data are presented as a percentage of vehicle or inhibitor control colony formation. Points represent the mean of ≥ 3 independent experiments, each in triplicate, $\pm$ standard error. (**B**) LC_{90} data are presented as the LC_{90} means $\pm$ standard error. Asterisk indicates a statistically significant difference using the Student's unpaired *t*-test when compared with the LC_{90} for IR alone (** *p<0.01*).

The A2780 and A2780-TX1000 cell line were then examined for their responses to ionising radiation alone or in combination with NU7441 or KU55933. Interestingly, in this cell line pair, a different pattern of radiosensitivity to that seen in the growth inhibition experiments was observed. There was no significant difference in the ionising radiation LC_{90} dose between the parental A2780 and the A2780-TX1000 cells (Figure 5-5), in contrast to the growth inhibition data where A2780 cells were 5.7-fold more sensitive. In the A2780 cells, NU7441 (1 µM) caused a 2.1-fold (p=0.006) sensitisation at the ionising radiation LC_{90} dose, and KU55933 (10 µM) caused a 3.1-fold (p=0.002) sensitisation. KU55933 (10 µM) significantly sensitised the A2780-TX1000 cells 2.2-fold (p=0.004) at the LC_{90} dose, whereas NU7441 (1 µM) did not significantly increase ionising radiation sensitivity.
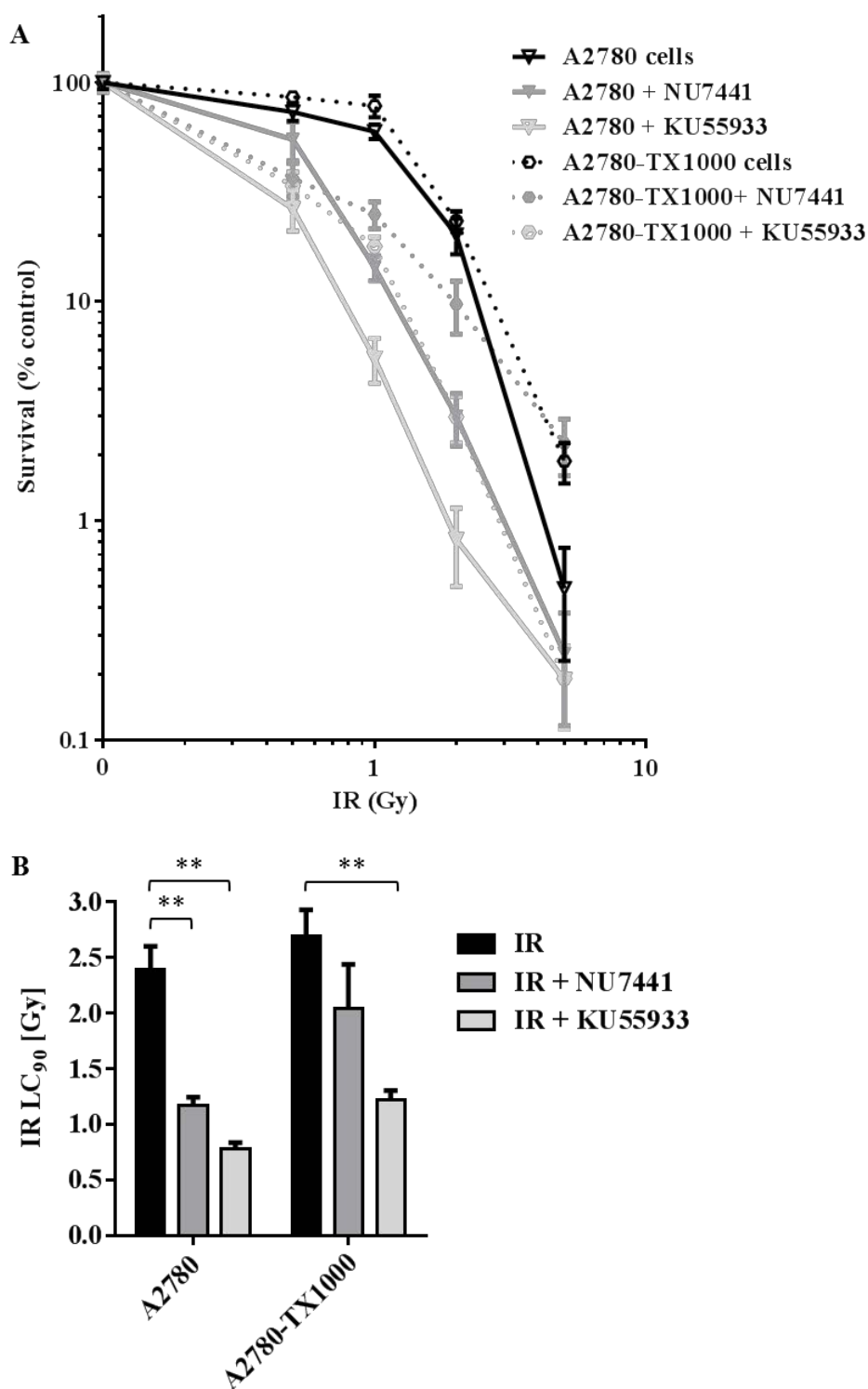
Figure 5-5: Both A2780 and A2780-TX1000 cells are sensitised to ionising radiation by NU7441 and KU55933. A2780 and A2780-TX1000 cells were treated with ionising radiation (IR) alone or in combination with 1 μM NU7441 or 10 μM KU55933 for 24 hours. % Survival was analysed by clonogenic assay (Section 2.4). (**A**) Data are presented as a percentage of vehicle or inhibitor control colony formation. Points represent the mean of ≥3 independent experiments, each in triplicate, ± standard error. (**B**) LC_{90} data are presented as the LC_{90} means ± standard error. Asterisk indicates a statistically significant difference using the Student's unpaired *t*-test when compared with the LC_{90} for IR alone (** *p<0.01*).

	CCRF-CEM cells				CCRF-CEM VCR/R cells		
	IR	**IR + NU7441**	**IR + KU55933**		**IR**	**IR + NU7441**	**IR + KU55933**
IR GI_{50}	1.4 ± 0.06	1.3 ± 0.3^{ns}	2.0 ± 0.3^{ns}		$8.9 \pm 1.3_{p=0.005}$	6.5 ± 2.0^{ns}	8.7 ± 0.7^{ns}
IR LC_{90}	1.5 ± 0.3	1.1 ± 0.1^{ns}	-		$4.0 \pm 0.2_{p=0.002}$	3.7 ± 1.3^{ns}	-
	A2780 cells				A2780-TX1000 cells		
	IR	**IR + NU7441**	**IR + KU55933**		**IR**	**IR + NU7441**	**IR + KU55933**
IR GI_{50}	2.2 ± 0.5	$0.7 \pm 0.1^{p=0.04}$	3.1 ± 2.2^{ns}		>10	>10	>10
IR LC_{90}	2.4 ± 0.2	$1.2 \pm 0.1^{p=0.006}$	$0.8 \pm 0.1^{p=0.002}$		$2.7 \pm 0.2_{ns}$	2.0 ± 0.4^{ns}	$1.2 \pm 0.1^{p=0.004}$
	SKOV3 cells				SKOV3-TR cells		
	IR	**IR + NU7441**	**IR + KU55933**		**IR**	**IR + NU7441**	**IR + KU55933**
IR GI_{50}	11 ± 1.1	$3.7 \pm 0.2^{p=0.003}$	7.5 ± 2.3^{ns}		>20	>20	>20

Table 5-1: GI_{50} and LC_{90} concentrations for ionising radiation alone or in the presence of the NU7441 or KU55933 in three paired sensitive and multidrug-resistant cell lines. GI_{50} data from cells treated with ionising radiation (IR) alone or in combination with 1 µM NU7441 or 10 µM KU55933 for 72 hours with growth analysed by XTT assay (Section 2.3). LC_{90} data from cells treated with ionising radiation (IR) alone or in combination with 1 µM NU7441 or 10 µM KU55933 for 24 hours with survival analysed by clonogenic assay (Sections 2.4 and 2.5). The data are presented as the GI_{50} or LC_{90} mean (Gy) of ≥ 3 independent experiments, each in triplicate, ± standard error. Significant differences between parental and multidrug-resistant cells treated with IR alone were calculated using an unpaired t-test and are shown as a subscript. Significant differences between cells treated with IR alone and cells treated with IR + inhibitor were calculated using an unpaired t-test and are shown as a superscript. ns = not-significant.

5.4   Discussion and future work

Ionising radiation was used as a control in the studies described in this thesis, as a physical, as opposed to a chemical, DNA damaging agent. The response to ionising radiation is known to involve DNA repair proteins, including ATM and DNA-PK, but it was assumed that this would be independent of multidrug-resistance through efflux transporter overexpression. Therefore radiation treatment was used alongside cytotoxic drug treatment in the experiments in Chapter 3.

However, unexpectedly, the multidrug-resistant cells from three different paired cell lines; CCRF-CEM and CCRF-CEM VCR/R cells, A2780 and A2780-TX1000 cells and SKOV3 and SKOV3-TR cells all demonstrated not only chemo-resistance, as seen in Chapter 3, but also radio-resistance in growth inhibition assays (summary in Table 5-1).

The findings in this chapter are consistent with a study demonstrating that vincristine-resistant SKOV3 cells were resistant to radiation relative to parental SKOV3 cells, an effect that was attributed to higher levels of autophagy in the vincristine-resistant cells; a pro-survival and self-protective mechanism in these cells (Liang *et al.*, 2012). It would therefore be interesting to investigate the ionising radiation-induced apoptosis levels using a caspase 3/7 assay or flow cytometry, and to examine the expression of pro-survival proteins and NF-κB. Furthermore, autophagy measured using an MDC assay (which evaluates incorporation of monodansylcadaverine into vacuoles by fluorescent microscopy (Munafo and Colombo, 2001)) could be studied in the parental and multidrug-resistant cells before and after ionising radiation.

The findings in this chapter are however in contrast to a study by Lee *et al.* (2013), which demonstrated reduced DNA-PK-mediated repair and reduced survival in vincristine-resistant KB cells, derived from parental KB cells by exposure to stepwise increments of vincristine, in response to ionising radiation compared with the parental KB cells. Therefore it is possible that the effects of MDR1 on radio-sensitivity are cell-line dependent and further studies using additional parental and multidrug-resistant cell lines should be undertaken to substantiate these conflicting findings.

A number of papers reported the effect of ionising radiation on the expression of MDR1 and other transporters (reviewed in Rendic and Guengerich (2012)). In general, ionising radiation (delivered in various forms) causes an increase in the mRNA and protein expression of a number of transporters, including MDR1, MRP1 (multidrug

resistance-associated protein 1, ABCC1) and LRP (lung resistance-related protein), and increases in transporter expression have been associated with resistance to chemotherapeutic agents in a number of human cancer models (Osmak *et al.*, 1994; Harvie *et al.*, 1997; Bottke *et al.*, 2008; Korystov *et al.*, 2008; Tsang *et al.*, 2009). Some of these findings were tissue-specific, as in the study by Bottke *et al.* (2008) who demonstrated that three breast cancer cell lines displayed increased mRNA and protein levels for MDR1, MRP1 and LRP following irradiation, whereas there was no mRNA increase but a large increase in functional protein in colon cancer cell lines associated with resistance to chemotherapeutic agents. These findings suggest that radiation treatment may lead to a highly resistant phenotype which could affect the response of tumours to concurrent or subsequent chemotherapeutic agents that are MDR1 substrates. However, there are also data to suggest that low doses of fractionated irradiation can have the opposite effect of decreasing MDR1 expression and increasing drug sensitivity (Sanchez *et al.*, 1998; Ryu *et al.*, 2004; Shareef *et al.*, 2008). Together these data suggest that the expression and activity of the transporters in response to radiation is complex, and that the radiation regimen may determine expression changes and subsequent tumour chemo-sensitivity.

Most of the above studies have investigated the effects of ionising radiation on the expression and activity of drug transporters in parental cell lines. Clinically, radiation can be administered before, during and after chemotherapy, depending on the regimen required for each cancer type. Therefore the findings in this chapter are clinically relevant as it is possible that a cancer could become chemo-resistant *via* overexpression of transporters such as MDR1 before the radiation is administered.

Fractionated irradiation is widely used clinically as it has been demonstrated that the delivery of small fractionated doses of ionising radiation causes less damage to normal tissue, whilst having the same effect on tumour growth control, as a single large dose of radiation (Dahlberg *et al.*, 1999). One study in particular investigated the effect of fractionated irradiation in sensitive and multidrug-resistant cells and on MDR1 and DNA-PK expression and activity. Ryu *et al.* (2004) used CCRF-CEM and MDR1-overexpressing CCRF-CEM MDR cells, along with a number of CCRF-CEM IR cells, which they derived following different doses of fractionated irradiation. The authors found that CCRF-CEM MDR cells exhibited lower Ku DNA binding and DNA-PK activity, and reduced MDR1 expression, along with drug sensitivity comparable to that seen in the parental CCRF-CEM cells, following fractionated irradiation. In contrast, the CCRF-CEM parental cells demonstrated radioresistance, increased Ku70/80 levels

and DNA-PKcs levels and activity in response to ionising radiation in a dose-dependent manner (Ryu *et al.*, 2004). This result suggests that the effect of ionising radiation on DNA-PK activity may be different in parental and multidrug-resistant cells, and hence DNA-PK activity should be investigated in all of the paired cell lines used in this thesis. The results presented by Ryu *et al.* (2004) are in contrast to the data generated in Chapter 3 (in relation to the CCRF-CEM and CCRF-CEM VCR/R cell line used in this thesis) where the CCRF-CEM VCR/R cells had higher DNA-PK activity. Therefore the MDR cells used by Ryu *et al.* (2004) (CCRF-CEM MDR) clearly have a very different phenotype to those used here (CCRF-CEM VCR/R).

Inhibition of DNA-PK and ATM using NU7441 and KU55933 has been consistently shown to cause radiosensitisation in a number of different studies (Hickson *et al.*, 2004; Cowell *et al.*, 2005; Zhao *et al.*, 2006; White *et al.*, 2008; Shaheen *et al.*, 2011; Ciszewski *et al.*, 2014; Tichy *et al.*, 2014). Therefore, the effect of these inhibitors on the radiation response in the three paired parental and multidrug-resistant cell lines was investigated.

The interesting finding in this chapter was the lack of sensitisation of cells to ionising radiation using the ATM inhibitor, KU55933, in the growth inhibition assays; although KU55933 did significantly sensitise A2780 and A2780-TX1000 cells in the clonogenic survival assay. This suggested that ATM inhibition effects are revealed in cytotoxicity and cell survival, but not growth inhibition assays. NU7441 significantly sensitised SKOV3 and A2780 cells to ionising radiation in the growth inhibition assays and sensitised the A2780 cells in the clonogenic survival assay. However, NU7441 did not sensitise any of the multidrug-resistant cell lines to ionising radiation in either the growth inhibition or clonogenic survival assays. Hence DNA-PK may not play such a significant role in the response of multidrug-resistant cells to ionising radiation as it does in parental cells. This finding is similar to the conclusions drawn by Ryu *et al.* (2004) in relation to the observed changes in DNA-PK activity following fractionated irradiation discussed above.

The effect of ionising radiation on DNA-PK autophosphorylation at serine 2056 in the CCRF-CEM and CCRF-CEM VCR/R cells and the effects of NU7441 were examined in Chapter 3. There was a similar level of DNA-PK autophosphorylation in response to ionising radiation in both the parental and multidrug-resistant cell lines, and the same inhibition profile with NU7441 in both cell lines. Therefore it is known that DNA-PK can be autophosphorylated in both cell lines following ionising radiation and that autophosphorylation can be inhibited to the same degree. Therefore the differences

in sensitisation in the parental and multidrug-resistant cell lines caused by NU7441 are not due to a difference in the effect of NU7441 on DNA-PK autophosphorylation. It would be interesting to investigate the DNA-PK catalytic activity in both the parental and multidrug-resistant cells, along with the Ku70/80 binding activity.

Studies of MDR1 expression and DNA-PK activity and expression in patients following ionising radiation would be useful to determine if there is a relationship between radiation and transporters or DNA repair enzyme function in clinical material. Such studies could lead to the use of MDR expression and/or DNA-PK activity as predictive biomarkers for ionising radiation sensitivity and lead to the use of these measurements in personalised medicine.

5.5   Summary

Three pairs of parental and multidrug-resistant cells were investigated for their response to ionising radiation. A2780-TX1000, CCRF-CEM VCR/R cells and SKOV3-TR multidrug-resistant cell lines were all found to be more resistant to ionising radiation than their parental cell lines in growth inhibition assays. The DNA-PK inhibitor NU7441 caused radiosensitisation in the A2780 and SKOV3 cell lines but had no effect on radiation sensitivity in any of the multidrug-resistant cell lines. The ATM inhibitor KU55933 sensitised the A2780 and A2780-TX1000 cells when determined by clonogenic survival assay but not by growth inhibition assay, and had no effect on any of the other cell lines. In conclusion, the multidrug-resistant cell lines that overexpress MDR1 used in this thesis display both chemo- and radioresistance and further investigation is needed to elucidate the mechanism behind the unexpected radioresistance observed.

Chapter 6: Investigation of the role of DNA-PK and ATM as a determinant of ionising radiation and vincristine response using paired DNA-PK proficient and deficient cell lines

6.1 Introduction

Comparing the effects of a lack of functional protein *versus* chemical inhibition is an important area of research in the discovery and development of targeted agents. Specifically, the cellular impact of an inhibited as opposed to an absent protein may be different, particularly when the target protein has dual catalytic and structural functions. However, finding a model of proficient and deficient cell lines that are truly isogenic is extremely difficult.

There are four reported incidences of spontaneous germline mutations in the DNA-PK gene in mammalian species; two in mice (Bosma *et al.*, 1983; Jhappan *et al.*, 1997), one in a horse (McGuire and Poppie, 1973) and one in a dog (Meek *et al.*, 2001), which have resulted in viable animals. However, there are only two cases of reported human germline *PRKDC* mutations. The first patient identified had a homozygous missense mutation that did not affect DNA-PKcs expression or kinase activity. The patient had severe combined immunodeficiency (SCID), and impaired NHEJ and Artemis activation, but was otherwise developmentally normal (van der Burg *et al.*, 2009). However, the second SCID patient to be identified with mutated *PRKDC*, resulting in substantially reduced DNA-PKcs protein levels, undetectable DNA-PK activity and impaired NHEJ, displayed neurological abnormalities resulting from neuronal atrophy postnatally, indicating a role for DNA-PKcs during neuronal development (Woodbine *et al.*, 2013). However, it is surprising that more DNA-PKcs germline mutations have not been reported.

The first animal model with defective DNA double-strand break repair attributed to a defect in the catalytic subunit of DNA-PK was the SCID mouse, which is viable but radiation hypersensitive and defective in V(D)J recombination (Bosma *et al.*, 1983; Kirchgessner *et al.*, 1995). However, the SCID mouse is not null for DNA-PKcs but rather has a single base mutation that allows the formation of an unstable, but almost full-length (excluding the last 83 amino acids), DNA-PKcs protein which may have residual function (Blunt *et al.*, 1996; Danska *et al.*, 1996; Araki *et al.*, 1997). Therefore a better isogenic model for investigating the function of DNA-PK and the effects of DNA-PK inhibition was required.

The M059J and M059K cell lines were derived from different areas of the same human malignant glioblastoma tumour and were found to have altered radiation sensitivity profiles resulting from different levels of DNA-PK activity, subsequently attributed to defects in human chromosome 8 where DNA-PK is located (Allalunis-

Turner *et al.*, 1993; Lees-Miller *et al.*, 1995). The M059J cell line, in contrast to mouse SCID cells, are deficient in DNA-PKcs protein expression through a nonsense frameshift mutation and are highly radiosensitive, whereas the M059K cells are relatively radioresistant and display DNA-PK activity. However, tumours often display genomic instability and rarely have only one gene mutation, and it was found that the M059J and M059K cells also have different expression profiles of ATM (Chan *et al.*, 1998; Gately *et al.*, 1998); therefore the M059J and M059K cells are not an isogenic matched pair of cells with only a mutation in DNA-PK. An isogenic M059J-matched cell line, the M059J-Fus1 cell line, was created by chromosome transfer by fusing M059J cells with a SCID cell line containing 1 copy of human chromosome 8, SCID/hu8 cells (Hoppe *et al.*, 2000). The M059J-Fus1 cells are thus complemented with an extra copy of chromosome 8 and are relatively radioresistant and have functional DNA-PK activity. The M059J and M059J-Fus1 cells were used initially in this study as an isogenic cell line pair, with the M059J-Fus1 cells grown under antibiotic selection. The M059J cells have previously been shown to be more radiosensitive and doxorubicin-sensitive than the M059J-Fus1 cells, and only the M059J-Fus1 cells were chemo- and radio-sensitised by the selective DNA-PK inhibitor, NU7441 (Tavecchio *et al.*, 2012).

A more modern and accurate technique for gene targeted knock-out involves the use of recombinant adeno-associated virus vectors (rAAV) which act by initiating homologous recombination to accurately deliver and incorporate the vector at the correct site on the DNA (Kohli *et al.*, 2004). The cells used in this chapter were purchased from Horizon Discovery Group plc and the original cell line is the human adenocarcinoma HCT116 cell line (DNA-PK +/+). The targeting vectors contained ~900-bp-long left and right homology arms for the DNA-PKcs exon 81 to 83, constructed by PCR from HCT116 genomic DNA, which were flanked by a Neo resistance selection cassette which itself was flanked by LoxP sites. Correct targeting of exons 81-83 at the 3' end of the locus results in catalytically inactive DNA-PKcs (as these exons are in the catalytic domain) (Ruis *et al.*, 2008). This technique first produces a heterozygous knockout cell line (DNA-PK +/-) as it can only target one allele at a time; however, the heterozygous cell line allows analysis of haploinsufficient gene function. A second round of gene targeting, where cells will either have random targeting, retargeting (correct targeting but of the already inactivated gene) or correct targeting of the remaining functional allele, produced the HCT116 -/- cells (Ruis *et al.*, 2008). These cells were found to display slow growth and radiation sensitivity, with

shortened telomeres and genetic instability. Another cell line was also produced from the DNA-PK -/- cells that had DNA-PK reintroduced using cDNA, and are referred to in this Chapter as DNA-PK RE (re-expressing) cells.

6.2   Aims

Following the observations that DNA-PK and ATM appear to play a role in the response of cells to microtubule-targeting agents, and that NU7441 and KU55933 are acting as dual DNA-PK and MDR1 or ATM and MDR1 inhibitors, respectively, the roles of DNA-PK and ATM were further investigated by using paired DNA-PK deficient and proficient cell lines. The use of paired cell lines allows the distinctions to be made between DNA-PK-, ATM- and MDR1-mediated effects that complement results obtained using inhibitors. Growth inhibition of the M059J (DNA-PK deficient) and M059J-Fus1 (DNA-PK proficient) cells was examined with the microtubule-targeting agent, docetaxel alone and in the presence of NU7441 to investigate any differences in sensitivity based on DNA-PK status. The HCT116 parental, DNA-PK +/-, DNA-PK -/- and DNA-PK RE cells were characterised and their responses to ionising radiation and microtubule-targeting agents was investigated in the presence and absence of NU7441 and KU55933. Activity and expression of DNA-PK in response to IR and vincristine was also established. Clonogenic assays were undertaken to investigate the effects of ionising radiation, vincristine or a combination of both in succession on survival of HCT116 cells with different DNA-PK activity profiles.

6.3   Results

6.3.1   DNA-PK-deficient M059J cells were more sensitive to docetaxel than DNA-PK proficient M059J-Fus1 cells

Following the findings of Chapter 3 that cells could be sensitised to microtubule-targeting agents by the DNA-PK and ATM inhibitors, sensitisation to these agents was investigated in isogenic cell lines with different DNA-PK expression profiles.

Total DNA-PK expression was investigated in the M059J and M059J-Fus1 cells. The M059J-Fus1 cells were maintained under antibiotic selection using G418 disulfate to ensure retention of the transferred chromosome 8 which carries a G418 resistance

gene. Figure 6-1 demonstrates that total DNA-PKcs was readily detectable in the M059J-Fus1 cells and that these are therefore DNA-PK proficient, but was not detectable in the M059J cells which are therefore DNA-PK deficient.
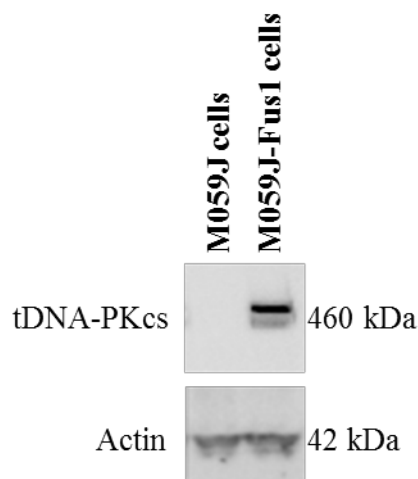
Figure 6-1: DNA-PK is expressed in M059J-Fus1 cells but not in M059J cells.
M059J and M059J-Fus1 cell lysates were prepared from exponentially-growing cells and total DNA-PKcs and actin expression was determined by Western blotting using the indicated specific antibodies (Section 2.7.4).Data are representative of 3 independent experiments.

The growth inhibition of M059J and M059J-Fus1 cells in response to the microtubule-targeting agent, docetaxel, alone or in combination with the DNA-PK inhibitor, NU7441, was investigated to highlight any differences in the response of cells caused by chemical inhibition *versus* lack of expression. The M059J DNA-PK deficient cells were 2.2-fold (p=0.04) more sensitive to docetaxel than the M059J-Fus1 cells (Figure 6-2A). The specificity of NU7441 was demonstrated by lack of sensitisation in the M059J cells to docetaxel (Figure 6-2B) in comparison to 2.3-fold (p=0.03) sensitisation in the M059J-Fus1 cells (Figure 6-2C). The sensitisation caused by NU7441 in the M059J-Fus1 cells reduced the GI_{50} concentration to the same level as in the DNA-PK deficient M059J cells (0.8 µM).
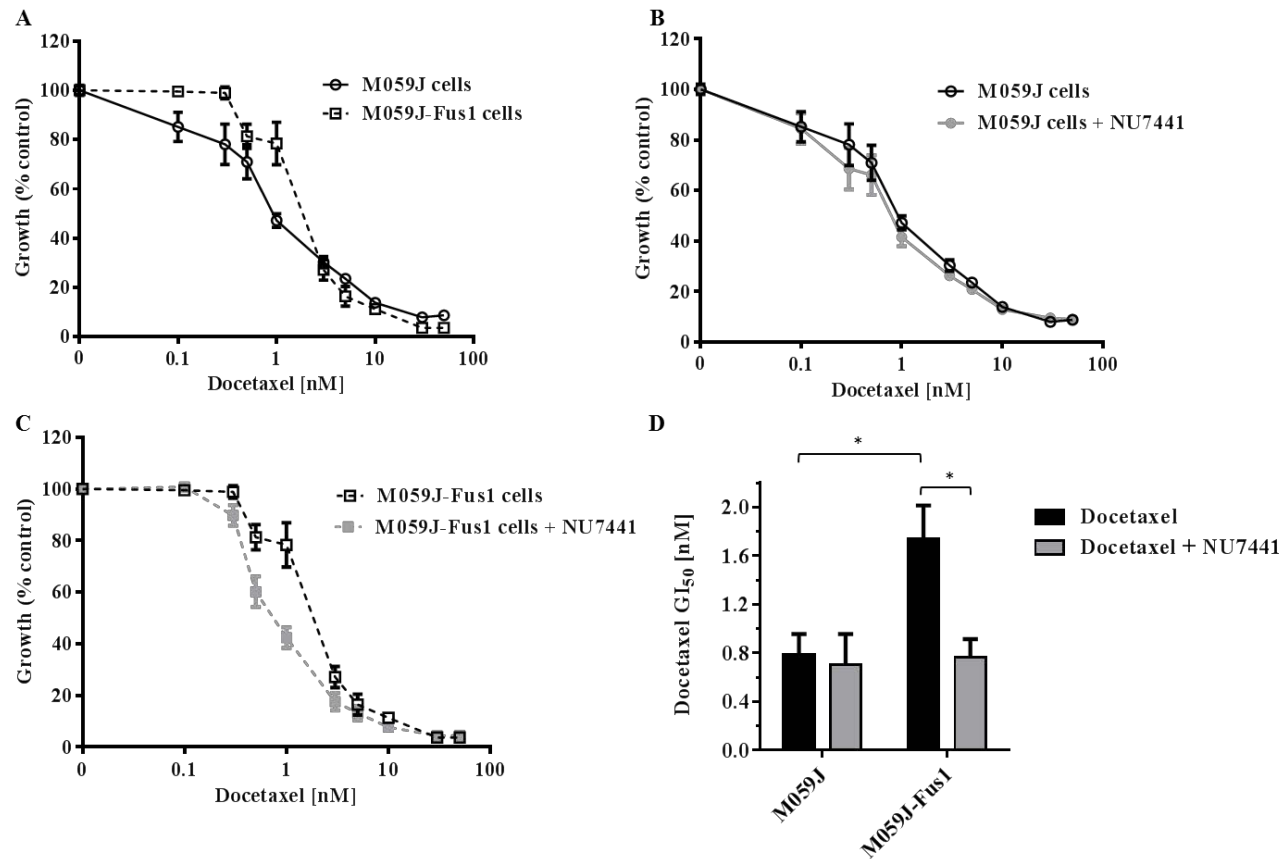
Figure 6-2: DNA-PK proficient cells are less sensitive to docetaxel than DNA-PK deficient cells. M059J (**A** and **B**) and M059J-Fus1 (**A** and **C**) cells were treated with docetaxel alone or in combination with 1 μM NU7441 for 72 hours and growth was analysed by XTT assay (Section 2.3). Data are presented as a percentage of vehicle control cells. Points represent the mean of ≥3 independent experiments, each in triplicate, ± standard error. (**D**) GI_{50} data are presented as the GI_{50} means ± standard error. Asterisk indicates a statistically significant difference using the Student's unpaired t-test when compared with the GI_{50} for docetaxel alone (* $p<0.05$).

	M059J cells		M059J-Fus1 cells	
	Drug [nM]	Drug + NU7441 [nM]	Drug [nM]	Drug + NU7441 [nM]
Docetaxel GI$_{50}$	0.79 ± 0.17	0.70 ± 0.25^{ns}	1.74 ± 0.27$_{p=0.04}$	0.76 ± 0.15$^{p=0.03}$

Table 6-1: GI$_{50}$ concentrations for docetaxel alone or in the presence of the NU7441 in M059J and M059J-Fus1 cells. Cells were treated with docetaxel alone or in combination with 1 µM NU7441 for 72 hours and % growth was analysed by XTT assay (Section 2.3). The data are presented as the GI$_{50}$ mean (nM) of ≥3 independent experiments, each in triplicate, ± standard error. Significant differences between M059J and M059J-Fus1 cells treated with drug alone were calculated using an unpaired *t*-test and are shown as a subscript. Significant differences between cells treated with drug alone and cells treated with drug + inhibitor were calculated using an unpaired *t*-test and are shown as a superscript. ns = non-significant.

The effect of DNA-PK expression on cytotoxicity in response to docetaxel was then investigated in the M059J and M059J-Fus1 cells using a clonogenic assay. Figure 6-3 indicates that the M059J cells were more sensitive to docetaxel than the M059J cells, consistent with the growth inhibition results shown in Figure 6-2.

However, the cloning efficiency calculated for both the M059J and M059J-Fus1 cells was low (≤ 8 %). It was also noted that the M059J cells had approximately half the growth rate of the M059J-Fus1 cells and therefore the colonies in the M059J cells were smaller and more difficult to count.

The low plating efficiency and different growth rates complicate interpretation of these data and therefore the HCT116 panel of cell lines (described in Section 6.1) were investigated.
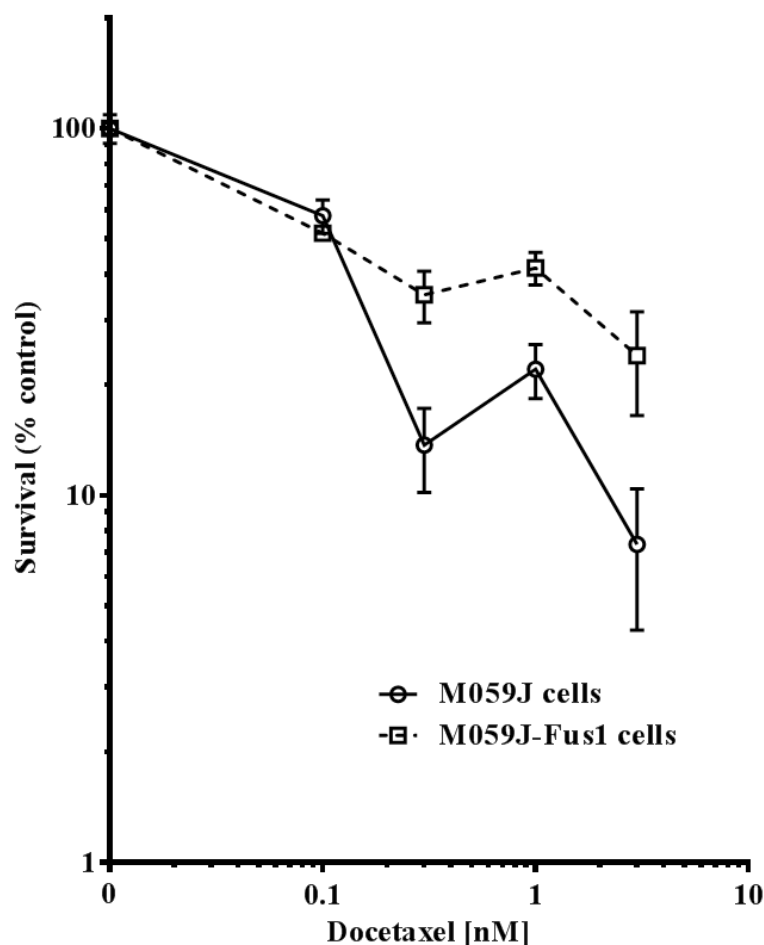
Figure 6-3: M059J cells are more sensitive to docetaxel than M059J-Fus1 cells.
M059J and M059J-Fus1 cells were treated with docetaxel alone or in combination with
1 μM NU7441 for 24 hours. % Survival was analysed by clonogenic assay (Section
2.4). Data are presented as a percentage of vehicle control cells. Points represent the
mean of 2 independent experiments, each in triplicate, ± standard error.

6.3.2   Characterisation of the HCT116 cell line panel

HCT116 parental, DNA-PK +/-, DNA-PK -/- and DNA-PK RE cells were
obtained from Horizon Discovery plc and all were shown to have a similar growth rate.

To characterise the DNA-PK expression, mRNA and protein levels were
measured in the 4 cell lines. mRNA levels of *ABCB1* (MDR1), *XRCC6* (Ku70) and
XRCC5 (Ku80) were also investigated by PCR. The *PRKDC* Taqman gene expression
assay used in these PCR experiments spanned exons 27-28. The targeting vectors in the
HCT116 DNA-PK +/-, DNA-PK -/-, and DNA-PK RE cells targeted exons 81-83,
preventing endogenous protein expression. Therefore the *PRKDC* mRNA expression

level based on exons 27-28 was found to be similar for all cell lines (Figure 6-4), and a gene expression assay targeting exons 81-83 would be needed to demonstrate differences in *PRKDC* mRNA expression levels. The mRNA levels of the other DNA-PK subunits, *XRCC6* and *XRCC5* were the same, as was the expression of *ABCB1* which was measured to ensure any differences in drug response in these cell lines were independent of MDR1 (Figure 6-4).
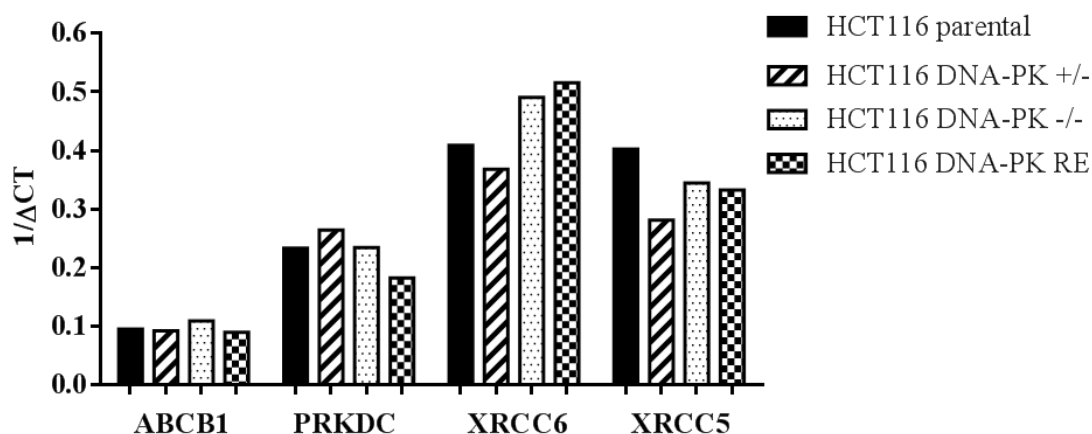
Figure 6-4: Characterisation of HCT116 cell line panel showing similar levels of *ABCB1, PRKDC, XRCC6* and *XRCC5* mRNA. Cell pellets were prepared from exponentially-growing cells and *ABCB1, PRKDC, XRCC6, XRCC5* and *β-actin* mRNA levels determined by real-time quantitative PCR using the indicated gene expression assays (Section 2.9.5). The cycle threshold (CT) value was determined using a 7500 Fast RT PCR system and data are presented as $1/\Delta CT$ relative to β-actin. Results are mean of one independent experiment carried out in duplicate.

DNA-PK protein expression and activity was determined in the HCT116 cell line panel by Western blotting. In HCT116 DNA-PK +/- cells, DNA-PK expression level was approximately half of that seen in the parental HCT116 DNA-PK +/+ cells (Figure 6-5). The total DNA-PK expression level in the HCT116 DNA-PK RE cells was similar to the HCT116 DNA-PK +/- cells, indicating that reintroduction of DNA-PK did not achieve the same level of DNA-PK expression as the parental cells. No DNA-PK expression was seen in the HCT116 DNA-PK -/- cells, as expected. DNA-PK was activated at its autophosphorylation site (serine 2056) in the HCT116 DNA-PK +/+, DNA-PK +/- and DNA-PK RE cells in response to ionising radiation (Figure 6-5);

however, the high basal expression of phosphorylated DNA-PK in DNA-PK +/- cells shown in Figure 6-5 was not a consistent finding.

	DNA-PK +/+		DNA-PK -/-		DNA-PK +/-		DNA-PK RE		
IR [Gy]	0	10	0	10	0	10	0	10	
pDNA-PK (Ser2056)									460 kD
tDNA-PKcs									460 kD
Actin									42 kD
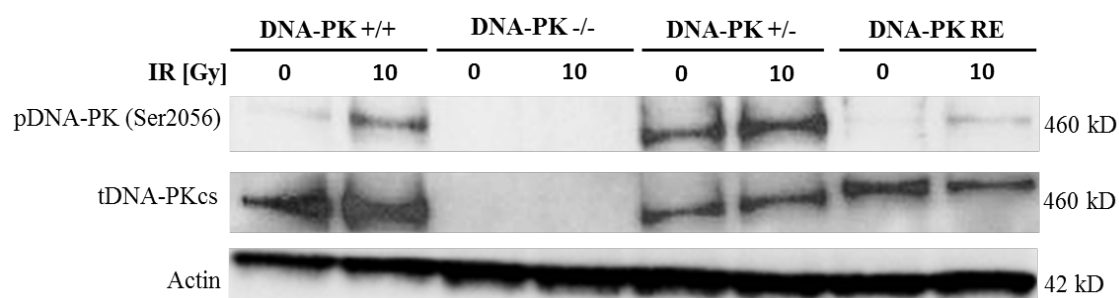
Figure 6-5: DNA-PK activation and expression profiles of the HCT116 cell line panel prior to or following 10 Gy IR. HCT116 DNA-PK +/+, DNA-PK +/-, DNA-PK -/- and DNA-PK RE cells were irradiated with 10 Gy IR and cell lysates were collected after 30 minutes. DNA-PK activity and expression, and actin expression, were determined by Western blotting using the indicated specific antibodies (Section 2.7.4). Data are representative of 3 independent experiments.

6.3.3   HCT116 DNA-PK -/- cells were more sensitive to ionising radiation than DNA-PK proficient cells

Following characterisation, growth inhibition and cytotoxicity was investigated in the HCT116 DNA-PK +/+, DNA-PK +/-, DNA-PK -/- and DNA-PK RE cells in response to ionising radiation.

In a growth inhibition assay, the HCT116 DNA-PK -/- cells were 3.2-fold more sensitive to ionising radiation than the parental HCT116 DNA-PK +/+ cells, indicating that DNA-PK expression is important in the response of these cells to ionising radiation (Figure 6-6). There was no difference in the response of the HCT116 DNA-PK +/- cells compared to the parental cells, indicating that a single DNA-PK allele is sufficient to maintain DNA-PK activity. The HCT116 DNA-PK RE cells were marginally (1.6-fold) more sensitive to ionising radiation than the HCT116 DNA-PK +/+ cells and 2-fold less sensitive than the HCT116 DNA-PK -/- cells, indicating that DNA-PK function present in the HCT116 DNA-PK RE cells is not as high as in the parental cells but greater than in the HCT116 DNA-PK -/- cells. However, these differences were not statistically significant at the GI_{50} concentration.

NU7441 and KU55933 were used in combination with ionising radiation in the HCT116 cell lines to explore the effects of chemical inhibiton of DNA-PK or ATM.

The parental HCT116 DNA-PK +/+ cells were sensitised 2.3-fold (p=0.02) to ionising radiation by 1 µM NU7441 and 2.4-fold (p=0.02) by 10 µM KU55933 (Figure 6-7A) (Table 6-2). A similar pattern of sensitisation was observed in the HCT116 DNA-PK +/- cells and the HCT116 DNA-PK RE cells but was not significant at the GI_{50} concentration due to experimental variation. There was no effect of 1 µM NU7441 in the HCT116 DNA-PK -/- cells and there was a 2.2-fold sensitisation with 10 µM KU55933, but again this was not significant at the GI_{50} concentration.
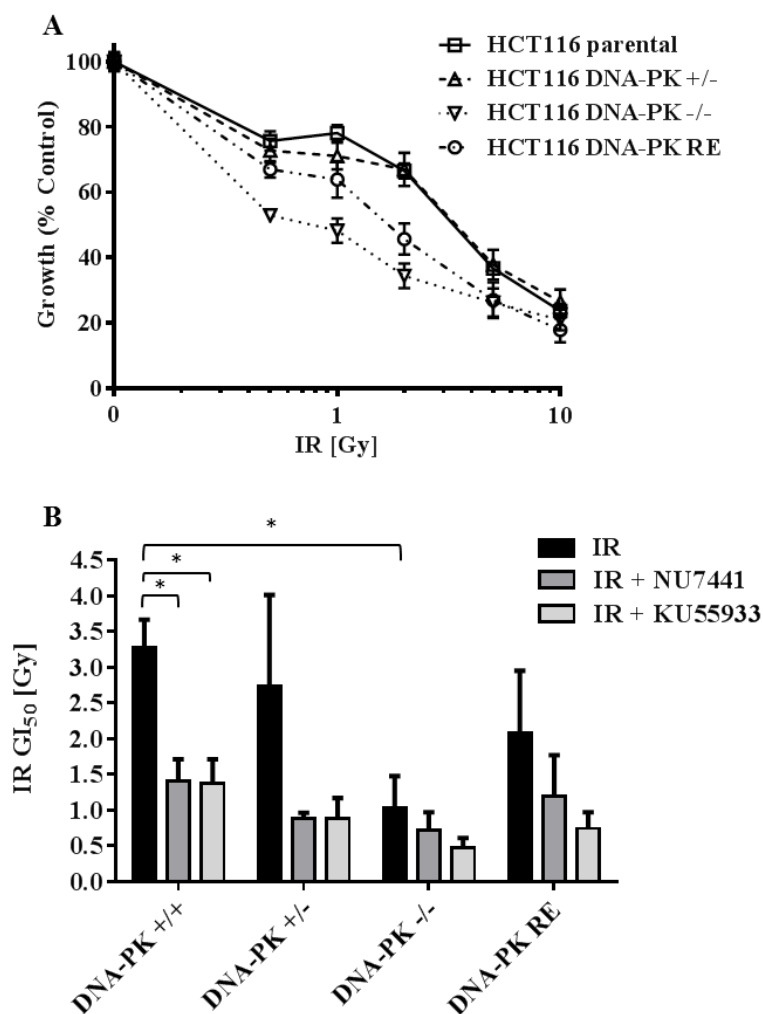
Figure 6-6: DNA-PK -/- cells are more sensitive to IR than DNA-PK proficient cells. HCT116 parental, DNA-PK +/-, DNA-PK -/- and DNA-PK RE cells were treated with IR alone or in combination with 1 µM NU7441 or 10 µM KU55933 for 72 hours and % growth was analysed by XTT assay (Section 2.3). (**A**) IR alone data are presented as a percentage of vehicle control cells. Points represent the mean of ≥3 independent experiments, each in triplicate, ± standard error. (**B**) IR plus inhibitors GI_{50} data are presented as the GI_{50} means ± standard error. Asterisk indicates a statistically significant difference using the Student's unpaired *t*-test when compared with the GI_{50} for IR alone (* *p<0.05).*
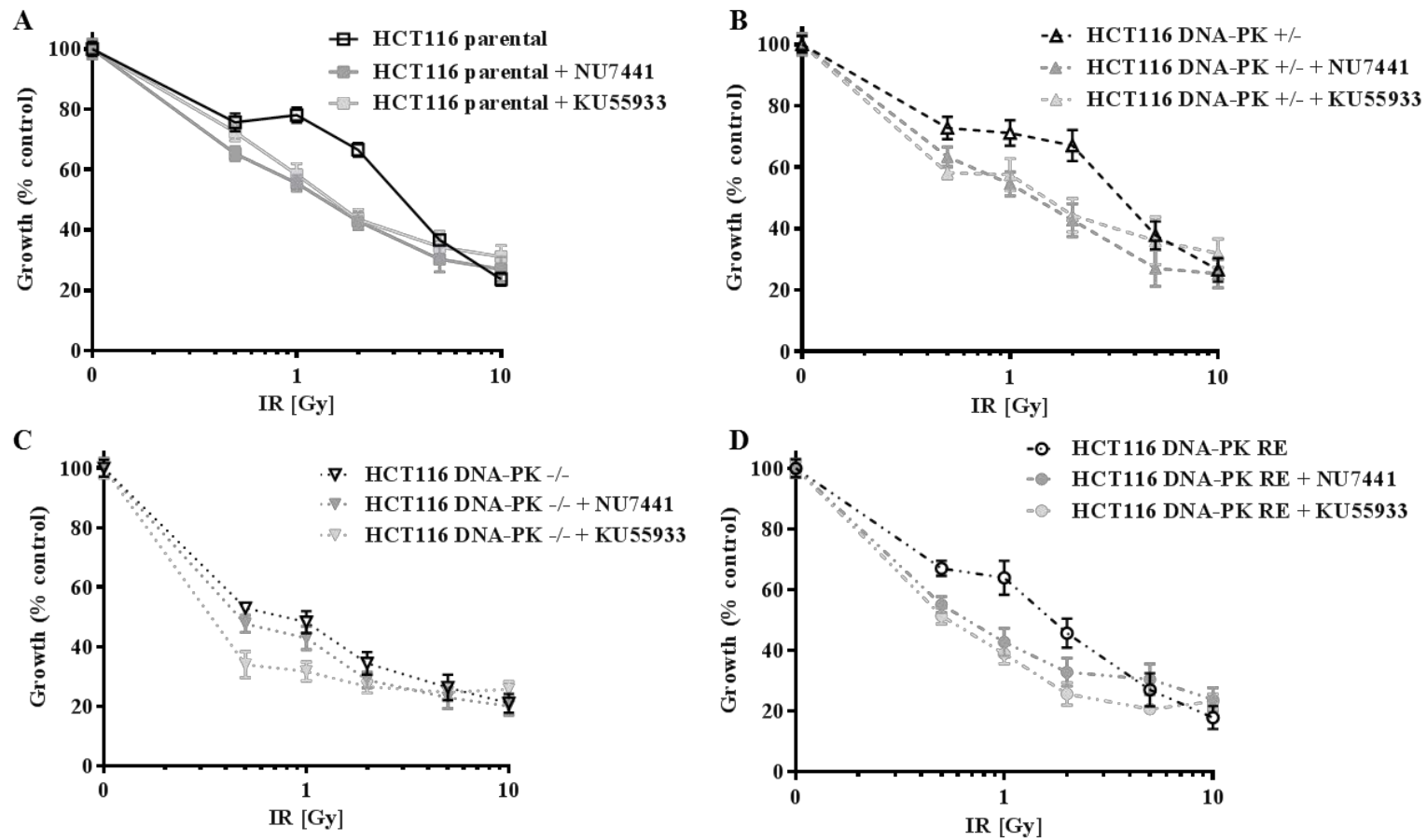
Figure 6-7: HCT116 cell lines are sensitised to IR by NU7441 and KU55933. HCT116 parental, DNA-PK +/-, DNA-PK -/- and DNA-PK RE cells were treated with IR alone or in combination with 1 µM NU7441 or 10 µM KU55933 for 72 hours and % growth was analysed by XTT assay (Section 2.3). Data are presented as a percentage of vehicle control cells. Points represent the mean of ≥3 independent experiments, each in triplicate ± standard error.

The HCT116 cell line panel was then treated with ionising radiation and cytotoxicity determined using a clonogenic assay. There was no difference in cytotoxicity to ionising radiation in the parental HCT116 DNA-PK +/+, DNA-PK +/- and DNA-PK RE cells but the HCT116 DNA-PK -/- cells were 3.4-fold more sensitive at the LC_{90} concentration (Figure 6-8).
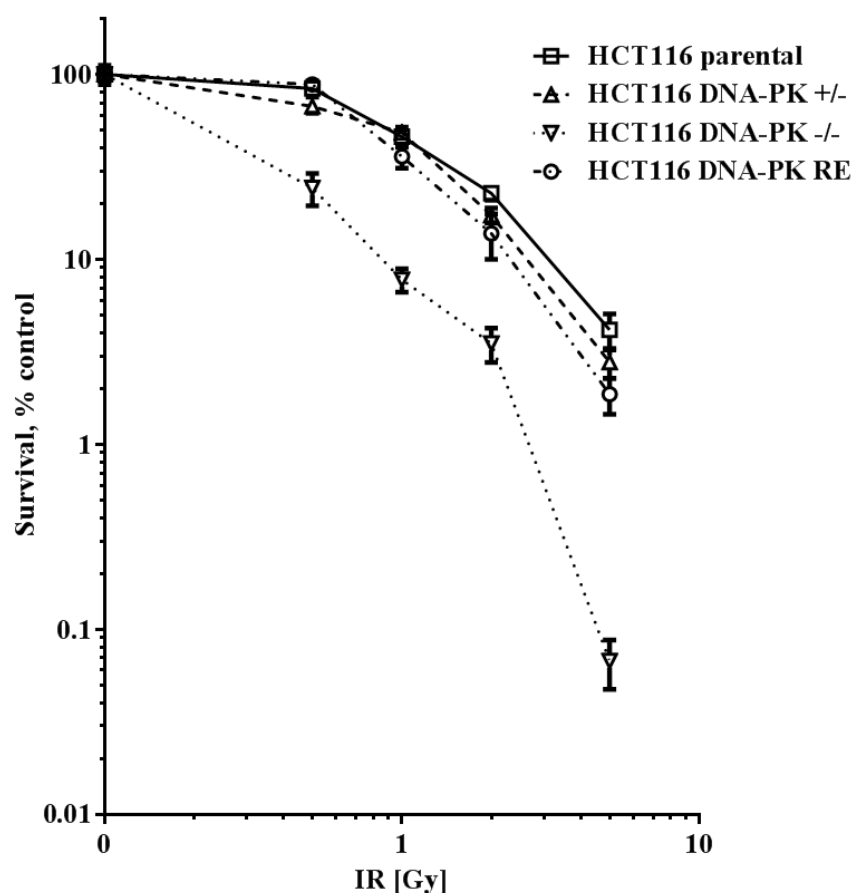
Figure 6-8: HCT116 DNA-PK -/- cells are significantly more sensitive to IR than the HCT116 parental cell line. HCT116 parental, DNA-PK +/-, DNA-PK -/- and DNA-PK RE cells were treated with IR and incubated for 24 hours. % survival was analysed by clonogenic assay (Section 2.4). Data are presented as a percentage of control cells. Points represent the mean of 3 independent experiments, each in triplicate, ± standard error.

Cell line	Ionising Radiation (IR) [Gy]			
	GI_{50} IR	GI_{50} IR + NU7441	GI_{50} IR + KU55933	LC_{90} IR
DNA-PK +/+	3.28 ± 0.38	$1.41 \pm 0.30^{p=0.02}$	$1.38 \pm 0.33^{p=0.02}$	2.99 ± 0.26
DNA-PK +/-	$2.74 \pm 1.28_{ns}$	0.89 ± 0.08^{ns}	0.89 ± 0.28^{ns}	$2.54 \pm 0.32_{ns}$
DNA-PK -/-	$1.03 \pm 0.45_{p=0.02}$	0.72 ± 0.25^{ns}	0.47 ± 0.14^{ns}	$0.87 \pm 0.07_{p=0.001}$
DNA-PK RE	$2.08 \pm 0.87_{ns}$	1.19 ± 0.58^{ns}	0.74 ± 0.23^{ns}	$2.29 \pm 0.38_{ns}$

Table 6-2: DNA-PK proficient HCT116 cell lines are sensitised to IR by NU7441 and KU55933. GI_{50} data: HCT116 parental, DNA-PK +/-, DNA-PK -/- and DNA-PK RE cells were treated with IR alone or in combination with 1 µM NU7441 or 10 µM KU55933 for 72 hours and % growth was analysed by XTT assay (Section 2.3). LC_{90} data: HCT116 parental, DNA-PK +/-, DNA-PK -/- and DNA-PK RE cells were treated with IR and incubated for 24 hours. % survival was analysed by clonogenic assay (Section 2.4). The data are presented as the GI_{50} mean or LC_{90} mean (Gy) of ≥3 independent experiments, each in triplicate, ± standard error. Significant differences between cell lines treated with IR alone were calculated using an unpaired *t*-test and are shown as subscripts. Significant differences between cells treated with IR alone and cells treated with IR + inhibitor were calculated using an unpaired *t*-test and are shown as superscripts. ns = non-significant.

This data demonstrates that the HCT116 cell line panel respond as expected to ionising radiation with respect to the DNA-PK expression status.

6.3.4   *HCT116 DNA-PK -/- cells and DNA-PK RE cells were more sensitive to vincristine than parental cells*

Following the ionising radiation growth inhibition and cytotoxicity studies in the HCT116 cell line panel, the cells were examined to measure their response to vincristine. There was no difference in growth inhibition in response to vincristine between the parental HCT116 DNA-PK +/+ and HCT116 DNA-PK +/- cells, again demonstrating no haploinsufficiency effect in the HCT116 DNA-PK +/- cells (Figure 6-9A). Although the HCT116 DNA-PK -/- cells were 1.5-fold more sensitive at the GI_{50} concentration, and the HCT116 DNA-PK RE cells were 3.9-fold more sensitive, sensitisation was not significant at the GI_{50} level. NU7441 (1 µM) had no significant effect on any of the cell lines' vincristine GI_{50} concentrations (Figure 6-10) (Table 6-3). KU55933 sensitised the DNA-PK +/+ cells 6.1-fold (p=0.046), the DNA-PK +/- cells

5.5-fold (p=0.02) and the DNA-PK -/- cells 16.2-fold (p=0.02), demonstrating that ATM may play a greater role in the response of these cells to vincristine than DNA-PK, especially in the absence of DNA-PK.
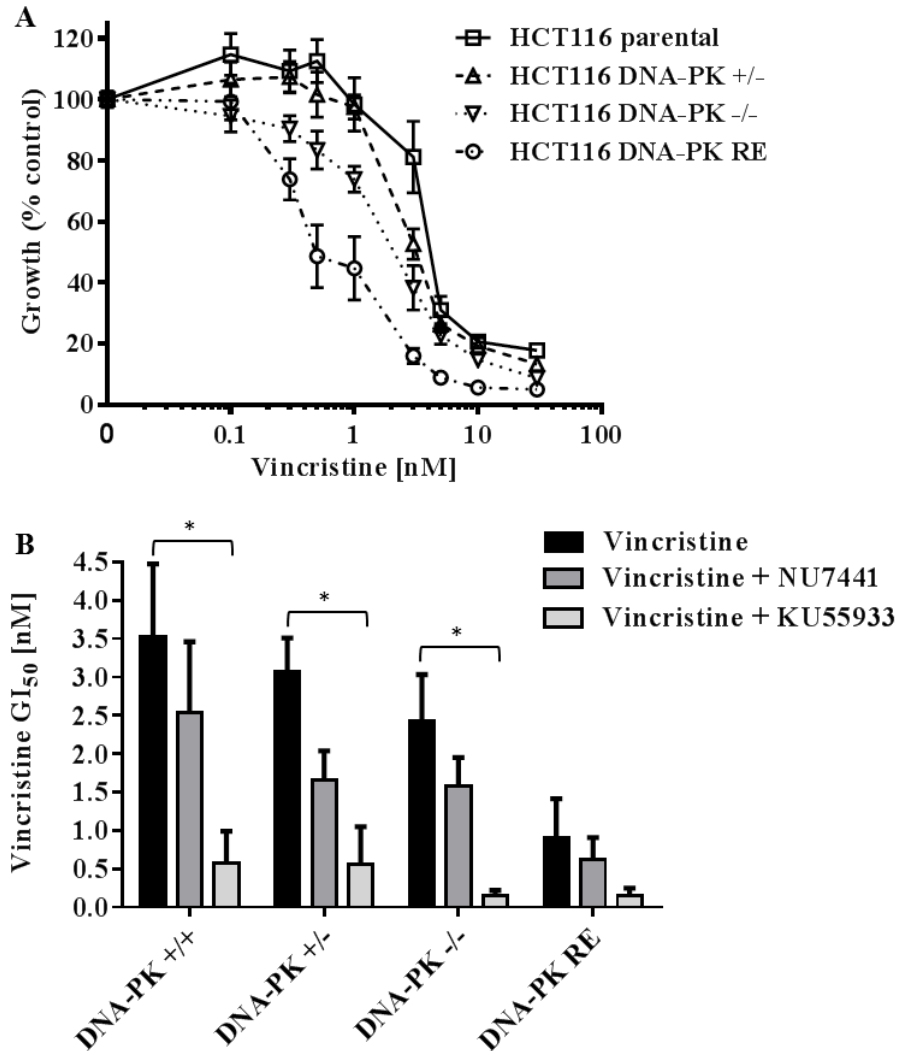
Figure 6-9: KU55933 sensitises HCT116 DNA-PK +/+, DNA-PK +/- and DNA-PK -/- cells to vincristine. HCT116 parental, DNA-PK +/-, DNA-PK -/- and DNA-PK RE cells were treated with vincristine alone or in combination with 1 μM NU7441 or 10 μM KU55933 for 72 hours and % growth was analysed by XTT assay (Section 2.3). (**A**) Vincristine alone data are presented as a percentage of vehicle control cells. Points represent the mean of ≥3 independent experiments, each in triplicate, ± standard error. (**B**) Vincristine plus inhibitors GI_{50} data are presented as the GI_{50} means ± standard error. Asterisk indicates a statistically significant difference using the Student's unpaired *t*-test when compared with the GI_{50} for drug alone (* *p<0.05*).
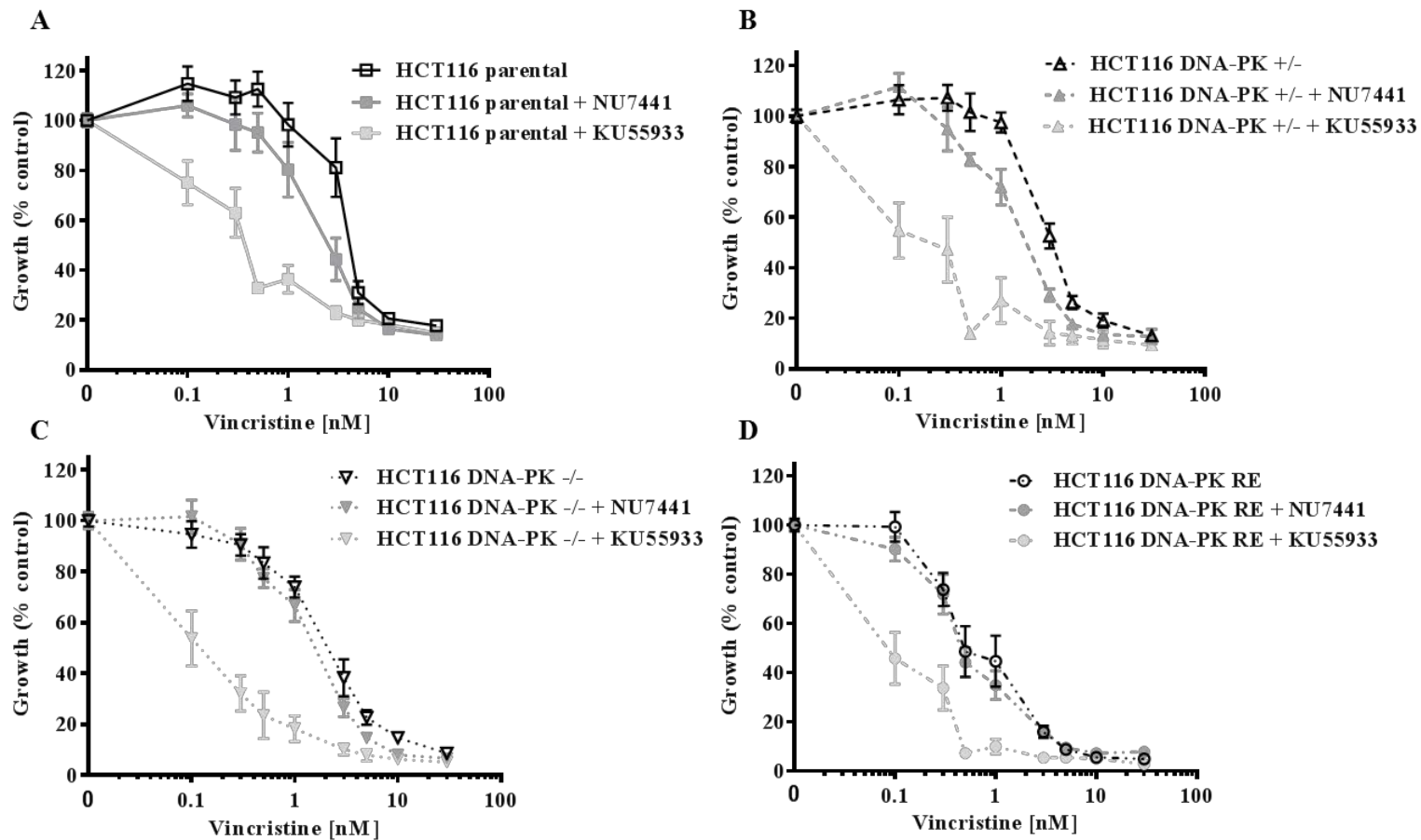
Figure 6-10: The effect of NU7441 and KU55933 on the response of DNA-PK proficient and deficient HCT116 cell lines to vincristine. HCT116 parental, DNA-PK +/-, DNA-PK -/- and DNA-PK RE cells were treated with vincristine alone or in combination with 1 µM NU7441 or 10 µM KU55933 for 72 hours and % growth was analysed by XTT assay (Section 2.3). Data are presented as a percentage of vehicle control cells. Points represent the mean of ≥3 independent experiments, each in triplicate, ± standard error.

The cytotoxic effect of vincristine in the HCT116 cell lines was then investigated using a clonogenic assay. There was no significant difference in vincristine response at the LC_{90} concentration in any of the cell lines (Figure 6-11). However, at concentrations of vincristine higher than 10 nM, the HCT116 DNA-PK -/- cells, along with the HCT116 DNA-PK RE cells, were more sensitive than the HCT116 DNA-PK +/+ and HCT116 DNA-PK +/- cells. At 100 nM vincristine, survival was 0.002 % in the HCT116 DNA-PK -/- and HCT116 DNA-PK RE cells whereas there was still 1 % survival in the HCT116 DNA-PK +/+ and HCT116 DNA-PK +/- cells, a 500-fold difference in survival.
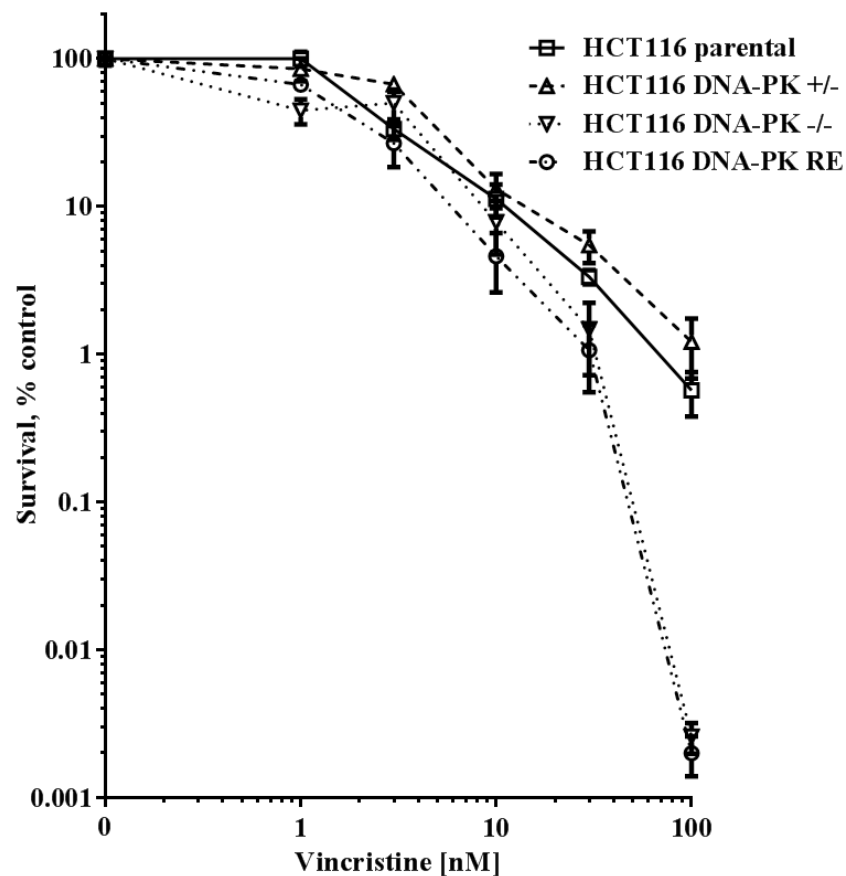
Figure 6-11: HCT116 DNA-PK -/- cells are more sensitive to vincristine than the HCT116 parental cell line at higher vincristine concentrations. HCT116 parental, DNA-PK +/-, DNA-PK -/- and DNA-PK RE cells were treated with vincristine and incubated for 24 hours. % survival was analysed by clonogenic assay (Section 2.4). Data are presented as a percentage of control cells. Points represent the mean of 3 independent experiments, each in triplicate, ± standard error.

Cell line	Vincristine (VCR) [nM]			
	GI_{50} VCR	GI_{50} VCR + NU7441	GI_{50} VCR + KU55933	LC_{90} VCR
DNA-PK +/+	3.53 ± 0.95	2.53 ± 0.93^{ns}	$0.58 \pm 0.41^{p=0.046}$	10.6 ± 3.41
DNA-PK +/-	3.07 ± 0.44^{ns}	1.66 ± 0.38^{ns}	$0.56 \pm 0.49^{p=0.018}$	16.4 ± 4.60^{ns}
DNA-PK -/-	2.43 ± 0.60^{ns}	1.58 ± 0.37^{ns}	$0.15 \pm 0.07^{p=0.02}$	7.57 ± 2.58^{ns}
DNA-PK RE	0.90 ± 0.52^{ns}	0.62 ± 0.29^{ns}	0.15 ± 0.10^{ns}	5.33 ± 3.07^{ns}

Table 6-3: HCT116 cell lines are sensitised to vincristine by KU55933. GI_{50} data: HCT116 parental, DNA-PK +/-, DNA-PK -/- and DNA-PK RE cells were treated with vincristine alone or in combination with 1 µM NU7441 or 10 µM KU55933 for 72 hours and % growth was analysed by XTT assay (Section 2.3). LC_{90} data: HCT116 parental, DNA-PK +/-, DNA-PK -/- and DNA-PK RE cells were treated with vincristine and incubated for 24 hours. % survival was analysed by clonogenic assay (Section 2.4). The data are presented as the GI_{50} mean or LC_{90} mean (nM) of ≥ 3 independent experiments, each in triplicate, $\pm$ standard error. Significant differences between cell lines treated with vincristine alone were calculated using an unpaired *t*-test and are shown as subscripts. Significant differences between cells treated with vincristine alone and cells treated with vincristine + inhibitor were calculated using an unpaired *t*-test and are shown as superscripts. ns = non-significant.

6.3.5 *HCT116 DNA-PK -/- cells and HCT116 DNA-PK RE cells were more sensitive to docetaxel than HCT116 DNA-PK +/+ and HCT116 DNA-PK +/- cells*

The HCT116 cell line panel was also tested for the growth-inhibitory response to a mechanistically-distinct microtubule-targeting agent, docetaxel.

The HCT116 DNA-PK -/- cells and the HCT116 DNA-PK RE cells were more sensitive to docetaxel than the parental and DNA-PK +/- cells; however, the effect was only significant at the docetaxel GI_{50} level in the DNA-PK RE cells (2.4-fold, p=0.03) (Figure 6-12B) (Table 6-4).

NU7441 did not significantly sensitise any of the cell lines to docetaxel (Figure 6-13). However, KU55933 significantly sensitised the HCT116 parental DNA-PK +/+ cells to docetaxel (1.9-fold, p=0.04) (Figure 6-13) (Table 6-4).
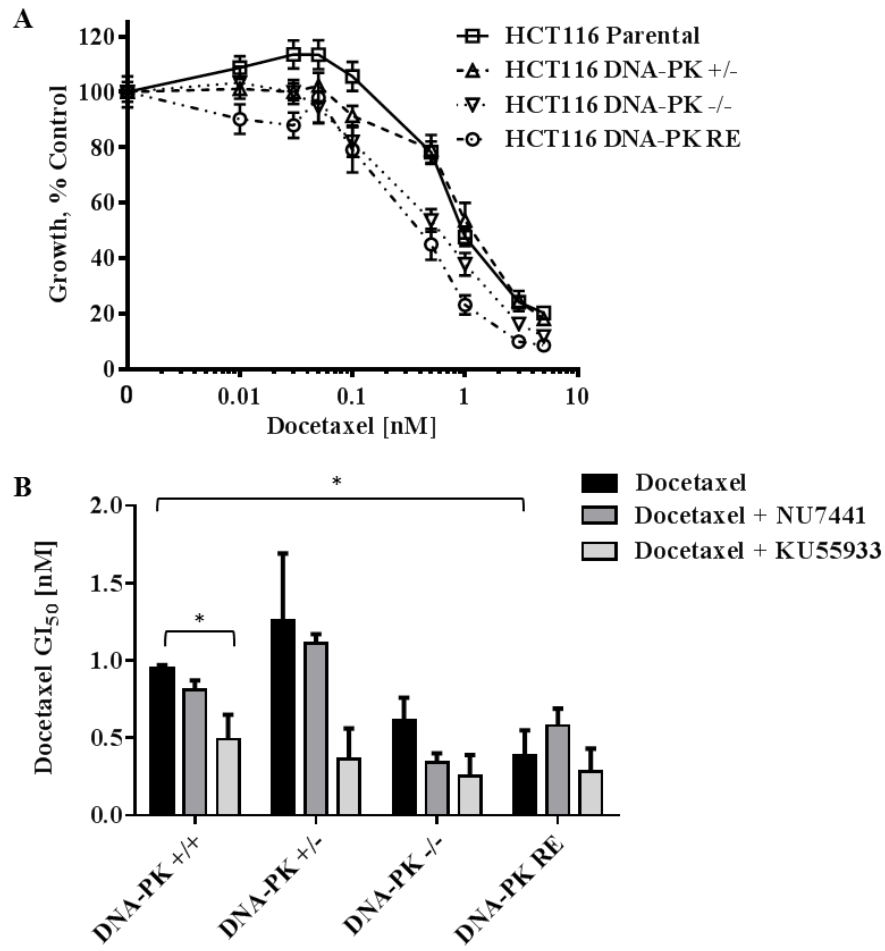
Figure 6-12: DNA-PK -/- cells are more sensitive to docetaxel than DNA-PK proficient cells. HCT116 parental, DNA-PK +/-, DNA-PK -/- and DNA-PK RE cells were treated with docetaxel alone or in combination with 1 µM NU7441 or 10 µM KU55933 for 72 hours and % growth was analysed by XTT assay (Section 2.3). (**A**) Docetaxel alone data are presented as a percentage of vehicle control cells. Points represent the mean of ≥3 independent experiments, each in triplicate, ± standard error. (**B**) Docetaxel plus inhibitors GI_{50} data are presented as the GI_{50} means ± standard error. Asterisk indicates a statistically significant difference using the Student's unpaired *t*-test when compared with the GI_{50} for drug alone (* *p<0.05).*
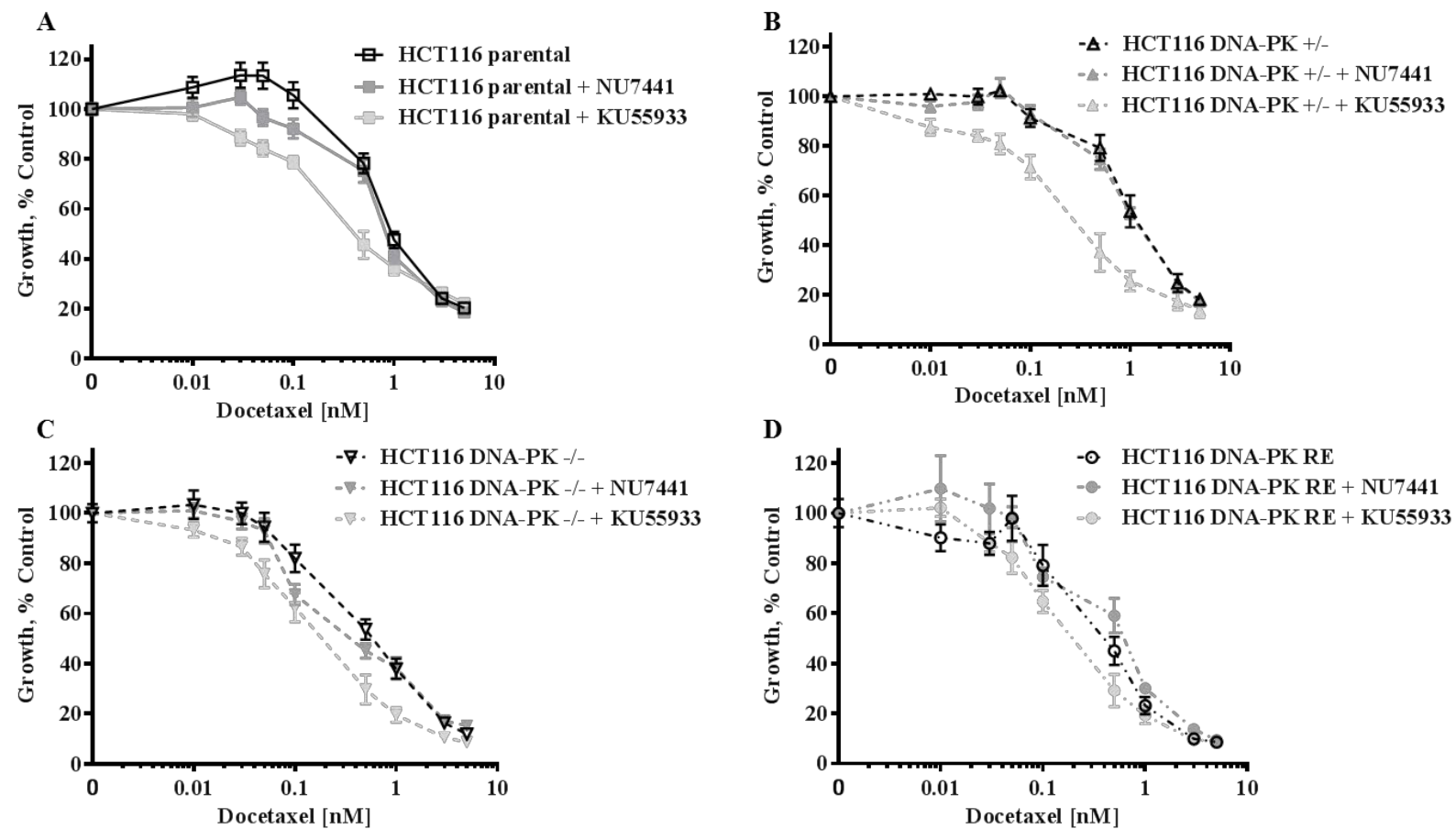
Figure 6-13: The effect of NU7441 and KU55933 on the response of DNA-PK proficient and deficient HCT116 cell lines to docetaxel. HCT116 parental, DNA-PK +/-, DNA-PK -/- and DNA-PK RE cells were treated with docetaxel alone or in combination with 1 µM NU7441 or 10 µM KU55933 for 72 hours and % growth was analysed by XTT assay (Section 2.3). Data are presented as a percentage of vehicle control cells. Points represent the mean of ≥3 independent experiments, each in triplicate, ± standard error.

Cell line	Docetaxel (DOC) [nM]		
	GI_{50} DOC	GI_{50} DOC + NU7441	GI_{50} DOC + KU55933
DNA-PK +/+	0.95 ± 0.02	0.81 ± 0.06^{ns}	$0.49 \pm 0.16^{p=0.043}$
DNA-PK +/-	$1.26 \pm 0.43_{ns}$	1.11 ± 0.06^{ns}	0.36 ± 0.20^{ns}
DNA-PK -/-	$0.61 \pm 0.15_{ns}$	0.34 ± 0.06^{ns}	0.25 ± 0.14^{ns}
DNA-PK RE	$0.39 \pm 0.16_{p=0.03}$	0.58 ± 0.11^{ns}	0.28 ± 0.15^{ns}

Table 6-4: DNA-PK RE cells are more sensitive to docetaxel than parental cells but only the parental cells were sensitised to docetaxel by KU55933. HCT116 parental, DNA-PK +/-, DNA-PK -/- and DNA-PK RE cells were treated with docetaxel alone or in combination with 1 µM NU7441 or 10 µM KU55933 for 72 hours and % growth was analysed by XTT assay (Section 2.3). The data are presented as the GI_{50} mean (nM) of ≥3 independent experiments, each in triplicate, ± standard error. Significant differences between cell lines treated with docetaxel alone were calculated using an unpaired *t*-test and are shown as subscripts. Significant differences between cells treated with docetaxel alone and cells treated with docetaxel + inhibitor were calculated using an unpaired *t*-test and are shown as superscripts. ns = non-significant.

The growth inhibitory data with vincristine and docetaxel demonstrates that the lack of DNA-PK in the HCT116 DNA-PK -/- cells sensitises cells to these agents. ATM inhibition sensitised cells to both vincristine and docetaxel, suggesting a role for both DNA-PK and ATM in the response of cells to these agents.

6.3.6 DNA-PK activation was observed in a concentration-dependent manner in response to vincristine in all of the DNA-PK-expressing HCT116 cells

The activation of DNA-PK in response to vincristine in the HCT116 cell lines was investigated by Western blotting. DNA-PK activation was observed in the HCT116 DNA-PK +/+, DNA-PK +/- and DNA-PK RE cells following treatment with 10 nM vincristine in a concentration-dependent manner (Figure 6-14). The greatest level of activation was seen in the parental DNA-PK +/+ cells which have the highest DNA-PK protein expression level (Figure 6-5). DNA-PK activation was very weak in the HCT116 DNA-PK RE cells but these cells also had lower total DNA-PKcs expression. There was no expression or activity in the DNA-PK -/- cells, as expected.

Vincristine [μM]	DNA-PK +/+	DNA-PK +/-	DNA-PK -/-	DNA-PK RE	
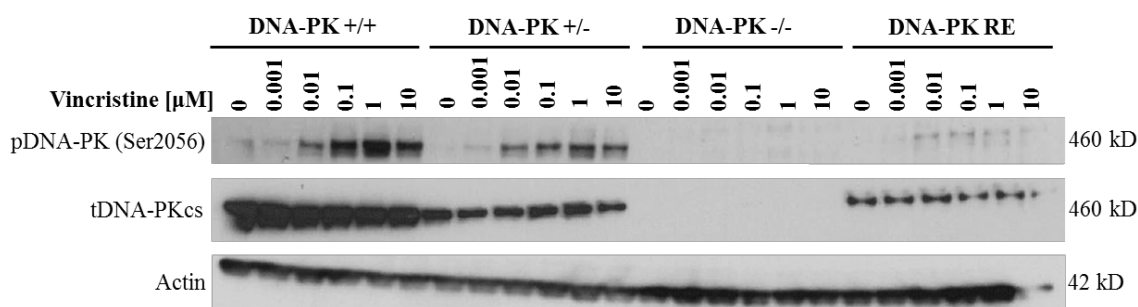
Figure 6-14: Vincristine activates DNA-PK in a concentration-dependent manner in all DNA-PK-expressing cells. HCT116 parental, DNA-PK +/-, DNA-PK -/- and DNA-PK RE cells were treated with vincristine (0-10 μM) and incubated for 24 hours. Cell lysates were prepared and DNA-PK activity and expression, and actin expression, were determined by Western blotting using the indicated specific antibodies (Section 2.7.4). Data are representative of 3 independent experiments.

6.3.7 The effects of vincristine, ionising radiation and a combination of both in the HCT116 cell lines to investigate the differences in response using chemical inhibition or absence of DNA-PK expression

The previous results in this chapter are consistent with a role for DNA-PK and ATM in the response of cells to both DNA-damaging ionising radiation and non-DNA-damaging microtubule-targeting agent treatment. Therefore, an investigation into whether the combination of vincristine treatment and ionising radiation would have an additive cytotoxic effect on cells, whether this would be dependent on DNA-PK expression status, and whether DNA-PK or ATM inhibition would increase combination cytotoxicity, was performed.

The 2 nM concentration of vincristine and 1 Gy dose of ionising radiation were chosen as being equally cytotoxic in the parental HCT116 cell line but to only reduce survival by around 30 % so any further impact on survival with the combination treatment could be accurately determined. Cells were incubated with 2 nM vincristine for 48 hours, or with 1 Gy ionising radiation and incubated for 24 hours, or were treated with 2 nM vincristine for 24 hours followed by 1 Gy ionising radiation and then incubation for a further 24 hours, in the presence of vincristine throughout. The inhibitors, NU7441 (1 μM) and KU55933 (10 μM), were applied for 48 hours with each treatment before the cells were plated out for the clonogenic assay in drug-free medium. HCT116 DNA-PK +/+ cells were treated in combination with 1 μM NU7441 or 10 μM KU55933 for 48 hours before treatment, which was also added to the medium after the

180

cells were plated out. However, results generated with cells in inhibitor-containing medium throughout compared to data generated using cells that only had 48 hour inhibitor incubation, followed by cloning in drug-free medium, were not significantly different and so the continual exposure data are not included in Figure 6-15.

The treatments all significantly reduced the survival of all of the cell lines compared to the respective untreated controls, confirming that the treatments alone at the concentrations/doses used were active. Vincristine alone or ionising radiation alone reduced the survival of the parental HCT116 cells to 72 %, and the combination of vincristine for 24 hours followed by ionising radiation and further 24 hour incubation reduced survival to 42 %.

There were no differences in plating efficiency between the different cell lines or the parental HCT116 DNA-PK +/+ cells treated with NU7441 or KU55933 alone. Figure 6-15 displays the results for all of the cell lines, each normalised to their respective untreated control. There was no significant difference in response of the HCT116 DNA-PK +/- cells to any of the treatments compared to the HCT116 DNA-PK +/+ cells, indicating that one copy of *PRKDC* is enough to maintain the response seen in the parental cells.

The HCT116 DNA-PK -/- cells were 1.6-fold (p=0.02) more sensitive to vincristine and 5-fold (p<0.0001) more sensitive to ionising radiation than the parental cells at the concentrations tested; in keeping with the sensitisation observed earlier in this chapter (Figure 6-8). However, interestingly, the DNA-PK -/- cells were 13.6-fold (p<0.0001) more sensitive to the vincristine-ionising radiation combination than the parental cells, which reduced the cell survival to 3 % suggesting a role for DNA-PK in the response of cells to this combination treatment.

The same treatments were also tested in HCT116 DNA-PK +/+ cells in combination with NU7441 to compare the response of HCT116 cells following chemical DNA-PK inhibition to effects observed in the HCT116 DNA-PK -/- cells. NU7441 caused a 3.6-fold (p<0.0001) reduction in survival in response to vincristine and a 2.5-fold (p<0.0001) reduction in survival in response to ionising radiation. However, there was a 5.3-fold (p<0.0001) survival reduction in the combination-treated cells with NU7441 compared with DNA-PK +/+ cells, which is considerably less than the 13.6-fold sensitisation observed in the DNA-PK -/- cells. These results demonstrate differences in the response of cells to these agents dependent on the method of DNA-PK manipulation.

The effects of ATM inhibition on the DNA-PK +/+ cells were also investigated. KU55933 (10 µM) caused a 14-fold (p<0.0001) reduction in survival in response to vincristine (Figure 6-15), which is consistent with the greater sensitisation observed with 10 µM KU55933 compared with 1 µM NU7441 (Figure 6-10). There was a 1.4-fold (p=0.03) reduction in ionising radiation survival (Figure 6-15), which is similar to the sensitisation caused by NU7441 and consistent with the data shown in Figure 6-7; namely that 1 µM NU7441 and 10 µM KU55933 have the same sensitisation effects for ionising radiation in the HCT116 DNA-PK +/+ cells in XTT growth inhibition assays. In the vincristine-IR combination-treated HCT116 DNA-PK +/+ cells with KU55933, there was an 18.7-fold (p<0.0001) reduction in cell survival compared with the parental cells (Figure 6-15), and this result indicates that chemical inhibition of ATM is highly effective at sensitising cells to a combination of these agents.

The HCT116 DNA-PK RE cells were 6.8-fold (p<0.0001) more sensitive to vincristine cytotoxicity than the HCT116 DNA-PK -/- cells, which is again consistent with the findings in the growth inhibition assays, i.e. that the HCT116 DNA-PK RE cells were highly sensitive to microtubule-targeting agents. HCT116 DNA-PK RE cell survival following 1 Gy IR was decreased 1.5-fold (p=0.008), indicating that the DNA-PK that has been re-expressed in the HCT116 DNA-PK RE cells reduces sensitivity to ionising radiation compared to the HCT116 DNA-PK -/- cells. There was a 2.7-fold (p=0.005) survival reduction with vincristine and ionising radiation combination-treatment in HCT116 DNA-PK RE cells compared with the HCT116 DNA-PK +/+ cells, but the combination of vincristine and ionising radiation in the HCT116 DNA-PK RE cells did not cause a further reduction in the cell survival beyond that observed with vincristine alone. The results in the HCT116 DNA-PK RE cell line demonstrate differences in the response of cells to microtubule-targeting agents if the DNA-PK is reintroduced on a cDNA construct compared with endogenous DNA-PK expression.
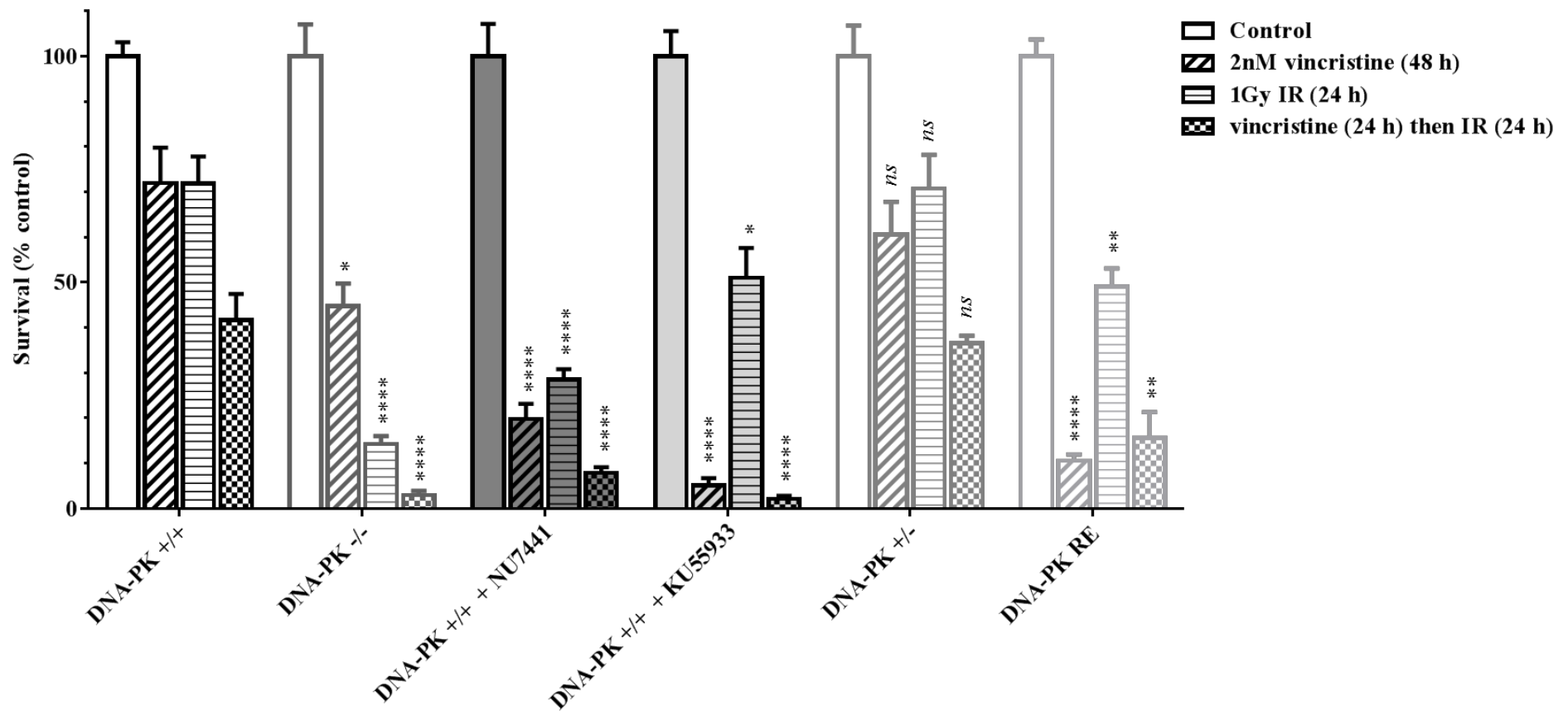
Figure 6-15: The effect of vincristine and ionising radiation alone and in combination in HCT116 cell lines. HCT116 parental, DNA-PK +/-, DNA-PK -/- and DNA-PK RE cells were treated with 2 nM vincristine (48h), 1 Gy IR or vincristine (24h) then IR and vincristine for a further 24h. % survival was analysed by clonogenic assay (Section 2.4). Data are presented as a percentage of control cells. Bars represent the mean of ≥3 independent experiments, each in triplicate, ± standard error. Asterisk indicates a statistically significant difference between that treatment compared with the same treatment in the DNA-PK +/+ cells using the Student's unpaired *t*-test (* *p<0.05, ** p<0.01, ****p<0.0001*).

6.4   Discussion and future work

The studies described in Chapter 3 demonstrated that cells could be sensitised to microtubule-targeting agents by the DNA-PK inhibitor NU7441, and the ATM inhibitor KU55933. However, Chapter 4 demonstrated that these selective inhibitors were also affecting drug efflux *via* MDR1. Therefore the work in this chapter aimed to investigate the role of DNA-PK and ATM in the response to microtubule-targeting agents using isogenic cell lines with different DNA-PK expression profiles. The use of the isogenic cell lines removes any non-specific effect of the inhibitors and also allows a comparison of the effects of lack of DNA-PK protein *vs* chemical inhibition of the protein. The effect of the ATM inhibitor in the absence of DNA-PK protein was also investigated.

The M059J and M059J-Fus1 cells were investigated initially. The M059J cells are DNA-PK deficient and the M059J-Fus1 cells are complemented with a copy of human chromosome 8 containing the DNA-PK locus, and are therefore DNA-PK proficient (Hoppe *et al.*, 2000). The DNA-PK deficient M059J cells were shown to be significantly more sensitive to docetaxel than the DNA-PK proficient M059J-Fus1 cells, and only the DNA-PK proficient cells could be sensitised to docetaxel by the DNA-PK inhibitor, NU7441. The sensitisation caused by NU7441 in the DNA-PK proficient cells reduced cell growth to the same level as observed in the DNA-PK deficient cells, indicating a role for DNA-PK in the response of these cells to docetaxel.

Hoppe *et al.* (2000) reported that the M059J and M059J-Fus1 cells display the same growth rate; however, here it was noted that the M059J cells grew at half the rate of the M059J-Fus1 cells, which complicated the interpretation of the growth inhibition results as the M059J-Fus1 cells doubled approximately four times over the 96-hour assay whereas the M059J cells only doubled approximately twice. Also, in the clonogenic assay, the differences in growth rate will have resulted in fewer M059J cells dividing in the presence of drug before the cells were plated out, and then had less time to divide and form colonies large enough for detection and counting. The timing of the experiments could be adjusted to take into account the differences in doubling time; however, Tavecchio *et al.* (2012) noted that the plating efficiency in the clonogenic assay was very low for both of the M059J (3.4±0.7 %) and the M059J-Fus1 (4.4±2.1 %) cells. A low level of plating efficiency was also observed here with the plating efficiency of both cell lines being approximately 5 %. If only 5 % of the cells in a population are surviving in the absence of any treatment, the clonogenic assay data are by definition limited to a small and potentially non-representative population, which

may be more resistant to treatment than those untreated cells that were unable to survive and form colonies.

Due to the introduction of a whole human chromosome 8 into the M059J-Fus1 cells, numerous other genes, and hence proteins, as well as DNA-PK will potentially be overexpressed in these cells. The M059J cells have been shown to have reduced ATM function due to a truncating ATM mutation (Tsuchida *et al.*, 2002) and have a *TP53* mutation (Anderson and Allalunis-Turner, 2000). Furthermore, numerous proteins involved in DNA biology reside on chromosome 8, including Nbs1. Nbs1 is one of the components of the MRN complex which stabilises ATM (reviewed in (Lee and Paull, 2007)) and could therefore enhance ATM function in the M059J-Fus1 cells, resulting in some of the resistance to docetaxel demonstrated in these experiments. Due to the presence of other genes on chromosome 8, it is difficult to state with confidence that the resistance effects seen in the M059J-Fus1 cells were solely due to DNA-PK, and therefore a better model of isogenic DNA-PK proficient and deficient cell lines was used.

The HCT116 DNA-PK cell line panel with parental DNA-PK +/+, heterozygous DNA-PK +/-, homozygous DNA-PK -/- and DNA-PK -/- cells with DNA-PK reintroduced on cDNA (DNA-PK RE cells) were obtained from Horizon Discovery Group plc.

The original study that describes the creation of the cell lines reported that the DNA-PKcs null cells have growth retardation as well as genetic instability, shortened telomeres and enhanced IR sensitivity (Ruis *et al.*, 2008). The growth retardation is reported to be extremely severe with the HCT116 DNA-PK +/- cells having reduced growth compared with the parental HCT116 DNA-PK +/+ cells and the HCT116 DNA-PK -/- cells barely growing after 9 days with doubling times for the HCT116 DNA-PK +/+, DNA-PK +/- and DNA-PK-/- cells being 23, 24 and 40 hours, respectively. Also the plating efficiency of the cells was determined and were found to be very different, being 59 %, 35 % and 2.3 % in the HCT116 DNA-PK +/+, DNA-PK +/- and DNA-PK-/- cells, respectively. From these data it was concluded that the HCT116 DNA-PK +/- cells were haploinsufficient and that HCT116 DNA-PK -/- cells were highly growth and survival defective. These growth deficiencies related to DNA-PK expression would be in keeping with the observations in this thesis relating to the M059J cells; however, growth of the HCT116 cell line panel used in this thesis was highly consistent. The growth rate of all of the cell lines was the same, tested after 96 hours and after 9 days (as done in Ruis *et al.* (2008)), and the plating efficiency of all the cell lines tested in the

clonogenic assays were found to be approximately 50 %. Therefore, it is likely that the genotype of the DNA-PK +/- and DNA-PK -/- cells must have been modified during the time between the creation of the cell lines using the technique in Ruis *et al.* (2008), and the acquisition of the commercially-available cell lines from Horizon Discovery Group plc to account for the lack of growth retardation and poor survival seen in the DNA-PK +/- and DNA-PK -/- cells used in this study.

Although DNA-PK activity and expression were investigated at the protein level by Western blotting, it would be useful to obtain PCR primers that target exons 81-83 to demonstrate the specificity of the targeted DNA-PK-interfering vectors in these cells. The measurement of DNA-PK protein expression demonstrated that the HCT116 DNA-PK +/- cells express approximately half the amount of total DNA-PKcs protein than that of the parental HCT116 DNA-PK +/+ cells and that the HCT116 DNA-PK -/- cells did not express detectable DNA-PKcs protein, as expected. The HCT116 DNA-PK RE cells were called "DNA-PK -/-, cDNA overexpressing cells" when obtained from Horizon Discovery Group plc, and these cells were shown to express a similar level of total DNA-PKcs protein as the HCT116 DNA-PK +/- cells, indicating the DNA-PK cDNA introduction did not restore the total protein levels to that of the parental cells, and therefore these cells are described as DNA-PK re-expression (DNA-PK RE) cells in this thesis.

The importance of non-homologous end-joining in response of cells to DNA damage caused by ionising radiation has been extensively studied (discussed in Chapter 1 and reviewed in Mahaney *et al.* (2009); Wang and Lees-Miller (2013)), and cells deficient in DNA-PKcs have previously been shown to be highly radiosensitive. Therefore, the response of the HCT116 cell line panel to ionising radiation was examined to determine the impact of DNA-PK activity. The HCT116 DNA-PK -/- cells were more than 3-fold more sensitive to ionising radiation (in both the growth inhibition and clonogenic survival assays) than the HCT116 DNA-PK +/+ cells, and the HCT116 DNA-PK +/+ cells were sensitised more than 2-fold by the DNA-PK inhibitor, NU7441. This finding confirms the importance of DNA-PK in the response of cells to ionising radiation.

ATM and homologous recombination are also involved in the repair of DSBs caused by ionising radiation, although this type of repair can only happen after DNA replication and before mitosis when there is a complementary sister strand to use as a template for repair. Inhibition of KU55933 had a very similar sensitisation effect to NU7441 in the HCT116 DNA-PK +/+, DNA-PK +/- and DNA-PK RE cells, suggesting

that when one double-strand break pathway is inhibited, although repair is hindered and cells are sensitised, the other pathway functions in a redundant fashion and that neither pathway is dominant in DNA repair in cells that have at least one functional DNA-PK allele. However, in HCT116 DNA-PK -/- cells, the inhibition of ATM led to further sensitisation, indicating that a lack of a functional double-strand break repair pathway is highly detrimental to cells that lack non-homologous end-joining function.

The HCT116 cell line panel was investigated to determine sensitivity to the microtubule-targeting agents, vincristine and docetaxel. Although the effects were not as marked as in response to ionising radiation, the HCT116 DNA-PK -/- cells were more sensitive to both vincristine and docetaxel than the parental HCT116 DNA-PK +/+ cells. The role of Ku70 and Ku80 in the response of cells to microtubule-targeting agents has been investigated previously and Ku70 -/- and Ku80 -/- cells were found to be more sensitive to both vincristine and paclitaxel (Kim *et al.*, 1999). Additionally, Ku protein levels were decreased after treatment with these agents in Ku-proficient cells, which was prevented by a specific caspase-3 inhibitor, suggesting proteolytic cleavage during drug-induced apoptosis (Kim *et al.*, 1999). Results presented in Chapter 3 demonstrated that there is an increase in caspase 3/7-dependent apoptosis in response to vincristine. The findings in this Chapter, and previous works (Kim *et al.*, 1999), indicate a role for DNA-PK, which is composed of DNA-PKcs, Ku70 and Ku80 subunits, in the response of cells to these agents. There are HCT116 cell lines available from Horizon Discovery Group plc that are Ku70 +/-, Ku80 +/- or DNA-PK -/-; Ku70 +/- which would be interesting to study for their response to microtubule-targeting agents.

An interesting observation was that the HCT116 DNA-PK RE cells were hyper-sensitive to both vincristine and docetaxel. This result suggests that the reintroduction of DNA-PKcs into the HCT116 DNA-PK -/- cells using a cDNA construct, although restoring protein expression and some resistance to ionising radiation, changes the response of the cells to microtubule-targeting agents. Despite having a similar amount of total DNA-PKcs protein as the HCT116 DNA-PK +/- cells, the HCT116 DNA-PK RE cells have very low levels of DNA-PK activation in response to either ionising radiation or vincristine, which suggests that the protein that is expressed is not being activated fully. Reduced sensitivity to vincristine or docetaxel was expected (compared to the level of the HCT116 DNA-PK -/- cells), based on the response to ionising radiation. However, the response of the HCT116 DNA-PK RE cells was the same or greater than the HCT116 DNA-PK -/- cells, an observation that has been reported in the literature previously.

Although not significant due to intra-experiment variation, NU7441 reduced the vincristine GI_{50} concentration in HCT116 DNA-PK +/+ cells to the same value as the GI_{50} in the HCT116 DNA-PK -/- cells. NU7441 did not cause any sensitisation of any of the HCT116 cells to docetaxel, indicating a potential difference in response between chemical inhibition of DNA-PK and the absence of DNA-PK protein. Thus DNA-PK protein may play a structural rather than a catalytic role in this scenario.

Similar to the patterns of NU7441- and KU55933-induced sensitisation seen in the parental and multidrug-resistant cells used in Chapter 3, the sensitisation of HCT116 cells to vincristine and docetaxel by 10 µM KU55933 was greater than that caused by 1 µM NU7441. KU55933 sensitised all of the HCT116 cell lines to both vincristine and docetaxel, with greater sensitisation seen in combination with vincristine than with docetaxel. KU55933 sensitisation in the HCT116 DNA-PK +/+ cells to vincristine was 6.1-fold whereas it was 16.2-fold in the HCT116 DNA-PK -/- cells, suggesting that lack of both DNA-PK and ATM function causes additional sensitisation compared to the absence or inhibition of just one of these proteins, and that both may have a role in the response of cells to these agents (although ATM appears to have a greater role). These results demonstrate the potential of an ATM inhibitor to be given in combination with microtubule-targeting agents clinically.

Although no MDR1 protein could be detected in any of the HCT116 cell lines by Western blot, these HCT116 cell lines should be investigated for sensitisation to microtubule-targeting agents by the known MDR1 blocker verapamil, to determine any MDR1-mediated sensitisation caused by NU7441 and KU55933.

To extend the studies described here, experiments could be performed using ATM proficient and deficient cells, with microtubule-targeting agents alone or in combination with NU7441. Such studies would allow a comparison of the effects of ATM absence with inhibition by KU55933, in relation to both sensitisation and the effect of inhibition with NU7441. Inactivating mutations in ATM occur in a number of cancers and it would be interesting to study cell lines with one or both copies of ATM being non-functional, and to investigate the sensitivity of these cells to microtubule-targeting agents. Such a study might indicate a possible clinical opportunity for the treatment of ATM-mutant or non-functional patients with microtubule-targeting agents, and whether DNA-PK inhibition in these patients would be a potentially synthetically lethal combination.

It would also be interesting to examine other DNA repair proteins that are downstream of ATM, e.g. Chk2, and whether sensitisation is generated by inhibitors of

these proteins e.g. the Chk1 and Chk2 inhibitor, AZD7762 (Mitchell *et al.*, 2010). The primary publication that identified the role of DNA-PK in spindle disruption and mitotic catastrophe also demonstrated reduced Chk2 phosphorylation (Shang *et al.*, 2010), and therefore a dual Chk1/2 inhibitor may also sensitise cells to microtubule-targeting agents. Lastly, other DNA repair proteins such as Chk1 and ATR should also be examined for a potential role in the response of microtubule-targeting agent-treated cells.

In the DNA-PK +/+ parental HCT116 cells, the combination of ionising radiation and vincristine was significantly more cytotoxic than a low dose of either agent alone (42 % survival with the combination compared with 72 % for each agent alone), and this pattern of cytotoxicity was also seen in the HCT116 DNA-PK +/- cells, demonstrating no haploinsufficiency effect. The findings in this thesis are in contrast with a study in medulloblastoma which demonstrated no additional effect on cell death with the combination of vincristine and ionising radiation compared with ionising radiation alone, although the schedule of treatments were different (Kumar *et al.*, 2007). Interestingly, the HCT116 DNA-PK -/- cells, which were more sensitive to ionising radiation and vincristine alone (2- and 5-fold, respectively), were 14-fold more sensitive to the combination of ionising radiation and vincristine than the HCT116 DNA-PK +/+ cells, demonstrating additional cytotoxicity with the combination compared with the two agents alone. The HCT116 DNA-PK +/+ cells were sensitised to the combination treatment by NU7441 but not to the same degree as seen in the HCT116 DNA-PK -/- cells, again indicating a possible difference in cell response between cells lacking DNA-PK and those with inhibited DNA-PK. HCT116 DNA-PK +/+ cells treated with KU55933 were highly sensitive to vincristine alone and were further sensitised in the combination treatment group.

In clonogenic cytotoxicity studies, prolonged inhibition of DNA-PK or ATM by adding NU7441 or KU55933 to the growth medium for the two week period required for colony formation, compared to the inhibitors only being present for 48 hours during the drug or ionising radiation treatments, resulted in no difference in cytotoxicity. This result suggests that DNA-PK and ATM only need to be inhibited during and/or immediately after the drug or radiation treatments, and that the impact of inhibition is maintained thereafter. NU7441 and KU55933 are known to be stable compounds (Celine Cano, personal communication) and so compound instability during prolonged inhibition is not anticipated, however, stability could be confirmed by LC-MS analysis

of NU7441 or KU55933 in the medium at the end of the two week colony forming assay.

Taxanes interfere with the mitotic spindle and cause cells to arrest in the G2/M phase of the cell cycle (Jordan *et al.*, 1996), which is also the phase in which cells are most sensitive to ionising radiation (Terasima and Tolmach, 1963), suggesting that microtubule-targeting agents and ionising radiation could interact positively and the enhanced cytotoxicity of vincristine and ionising radiation combination, particularly when DNA-PK was absent or inhibited (Figure 6-15) was of interest in this context. It would be useful to investigate the cell cycle distribution of the cells used in the combination experiment before they are plated out for the clonogenic assay to determine whether a G2/M block is observed. Increased radiosensitivity for combinations of paclitaxel or docetaxel with ionising radiation has been shown in a number of studies; an effect that is independent of p53 status (Liebmann *et al.*, 1994; Milas *et al.*, 1994; Koukourakis *et al.*, 1999; Niero *et al.*, 1999; Zhang *et al.*, 2007a). Some of these authors have highlighted that paclitaxel treatment before ionising radiation is key to the response observed, and that paclitaxel should be administered at least 24 hours before ionising radiation (Milas *et al.*, 1994; Niero *et al.*, 1999); consistent with the schedule used in this study.

Currently, there are a large number of clinical trials underway that are investigating the effects of vincristine in chemotherapy regimens in combination with radiotherapy in adult and childhood cancers, e.g. rhabdomyosarcoma (NCT00075582), high-risk CNS embryonal tumors (NCT00003203), primary CNS lymphoma (NCT01399372), Wilm's tumour (NCT00352534) and brain stem glioma (NCT00003935) (Clinicaltrials.gov, 2014). There are also a large number of trials with radiation in combination with paclitaxel in cancers such as bladder cancer (NCT00238420), uterine cancer (NCT01367301), head and neck squamous cell carcinoma (NCT00736619), cervical cancer (NCT01295502) and oesophageal cancer (NCT01196390) (Clinicaltrials.gov, 2014).

It would be interesting to investigate the effects of pre-treatment with NU7441 or KU55933 on chemo- and radio-sensitisation in an *in vivo* model. DNA-PK inhibition in cancer cells that are defective in HR repair should allow tumour selective cell killing, and this hypothesis could be investigated in a mouse model. If similar results to the vincristine results obtained in this study were seen with a taxane, it would be interesting to develop a mouse xenograft using the HCT116 cells from Horizon Discovery plc, then treat with a DNA-PK inhibitor or an ATM inhibitor for approximately an hour before

190

treatment with a non-toxic dose of a taxane, leave for 24 hours and then treat with a non-toxic dose of ionising radiation. In the same study, the potentiation of these doses of drug and ionising radiation alone, with NU7441 or KU55933 alone, should be investigated.

The study here demonstrates that vincristine and ionising radiation can be combined with a DNA-PK or ATM inhibitor to produce enhanced cytotoxicity. The *in vitro* experiment carried out in this Chapter should also be undertaken with paclitaxel and docetaxel, as the clinical use of radiation and taxanes would be greater than that of vincristine with radiation. Furthermore, the effects of a combination of microtubule-targeting agents and radiation should be examined in further *in vitro* and *in vivo* models.

6.5   Summary

The M059J and M059J-Fus1 cell line pair was used to demonstrate that the absence or inhibition of DNA-PK sensitised cells to docetaxel. HCT116 DNA-PK +/+, DNA-PK +/-, DNA-PK -/- and DNA-PK RE cells were characterised by mRNA and protein expression, and their response to ionising radiation, vincristine and docetaxel was investigated, alone or in combination with 1 µM NU7441 and 10 µM KU55933. There was no difference in the sensitivity of the HCT116 DNA-PK +/- cells to ionising radiation or the microtubule-targeting agents compared with the HCT116 DNA-PK +/+ cells. HCT116 DNA-PK -/- cells were more sensitive to ionising radiation, vincristine and docetaxel, demonstrating a role for DNA-PK in the response of cells to all of these agents. NU7441 (1 µM) sensitised DNA-PK +/+ cells to ionising radiation but did not have an effect on growth inhibition in response to vincristine or docetaxel. However, NU7441 (1 µM) did significantly sensitise HCT116 DNA-PK +/+ cells to vincristine in a cytotoxicity assay. KU55933 (10 µM) caused significant sensitisation in the HCT116 DNA-PK +/+, DNA-PK +/- and DNA-PK -/- cells to ionising radiation, vincristine and docetaxel, demonstrating a role for ATM in the response to these agents. The combination of vincristine and ionising radiation was significantly more active in the absence of DNA-PK or following inhibition of DNA-PK. Overall, these findings extend the clinical potential of targeted inhibition of DNA-PK and ATM to ionising radiation, microtubule-targeting agents and combinations of both of these treatments.

Chapter 7: The effect of ionising radiation, microtubule-targeting agents and DNA-PK deletion or inhibition on mitosis, and the subcellular localisation and activity of DNA-PK

7.2   Introduction

High fidelity mitosis and the spindle checkpoint are important factors in maintaining genomic stability. During the majority of the cell cycle, the microtubules function to traffic proteins around the cell, and are involved in maintaining cell shape and polarity. However, during mitosis microtubules are organised to form the mitotic spindle to accurately segregate sister chromatids (Risinger *et al.*, 2009). The centrosome functions as a microtubule organising centre, and the centrosome duplicates in S phase to form the mitotic spindle poles and to direct the microtubules to ensure the correct assembly of the spindle (Hinchcliffe and Sluder, 2001). Centrosome amplification causes the formation of multipolar spindles, and can occur following defective cell division and multinucleation or following the failure of the G2/M checkpoint to halt the progression of a cell containing DNA damage (Borel *et al.*, 2002; Ko *et al.*, 2006).

DNA repair proteins have not been conventionally associated with mitotic regulation, but recently a number of publications have shown that various DNA repair proteins localise to mitotic structures during mitosis in the absence of DNA damage, and these include DNA-PKcs, ATM, ATR, p53, TopBP1, BRCA1, Chk1 and Chk2 (Hsu and White, 1998; Tsvetkov *et al.*, 2003; Reini *et al.*, 2004; Tritarelli *et al.*, 2004; Zhang *et al.*, 2007b; Lee *et al.*, 2011).

Double-strand break repair during mitosis is atypical and incomplete; suggesting that the timely passage through mitosis takes precedence over a complete DNA damage response. However, this does not mean that there is a total absence of a DNA damage response during mitosis. Giunta *et al.* (2010) demonstrated that DNA-PK and ATM were activated, γH2AX was phosphorylated and MDC1 and MRN were recruited to sites of DNA damage (ionising radiation-induced foci in this case), but there was no recruitment of the ubiquitin ligases RNF8 or RNF168, BRCA1 or 53BP1, all of which are required to complete double-strand break repair. It was hypothesised that this incomplete repair may effectively "mark" the sites of damage to allow identification in the following cell cycle, and that the sequestration of DNA damage proteins to mitotic structures may aid the cell in progressing through mitosis rather than activating a full DNA damage cascade (Giunta *et al.*, 2010; Giunta and Jackson, 2011).

Phosphorylated DNA-PKcs was initially identified as being localised to the centrosomes, kinetochores and the midbody following ionising radiation (Shang *et al.*, 2010), and was found to be important in the maintenance of mitotic spindle function and centrosome stability following ionising radiation. Shang *et al.* (2010) also demonstrated

that inactivation of DNA-PKcs by siRNA caused multinucleated cells, aberrant spindles and mitotic catastrophe, along with reduced Chk2 phosphorylation, following DNA damage. DNA-PK was subsequently shown to be a critical regulator of mitosis and T2609 phosphorylation of DNA-PK was closely associated with spindle structures and microtubule dynamics during progression through mitosis (Lee *et al.*, 2011). In the DNA damage response, DNA-PKcs undergoes autophosphorylation at serine 2056, and ATM and ATR have been shown to be required for phosphorylation of DNA-PK at threonine 2609 (Yajima *et al.*, 2006; Chen *et al.*, 2007), the other main site of DNA-PKcs phosphorylation. However, depletion of ATM or ATR by siRNA, or inhibition of ATM using KU55933, did not affect mitotic DNA-PKcs phosphorylation at T2609, suggesting that both S2056 and T2609 DNA-PKcs autophosphorylation occurs in mitosis (Lee *et al.*, 2011). Regulation of mitotic spindle dynamics and chromosome segregation was recently specifically attributed to DNA-PKcs activating the Chk2-BRCA1 signalling pathway during mitosis (Shang *et al.*, 2014).

Polo-like kinase 1 (PLK1) is a key regulator of cell division and is differentially localised to various subcellular structures during mitotic progression in a dynamic fashion. PLK1 associates with the centrosomes during prophase, the kinetochores in prometaphase and metaphase, the central mitotic spindle during anaphase and the midbody during cytokinesis, after which it is rapidly degraded during mitotic exit (Lindon and Pines, 2004; Petronczki *et al.*, 2008; Takaki *et al.*, 2008). Therefore PLK1 is an extremely useful protein to monitor by fluorescence microscopy, as its location allows the determination of the mitotic stage of a cell as well as visualisation of the location of mitotic structures. Phosphorylated DNA-PK (T2609) colocalises with PLK1 throughout mitosis at the centrosomes (prophase to anaphase), kinetochores (prometaphase and metaphase) and midbody (cytokinesis), and the two proteins were shown to be functionally associated and involved in chromosomal segregation and the control of cytokinesis (Huang *et al.*, 2014). Absence or inhibition of DNA-PKcs caused an increase in PLK1 protein stability, and a reduction of PLK1 localisation at the midbody; roles that could account for the increase in cytokinesis failure observed in DNA-PKcs-deficient cells.

Many of the papers discussed above that have investigated mitotic cells have achieved cell cycle synchronisation through chemical approaches such as thymidine and nocodazole blocks. The thymidine block procedure synchronises cells in S phase whereas nocodazole is a microtubule inhibitor and causes cell cycle arrest in mitosis (Bostock *et al.*, 1971; Zieve *et al.*, 1980). However, the use of chemicals or

biochemicals to synchronise cells can be compromised by the cytotoxic effects of treatment, and there is some debate over the efficacy and reliability of the chemical inhibitors in causing genuine synchronisation (Cooper *et al.*, 2006; Cooper *et al.*, 2008). In the studies described in this chapter, cells were not synchronised allowing the comparison of the subcellular localisation of proteins in a mixed cell cycle population using microscopic evaluation of individual cells.

7.3   Aims

Recent studies have demonstrated that DNA-PK has roles beyond DNA repair, including localisation to and regulation of mitotic structures. Experiments described in the previous chapters in this thesis demonstrated that DNA-PK can play a role in the response of cells to microtubule-targeting agents. Therefore, the aims of the studies described in this chapter were to investigate the subcellular localisation of DNA-PKcs and its activation in untreated, ionising radiation-treated and vincristine-treated cells by analysing the location and occurrence of phosphorylated forms of DNA-PK, and changes to mitotic spindle structure and mitotic progression, in DNA-proficient cells treated with NU7441 or in DNA-deficient cells, compared with parental cells, by using confocal microscopy.

7.4 Results

7.4.1 Confocal microscopy to visualise mitotic events in DNA-PK +/+ cells

The previous chapters in this thesis have focussed on the effect of the absence or inhibition of DNA-PK on cellular responses to microtubule-targeting agents by studying growth inhibition and cytotoxicity, apoptosis and DNA-PK activity and expression. Following the publications, discussed in Section 7.2 (demonstrating that DNA-PK plays a regulatory role in mitosis), investigations were undertaken to study DNA-PK expression and activity during mitosis, and the localisation of DNA-PK in the parental HCT116 DNA-PK +/+ cells and the HCT116 DNA-PK -/- cells.

Initially, it was necessary to optimise techniques for the fixation, permeabilisation and immunostaining of cells prior to microscopy. Three different techniques were evaluated and modified to achieve a balance between sufficient permeabilisation to allow the antibodies to enter the cells, and toxicity resulting in a loss of cells from the coverslips. Fixation and permeabilisation with 100 % methanol was found to maintain cells on the coverslips; however, antibody staining was not detected at the correct subcellular locations, demonstrating the need for greater permeabilisation. The technique described by Shang *et al.* (2010) was attempted which uses a harsher permeabilisation reagent (0.5 % (v/v) Triton X-100 in PBS), and this technique resulted in good staining but very few cells remaining on the coverslips, even with the introduction of poly L-lysine-coated coverslips. Therefore the fixation step from Shang *et al.* (2010) was combined with another permeabilisation technique (KCM-T buffer (0.1 % (v/v) Triton X-100 in KCM buffer), Ian Cowell, personal communication), resulting in the optimal technique. Locating cells on the coverslips that were in different stages of mitosis also required optimisation, because cells undergoing mitosis become rounded and are less adherent than cells in interphase, and therefore are the first cells to be lost if the technique is too severe. The optimised technique allowed the easy detection of mitotic cells and a representative microscopy image is shown in Figure 7-1.

Each microscopy image shown throughout this chapter is taken from at least 3 fields of view for each treatment group with at least 10 cells *per* field, and on average 35-40 cells, from two independent experiments.
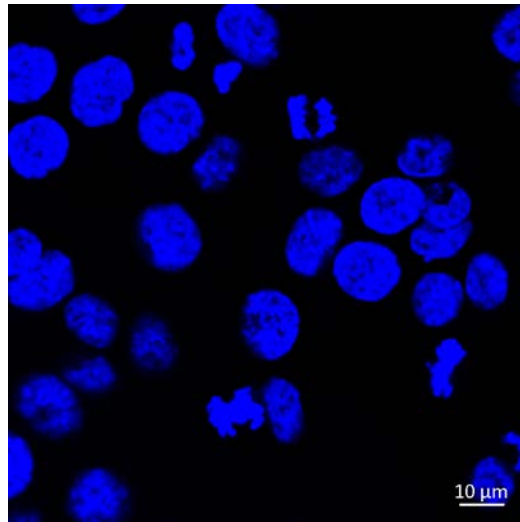
Figure 7-1: Representative view of HCT116 cells. HCT116 DNA-PK +/+ cells were seeded onto poly L-lysine-coated coverslips and left to establish for 48 hours. DAPI DNA staining (blue) was analysed by confocal microscopy (Section 2.12). Cell images are representative of ≥ 3 fields captured, in 2 independent experiments.

Figure 7-2 shows untreated HCT116 DNA-PK +/+ cells in different stages of mitosis. The cells were stained with antibodies against α-tubulin and γ-tubulin to visualise the mitotic structures. The γ-tubulin staining pattern observed was not as expected. γ-Tubulin localises at the centrosomes and so centrosome staining would be expected with microtubules (stained for α-tubulin) protruding from the centrosome. However, the γ-tubulin staining was in fact relatively diffuse throughout the cell, excluding the chromosomes. The DNA was stained with DAPI and merged images generated. Figure 7-2A displays a cell in metaphase with the chromosomes arranged along the metaphase plate with the microtubules radiating out from the centrosomes and connecting to the chromosomes. The lower cell in Figure 7-2B demonstrates early anaphase, Figure 7-2C demonstrates late anaphase/early telophase and the upper cell in Figure 7-2B and the cell in Figure 7-2D are in late telophase before cytokinesis.
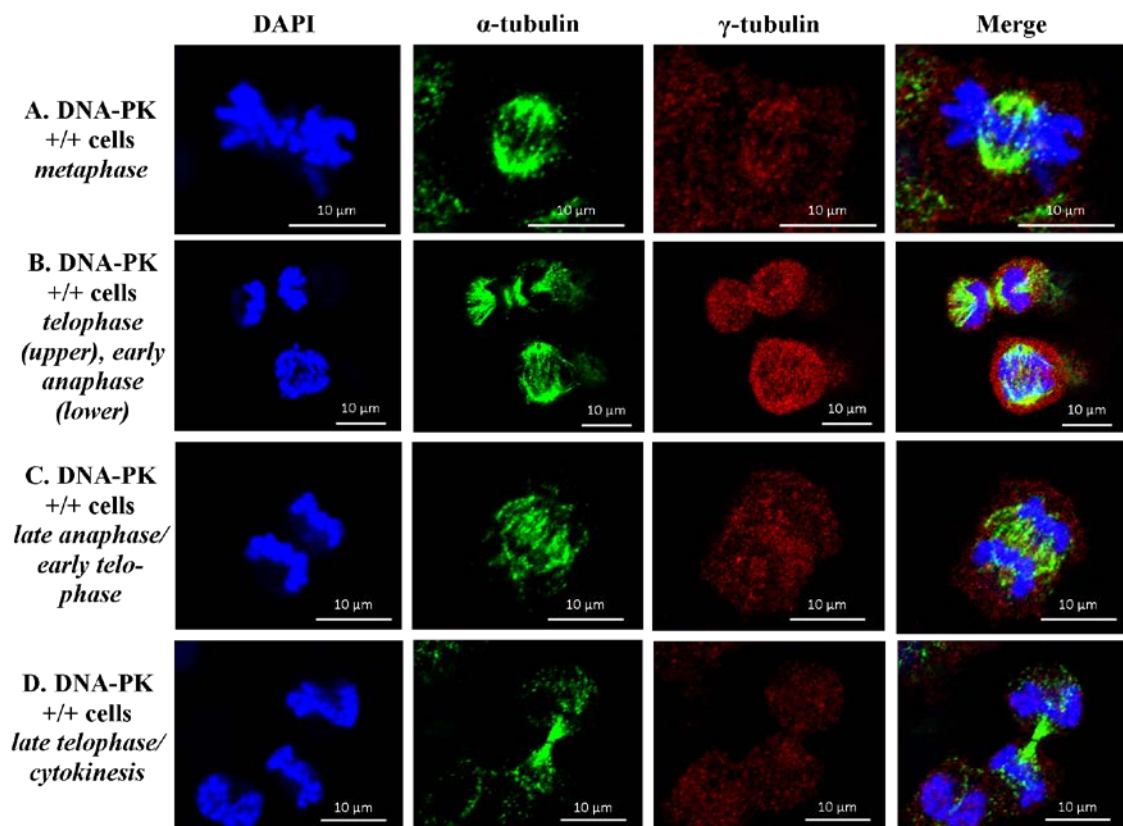
Figure 7-2: HCT116 cells in different stages of mitosis. (**A-D**) HCT116 DNA-PK +/+ cells were seeded onto poly L-lysine-coated coverslips and left to establish for 48 hours. Immunodetection of α-tubulin (green) and γ-tubulin (red), using the indicated antibodies, and DAPI DNA staining (blue) were analysed by confocal microscopy (Section 2.12). Mitotic cell images are representative of ≥ 3 fields captured, in 2 independent experiments.

7.4.2   The deletion or inhibition of DNA-PK increased the incidence of aberrant mitotic events, including multipolar spindles and lagging chromosomes

Cells undergoing "abnormal" mitosis (defined as cells with lagging chromosomes not correctly aligned on the mitotic spindle, cells containing multiple centrosomes or cells with disregular polarity resulting in the incorrect separation of chromosomes) were not identified in the untreated DNA-PK +/+ cells (8 fields captured with 30-40 cells *per* field).

The mitotic structures in DNA-PK +/+ cells treated with NU7441, and in untreated DNA-PK -/- cells, were then examined. Although the majority of the mitotic cells detected were undergoing normal mitosis, there were a number of cells in both DNA-PK +/+ cells treated with NU7441 and in DNA-PK -/- cells that were undergoing incorrect mitosis, estimated at around 10-30 % of mitotic cells examined. The most common aberrations observed are illustrated in Figure 7-3. The cell in Figure 7-3A and the left cell in Figure 7-3C are multipolar; there are three centrosomes from which microtubules are extending and therefore these cells will not complete accurate mitosis. The α-tubulin staining in the left cell in Figure 7-3B shows this cell has irregular polarity and misalignment of the chromosomes.
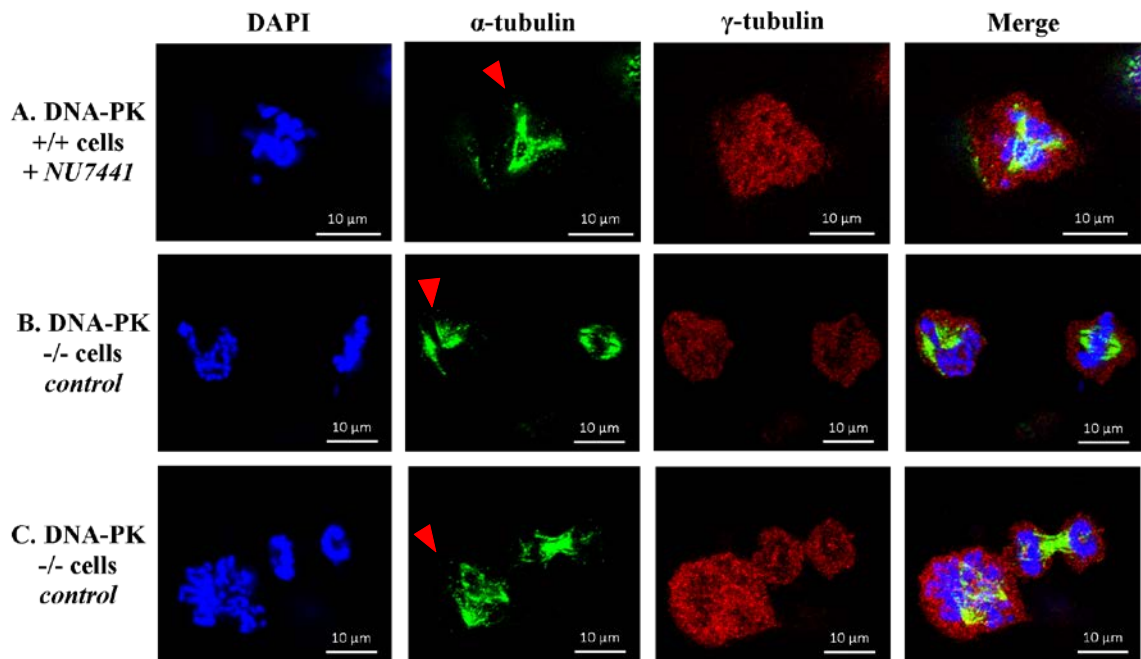
Figure 7-3: The deletion or inhibition of DNA-PK increases the incidence of multipolar spindles. (**A**) HCT116 DNA-PK +/+ cells or (**B**-**C**) DNA-PK -/- cells were seeded onto poly L-lysine-coated coverslips and left to establish for 24 hours before treatment with 1 µM NU7441 where indicated, and then incubated for a further 24 hours. Immunodetection of α-tubulin (green) and γ-tubulin (red), using the indicated antibodies, and DAPI DNA staining (blue) were analysed by confocal microscopy (Section 2.12). Mitotic cell images are representative of ≥ 3 fields captured for each treatment group, in 2 independent experiments. Red arrowheads indicate α-tubulin abnormalities.

7.4.3 A greater number of mitotic abnormalities were observed following vincristine treatment in cells with inhibited or deleted DNA-PK

The DNA-PK +/+ cells and the DNA-PK -/- cells were then treated with 2 nM vincristine alone or in combination with 1 µM NU7441 for 24 hours. This vincristine concentration was chosen because it is below the vincristine GI_{50} for both the DNA-PK +/+ and DNA-/- cells (Section 6.3.4), and therefore the cells would still adhere to the coverslips but there would be an effect on tubulin formation. In the DNA-PK +/+ cells, vincristine treatment caused the majority of the cells undergoing mitosis to arrest in what appears to be prometaphase (Figure 7-4A), with the chromosomes condensed and microtubules visible and extending, prior to chromosomal organisation on the mitotic spindle, with the remaining mitotic cells in metaphase. However, in cells treated with NU7441 in combination with vincristine, or in DNA-PK -/- cells treated with vincristine

alone, many of the mitotic cells appeared to have progressed further through mitosis to metaphase, and a large number of mitotic abnormalities were observed (see red arrowheads) (seen in approximately 30-50 % of mitotic cells), such as chromosomal misalignments and cells with either only one, or more than two, centrosomes (Figure 7-4B-D).
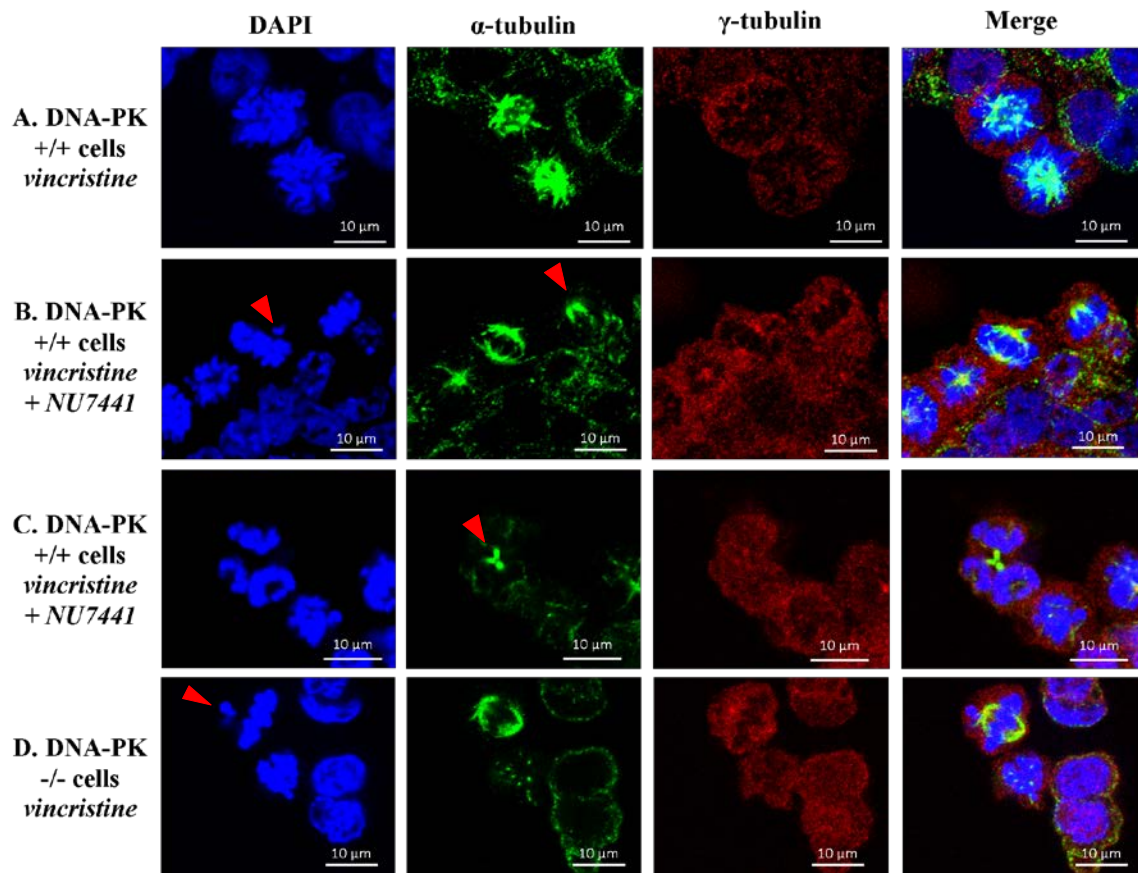
Figure 7-4: Vincristine treatment in combination with either deletion or inhibition of DNA-PK increases the incidence of incorrect mitotic spindle formation and chromosome misalignment. (**A**-**C**) HCT116 DNA-PK +/+ cells or (**D**) DNA-PK -/- cells were seeded onto poly L-lysine-coated coverslips and left to establish for 24 hours before treatment with 2 nM vincristine alone or in combination with 1 μM NU7441 where indicated, and then incubated for a further 24 hours. Immunodetection of α-tubulin (green) and γ-tubulin (red), using the indicated antibodies, and DAPI DNA staining (blue) were analysed by confocal microscopy (Section 2.12). Mitotic cell images are representative of ≥ 3 fields captured for each treatment group, in 2 independent experiments. Red arrowheads indicate DNA or α-tubulin abnormalities.

One of the aberrant mitotic events following ionising radiation reported to occur in DNA-PK deficient cells is the formation of multinucleated cells (Shang *et al.*, 2010). There were no multinucleated cells observed among the DNA-PK +/+ cells but multinucleated cells were observed in untreated DNA-PK -/- cells (red arrows, Figure 7-5B), and vincristine-treated DNA-PK -/- cells (Figure 7-5C and D). These cells appeared to have multiple nuclei of normal size.
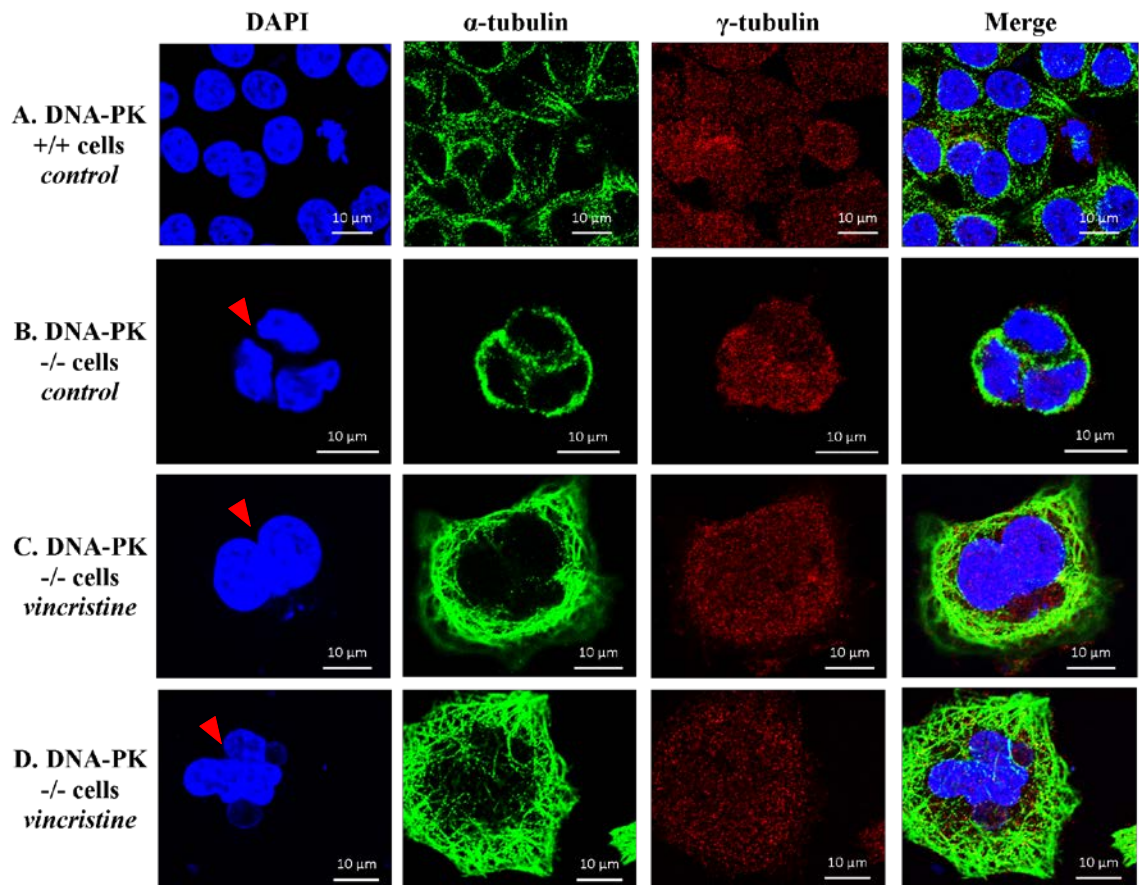
Figure 7-5: Untreated or vincristine-treated DNA-PK deficient cells display multinucleated cells. (**A**) HCT116 DNA-PK +/+ cells or (**B-D**) DNA-PK -/- cells were seeded onto poly L-lysine-coated coverslips and left to establish for 24 hours before treatment with 2 nM vincristine where indicated, and then incubated for a further 24 hours. Immunodetection of α-tubulin (green) and γ-tubulin (red), using the indicated antibodies, and DAPI DNA staining (blue) were analysed by confocal microscopy (Section 2.12). Mitotic cell images are representative of ≥ 3 fields captured for each treatment group, in 2 independent experiments. Red arrowheads indicate DNA abnormalities.

7.4.4 Total DNA-PK expression was lower in mitotic cells compared with non-mitotic cells, and was significantly reduced in mitotic cells following vincristine treatment

Total DNA-PKcs protein expression and phosphorylated DNA-PK (S2056) localisation were examined in the DNA-PK +/+ cells. DNA-PK phosphorylation at serine 2056 was seen in response to ionising radiation and vincristine treatment (Figure 7-6C and D). There was no difference in phosphorylated DNA-PK (S2056) foci in mitotic and non-mitotic cells. There was less total DNA-PKcs expression in mitotic cells both before treatment and after ionising radiation treatment, and the remaining expression was extra-chromosomal (red arrowheads, Figure 7-6A-C). Total DNA-PKcs levels in mitotic cells following vincristine treatment were very low compared with levels in untreated or ionising radiation-treated cells (red arrowheads, Figure 7-6D), whereas the total DNA-PKcs level in non-mitotic cells was not changed by vincristine treatment.
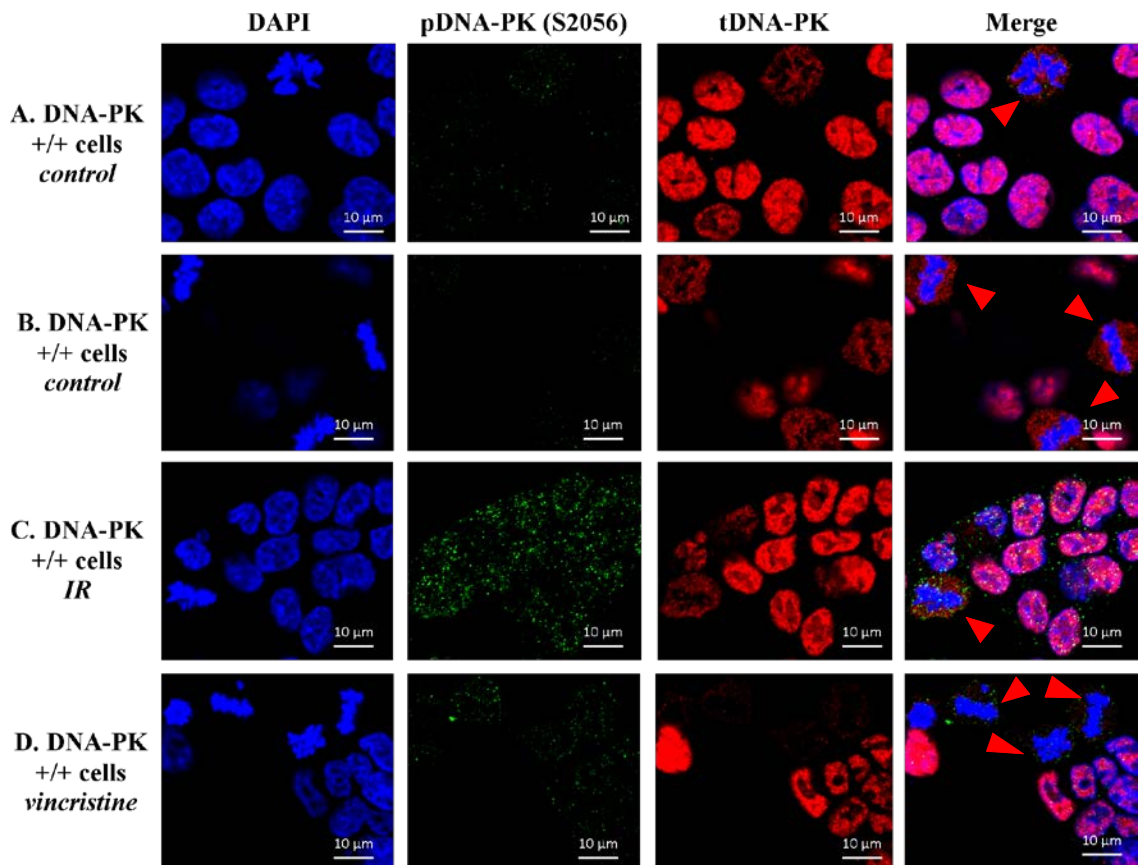
Figure 7-6: Vincristine treatment causes a reduction in total DNA-PK expression in mitotic cells. (**A-D**) HCT116 DNA-PK +/+ cells were seeded onto poly L-lysine-coated coverslips and left to establish for 24 hours before treatment with 2 nM vincristine or 2 Gy ionising radiation (IR), where indicated, and then incubated for a further 24 hours. Immunodetection of phosphorylated DNA-PK at serine 2056 (pDNA-PK (S2056)) (green) and total DNA-PK (tDNA-PK) (red), using the indicated antibodies, and DAPI DNA staining (blue) were analysed by confocal microscopy (Section 2.12). Mitotic cell images are representative of ≥ 3 fields captured for each treatment group, in 2 independent experiments. Red arrowheads indicate cells with lower total DNA-PK levels.

7.4.5 Phosphorylated DNA-PK (T2609) localises with chromosomes and PLK1 during mitosis

Phosphorylated DNA-PK (T2609) has previously been shown to co-localise with PLK1 at the centrosomes, kinetochores and midbody during normal mitotic progression and during mitosis following ionising radiation (Shang *et al.*, 2010; Huang *et al.*, 2014). Therefore the localisation of phosphorylated DNA-PK (T2609) and PLK1 were investigated in untreated, ionising radiation-treated and vincristine-treated DNA-PK +/+ cells and DNA-PK -/- cells.

In untreated DNA-PK +/+ cells, phosphorylated DNA-PK (T2609) was found to localise with the condensed chromosomes in prometaphase (Figure 7-7A), metaphase (Figure 7-7D) and early anaphase (Figure 7-7C). DNA-PK appears to surround the chromosomes in these early stages of mitosis, but is not detectable in cells in late anaphase/telophase or during cytokinesis. Phosphorylated DNA-PK (T2609) was found to co-localise with PLK1 at the centrosomes (Figure 7-7B) and midbody (Figure 7-7F). However, phosphorylated DNA-PK (T2609) co-localisation with PLK1 was not detected in cells in late anaphase/telophase (lower cell in Figure 7-7D and Figure 7-7E).
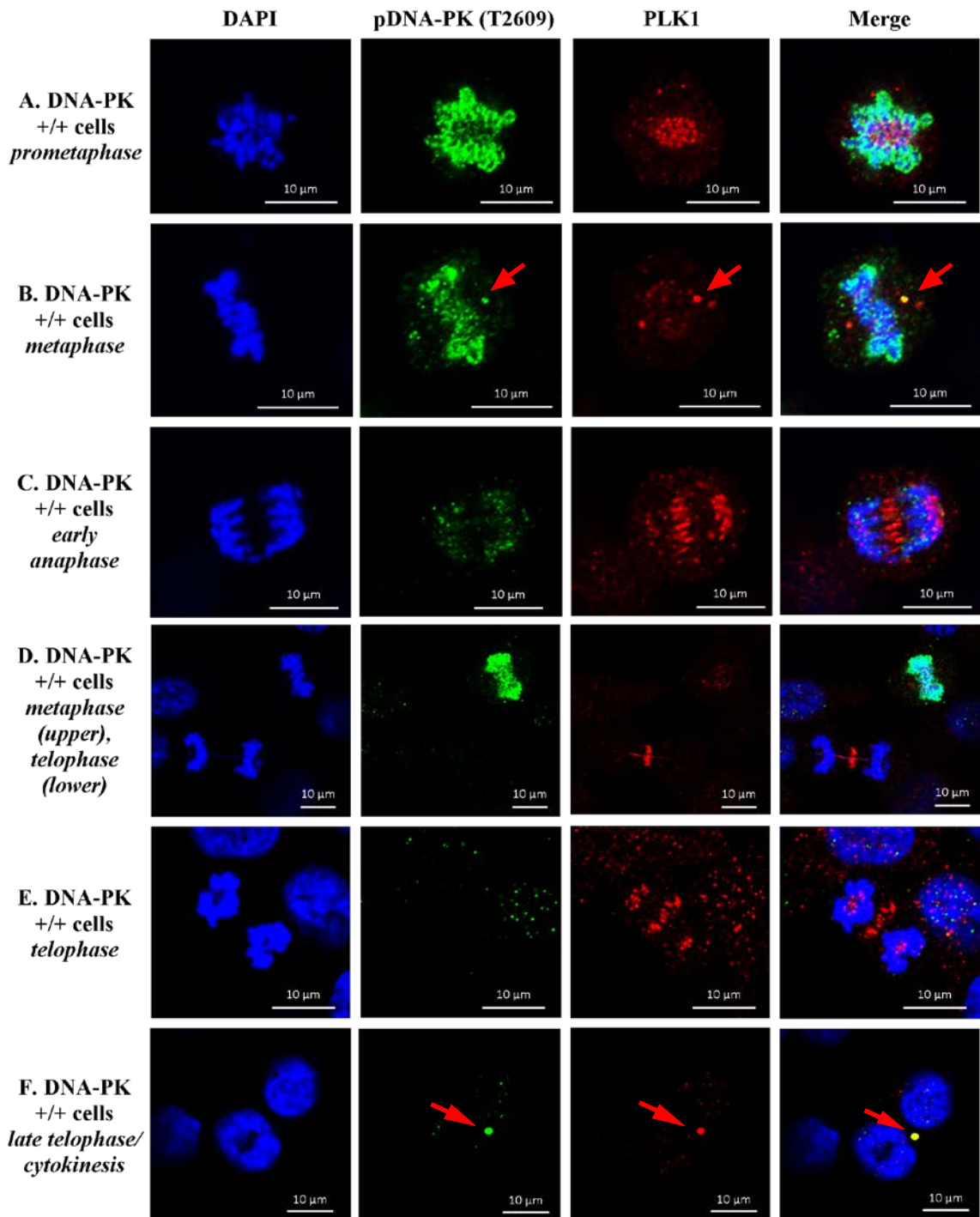
Figure 7-7: Phosphorylated DNA-PK co-localises with PLK1 at the centrosomes and the midbody during mitosis. (**A-F**) HCT116 DNA-PK +/+ cells were seeded onto poly L-lysine-coated coverslips and left to establish for 48 hours. Immunodetection of phosphorylated DNA-PK at threonine 2609 (pDNA-PK (T2609)) (green) and PLK1 (red), using the indicated antibodies, and DAPI DNA staining (blue) were analysed by confocal microscopy (Section 2.12). Mitotic cell images are representative of ≥ 3 fields captured for each treatment group, in 2 independent experiments. Red arrows indicate pDNA-PK T2609 and PLK1 co-localisation.

Figure 7-8 shows DNA-PK +/+ cells following treatment with ionising radiation. Phosphorylated DNA-PK (T2609) foci were seen across the nuclei of irradiated cells not undergoing mitosis (Figure 7-8A). Phosphorylated DNA-PK (T2609) was found to localise with the chromosomes, even when the chromosomes were lagging and not correctly aligned on the mitotic spindle, and phosphorylated DNA-PK (T2609) is seen both on and around these chromosomes (red arrows, Figure 7-8B and C). Figure 7-8D demonstrates no phosphorylated DNA-PK (T2609) in the DNA-PK -/- cells, as expected.
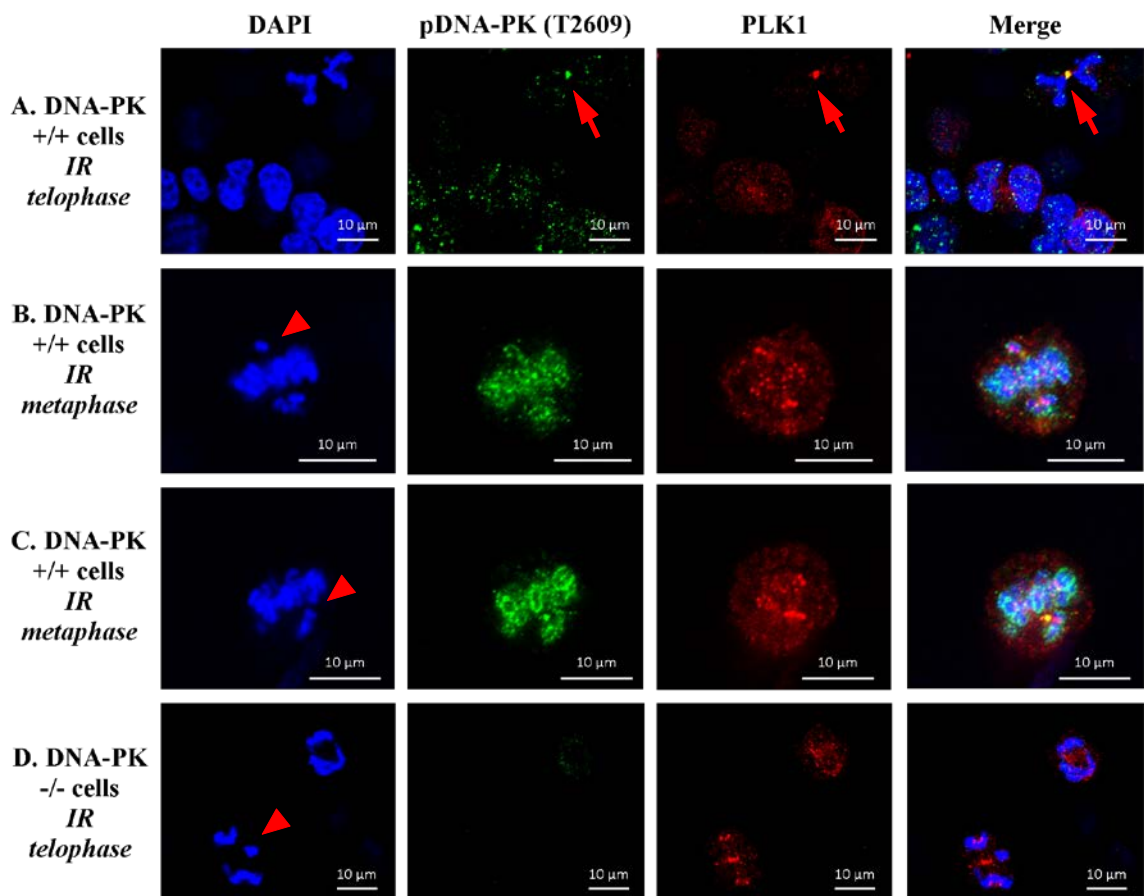
Figure 7-8: Ionising radiation causes chromosome misalignment and phosphorylated DNA-PK localises to the chromosomes during mitosis following ionising radiation treatment. (**A-C**) HCT116 DNA-PK +/+ cells and (**D**) DNA-PK -/- cells were seeded onto poly L-lysine-coated coverslips and left to establish for 24 hours before treatment with 2 Gy ionising radiation (IR), and then incubated for a further 24 hours. Immunodetection of phosphorylated DNA-PK at threonine 2609 (pDNA-PK (T2609)) (green) and PLK1 (red), using the indicated antibodies, and DAPI DNA staining (blue) were analysed by confocal microscopy (Section 2.12). Mitotic cell images are representative of ≥ 3 fields captured for each treatment group, in 2 independent experiments. Red arrowheads indicate DNA abnormalities and red arrows indicate pDNA-PK T2609 and PLK1 co-localisation.

Figure 7-9 shows that increases in centrosome number were observed in DNA-PK +/+ cells following vincristine treatment, and phosphorylated DNA-PK (T2609) was seen to localise with PLK1 at these centrosomes (red arrows, Figure 7-9A and B). An example of an untreated DNA-PK +/+ cell with two centrosomes and co-localisation of PLK1 and phosphorylated DNA-PK (T2609) is shown in Figure 7-7B. It was possible to observe cells undergoing cell death (red arrowheads, Figure 7-9A and C), as detected by DAPI staining of nuclear breakdown, and phosphorylated DNA-PK (T2609) staining was seen in DNA-PK +/+ cells (red arrowhead, Figure 7-9A).
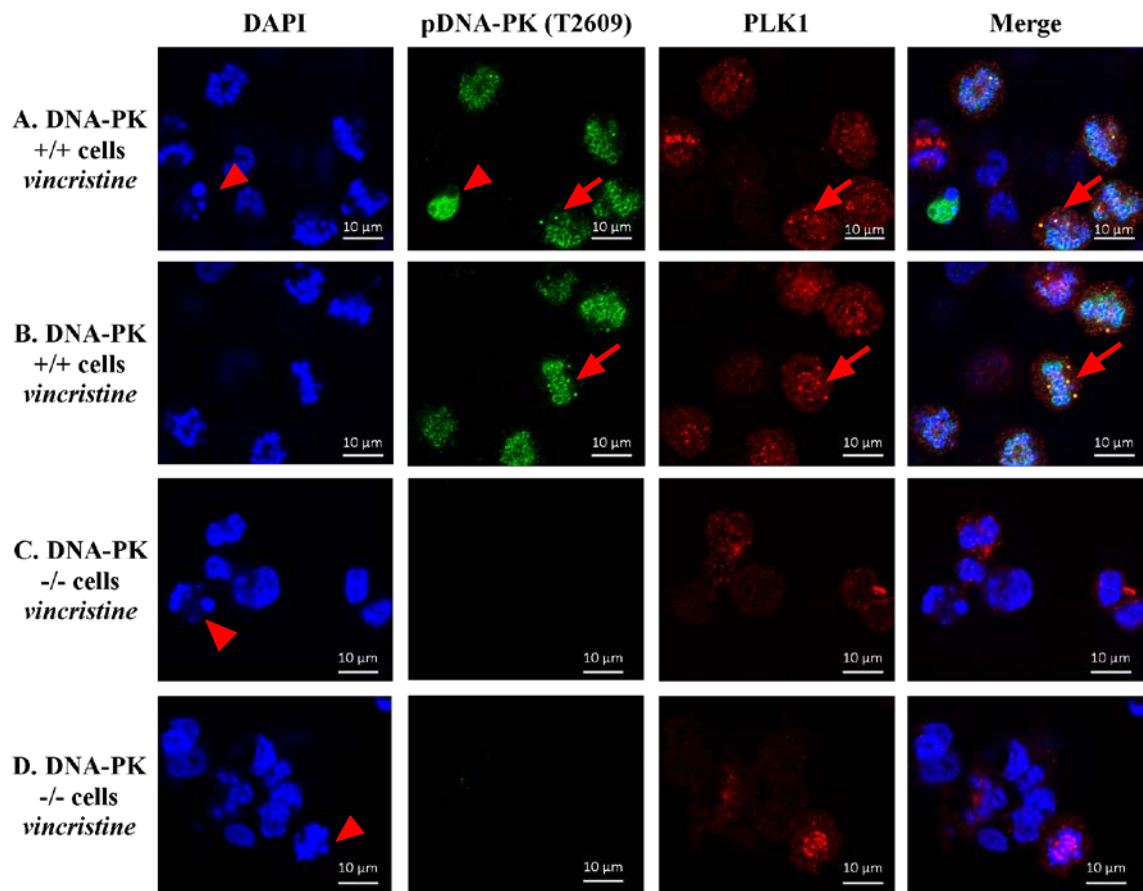
Figure 7-9: Vincristine treatment causes increases in centrosome number. (**A** and **B**) HCT116 DNA-PK +/+ cells and (**C** and **D**) DNA-PK -/- cells were seeded onto poly L-lysine-coated coverslips and left to establish for 24 hours before treatment with 2 nM vincristine and then incubated for a further 24 hours. Immunodetection of phosphorylated DNA-PK at threonine 2609 (pDNA-PK (T2609)) (green) and PLK1 (red), using the indicated antibodies, and DAPI DNA staining (blue) were analysed by confocal microscopy (Section 2.12). Mitotic cell images are representative of ≥ 3 fields captured for each treatment group, in 2 independent experiments. Red arrowheads indicate DNA abnormalities and red arrows indicate pDNA-PK T2609 and PLK1 co-localisation.

7.5   Discussion and future work

A number of publications have suggested a role for DNA-PKcs in chromosome segregation, and mitotic spindle stability and organisation (Shang *et al.*, 2010; Lee *et al.*, 2011; Huang *et al.*, 2014; Shang *et al.*, 2014). Following the observations in previous chapters that DNA-PK plays a role in the response of cells to microtubule-targeting agents, the effect of DNA-PK expression on mitosis and mitotic structures, and the activation and localisation of DNA-PKcs during mitosis, was investigated in the HCT116 DNA-PK +/+ and DNA-PK -/- cells by confocal microscopy.

The techniques for cell preparation, fixation and staining were optimised to allow visualisation of mitotic cells within a mixed cell population, thereby avoiding the use of chemical synchronisation. The optimised conditions and the use of the Zeiss LSM 700 confocal system allowed the visualisation of subcellular structures and protein localisation. Due to time constraints it was not possible to perform quantification of the results of the microscopy. More experiments would be necessary to allow quantification of the percentage of mitotic cells displaying aberrant mitotic events, such as multinucleated cells, multipolar spindles and cells displaying polyploidy, as previously performed in Shang *et al.* (2010). However, representative imaging of normal and aberrant mitotic events was undertaken.

Mitotic cells in untreated HCT116 DNA-PK +/+ cell cultures were normal and cells were observed in all stages of mitosis (Figure 7-1). However, the absence (in DNA-PK -/- cells) or inhibition (using NU7441) of DNA-PK caused an increase in the incidence of multipolar and multinucleated cells (Figure 7-3, Figure 7-5). This finding has also been reported by Lee *et al.* (2011) who demonstrated abnormal spindle formation and chromosome misalignment in NU7441- or DNA-PK siRNA-treated cells. There was an increase in the number of chromosome misalignments in ionising radiation-treated DNA-PK +/+ cells treated with NU7441 and in DNA-PK -/- cells (Figure 7-8) but there was no increase in multipolar or multinucleated cells. This result is in contrast to the data of Shang *et al.* (2010) who found increases in multipolar spindles, polyploidy and multinucleated cells. However, Shang *et al.* (2010) used a higher dose of irradiation (4 Gy) than used in this study (2 Gy), and the ionising radiation effects with the deletion or inhibition of DNA-PK should be investigated at a range of ionising radiation doses and at a range of time points post-irradiation.

Vincristine treatment of DNA-PK +/+ cells caused many of the mitotic cells to display condensed chromosomes and radiating microtubules (but no spindle

organisation) or chromosomes organised at the mitotic spindle, suggesting that these cells are arrested in prometaphase or metaphase. This result was expected as microtubule-targeting agents are known to arrest cells at metaphase in mitosis by triggering the mitotic spindle checkpoint, which ensures correct attachment of microtubules to the mitotic spindle. Mechanistically, vincristine alters the dynamics of the tubulin assembly and disassembly at the ends of the microtubules (Jordan *et al.*, 1991).

The results presented in Figure 7-4 suggest that DNA-PKcs activity may be necessary for correct chromosome organisation at the mitotic spindle, as lagging chromosomes and cells that have progressed past the mitotic checkpoint (and are dividing incorrectly) were observed in vincristine-treated DNA-PK +/+ cells co-treated with NU7441, and in vincristine-treated DNA-PK -/- cells (Figure 7-4B-D). It was estimated that between 10-30 % of untreated mitotic cells displayed aberrant mitotic events in the absence or inhibition of DNA-PK, and this percentage increased to around 30-50 % when these cells were treated with vincristine. DNA-PKcs has been shown to regulate Chk2 T68 phosphorylation during mitosis and DNA-PKcs organises microtubule attachment and spindle assembly through the Chk2/BRCA1 pathway (Shang *et al.*, 2014). The Chk2/BRCA1 pathway impacts on microtubule dynamics and chromosome segregation, and therefore it would be interesting to study Chk2 and its activation in response to microtubule-targeting agents. Also, it would be of interest to investigate whether similar aberrant mitotic events are observed in Chk2- and/or BRCA1-deficient cells, as Chk2 has previously been shown to colocalise with PLK1 at the centrosomes and midbody (Tsvetkov *et al.*, 2003).

The mitotic phase of the cell cycle should also be investigated in more detail to confirm differences observed in the presence and absence of DNA-PK function after vincristine treatment. It is difficult to define the individual phases of mitosis because anaphase in particular occurs relatively quickly; however, Matsui *et al.* (2012) recently developed a synchronisation technique to isolate cells in metaphase, anaphase and telophase. This technique could be used to generate positive control samples for each mitotic cell phase. Western blotting could also be carried out on mitotic cells collected by mitotic shake-off following vincristine treatment of DNA-PK +/+ cells co-treated with NU7441, or DNA-PK -/- cells, to examine the expression of cyclin B1 (which is necessary for mitotic progression and is degraded before mitotic exit (Lindqvist *et al.*, 2007)) and of phosphorylated histone H3 (S10), phosphorylation of which begins in early prophase but ceases in anaphase and telophase (Li *et al.*, 2005). Therefore, if

vincristine treatment in the absence of DNA-PK or following inhibition of DNA-PK has caused cells to progress past the metaphase block in the HCT116 +/+ cells, a decrease in phosphorylated histone H3 should be observed.

DNA-PKcs has previously been shown to co-localise with PLK1 at centrosomes, kinetochores and the midbody during mitosis, and this co-localisation is involved in correct chromosome segregation and cytokinesis (Shang *et al.*, 2010; Huang *et al.*, 2014). Therefore, the localisation of phosphorylated DNA-PKcs (T2609) and PLK1 was investigated in untreated, ionising radiation- and vincristine-treated DNA-PK +/+ and DNA-PK -/- cells. Phosphorylated DNA-PK (T2609) co-localised with centrosomes and the midbody during mitosis (Figure 7-7B and F) but, in contrast to previous findings (Lee *et al.*, 2011), DNA-PK phosphorylation (T2609) was not associated with PLK1 in anaphase cells (Figure 7-7D and E). DNA-PK phosphorylation (T2609) was apparent surrounding the condensed chromosomes in prometaphase, but not localised with PLK1 in untreated, ionising radiation- or vincristine-treated cells, even when there were lagging chromosomes and chromosome misalignment. Previous studies have reported that phosphorylated DNA-PK (T2609) co-localises with PLK1 at the kinetochores during prometaphase (Lee *et al.*, 2011). The findings presented in this chapter suggest that in HCT116 cells, phosphorylated DNA-PKcs (T2609) localises to the chromosomes, in addition to the kinetochores, and may play a role before anaphase.

DNA-PKcs has been shown to be phosphorylated on serine 2056, threonine 2609 and threonine 2647 during mitosis. Furthermore, these phosphorylation events during mitosis are dependent on the kinase activity of DNA-PK (Shang *et al.*, 2010; Lee *et al.*, 2011). Recently, two further DNA-PKcs sites that are phosphorylated during mitosis have been identified. Firstly, DNA-PKcs is phosphorylated on threonine 3950, which is also DNA-PK-dependent and results in phosphorylated DNA-PK (T3950) localising to centrosomes and the midbody. Secondly, there is phosphorylation of DNA-PK at serine 3205, which is PLK1-dependent and results in a diffuse staining pattern in metaphase cells but localisation at the midbody in cytokinesis (Douglas *et al.*, 2014). DNA-PK phosphorylation during mitosis was also shown to be regulated by protein phosphatase 6 (PP6) (Douglas *et al.*, 2014). It would be interesting to investigate these two additional phosphorylation sites in untreated and vincristine-treated HCT116 DNA-PK +/+ cells.

The phosphorylation of H2AX at serine 139 (γH2AX) is an early event in DNA double-strand break repair and this phosphorylation event can be performed by ATM, DNA-PK and ATR (Burma *et al.*, 2001; Wang *et al.*, 2005; An *et al.*, 2010). Recently,

γH2AX phosphorylation has been detected in mitotic cells that have not been exposed to DNA damaging agents (McManus and Hendzel, 2005) and γH2AX phosphorylation at serine 139 is DNA-PKcs-dependent and mediated by Chk2 (Tu *et al.*, 2013). Therefore γH2AX phosphorylation would be another interesting DNA-damage-associated protein phosphorylation event to investigate in untreated and vincristine-treated cells, and this protein is also likely to have novel roles in mitosis.

Total DNA-PK expression was investigated along with phosphorylated DNA-PK (S2056) levels in mitotic cells. As with threonine 2609 phosphorylation, serine 2056 DNA-PK phosphorylation was observed in response to both ionising radiation and vincristine in non-mitotic cells, in the form of foci. However, there was no difference in serine 2056 phosphorylation in mitotic cells compared with non-mitotic cells. Both serine 2056 and threonine 2609 phosphorylated DNA-PKcs has previously been shown to be localised to the centrosomes and kinetochores in HCT116 cells (Lee *et al.*, 2011). Figure 7-6 demonstrates that the total DNA-PKcs levels were reduced in mitotic HCT116 cells compared to surrounding non-mitotic cells. This reduced level is also observed after ionising radiation treatment and is reduced further by vincristine treatment, to a point where total DNA-PKcs expression is barely detectable in vincristine-treated mitotic cells (Figure 7-6D). This result suggests that total DNA-PK is degraded in response to vincristine treatment, although interestingly DNA-PKcs that is phosphorylated at serine 2056 and threonine 2609 is detectable. Loss of total DNA-PK following vincristine treatment in CCRF-CEM cells was demonstrated by Western blotting in Chapter 3 and was associated with an increase in phosphorylated DNA-PKcs (S2056) levels. These microscopy results are consistent with the Western blotting data, and further investigation into how DNA-PK is being degraded, and at what stage total DNA-PK levels are re-established, is warranted.

The results presented in this Chapter suggest that inhibition of DNA-PK in conjunction with vincristine treatment causes mitotic spindle and centrosome disruption, resulting in mitotic catastrophe. This could explain the lack of an increase in caspase 3/7-mediated apoptosis with combinations of microtubule-targeting agents and NU7441, despite the increase in sensitivity observed in growth inhibition assays (Chapter 3). Lastly, these microscopy experiments should be extended to investigate ATM phosphorylation as ATM has also been shown to localise to mitotic structures during mitosis (Zhang *et al.*, 2007b).
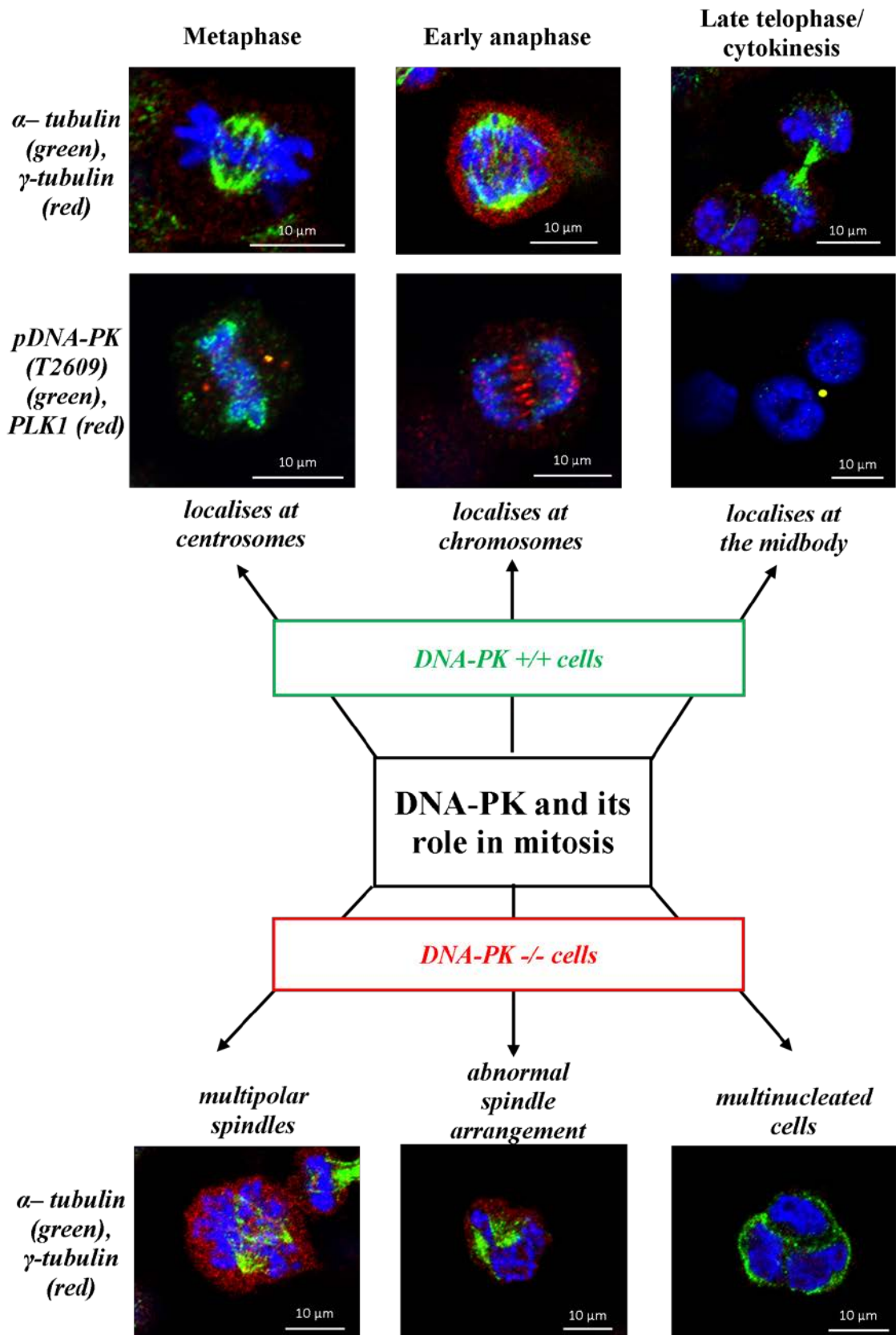
Figure 7-10: Model demonstrating the localisation of DNA-PK during mitosis and the effect of DNA-PK deficiency on cellular and mitotic structures

7.6   Summary

These microscopy data, along with previous studies, confirm that DNA-PK plays a role in mitosis and mitotic regulation, and that lack or inhibition of DNA-PKcs causes an increase in aberrant mitotic events including chromosome misalignment, increases in centrosome number and multipolar spindle formation. Phosphorylated DNA-PK (T2609) co-localises with PLK1 at the centrosomes and midbody during mitosis, and localises with chromosomes during prometaphase. These microscopy data also support extending the therapeutic potential of DNA-PK inhibition beyond use in combination with DNA-damaging agents, to combinations with microtubule-targeting agents, due to the role that DNA-PK plays in mitosis and mitotic spindle regulation.

Chapter 8: Discussion and further work

The enzymes DNA-PK and ATM have been extensively studied for their roles in the NHEJ and HR DNA repair pathways, respectively. However, as is the case with many of the protein kinases that have been investigated for their role in cancer and treatment response that were initially identified as having specific functions in a signalling pathway, these proteins have additional roles. As reviewed in Chapter 1, DNA-PK has recently been shown to have functions beyond its classical role in NHEJ, with roles in genomic stability, HR, cell cycle checkpoint maintenance, inflammation and innate immunity, metabolic gene regulation, hypoxia and spindle dynamics (Figure 1-4). The roles of ATM beyond HR extend to replication stress, hypoxia, redox signalling and regulation, neuronal function, insulin signalling and secretion, NFκB activation and mitotic spindle assembly and mitosis (Figure 1-6).

Microtubule-targeting agents are widely-used to treat a range of solid and haematological cancers. These agents act upon cells undergoing mitosis to inhibit mitotic spindle function and also upon cells in interphase by interfering with intracellular protein trafficking (Figure 1-8).

A previous Newcastle University Master's degree project demonstrated that the ALL cell line, CCRF-CEM, could be sensitised not only to DNA damaging agents by the DNA-PK and ATM selective inhibitors NU7441 and KU55933, respectively, but also to the microtubule-targeting agent vincristine (NJ Tan, unpublished results). This project also demonstrated that the vincristine-resistant CCRF-CEM VCR/R cell line, which was created by stepwise exposure to increasing concentrations of vincristine and which overexpressed the drug efflux transporter MDR1, could be sensitised to DNA-damaging and microtubule-targeting drugs to a much greater degree by NU7441 and KU55933 than parental CCRF-CEM cells.

Therefore, based on published findings that DNA-PK and ATM may play a role in mitotic spindle formation, and the initial findings that cells can be sensitised to MTAs by small molecule inhibitors of DNA-PK and ATM, it was hypothesised that DNA-PK and ATM may play a role in the response of cells to MTAs. The aims of this project were therefore to investigate the sensitisation of cells to MTAs using NU7441 and KU55933, in relation to DNA-PK and ATM activation and expression, and to compare the results of chemical inhibition of DNA-PK and ATM with the lack of DNA-PK by using DNA-PK proficient and deficient cell lines. Another set of aims was to determine if the sensitisation observed with NU7441 and KU55933 in MDR1-overexpressing cell lines was due to these agents interacting with drug efflux *via* MDR1, and also to investigate the localisation and activation of DNA-PK in mitotic cells, the effect of

MTAs on DNA-PK localisation and activation, and the effects of a lack of DNA-PK on spindle assembly and mitosis.

Growth inhibition data in Chapter 3 demonstrated that 1 µM NU7441 sensitised the parental CCRF-CEM cells to vincristine, whereas three other parental cell lines (A2780, SKOV3 or KK47 cells) were not sensitised to either vincristine or docetaxel/paclitaxel. KU55933 (10 µM) sensitised CCRF-CEM cells to vincristine and A2780 cells to paclitaxel, but had no effect with the other MTAs in these cell lines or with either MTA in the other parental cell lines. These results suggest that sensitisation to MTAs using NU7441 or KU55933 is cell line- and MTA-specific, and that sensitisation is quite modest with 1 µM NU7441 (1.5-fold) but larger with 10 µM KU55933 (6- to 20-fold). In four multidrug-resistant MDR1-overexpressing cell lines, 1 µM NU7441 and 10 µM KU55933 caused sensitisation to both vincristine and taxanes to a greater degree (3.4- to 17-fold for NU7441, 11- to 48-fold for KU55933) than demonstrated in the parental cell lines. This observation led to the hypothesis that the DNA-PK and ATM inhibitors were affecting vincristine and taxane efflux *via* MDR1.

Chapter 4 therefore investigated whether NU7441 and KU55933 had any effect on drug accumulation *via* MDR1. The DNA-PK inhibitors NU7441 and NDD0004 were shown, using fluorescence microscopy, to cause doxorubicin accumulation in MDR1-overexpressing MDCKII-MDR1 cells. A more quantitative LC-MS assay demonstrated that regardless of DNA-PK-inhibitory activity, a panel of NU7441-based derivatives and KU55933 caused an increase in intracellular vincristine levels in MDR1-overexpressing CCRF-CEM VCR/R cells. There was no effect on intracellular vincristine in CCRF-CEM cells, and no MDR1 expression was detected by Western blot in these cells, indicating low endogenous expression of MDR1. Therefore, the effects of NU7441 and KU55933 in the parental cell lines are unlikely to be due to the MDR1-inhibitory action of the compounds. The optimal concentrations for DNA-PK and ATM inhibition were 1 µM NU7441 and 10 µM KU55933, respectively. Both 1 µM NU7441 and 10 µM KU55933 produced a very similar increase in intracellular vincristine concentration, indicating that although there is a 10-fold difference in the absolute molar concentration of these two inhibitors, 10 µM KU55933 did not result in a greater drug accumulation, and therefore the greater effects seen with 10 µM of KU55933 in the multidrug-resistant cell lines compared with 1 µM of NU7441 were not a result of greater drug accumulation.

Despite the lack of sensitisation with the DNA-PK inhibitor in the parental cell lines tested, activation of DNA-PK at an autophosphorylation site in response to

vincristine treatment was demonstrated in both the CCRF-CEM and CCRF-CEM VCR/R cells, and in the HCT116 DNA-PK +/+, DNA-PK +/- and DNA-PK RE cells. However, this autophosphorylation was not a result of DNA damage, because cytotoxic concentrations of vincristine and docetaxel did not cause DNA damage as demonstrated by the COMET assay. Also, the ATM inhibitor caused sensitisation to MTAs, suggesting that ATM is also activated in response to these agents. However, autophosphorylation of ATM at serine 1981 was not demonstrated in response to vincristine treatment, which would be expected if vincristine was causing DNA double-strand breaks.

There was a concentration-dependent increase in caspase 3/7-mediated apoptosis in response to the MTAs, but NU7441 did not consistently cause a significant further increase in apoptosis in either parental or multidrug-resistant cells. The intracellular concentration of the MTAs increased with the combination of NU7441 in the multidrug-resistant cell lines, and an increase in caspase 3/7-mediated apoptosis would be expected if this was the main mechanism of cell death. It was not possible to measure caspase 3/7-mediated apoptosis in combination with KU55933 as this compound interacted with the Caspase-Glo assay. Therefore, further investigation into the mechanisms of cell death need to be studied.

The HCT116 cell line panel with differing DNA-PK expression levels was obtained to allow investigation of the effects of DNA-PK absence as opposed to inhibition. In line with previous observations that DNA-PK is involved in cellular responses to ionising radiation, and that NU7441-treated or DNA-PK-deficient cells were more radio-resistant than DNA-PK-proficient cells (Tavecchio *et al.*, 2012), Chapter 6 demonstrated that HCT116 DNA-PK +/+ cells were sensitised to ionising radiation by 1 µM NU7441, and the HCT116 DNA-PK -/- cells were more sensitive to ionising radiation than DNA-PK +/+ cells. There was no difference in ionising radiation sensitivity between parental DNA-PK +/+ cells and DNA-PK +/- cells, indicating that there was no haploinsufficiency effect.

However, DNA-PK absence or inhibition in the panel of HCT116 cell lines had no significant effect on sensitisation to vincristine or docetaxel, except that the HCT116 DNA-PK -/- cells were more sensitive in the clonogenic assay at higher vincristine concentrations. KU55933 (10 µM) caused sensitisation to vincristine in the HCT116 DNA-PK +/+, DNA-PK +/- cells and DNA-PK -/- cells, and sensitisation to docetaxel in the HCT116 DNA-PK +/+ cells. These data complement the findings described in

Chapter 3 and suggest that inhibition of ATM using 10 μM KU55933 causes more effective sensitisation to MTAs than inhibition of DNA-PK using 1 μM NU7441.

Loss of DNA-PK expression is not a common event in cancer, whereas loss or mutation of ATM occurs more frequently (reviewed briefly in Chapter 1 and extensively in Cremona and Behrens (2014)). Therefore, sensitisation with NU7441 to DNA-damaging drugs or MTAs could be more marked in the setting of loss of ATM function, as it would be predicted that loss of both DNA repair pathways would result in synthetic lethality in response to DNA double strand breaks. Although increased sensitivity to MTAs was observed in the DNA-PK -/- cells treated with KU55933, this result needs to be investigated further in clonogenic survival assays. Whilst it is tempting to speculate that dual inhibition of DNA-PK and ATM would produce synthetic lethality, there is a concern that toxicity to normal healthy cells would also increase. A clinical trial using a similar approach has recently completed (although with no results as yet) which investigated the effect of the PARP inhibitor olaparib in combination with paclitaxel *versus* paclitaxel alone in gastric cancer patients (NCT01063517, Clinicaltrials.gov (2014)). Progression-free survival was recorded for the whole population but stratified for patients who were HR-deficient (defined by loss of ATM protein). Modification inhibition of the base-excision repair pathway in the setting of HR-deficiency could increase sensitivity in these patients as low ATM expression or ATM deficiency is known to confer sensitivity to PARP inhibition (Williamson *et al.*, 2010; Gilardini Montani *et al.*, 2013).

Interestingly, although the combination of vincristine and ionising radiation was more cytotoxic to HCT116 DNA-PK +/+ cells and DNA-PK +/- cells than either treatment alone, the vincristine-ionising radiation combination was 14-fold more toxic to HCT116 DNA-PK -/- cells compared with the parental DNA-PK +/+ cells. This combination study should be extended to investigating the effect of ionising radiation in combination with a taxane. Also, the effect of DNA-PK or ATM inhibition in combination with dual MTA and ionising radiation treatment should be investigated in an *in vivo* model, and there are a large number of clinical trials currently that are already investigating the combination of ionising radiation with MTAs. On the basis of the data presented here, the MTA would need to be administered 24 hours prior to ionising radiation treatment. Furthermore, combination of a DNA-PK or ATM inhibitor with an MTA and ionising radiation should be fully characterised in preclinical models and should include toxicity studies.

The Genomics of Drug Sensitivity in Cancer Project is a collaboration between the Cancer Genome Project at the Wellcome Trust Sanger Institute (UK) and the Center for Molecular Therapeutics, Massachusetts General Hospital Cancer Center (USA), and is a freely accessible service with drug sensitivity data on 140 compounds and genomic datasets for 70 commonly mutated genes in a panel of over 600 cell lines. Neither DNA-PK nor ATM has been studied in the gene profiling; however, NU7441 and KU55933 have been tested against the panel of cell lines, as well as docetaxel, paclitaxel and vinblastine (but not vincristine). Multivariate ANOVA is used to investigate genomic determinants of sensitivity to a specific drug, and effects with a p-value of $p<0.01$ are significantly associated with drug sensitivity (effect <1) or resistance (effect >1). FLT3 (a cytokine receptor frequently mutated in acute myeloid leukaemia) mutation was the only predictor for sensitivity to NU7441 treatment alone (effect 0.17, p=0.001), and FLT3 mutation was also a predictor of sensitivity to KU55933 alone (effect 0.25, p=0.0001) and paclitaxel (effect 0.15, p=0.0004). This result suggests that combinations of these compounds should be studied further to determine whether FLT3 expression or mutation determines response to NU7441 or KU55933, alone or in combination with an MTA (Yang *et al.*, 2013; Genomics of Drug Sensitivity in Cancer, 2014). The CCRF-CEM, SKOV3 and HCT116 cell lines all have FLT3 mutations (COSMIC, 2014) and the CCRF-CEM cells are relatively sensitive to NU7441 and KU55933 treatments alone (low Z-scores) compared with all of the other cell lines in the panel. Mutation of EZH2, a histone-lysine N-methyltransferase where mutations can lead to increases in histone methylation and silencing tumour suppressor genes, predicted sensitivity to vinblastine (effect 0.33, p=0.007) and KU55933 (effect 0.33, p=0.002), indicating another gene mutation which could be exploited to enhance sensitivity to a combination of these agents, and which is also mutated in the CCRF-CEM cells.

An interesting finding in this thesis was that three multidrug-resistant cell lines, all generated by exposure to increasing concentrations of an MTA resulting in overexpression of MDR1, demonstrated not only chemo-resistance but also radio-resistance. A number of previous studies, as discussed in Chapter 5, have reported that ionising radiation can cause an increase in MDR1 (and a number of other transporters) mRNA and protein expression, which has been associated with resistance to chemotherapeutic agents. The data presented in Chapter 5 needs to be validated in additional MDR1-overexpressing cell lines and these studies should be extended to an *in vivo* model of MDR1-overexpressing resistant cancer. These data raise the possibility

that chemotherapy treatment that generates a chemo-resistant tumour could also influence the subsequent response to radiotherapy. It is therefore important for these findings to be confirmed, as the order and timing of chemo- and radiotherapy may be very important in determining outcome.

DNA-PKcs content and activity has previously been shown to correlate with radiosensitivity in lung, oesophageal and early breast cancer (Sirzen *et al.*, 1999; Noguchi *et al.*, 2002; Soderlund Leifler *et al.*, 2010), but not nasopharyngeal cancer (Lee *et al.*, 2005b). However, Beskow *et al.* (2006) found no difference in DNA-PKcs, Ku70 or Ku80 expression in cervical cancer patient biopsies before and following radiation, whereas Shintani *et al.* (2003) and Beskow *et al.* (2009) found that DNA-PKcs and Ku proteins were upregulated after radiation treatment. The results presented in Chapter 5 demonstrated that NU7441 did not sensitise any of the multidrug-resistant cell lines to ionising radiation.

The CCRF-CEM VCR/R cells were shown to have more total DNA-PK and ATM expression, and therefore resistant cells may upregulate DNA double-strand break repair enzymes to enable fast and complete repair of DNA damage. However, whether increased DNA-PK or ATM protein expression and activity confers sensitivity or resistance to small molecule inhibition in resistant cell lines is still to be proven; resistant cell lines could be more sensitive to treatment with small molecule inhibitors due to an increased dependency on these proteins, or conversely could be more resistant to inhibition due to the fact that there is more protein present in the cells. It is difficult to separate the effects of NU7441 and KU55933 on DNA-PK or ATM and MDR1 in determining the effect of MTAs on the multidrug-resistant cell lines; however, the lack of sensitisation to ionising radiation using NU7441 and KU55933 in the multidrug-resistant cell lines suggests that DNA-PK and ATM do not play as large a role in the response of resistant cells to ionising radiation as they do in parental cells. Investigation of other DNA repair proteins such as ATR may reveal repair mechanisms responsible for the radio-resistance observed in these multidrug-resistant cell lines. The studies in Chapter 5 demonstrate that DNA-PK plays a role in the response of non-MDR1 expressing cells to ionising radiation and that these cells can be sensitised using a DNA-PK inhibitor, NU7441, but that ionising radiation sensitisation is lost in multidrug-resistant cells. This contrasts with the enhancement in sensitisation with MTAs in multidrug-resistant cells which is most likely due to the dual DNA-PK and MDR1 inhibition properties of NU7441.

To investigate further the expression of DNA-PK and ATM in parental and multidrug-resistant cells, the development of a resistant cell line would be useful as this would allow cells at different stages of resistance to be collected and changes in DNA-PK and ATM expression and activity monitored as resistance evolved. Initial studies undertaken previously, generated a super-resistant version of the CCRF-CEM VCR/R cell line which had further increases in DNA-PK and ATM expression and activity (NJ Tan, unpublished results). Access to a panel of isogenic cell lines with increasing MTA resistance would allow investigation of DNA-PK and ATM inhibitor effects, using NU7441 and KU55933, in parallel with MDR1 modulation and provide further insights into the role of DNA-PK and ATM in the development of resistance to MTAs.

To provide more mechanistic evidence for the involvement of DNA-PK in mitosis, DNA-PK localisation and activation was examined in mitotic cells in Chapter 7, and the effect of the absence of DNA-PK on spindle assembly studied. In line with previous studies, DNA-PK phosphorylated on T2609 co-localised with the mitotic protein PLK1 at mitotic structures such as the chromosomes in prometaphase and metaphase, the centrosomes and the midbody. The novel findings were that lack of DNA-PK, or inhibition using NU7441, resulted in an increase in aberrant mitotic events including chromosome misalignments, multipolar spindles and an increase in centrosome numbers in untreated, ionising radiation-treated or MTA-treated cells. An additional finding was that total DNA-PK expression was reduced in mitotic cells following vincristine treatment. As discussed in Chapter 1, many proteins, including DNA repair proteins, associate with or traffic along the microtubules, and DNA-PK may be trafficked along the microtubules before the commencement of mitosis; a process that could be disrupted by vincristine treatment leading to decreased DNA-PK expression in mitotic cells. The reduced total DNA-PK expression observed needs to be further investigated because cells in prometaphase and metaphase were found to have no detectable total DNA-PK expression whereas others had phosphorylated DNA-PK (T2609). Therefore, it is difficult to understand the time course of DNA-PK activation and reduced expression; for example, whether the protein is activated and then degraded or if there is reduced total protein before activation. The role of DNA-PK in mitosis in cells treated with vincristine is an important area for clarification if a DNA-PK inhibitor was to be used in combination with vincristine, and these studies should also be extended to investigate the role of ATM.

Phosphorylated DNA-PK foci formation has been incorporated as a biomarker for the integrity of DNA repair pathways in pancreatic cancer, along with Rad51 foci, and

was found to be related to tumour response to radiotherapy, chemotherapy and overall survival in a recently completed clinical trial (NCT00900003, Clinicaltrials.gov (2014)). It will be interesting to see the results of this study in full because it suggests that phosphorylated DNA-PK foci could therefore be measured in patients with a wide variety of cancers or treatments if this initial trial finds a data correlation between DNA-PK phosphorylation and outcome. It would be of interest to investigate the DNA-PK and ATM activity and expression by immunohistochemistry of phosphorylated DNA-PK (Ser2056) and phosphorylated ATM (Thr2609) in xenograft models that have had no treatment or ionising radiation or MTA treatment.

Due to the large range of functions and processes, such as hypoxia, genomic stability, inflammation, immune response and oxidative stress in which DNA-PK and ATM have been implicated, along with their roles in DNA repair, this work needs to be extended beyond *in vitro* cell line work. *In vivo* studieswill aid in understanding the effects of inhibition of these proteins. The development of more soluble compounds suitable for *in vivo* investigation would facilitate such studies. The complexity and heterogeneity of a tumour *in situ* cannot be modelled using a cell line growing in two dimensions *in vitro*. The effects of DNA-PK and ATM inhibition stretch far beyond DNA double-strand break repair to other tumour growth and signalling pathways, the comprehensive study of which requires three dimensional whole tumour models.

In summary, this thesis has extended our understanding of the roles of DNA-PK and ATM by demonstrating the involvement of these proteins in the cellular response to MTAs. In turn, this understanding extends the therapeutic potential of targeting DNA-PK and ATM. This thesis has provided insights into the pharmacology of NU7441 and KU55933; two well-established compounds used widely for *in vitro* work, and demonstrated that these two compounds interact with the drug efflux transporter, MDR1, to increase intracellular drug concentrations.

Appendices

References

Al-Ejeh, F., Kumar, R., Wiegmans, A., Lakhani, S.R., Brown, M.P. and Khanna, K.K. (2010) 'Harnessing the complexity of DNA-damage response pathways to improve cancer treatment outcomes', *Oncogene*, 29(46), pp. 6085-98.

Alexander, A., Cai, S.L., Kim, J., Nanez, A., Sahin, M., MacLean, K.H., Inoki, K., Guan, K.L., Shen, J., Person, M.D., Kusewitt, D., Mills, G.B., Kastan, M.B. and Walker, C.L. (2010) 'ATM signals to TSC2 in the cytoplasm to regulate mTORC1 in response to ROS', *Proc Natl Acad Sci U S A*, 107(9), pp. 4153-8.

Alexandrova, N., Niklinski, J., Bliskovsky, V., Otterson, G.A., Blake, M., Kaye, F.J. and Zajac-Kaye, M. (1995) 'The N-terminal domain of c-Myc associates with alpha-tubulin and microtubules in vivo and in vitro', *Mol Cell Biol*, 15(9), pp. 5188-95.

Allalunis-Turner, M.J., Barron, G.M., Day, R.S., 3rd, Dobler, K.D. and Mirzayans, R. (1993) 'Isolation of two cell lines from a human malignant glioma specimen differing in sensitivity to radiation and chemotherapeutic drugs', *Radiat Res*, 134(3), pp. 349-54.

Allen, J.D., Brinkhuis, R.F., van Deemter, L., Wijnholds, J. and Schinkel, A.H. (2000) 'Extensive contribution of the multidrug transporters P-glycoprotein and Mrp1 to basal drug resistance', *Cancer Res*, 60(20), pp. 5761-6.

Amatya, P.N., Kim, H.B., Park, S.J., Youn, C.K., Hyun, J.W., Chang, I.Y., Lee, J.H. and You, H.J. (2012) 'A role of DNA-dependent protein kinase for the activation of AMP-activated protein kinase in response to glucose deprivation', *Biochim Biophys Acta*, 1823(12), pp. 2099-108.

An, J., Huang, Y.C., Xu, Q.Z., Zhou, L.J., Shang, Z.F., Huang, B., Wang, Y., Liu, X.D., Wu, D.C. and Zhou, P.K. (2010) 'DNA-PKcs plays a dominant role in the regulation of H2AX phosphorylation in response to DNA damage and cell cycle progression', *BMC Mol Biol*, 11, p. 18.

Anderson, C.W. and Allalunis-Turner, M.J. (2000) 'Human TP53 from the malignant glioma-derived cell lines M059J and M059K has a cancer-associated mutation in exon 8', *Radiat Res*, 154(4), pp. 473-6.

Andreu, J.M., Bordas, J., Diaz, J.F., Garcia de Ancos, J., Gil, R., Medrano, F.J., Nogales, E., Pantos, E. and Towns-Andrews, E. (1992) 'Low resolution structure of microtubules in solution. Synchrotron X-ray scattering and electron microscopy of taxol-induced microtubules assembled from purified tubulin in comparison with glycerol and MAP-induced microtubules', *J Mol Biol*, 226(1), pp. 169-84.

Aplan, P.D. (2006) 'Causes of oncogenic chromosomal translocation', *Trends Genet*, 22(1), pp. 46-55.

Araki, R., Fujimori, A., Hamatani, K., Mita, K., Saito, T., Mori, M., Fukumura, R., Morimyo, M., Muto, M., Itoh, M., Tatsumi, K. and Abe, M. (1997) 'Nonsense mutation at Tyr-4046 in the DNA-dependent protein kinase catalytic subunit of severe combined immune deficiency mice', *Proc Natl Acad Sci U S A*, 94(6), pp. 2438-43.

Arcaro, A. and Wymann, M.P. (1993) 'Wortmannin is a potent phosphatidylinositol 3-kinase inhibitor: the role of phosphatidylinositol 3,4,5-trisphosphate in neutrophil responses', *Biochem J*, 296 (Pt 2), pp. 297-301.

Arva, N.C., Talbott, K.E., Okoro, D.R., Brekman, A., Qiu, W.G. and Bargonetti, J. (2008) 'Disruption of the p53-Mdm2 complex by Nutlin-3 reveals different cancer cell phenotypes', *Ethn Dis*, 18(2 Suppl 2), pp. S2-1-8.

Auckley, D.H., Crowell, R.E., Heaphy, E.R., Stidley, C.A., Lechner, J.F., Gilliland, F.D. and Belinsky, S.A. (2001) 'Reduced DNA-dependent protein kinase activity is associated with lung cancer', *Carcinogenesis*, 22(5), pp. 723-7.

Azad, A., Jackson, S., Cullinane, C., Natoli, A., Neilsen, P.M., Callen, D.F., Maira, S.M., Hackl, W., McArthur, G.A. and Solomon, B. (2011) 'Inhibition of DNA-dependent protein kinase induces accelerated senescence in irradiated human cancer cells', *Mol Cancer Res*, 9(12), pp. 1696-707.

Bai, R.L., Pettit, G.R. and Hamel, E. (1990) 'Binding of dolastatin 10 to tubulin at a distinct site for peptide antimitotic agents near the exchangeable nucleotide and vinca alkaloid sites', *J Biol Chem*, 265(28), pp. 17141-9.

Baker, J., Ajani, J., Scotte, F., Winther, D., Martin, M., Aapro, M.S. and von Minckwitz, G. (2009) 'Docetaxel-related side effects and their management', *Eur J Oncol Nurs*, 13(1), pp. 49-59.

Bakkenist, C.J. and Kastan, M.B. (2003) 'DNA damage activates ATM through intermolecular autophosphorylation and dimer dissociation', *Nature*, 421(6922), pp. 499-506.

Bates, S., Kang, M., Meadows, B., Bakke, S., Choyke, P., Merino, M., Goldspiel, B., Chico, I., Smith, T., Chen, C., Robey, R., Bergan, R., Figg, W.D. and Fojo, T. (2001) 'A Phase I study of infusional vinblastine in combination with the P-glycoprotein antagonist PSC 833 (valspodar)', *Cancer*, 92(6), pp. 1577-90.

Ben-Chetrit, E. and Levy, M. (1998) 'Colchicine: 1998 update', *Semin Arthritis Rheum*, 28(1), pp. 48-59.

Benard, J., Da Silva, J., Teyssier, J.R. and Riou, G. (1989) 'Over-expression of MDR1 gene with no DNA amplification in a multiple-drug-resistant human ovarian carcinoma cell line', *Int J Cancer*, 43(3), pp. 471-7.

Bencokova, Z., Kaufmann, M.R., Pires, I.M., Lecane, P.S., Giaccia, A.J. and Hammond, E.M. (2009) 'ATM activation and signaling under hypoxic conditions', *Mol Cell Biol*, 29(2), pp. 526-37.

Bennouna, J., Delord, J.P., Campone, M. and Nguyen, L. (2008) 'Vinflunine: a new microtubule inhibitor agent', *Clin Cancer Res*, 14(6), pp. 1625-32.

Bergen, L.G. and Borisy, G.G. (1980) 'Head-to-tail polymerization of microtubules in vitro. Electron microscope analysis of seeded assembly', *J Cell Biol*, 84(1), pp. 141-50.

Bergen, L.G., Kuriyama, R. and Borisy, G.G. (1980) 'Polarity of microtubules nucleated by centrosomes and chromosomes of Chinese hamster ovary cells in vitro', *J Cell Biol*, 84(1), pp. 151-9.

Beskow, C., Kanter, L., Holgersson, A., Nilsson, B., Frankendal, B., Avall-Lundqvist, E. and Lewensohn, R. (2006) 'Expression of DNA damage response proteins and complete remission after radiotherapy of stage IB-IIA of cervical cancer', *Br J Cancer*, 94(11), pp. 1683-9.

Beskow, C., Skikuniene, J., Holgersson, A., Nilsson, B., Lewensohn, R., Kanter, L. and Viktorsson, K. (2009) 'Radioresistant cervical cancer shows upregulation of the NHEJ proteins DNA-PKcs, Ku70 and Ku86', *Br J Cancer*, 101(5), pp. 816-21.

Blier, P.R., Griffith, A.J., Craft, J. and Hardin, J.A. (1993) 'Binding of Ku protein to DNA. Measurement of affinity for ends and demonstration of binding to nicks', *J Biol Chem*, 268(10), pp. 7594-601.

Block, W.D., Merkle, D., Meek, K. and Lees-Miller, S.P. (2004a) 'Selective inhibition of the DNA-dependent protein kinase (DNA-PK) by the radiosensitizing agent caffeine', *Nucleic Acids Res*, 32(6), pp. 1967-72.

Block, W.D., Yu, Y. and Lees-Miller, S.P. (2004b) 'Phosphatidyl inositol 3-kinase-like serine/threonine protein kinases (PIKKs) are required for DNA damage-induced phosphorylation of the 32 kDa subunit of replication protein A at threonine 21', *Nucleic Acids Res*, 32(3), pp. 997-1005.

Blunt, T., Gell, D., Fox, M., Taccioli, G.E., Lehmann, A.R., Jackson, S.P. and Jeggo, P.A. (1996) 'Identification of a nonsense mutation in the carboxyl-terminal region of DNA-dependent protein kinase catalytic subunit in the scid mouse', *Proc Natl Acad Sci U S A*, 93(19), pp. 10285-90.

Bohannon, R.A., Miller, D.G. and Diamond, H.D. (1963) 'Vincristine in the treatment of lymphomas and leukemias', *Cancer Res*, 23, pp. 613-21.

Bolderson, E., Richard, D.J., Zhou, B.B. and Khanna, K.K. (2009) 'Recent advances in cancer therapy targeting proteins involved in DNA double-strand break repair', *Clin Cancer Res*, 15(20), pp. 6314-20.

Borel, F., Lohez, O.D., Lacroix, F.B. and Margolis, R.L. (2002) 'Multiple centrosomes arise from tetraploidy checkpoint failure and mitotic centrosome clusters in p53 and RB pocket protein-compromised cells', *Proc Natl Acad Sci U S A*, 99(15), pp. 9819-24.

Bosma, G.C., Custer, R.P. and Bosma, M.J. (1983) 'A severe combined immunodeficiency mutation in the mouse', *Nature*, 301(5900), pp. 527-30.

Bostock, C.J., Prescott, D.M. and Kirkpatrick, J.B. (1971) 'An evaluation of the double thymidine block for synchronizing mammalian cells at the G1-S border', *Exp Cell Res*, 68(1), pp. 163-8.

Bottke, D., Koychev, D., Busse, A., Heufelder, K., Wiegel, T., Thiel, E., Hinkelbein, W. and Keilholz, U. (2008) 'Fractionated irradiation can induce functionally relevant multidrug resistance gene and protein expression in human tumor cell lines', *Radiat Res*, 170(1), pp. 41-8.

Bouquet, F., Ousset, M., Biard, D., Fallone, F., Dauvillier, S., Frit, P., Salles, B. and Muller, C. (2011) 'A DNA-dependent stress response involving DNA-PK occurs in hypoxic cells and contributes to cellular adaptation to hypoxia', *J Cell Sci*, 124(Pt 11), pp. 1943-51.

Brattain, M.G., Fine, W.D., Khaled, F.M., Thompson, J. and Brattain, D.E. (1981) 'Heterogeneity of malignant cells from a human colonic carcinoma', *Cancer Res*, 41(5), pp. 1751-6.

Broker, L.E., Huisman, C., Span, S.W., Rodriguez, J.A., Kruyt, F.A. and Giaccone, G. (2004) 'Cathepsin B mediates caspase-independent cell death induced by microtubule stabilizing agents in non-small cell lung cancer cells', *Cancer Res*, 64(1), pp. 27-30.

Burdak-Rothkamm, S., Rothkamm, K. and Prise, K.M. (2008) 'ATM acts downstream of ATR in the DNA damage response signaling of bystander cells', *Cancer Res*, 68(17), pp. 7059-65.

Burma, S., Chen, B.P., Murphy, M., Kurimasa, A. and Chen, D.J. (2001) 'ATM phosphorylates histone H2AX in response to DNA double-strand breaks', *J Biol Chem*, 276(45), pp. 42462-7.

Cancer Research UK (2014) *Cancer Stats: Key Facts*. Available at: http://publications.cancerresearchuk.org/downloads/Product/CS_KF_ALLCANCERS.pdf (Accessed: 13/05/2014).

Cano-Gauci, D.F. and Riordan, J.R. (1987) 'Action of calcium antagonists on multidrug resistant cells. Specific cytotoxicity independent of increased cancer drug accumulation', *Biochem Pharmacol*, 36(13), pp. 2115-23.

Chan, D.W., Gately, D.P., Urban, S., Galloway, A.M., Lees-Miller, S.P., Yen, T. and Allalunis-Turner, J. (1998) 'Lack of correlation between ATM protein expression and tumour cell radiosensitivity', *Int J Radiat Biol*, 74(2), pp. 217-24.

Chan, D.W., Son, S.C., Block, W., Ye, R., Khanna, K.K., Wold, M.S., Douglas, P., Goodarzi, A.A., Pelley, J., Taya, Y., Lavin, M.F. and Lees-Miller, S.P. (2000) 'Purification and characterization of ATM from human placenta. A manganese-dependent, wortmannin-sensitive serine/threonine protein kinase', *J Biol Chem*, 275(11), pp. 7803-10.

Chen, B.P., Chan, D.W., Kobayashi, J., Burma, S., Asaithamby, A., Morotomi-Yano, K., Botvinick, E., Qin, J. and Chen, D.J. (2005) 'Cell cycle dependence of DNA-dependent protein kinase phosphorylation in response to DNA double strand breaks', *J Biol Chem*, 280(15), pp. 14709-15.

Chen, B.P., Uematsu, N., Kobayashi, J., Lerenthal, Y., Krempler, A., Yajima, H., Lobrich, M., Shiloh, Y. and Chen, D.J. (2007) 'Ataxia telangiectasia mutated (ATM) is essential for DNA-PKcs phosphorylations at the Thr-2609 cluster upon DNA double strand break', *J Biol Chem*, 282(9), pp. 6582-7.

Chen, C.J., Chin, J.E., Ueda, K., Clark, D.P., Pastan, I., Gottesman, M.M. and Roninson, I.B. (1986) 'Internal duplication and homology with bacterial transport proteins in the mdr1 (P-glycoprotein) gene from multidrug-resistant human cells', *Cell*, 47(3), pp. 381-9.

Chico, I., Kang, M.H., Bergan, R., Abraham, J., Bakke, S., Meadows, B., Rutt, A., Robey, R., Choyke, P., Merino, M., Goldspiel, B., Smith, T., Steinberg, S., Figg, W.D., Fojo, T. and Bates, S. (2001) 'Phase I study of infusional paclitaxel in combination with the P-glycoprotein antagonist PSC 833', *J Clin Oncol*, 19(3), pp. 832-42.

Chin, C.F. and Yeong, F.M. (2010) 'Safeguarding entry into mitosis: the antephase checkpoint', *Mol Cell Biol*, 30(1), pp. 22-32.

Ciszewski, W.M., Tavecchio, M., Dastych, J. and Curtin, N.J. (2014) 'DNA-PK inhibition by NU7441 sensitizes breast cancer cells to ionizing radiation and doxorubicin', *Breast Cancer Res Treat*, 143(1), pp. 47-55.

Clapham, K.M., Rennison, T., Jones, G., Craven, F., Bardos, J., Golding, B.T., Griffin, R.J., Haggerty, K., Hardcastle, I.R., Thommes, P., Ting, A. and Cano, C. (2012) 'Potent

enantioselective inhibition of DNA-dependent protein kinase (DNA-PK) by atropisomeric chromenone derivatives', *Org Biomol Chem*, 10(33), pp. 6747-57.

Clarke, S.J. and Rivory, L.P. (1999) 'Clinical pharmacokinetics of docetaxel', *Clin Pharmacokinet*, 36(2), pp. 99-114.

Clinicaltrials.gov (2014) *clinicaltrials.gov*. Available at: https://clinicaltrials.gov/ct2/home (Accessed: 04/08/2014).

Constantinou, A., Tarsounas, M., Karow, J.K., Brosh, R.M., Bohr, V.A., Hickson, I.D. and West, S.C. (2000) 'Werner's syndrome protein (WRN) migrates Holliday junctions and co-localizes with RPA upon replication arrest', *EMBO Rep*, 1(1), pp. 80-4.

Convery, E., Shin, E.K., Ding, Q., Wang, W., Douglas, P., Davis, L.S., Nickoloff, J.A., Lees-Miller, S.P. and Meek, K. (2005) 'Inhibition of homologous recombination by variants of the catalytic subunit of the DNA-dependent protein kinase (DNA-PKcs)', *Proc Natl Acad Sci U S A*, 102(5), pp. 1345-50.

Cooper, S., Chen, K.Z. and Ravi, S. (2008) 'Thymidine block does not synchronize L1210 mouse leukaemic cells: implications for cell cycle control, cell cycle analysis and whole-culture synchronization', *Cell Prolif*, 41(1), pp. 156-67.

Cooper, S., Iyer, G., Tarquini, M. and Bissett, P. (2006) 'Nocodazole does not synchronize cells: implications for cell-cycle control and whole-culture synchronization', *Cell Tissue Res*, 324(2), pp. 237-42.

COSMIC (2014) *Catalogue of somatic mutations in cancer. Cell lines project*. Available at: http://cancer.sanger.ac.uk/cell_lines/cbrowse/all (Accessed: 07/05/2014).

Costantini, S., Woodbine, L., Andreoli, L., Jeggo, P.A. and Vindigni, A. (2007) 'Interaction of the Ku heterodimer with the DNA ligase IV/Xrcc4 complex and its regulation by DNA-PK', *DNA Repair (Amst)*, 6(6), pp. 712-22.

Cowell, I.G., Durkacz, B.W. and Tilby, M.J. (2005) 'Sensitization of breast carcinoma cells to ionizing radiation by small molecule inhibitors of DNA-dependent protein kinase and ataxia telangiectsia mutated', *Biochem Pharmacol*, 71(1-2), pp. 13-20.

Cremona, C.A. and Behrens, A. (2014) 'ATM signalling and cancer', *Oncogene*, 33(26), pp. 3351-60.

Crown, J., O'Leary, M. and Ooi, W.S. (2004) 'Docetaxel and paclitaxel in the treatment of breast cancer: a review of clinical experience', *Oncologist*, 9 Suppl 2, pp. 24-32.

Cutts, J.H., Beer, C.T. and Noble, R.L. (1960) 'Biological properties of Vincaleukoblastine, an alkaloid in Vinca rosea Linn, with reference to its antitumor action', *Cancer Res*, 20, pp. 1023-31.

Dahlberg, W.K., Azzam, E.I., Yu, Y. and Little, J.B. (1999) 'Response of human tumor cells of varying radiosensitivity and radiocurability to fractionated irradiation', *Cancer Res*, 59(20), pp. 5365-9.

Dai, C.L., Tiwari, A.K., Wu, C.P., Su, X.D., Wang, S.R., Liu, D.G., Ashby, C.R., Jr., Huang, Y., Robey, R.W., Liang, Y.J., Chen, L.M., Shi, C.J., Ambudkar, S.V., Chen, Z.S. and Fu, L.W. (2008) 'Lapatinib (Tykerb, GW572016) reverses multidrug resistance in cancer cells by inhibiting the activity of ATP-binding cassette subfamily B member 1 and G member 2', *Cancer Res*, 68(19), pp. 7905-14.

Danska, J.S., Holland, D.P., Mariathasan, S., Williams, K.M. and Guidos, C.J. (1996) 'Biochemical and genetic defects in the DNA-dependent protein kinase in murine scid lymphocytes', *Mol Cell Biol*, 16(10), pp. 5507-17.

Davies, H., Bignell, G.R., Cox, C., Stephens, P., Edkins, S., Clegg, S., Teague, J., Woffendin, H., Garnett, M.J., Bottomley, W., Davis, N., Dicks, E., Ewing, R., Floyd, Y., Gray, K., Hall, S., Hawes, R., Hughes, J., Kosmidou, V., Menzies, A., Mould, C., Parker, A., Stevens, C., Watt, S., Hooper, S., Wilson, R., Jayatilake, H., Gusterson, B.A., Cooper, C., Shipley, J., Hargrave, D., Pritchard-Jones, K., Maitland, N., Chenevix-Trench, G., Riggins, G.J., Bigner, D.D., Palmieri, G., Cossu, A., Flanagan, A., Nicholson, A., Ho, J.W., Leung, S.Y., Yuen, S.T., Weber, B.L., Seigler, H.F., Darrow, T.L., Paterson, H., Marais, R., Marshall, C.J., Wooster, R., Stratton, M.R. and Futreal, P.A. (2002) 'Mutations of the BRAF gene in human cancer', *Nature*, 417(6892), pp. 949-54.

de Grouw, E.P., Raaijmakers, M.H., Boezeman, J.B., van der Reijden, B.A., van de Locht, L.T., de Witte, T.J., Jansen, J.H. and Raymakers, R.A. (2006) 'Preferential expression of a high number of ATP binding cassette transporters in both normal and leukemic CD34+CD38- cells', *Leukemia*, 20(4), pp. 750-4.

de Laat, W.L., Jaspers, N.G. and Hoeijmakers, J.H. (1999) 'Molecular mechanism of nucleotide excision repair', *Genes Dev*, 13(7), pp. 768-85.

Dean, M., Rzhetsky, A. and Allikmets, R. (2001) 'The human ATP-binding cassette (ABC) transporter superfamily', *Genome Res*, 11(7), pp. 1156-66.

DeAngelis, L.M., Gnecco, C., Taylor, L. and Warrell, R.P., Jr. (1991) 'Evolution of neuropathy and myopathy during intensive vincristine/corticosteroid chemotherapy for non-Hodgkin's lymphoma', *Cancer*, 67(9), pp. 2241-6.

DeVita, V.T., Jr. and Chu, E. (2008) 'A history of cancer chemotherapy', *Cancer Res*, 68(21), pp. 8643-53.

Digweed, M. and Sperling, K. (2004) 'Nijmegen breakage syndrome: clinical manifestation of defective response to DNA double-strand breaks', *DNA Repair (Amst)*, 3(8-9), pp. 1207-17.

Dobbs, T.A., Tainer, J.A. and Lees-Miller, S.P. (2010) 'A structural model for regulation of NHEJ by DNA-PKcs autophosphorylation', *DNA Repair (Amst)*, 9(12), pp. 1307-14.

Dohse, M., Scharenberg, C., Shukla, S., Robey, R.W., Volkmann, T., Deeken, J.F., Brendel, C., Ambudkar, S.V., Neubauer, A. and Bates, S.E. (2010) 'Comparison of ATP-binding cassette transporter interactions with the tyrosine kinase inhibitors imatinib, nilotinib, and dasatinib', *Drug Metab Dispos*, 38(8), pp. 1371-80.

Doil, C., Mailand, N., Bekker-Jensen, S., Menard, P., Larsen, D.H., Pepperkok, R., Ellenberg, J., Panier, S., Durocher, D., Bartek, J., Lukas, J. and Lukas, C. (2009) 'RNF168 binds and amplifies ubiquitin conjugates on damaged chromosomes to allow accumulation of repair proteins', *Cell*, 136(3), pp. 435-46.

Douglas, P., Ye, R., Trinkle-Mulcahy, L., Neal, J.A., De Wever, V., Morrice, N.A., Meek, K. and Lees-Miller, S.P. (2014) 'Polo-like kinase 1 (PLK1) and protein phosphatase 6 (PP6) regulate DNA-dependent protein kinase catalytic subunit (DNA-PKcs) phosphorylation in mitosis', *Biosci Rep*, 34(3).

Durmus, S., Sparidans, R.W., van Esch, A., Wagenaar, E., Beijnen, J.H. and Schinkel, A.H. (2014) 'Breast Cancer Resistance Protein (BCRP/ABCG2) and P-glycoprotein (P-GP/ABCB1) Restrict Oral Availability and Brain Accumulation of the PARP Inhibitor Rucaparib (AG-014699)', *Pharm Res*.

Durmus, S., Sparidans, R.W., Wagenaar, E., Beijnen, J.H. and Schinkel, A.H. (2012) 'Oral availability and brain penetration of the B-RAFV600E inhibitor vemurafenib can be enhanced by the P-GLYCOprotein (ABCB1) and breast cancer resistance protein (ABCG2) inhibitor elacridar', *Mol Pharm*, 9(11), pp. 3236-45.

Dutertre, S., Descamps, S. and Prigent, C. (2002) 'On the role of aurora-A in centrosome function', *Oncogene*, 21(40), pp. 6175-83.

Dvorak, C.C. and Cowan, M.J. (2010) 'Radiosensitive severe combined immunodeficiency disease', *Immunol Allergy Clin North Am*, 30(1), pp. 125-42.

Edelman, M.J. and Shvartsbeyn, M. (2012) 'Epothilones in development for non--small-cell lung cancer: novel anti-tubulin agents with the potential to overcome taxane resistance', *Clin Lung Cancer*, 13(3), pp. 171-80.

Elie-Caille, C., Severin, F., Helenius, J., Howard, J., Muller, D.J. and Hyman, A.A. (2007) 'Straight GDP-tubulin protofilaments form in the presence of taxol', *Curr Biol*, 17(20), pp. 1765-70.

Elliott, S.L., Crawford, C., Mulligan, E., Summerfield, G., Newton, P., Wallis, J., Mainou-Fowler, T., Evans, P., Bedwell, C., Durkacz, B.W. and Willmore, E. (2011) 'Mitoxantrone in combination with an inhibitor of DNA-dependent protein kinase: a potential therapy for high risk B-cell chronic lymphocytic leukaemia', *Br J Haematol*, 152(1), pp. 61-71.

Erickson, H.P. and O'Brien, E.T. (1992) 'Microtubule dynamic instability and GTP hydrolysis', *Annu Rev Biophys Biomol Struct*, 21, pp. 145-66.

Eum, K.H., Ahn, S.K., Kang, H. and Lee, M. (2013) 'Differential inhibitory effects of two Raf-targeting drugs, sorafenib and PLX4720, on the growth of multidrug-resistant cells', *Mol Cell Biochem*, 372(1-2), pp. 65-74.

Evers, R., Kool, M., van Deemter, L., Janssen, H., Calafat, J., Oomen, L.C., Paulusma, C.C., Oude Elferink, R.P., Baas, F., Schinkel, A.H. and Borst, P. (1998) 'Drug export activity of the human canalicular multispecific organic anion transporter in polarized kidney MDCK cells expressing cMOAT (MRP2) cDNA', *J Clin Invest*, 101(7), pp. 1310-9.

Falck, J., Coates, J. and Jackson, S.P. (2005) 'Conserved modes of recruitment of ATM, ATR and DNA-PKcs to sites of DNA damage', *Nature*, 434(7033), pp. 605-11.

Fekairi, S., Scaglione, S., Chahwan, C., Taylor, E.R., Tissier, A., Coulon, S., Dong, M.Q., Ruse, C., Yates, J.R., 3rd, Russell, P., Fuchs, R.P., McGowan, C.H. and Gaillard, P.H. (2009) 'Human SLX4 is a Holliday junction resolvase subunit that binds multiple DNA repair/recombination endonucleases', *Cell*, 138(1), pp. 78-89.

Ferguson, B.J., Mansur, D.S., Peters, N.E., Ren, H. and Smith, G.L. (2012) 'DNA-PK is a DNA sensor for IRF-3-dependent innate immunity', *Elife*, 1, p. e00047.

Ferguson, D.O., Sekiguchi, J.M., Chang, S., Frank, K.M., Gao, Y., DePinho, R.A. and Alt, F.W. (2000) 'The nonhomologous end-joining pathway of DNA repair is required for genomic stability and the suppression of translocations', *Proc Natl Acad Sci U S A*, 97(12), pp. 6630-3.

Fisher Scientific (2014) *Anti-DNA-PKcs Ab-2, Clone: 25-4*. Available at: http://www.fishersci.com/ecomm/servlet/fsproductdetail_10652_1671351__-1_0 (Accessed: 26/07/2014).

Fitzgerald, D.P., Emerson, D.L., Qian, Y., Anwar, T., Liewehr, D.J., Steinberg, S.M., Silberman, S., Palmieri, D. and Steeg, P.S. (2012) 'TPI-287, a new taxane family

member, reduces the brain metastatic colonization of breast cancer cells', *Mol Cancer Ther*, 11(9), pp. 1959-67.

Fogh, J. and Trempe, G. (1975) *New human tumor cell lines*. New York: Plenum Publishing Corporation.

Fojo, A.T., Ueda, K., Slamon, D.J., Poplack, D.G., Gottesman, M.M. and Pastan, I. (1987) 'Expression of a multidrug-resistance gene in human tumors and tissues', *Proc Natl Acad Sci U S A*, 84(1), pp. 265-9.

Foley, E.A. and Kapoor, T.M. (2013) 'Microtubule attachment and spindle assembly checkpoint signalling at the kinetochore', *Nat Rev Mol Cell Biol*, 14(1), pp. 25-37.

Foley, G.E., Lazarus, H., Farber, S., Uzman, B.G., Boone, B.A. and McCarthy, R.E. (1965) 'Continuous Culture of Human Lymphoblasts from Peripheral Blood of a Child with Acute Leukemia', *Cancer*, 18, pp. 522-9.

Freireich, E.J., Bodey, G.P., McCredie, K.B., Hersh, E.M., Gehan, E.A., Hart, J., Gutterman, J.U., Rodriguez, V., Smith, T. and Hester, J.P. (1976) 'Developmental therapy in adult acute leukemia', *Arch Intern Med*, 136(12), pp. 1417-21.

Fu, Y.P., Yu, J.C., Cheng, T.C., Lou, M.A., Hsu, G.C., Wu, C.Y., Chen, S.T., Wu, H.S., Wu, P.E. and Shen, C.Y. (2003) 'Breast cancer risk associated with genotypic polymorphism of the nonhomologous end-joining genes: a multigenic study on cancer susceptibility', *Cancer Res*, 63(10), pp. 2440-6.

Galletti, E., Magnani, M., Renzulli, M.L. and Botta, M. (2007) 'Paclitaxel and docetaxel resistance: molecular mechanisms and development of new generation taxanes', *ChemMedChem*, 2(7), pp. 920-42.

Gan, P.P. and Kavallaris, M. (2008) 'Tubulin-targeted drug action: functional significance of class ii and class IVb beta-tubulin in vinca alkaloid sensitivity', *Cancer Res*, 68(23), pp. 9817-24.

Gandhi, A.K., Mendy, D., Parton, A., Wu, L., Kosek, J., Zhang, L.H., Capone, L., Lopez-Girona, A., Schafer, P.H. and Chopra, R. (2012) 'CC-122 Is a Novel Pleiotropic Pathway Modifier with Potent in Vitro Immunomodulatory and Anti-Angiogenic Properties and in Vivo Anti-Tumor Activity in Hematological Cancers', *54th ASH Annual Meeting and Exposition*. Atlanta, GA, Abstract number 2963.

Garcia-Rocha, M., Avila, J. and Lozano, J. (1997) 'The zeta isozyme of protein kinase C binds to tubulin through the pseudosubstrate domain', *Exp Cell Res*, 230(1), pp. 1-8.

Gately, D.P., Hittle, J.C., Chan, G.K. and Yen, T.J. (1998) 'Characterization of ATM expression, localization, and associated DNA-dependent protein kinase activity', *Mol Biol Cell*, 9(9), pp. 2361-74.

Genomics of Drug Sensitivity in Cancer (2014) *Genomics of Drug Sensitivity in Cancer*. Available at: http://www.cancerrxgene.org/ (Accessed: 21/09/2014).

Gewirtz, D.A. (2000) 'Growth arrest and cell death in the breast tumor cell in response to ionizing radiation and chemotherapeutic agents which induce DNA damage', *Breast Cancer Res Treat*, 62(3), pp. 223-35.

Gharbi, S.I., Zvelebil, M.J., Shuttleworth, S.J., Hancox, T., Saghir, N., Timms, J.F. and Waterfield, M.D. (2007) 'Exploring the specificity of the PI3K family inhibitor LY294002', *Biochem J*, 404(1), pp. 15-21.

Giannakakou, P., Sackett, D.L., Ward, Y., Webster, K.R., Blagosklonny, M.V. and Fojo, T. (2000) 'p53 is associated with cellular microtubules and is transported to the nucleus by dynein', *Nat Cell Biol*, 2(10), pp. 709-17.

Gilardini Montani, M.S., Prodosmo, A., Stagni, V., Merli, D., Monteonofrio, L., Gatti, V., Gentileschi, M.P., Barila, D. and Soddu, S. (2013) 'ATM-depletion in breast cancer cells confers sensitivity to PARP inhibition', *J Exp Clin Cancer Res*, 32, p. 95.

Giunta, S., Belotserkovskaya, R. and Jackson, S.P. (2010) 'DNA damage signaling in response to double-strand breaks during mitosis', *J Cell Biol*, 190(2), pp. 197-207.

Giunta, S. and Jackson, S.P. (2011) 'Give me a break, but not in mitosis: the mitotic DNA damage response marks DNA double-strand breaks with early signaling events', *Cell Cycle*, 10(8), pp. 1215-21.

Golding, S.E., Rosenberg, E., Valerie, N., Hussaini, I., Frigerio, M., Cockcroft, X.F., Chong, W.Y., Hummersone, M., Rigoreau, L., Menear, K.A., O'Connor, M.J., Povirk, L.F., van Meter, T. and Valerie, K. (2009) 'Improved ATM kinase inhibitor KU-60019 radiosensitizes glioma cells, compromises insulin, AKT and ERK prosurvival signaling, and inhibits migration and invasion', *Mol Cancer Ther*, 8(10), pp. 2894-902.

Goldstein, L.J., Galski, H., Fojo, A., Willingham, M., Lai, S.L., Gazdar, A., Pirker, R., Green, A., Crist, W., Brodeur, G.M. and et al. (1989) 'Expression of a multidrug resistance gene in human cancers', *J Natl Cancer Inst*, 81(2), pp. 116-24.

Goodwin, J.F. and Knudsen, K.E. (2014) 'Beyond DNA Repair: DNA-PK Function in Cancer', *Cancer Discov*.

Gottesman, M.M., Fojo, T. and Bates, S.E. (2002) 'Multidrug resistance in cancer: role of ATP-dependent transporters', *Nat Rev Cancer*, 2(1), pp. 48-58.

Gradishar, W.J., Tjulandin, S., Davidson, N., Shaw, H., Desai, N., Bhar, P., Hawkins, M. and O'Shaughnessy, J. (2005) 'Phase III trial of nanoparticle albumin-bound paclitaxel compared with polyethylated castor oil-based paclitaxel in women with breast cancer', *J Clin Oncol*, 23(31), pp. 7794-803.

Grawunder, U., Zimmer, D., Kulesza, P. and Lieber, M.R. (1998) 'Requirement for an interaction of XRCC4 with DNA ligase IV for wild-type V(D)J recombination and DNA double-strand break repair in vivo', *J Biol Chem*, 273(38), pp. 24708-14.

Griffin, R.J., Fontana, G., Golding, B.T., Guiard, S., Hardcastle, I.R., Leahy, J.J., Martin, N., Richardson, C., Rigoreau, L., Stockley, M. and Smith, G.C. (2005) 'Selective benzopyranone and pyrimido[2,1-a]isoquinolin-4-one inhibitors of DNA-dependent protein kinase: synthesis, structure-activity studies, and radiosensitization of a human tumor cell line in vitro', *J Med Chem*, 48(2), pp. 569-85.

Gu, J. and Lieber, M.R. (2008) 'Mechanistic flexibility as a conserved theme across 3 billion years of nonhomologous DNA end-joining', *Genes Dev*, 22(4), pp. 411-5.

Gu, J., Lu, H., Tippin, B., Shimazaki, N., Goodman, M.F. and Lieber, M.R. (2007a) 'XRCC4:DNA ligase IV can ligate incompatible DNA ends and can ligate across gaps', *EMBO J*, 26(4), pp. 1010-23.

Gu, J., Lu, H., Tsai, A.G., Schwarz, K. and Lieber, M.R. (2007b) 'Single-stranded DNA ligation and XLF-stimulated incompatible DNA end ligation by the XRCC4-DNA ligase IV complex: influence of terminal DNA sequence', *Nucleic Acids Res*, 35(17), pp. 5755-62.

Gu, Y., Seidl, K.J., Rathbun, G.A., Zhu, C., Manis, J.P., van der Stoep, N., Davidson, L., Cheng, H.L., Sekiguchi, J.M., Frank, K., Stanhope-Baker, P., Schlissel, M.S., Roth, D.B. and Alt, F.W. (1997) 'Growth retardation and leaky SCID phenotype of Ku70-deficient mice', *Immunity*, 7(5), pp. 653-65.

Guarini, A., Marinelli, M., Tavolaro, S., Bellacchio, E., Magliozzi, M., Chiaretti, S., De Propris, M.S., Peragine, N., Santangelo, S., Paoloni, F., Nanni, M., Del Giudice, I., Mauro, F.R., Torrente, I. and Foa, R. (2012) 'ATM gene alterations in chronic lymphocytic leukemia patients induce a distinct gene expression profile and predict disease progression', *Haematologica*, 97(1), pp. 47-55.

Guo, K., Shelat, A.A., Guy, R.K. and Kastan, M.B. (2014) 'Development of a cell-based, high-throughput screening assay for ATM kinase inhibitors', *J Biomol Screen*, 19(4), pp. 538-46.

Gupta, A.K., Cerniglia, G.J., Mick, R., Ahmed, M.S., Bakanauskas, V.J., Muschel, R.J. and McKenna, W.G. (2003) 'Radiation sensitization of human cancer cells in vivo by inhibiting the activity of PI3K using LY294002', *Int J Radiat Oncol Biol Phys*, 56(3), pp. 846-53.

Haber, M., Norris, M.D., Kavallaris, M., Bell, D.R., Davey, R.A., White, L. and Stewart, B.W. (1989) 'Atypical multidrug resistance in a therapy-induced drug-resistant

human leukemia cell line (LALW-2): resistance to Vinca alkaloids independent of P-glycoprotein', *Cancer Res*, 49(19), pp. 5281-7.

Hamel, E., Day, B.W., Miller, J.H., Jung, M.K., Northcote, P.T., Ghosh, A.K., Curran, D.P., Cushman, M., Nicolaou, K.C., Paterson, I. and Sorensen, E.J. (2006) 'Synergistic effects of peloruside A and laulimalide with taxoid site drugs, but not with each other, on tubulin assembly', *Mol Pharmacol*, 70(5), pp. 1555-64.

Hamilton, T.C., Young, R.C. and Ozols, R.F. (1984) 'Experimental model systems of ovarian cancer: applications to the design and evaluation of new treatment approaches', *Semin Oncol*, 11(3), pp. 285-98.

Hanahan, D. and Weinberg, R.A. (2000) 'The hallmarks of cancer', *Cell*, 100(1), pp. 57-70.

Hanahan, D. and Weinberg, R.A. (2011) 'Hallmarks of cancer: the next generation', *Cell*, 144(5), pp. 646-74.

Hardcastle, I.R., Cockcroft, X., Curtin, N.J., El-Murr, M.D., Leahy, J.J., Stockley, M., Golding, B.T., Rigoreau, L., Richardson, C., Smith, G.C. and Griffin, R.J. (2005) 'Discovery of potent chromen-4-one inhibitors of the DNA-dependent protein kinase (DNA-PK) using a small-molecule library approach', *J Med Chem*, 48(24), pp. 7829-46.

Hartley, K.O., Gell, D., Smith, G.C., Zhang, H., Divecha, N., Connelly, M.A., Admon, A., Lees-Miller, S.P., Anderson, C.W. and Jackson, S.P. (1995) 'DNA-dependent protein kinase catalytic subunit: a relative of phosphatidylinositol 3-kinase and the ataxia telangiectasia gene product', *Cell*, 82(5), pp. 849-56.

Harvie, R.M., Davey, M.W. and Davey, R.A. (1997) 'Increased MRP expression is associated with resistance to radiation, anthracyclines and etoposide in cells treated with fractionated gamma-radiation', *Int J Cancer*, 73(1), pp. 164-7.

Hasegawa, S., Abe, T., Naito, S., Kotoh, S., Kumazawa, J., Hipfner, D.R., Deeley, R.G., Cole, S.P. and Kuwano, M. (1995) 'Expression of multidrug resistance-associated protein (MRP), MDR1 and DNA topoisomerase II in human multidrug-resistant bladder cancer cell lines', *Br J Cancer*, 71(5), pp. 907-13.

Hayden, J.H., Bowser, S.S. and Rieder, C.L. (1990) 'Kinetochores capture astral microtubules during chromosome attachment to the mitotic spindle: direct visualization in live newt lung cells', *J Cell Biol*, 111(3), pp. 1039-45.

Hegedus, C., Ozvegy-Laczka, C., Apati, A., Magocsi, M., Nemet, K., Orfi, L., Keri, G., Katona, M., Takats, Z., Varadi, A., Szakacs, G. and Sarkadi, B. (2009) 'Interaction of nilotinib, dasatinib and bosutinib with ABCB1 and ABCG2: implications for altered

anti-cancer effects and pharmacological properties', *Br J Pharmacol*, 158(4), pp. 1153-64.

Hickson, I., Zhao, Y., Richardson, C.J., Green, S.J., Martin, N.M., Orr, A.I., Reaper, P.M., Jackson, S.P., Curtin, N.J. and Smith, G.C. (2004) 'Identification and characterization of a novel and specific inhibitor of the ataxia-telangiectasia mutated kinase ATM', *Cancer Res*, 64(24), pp. 9152-9.

Hill, C.R., Jamieson, D., Thomas, H.D., Brown, C.D., Boddy, A.V. and Veal, G.J. (2013) 'Characterisation of the roles of ABCB1, ABCC1, ABCC2 and ABCG2 in the transport and pharmacokinetics of actinomycin D in vitro and in vivo', *Biochem Pharmacol*, 85(1), pp. 29-37.

Hinchcliffe, E.H. and Sluder, G. (2001) '"It takes two to tango": understanding how centrosome duplication is regulated throughout the cell cycle', *Genes Dev*, 15(10), pp. 1167-81.

Hirokawa, N., Noda, Y., Tanaka, Y. and Niwa, S. (2009) 'Kinesin superfamily motor proteins and intracellular transport', *Nat Rev Mol Cell Biol*, 10(10), pp. 682-96.

Hoeijmakers, J.H. (2001) 'Genome maintenance mechanisms for preventing cancer', *Nature*, 411(6835), pp. 366-74.

Holgersson, A., Erdal, H., Nilsson, A., Lewensohn, R. and Kanter, L. (2004) 'Expression of DNA-PKcs and Ku86, but not Ku70, differs between lymphoid malignancies', *Exp Mol Pathol*, 77(1), pp. 1-6.

Hoppe, B.S., Jensen, R.B. and Kirchgessner, C.U. (2000) 'Complementation of the radiosensitive M059J cell line', *Radiat Res*, 153(2), pp. 125-30.

Hosoi, Y., Watanabe, T., Nakagawa, K., Matsumoto, Y., Enomoto, A., Morita, A., Nagawa, H. and Suzuki, N. (2004) 'Up-regulation of DNA-dependent protein kinase activity and Sp1 in colorectal cancer', *Int J Oncol*, 25(2), pp. 461-8.

Hotte, S.J. and Saad, F. (2010) 'Current management of castrate-resistant prostate cancer', *Curr Oncol*, 17 Suppl 2, pp. S72-9.

Hoyt, M.A., Totis, L. and Roberts, B.T. (1991) 'S. cerevisiae genes required for cell cycle arrest in response to loss of microtubule function', *Cell*, 66(3), pp. 507-17.

Hsu, F.M., Zhang, S. and Chen, B.P. (2012) 'Role of DNA-dependent protein kinase catalytic subunit in cancer development and treatment', *Transl Cancer Res*, 1(1), pp. 22-34.

Hsu, L.C. and White, R.L. (1998) 'BRCA1 is associated with the centrosome during mitosis', *Proc Natl Acad Sci U S A*, 95(22), pp. 12983-8.

Huang, B., Shang, Z.F., Li, B., Wang, Y., Liu, X.D., Zhang, S.M., Guan, H., Rang, W.Q., Hu, J.A. and Zhou, P.K. (2014) 'DNA-PKcs associates with PLK1 and is involved in proper chromosome segregation and cytokinesis', *J Cell Biochem*, 115(6), pp. 1077-88.

Huszar, D., Theoclitou, M.E., Skolnik, J. and Herbst, R. (2009) 'Kinesin motor proteins as targets for cancer therapy', *Cancer Metastasis Rev*, 28(1-2), pp. 197-208.

Hwang, L.H., Lau, L.F., Smith, D.L., Mistrot, C.A., Hardwick, K.G., Hwang, E.S., Amon, A. and Murray, A.W. (1998) 'Budding yeast Cdc20: a target of the spindle checkpoint', *Science*, 279(5353), pp. 1041-4.

Ip, S.C., Rass, U., Blanco, M.G., Flynn, H.R., Skehel, J.M. and West, S.C. (2008) 'Identification of Holliday junction resolvases from humans and yeast', *Nature*, 456(7220), pp. 357-61.

Israels, T., Damen, C.W., Cole, M., van Geloven, N., Boddy, A.V., Caron, H.N., Beijnen, J.H., Molyneux, E.M. and Veal, G.J. (2010) 'Malnourished Malawian patients presenting with large Wilms tumours have a decreased vincristine clearance rate', *Eur J Cancer*, 46(10), pp. 1841-7.

Jain, R.K. (2012) 'Delivery of molecular and cellular medicine to solid tumors', *Adv Drug Deliv Rev*, 64(Suppl), pp. 353-365.

Jensen, R.B., Carreira, A. and Kowalczykowski, S.C. (2010) 'Purified human BRCA2 stimulates RAD51-mediated recombination', *Nature*, 467(7316), pp. 678-83.

Jhappan, C., Morse, H.C., 3rd, Fleischmann, R.D., Gottesman, M.M. and Merlino, G. (1997) 'DNA-PKcs: a T-cell tumour suppressor encoded at the mouse scid locus', *Nat Genet*, 17(4), pp. 483-6.

Jordan, M.A., Margolis, R.L., Himes, R.H. and Wilson, L. (1986) 'Identification of a distinct class of vinblastine binding sites on microtubules', *J Mol Biol*, 187(1), pp. 61-73.

Jordan, M.A., Thrower, D. and Wilson, L. (1991) 'Mechanism of inhibition of cell proliferation by Vinca alkaloids', *Cancer Res*, 51(8), pp. 2212-22.

Jordan, M.A., Wendell, K., Gardiner, S., Derry, W.B., Copp, H. and Wilson, L. (1996) 'Mitotic block induced in HeLa cells by low concentrations of paclitaxel (Taxol) results in abnormal mitotic exit and apoptotic cell death', *Cancer Res*, 56(4), pp. 816-25.

Jordan, M.A. and Wilson, L. (2004) 'Microtubules as a target for anticancer drugs', *Nat Rev Cancer*, 4(4), pp. 253-65.

Ju, J., Naura, A.S., Errami, Y., Zerfaoui, M., Kim, H., Kim, J.G., Abd Elmageed, Z.Y., Abdel-Mageed, A.B., Giardina, C., Beg, A.A., Smulson, M.E. and Boulares, A.H.

(2010) 'Phosphorylation of p50 NF-kappaB at a single serine residue by DNA-dependent protein kinase is critical for VCAM-1 expression upon TNF treatment', *J Biol Chem*, 285(52), pp. 41152-60.

Juliano, R.L. and Ling, V. (1976) 'A surface glycoprotein modulating drug permeability in Chinese hamster ovary cell mutants', *Biochim Biophys Acta*, 455(1), pp. 152-62.

Kajita, M., McClinic, K.N. and Wade, P.A. (2004) 'Aberrant expression of the transcription factors snail and slug alters the response to genotoxic stress', *Mol Cell Biol*, 24(17), pp. 7559-66.

Kane, R.C., Farrell, A.T., Saber, H., Tang, S., Williams, G., Jee, J.M., Liang, C., Booth, B., Chidambaram, N., Morse, D., Sridhara, R., Garvey, P., Justice, R. and Pazdur, R. (2006) 'Sorafenib for the treatment of advanced renal cell carcinoma', *Clin Cancer Res*, 12(24), pp. 7271-8.

Kanthou, C. and Tozer, G.M. (2007) 'Tumour targeting by microtubule-depolymerizing vascular disrupting agents', *Expert Opin Ther Targets*, 11(11), pp. 1443-57.

Kardon, J.R. and Vale, R.D. (2009) 'Regulators of the cytoplasmic dynein motor', *Nat Rev Mol Cell Biol*, 10(12), pp. 854-65.

Kashishian, A., Douangpanya, H., Clark, D., Schlachter, S.T., Eary, C.T., Schiro, J.G., Huang, H., Burgess, L.E., Kesicki, E.A. and Halbrook, J. (2003) 'DNA-dependent protein kinase inhibitors as drug candidates for the treatment of cancer', *Mol Cancer Ther*, 2(12), pp. 1257-64.

Kavallaris, M. (2010) 'Microtubules and resistance to tubulin-binding agents', *Nat Rev Cancer*, 10(3), pp. 194-204.

Kavallaris, M., Kuo, D.Y., Burkhart, C.A., Regl, D.L., Norris, M.D., Haber, M. and Horwitz, S.B. (1997) 'Taxol-resistant epithelial ovarian tumors are associated with altered expression of specific beta-tubulin isotypes', *J Clin Invest*, 100(5), pp. 1282-93.

Kim, S.H., Kim, D., Han, J.S., Jeong, C.S., Chung, B.S., Kang, C.D. and Li, G.C. (1999) 'Ku autoantigen affects the susceptibility to anticancer drugs', *Cancer Res*, 59(16), pp. 4012-7.

Kimiya, K., Naito, S., Soejima, T., Sakamoto, N., Kotoh, S., Kumazawa, J. and Tsuruo, T. (1992) 'Establishment and characterization of doxorubicin-resistant human bladder cancer cell line, KK47/ADM', *J Urol*, 148(2 Pt 1), pp. 441-5.

Kirchgessner, C.U., Patil, C.K., Evans, J.W., Cuomo, C.A., Fried, L.M., Carter, T., Oettinger, M.A. and Brown, J.M. (1995) 'DNA-dependent kinase (p350) as a candidate gene for the murine SCID defect', *Science*, 267(5201), pp. 1178-83.

Kishi, K., van Vugt, M.A., Okamoto, K., Hayashi, Y. and Yaffe, M.B. (2009) 'Functional dynamics of Polo-like kinase 1 at the centrosome', *Mol Cell Biol*, 29(11), pp. 3134-50.

Kitazaki, T., Oka, M., Nakamura, Y., Tsurutani, J., Doi, S., Yasunaga, M., Takemura, M., Yabuuchi, H., Soda, H., Kohno, S. (2005) 'Gefitinib, an EGFR tyrosine kinase inhibitor, directly inhibits the function of P-glycoprotein in multidrug resistant cancer cells', *Lung Cancer*, 49(3), pp. 337-43.

Ko, M.J., Murata, K., Hwang, D.S. and Parvin, J.D. (2006) 'Inhibition of BRCA1 in breast cell lines causes the centrosome duplication cycle to be disconnected from the cell cycle', *Oncogene*, 25(2), pp. 298-303.

Kohli, M., Rago, C., Lengauer, C., Kinzler, K.W. and Vogelstein, B. (2004) 'Facile methods for generating human somatic cell gene knockouts using recombinant adeno-associated viruses', *Nucleic Acids Res*, 32(1), p. e3.

Koike, M. (2002) 'Dimerization, translocation and localization of Ku70 and Ku80 proteins', *J Radiat Res*, 43(3), pp. 223-36.

Kolas, N.K., Chapman, J.R., Nakada, S., Ylanko, J., Chahwan, R., Sweeney, F.D., Panier, S., Mendez, M., Wildenhain, J., Thomson, T.M., Pelletier, L., Jackson, S.P. and Durocher, D. (2007) 'Orchestration of the DNA-damage response by the RNF8 ubiquitin ligase', *Science*, 318(5856), pp. 1637-40.

Komlodi-Pasztor, E., Sackett, D., Wilkerson, J. and Fojo, T. (2011) 'Mitosis is not a key target of microtubule agents in patient tumors', *Nat Rev Clin Oncol*, 8(4), pp. 244-50.

Komlodi-Pasztor, E., Sackett, D.L. and Fojo, A.T. (2012) 'Inhibitors targeting mitosis: tales of how great drugs against a promising target were brought down by a flawed rationale', *Clin Cancer Res*, 18(1), pp. 51-63.

Kong, D., Yaguchi, S. and Yamori, T. (2009) 'Effect of ZSTK474, a novel phosphatidylinositol 3-kinase inhibitor, on DNA-dependent protein kinase', *Biol Pharm Bull*, 32(2), pp. 297-300.

Korystov, Y.N., Shaposhnikova, V.V., Korystova, A.F., Emel'yanov, M.O. and Kublik, L.N. (2008) 'Modification of multidrug resistance of tumor cells by ionizing radiation', *Cancer Chemother Pharmacol*, 61(1), pp. 15-21.

Koukourakis, M.I., Giatromanolaki, A., Schiza, S., Kakolyris, S. and Georgoulias, V. (1999) 'Concurrent twice-a-week docetaxel and radiotherapy: a dose escalation trial with immunological toxicity evaluation', *Int J Radiat Oncol Biol Phys*, 43(1), pp. 107-14.

Kowalski, R.J., Giannakakou, P. and Hamel, E. (1997) 'Activities of the microtubule-stabilizing agents epothilones A and B with purified tubulin and in cells resistant to paclitaxel (Taxol(R))', *J Biol Chem*, 272(4), pp. 2534-41.

Kumar, K.S., Sonnemann, J., Hong le, T.T., Buurman, C., Adler, F., Maass, M., Volker, U. and Beck, J.F. (2007) 'Histone deacetylase inhibitors, but not vincristine, cooperate with radiotherapy to induce cell death in medulloblastoma', *Anticancer Res*, 27(1A), pp. 465-70.

Kurimasa, A., Kumano, S., Boubnov, N.V., Story, M.D., Tung, C.S., Peterson, S.R. and Chen, D.J. (1999) 'Requirement for the kinase activity of human DNA-dependent protein kinase catalytic subunit in DNA strand break rejoining', *Mol Cell Biol*, 19(5), pp. 3877-84.

Lang, L. (2008) 'FDA approves sorafenib for patients with inoperable liver cancer', *Gastroenterology*, 134(2), p. 379.

Leahy, J.J., Golding, B.T., Griffin, R.J., Hardcastle, I.R., Richardson, C., Rigoreau, L. and Smith, G.C. (2004) 'Identification of a highly potent and selective DNA-dependent protein kinase (DNA-PK) inhibitor (NU7441) by screening of chromenone libraries', *Bioorg Med Chem Lett*, 14(24), pp. 6083-7.

Lee, H.S., Choe, G., Park, K.U., Park do, J., Yang, H.K., Lee, B.L. and Kim, W.H. (2007) 'Altered expression of DNA-dependent protein kinase catalytic subunit (DNA-PKcs) during gastric carcinogenesis and its clinical implications on gastric cancer', *Int J Oncol*, 31(4), pp. 859-66.

Lee, H.S., Yang, H.K., Kim, W.H. and Choe, G. (2005a) 'Loss of DNA-dependent protein kinase catalytic subunit (DNA-PKcs) expression in gastric cancers', *Cancer Res Treat*, 37(2), pp. 98-102.

Lee, J.H. and Paull, T.T. (2005) 'ATM activation by DNA double-strand breaks through the Mre11-Rad50-Nbs1 complex', *Science*, 308(5721), pp. 551-4.

Lee, J.H. and Paull, T.T. (2007) 'Activation and regulation of ATM kinase activity in response to DNA double-strand breaks', *Oncogene*, 26(56), pp. 7741-8.

Lee, K.J., Lin, Y.F., Chou, H.Y., Yajima, H., Fattah, K.R., Lee, S.C. and Chen, B.P. (2011) 'Involvement of DNA-dependent protein kinase in normal cell cycle progression through mitosis', *J Biol Chem*, 286(14), pp. 12796-802.

Lee, P.C., Lee, H.J., Kakadiya, R., Sanjiv, K., Su, T.L. and Lee, T.C. (2013) 'Multidrug-resistant cells overexpressing P-glycoprotein are susceptible to DNA crosslinking agents due to attenuated Src/nuclear EGFR cascade-activated DNA repair activity', *Oncogene*, 32(9), pp. 1144-54.

Lee, S.W., Cho, K.J., Park, J.H., Kim, S.Y., Nam, S.Y., Lee, B.J., Kim, S.B., Choi, S.H., Kim, J.H., Ahn, S.D., Shin, S.S., Choi, E.K. and Yu, E. (2005b) 'Expressions of Ku70 and DNA-PKcs as prognostic indicators of local control in nasopharyngeal carcinoma', *Int J Radiat Oncol Biol Phys*, 62(5), pp. 1451-7.

Lees-Miller, S.P., Godbout, R., Chan, D.W., Weinfeld, M., Day, R.S., 3rd, Barron, G.M. and Allalunis-Turner, J. (1995) 'Absence of p350 subunit of DNA-activated protein kinase from a radiosensitive human cell line', *Science*, 267(5201), pp. 1183-5.

Legha, S.S., Ring, S., Papadopoulos, N., Raber, M. and Benjamin, R.S. (1990) 'A phase II trial of taxol in metastatic melanoma', *Cancer*, 65(11), pp. 2478-81.

Legrand, O., Simonin, G., Beauchamp-Nicoud, A., Zittoun, R. and Marie, J.P. (1999) 'Simultaneous activity of MRP1 and Pgp is correlated with in vitro resistance to daunorubicin and with in vivo resistance in adult acute myeloid leukemia', *Blood*, 94(3), pp. 1046-56.

Leith, C.P., Kopecky, K.J., Chen, I.M., Eijdems, L., Slovak, M.L., McConnell, T.S., Head, D.R., Weick, J., Grever, M.R., Appelbaum, F.R. and Willman, C.L. (1999) 'Frequency and clinical significance of the expression of the multidrug resistance proteins MDR1/P-glycoprotein, MRP1, and LRP in acute myeloid leukemia: a Southwest Oncology Group Study', *Blood*, 94(3), pp. 1086-99.

Leonard, G.D., Fojo, T. and Bates, S.E. (2003) 'The role of ABC transporters in clinical practice', *Oncologist*, 8(5), pp. 411-24.

Li, D.W., Yang, Q., Chen, J.T., Zhou, H., Liu, R.M. and Huang, X.T. (2005) 'Dynamic distribution of Ser-10 phosphorylated histone H3 in cytoplasm of MCF-7 and CHO cells during mitosis', *Cell Res*, 15(2), pp. 120-6.

Li, J., Han, Y.R., Plummer, M.R. and Herrup, K. (2009) 'Cytoplasmic ATM in neurons modulates synaptic function', *Curr Biol*, 19(24), pp. 2091-6.

Li, M., Lin, Y.F., Palchik, G., Matsunaga, S., Wang, D. and Chen, B.P. (2014) 'The catalytic subunit of DNA-dependent protein kinase is required for cellular resistance to oxidative stress independent of DNA double strand break repair', *Free Radic Biol Med*.

Li, R. and Murray, A.W. (1991) 'Feedback control of mitosis in budding yeast', *Cell*, 66(3), pp. 519-31.

Liang, B., Kong, D., Liu, Y., Liang, N., He, M., Ma, S. and Liu, X. (2012) 'Autophagy inhibition plays the synergetic killing roles with radiation in the multi-drug resistant SKVCR ovarian cancer cells', *Radiat Oncol*, 7, p. 213.

Liebmann, J., Cook, J.A., Fisher, J., Teague, D. and Mitchell, J.B. (1994) 'In vitro studies of Taxol as a radiation sensitizer in human tumor cells', *J Natl Cancer Inst*, 86(6), pp. 441-6.

Lindahl, T. and Wood, R.D. (1999) 'Quality control by DNA repair', *Science*, 286(5446), pp. 1897-905.

Lindon, C. and Pines, J. (2004) 'Ordered proteolysis in anaphase inactivates Plk1 to contribute to proper mitotic exit in human cells', *J Cell Biol*, 164(2), pp. 233-41.

Lindqvist, A., van Zon, W., Karlsson Rosenthal, C. and Wolthuis, R.M. (2007) 'Cyclin B1-Cdk1 activation continues after centrosome separation to control mitotic progression', *PLoS Biol*, 5(5), p. e123.

Lingle, W.L., Barrett, S.L., Negron, V.C., D'Assoro, A.B., Boeneman, K., Liu, W., Whitehead, C.M., Reynolds, C. and Salisbury, J.L. (2002) 'Centrosome amplification drives chromosomal instability in breast tumor development', *Proc Natl Acad Sci U S A*, 99(4), pp. 1978-83.

Liu, Y.M., Chen, H.L., Lee, H.Y. and Liou, J.P. (2014) 'Tubulin inhibitors: a patent review', *Expert Opin Ther Pat*, 24(1), pp. 69-88.

Livak, K.J. and Schmittgen, T.D. (2001) 'Analysis of relative gene expression data using real-time quantitative PCR and the 2(-Delta Delta C(T)) Method', *Methods*, 25(4), pp. 402-8.

Long, X.D., Yao, J.G., Huang, Y.Z., Huang, X.Y., Ban, F.Z., Yao, L.M. and Fan, L.D. (2011) 'DNA repair gene XRCC7 polymorphisms (rs#7003908 and rs#10109984) and hepatocellular carcinoma related to AFB1 exposure among Guangxi population, China', *Hepatol Res*, 41(11), pp. 1085-93.

Louvard, D. (1980) 'Apical membrane aminopeptidase appears at site of cell-cell contact in cultured kidney epithelial cells', *Proc Natl Acad Sci U S A*, 77(7), pp. 4132-6.

Lovejoy, C.A. and Cortez, D. (2009) 'Common mechanisms of PIKK regulation', *DNA Repair (Amst)*, 8(9), pp. 1004-8.

Luduena, R.F. (1993) 'Are tubulin isotypes functionally significant', *Mol Biol Cell*, 4(5), pp. 445-57.

Ma, Y., Schwarz, K. and Lieber, M.R. (2005) 'The Artemis:DNA-PKcs endonuclease cleaves DNA loops, flaps, and gaps', *DNA Repair (Amst)*, 4(7), pp. 845-51.

Mahaney, B.L., Meek, K. and Lees-Miller, S.P. (2009) 'Repair of ionizing radiation-induced DNA double-strand breaks by non-homologous end-joining', *Biochem J*, 417(3), pp. 639-50.

Mao, Z., Bozzella, M., Seluanov, A. and Gorbunova, V. (2008) 'Comparison of nonhomologous end joining and homologous recombination in human cells', *DNA Repair (Amst)*, 7(10), pp. 1765-71.

Martin, C., Walker, J., Rothnie, A. and Callaghan, R. (2003) 'The expression of P-glycoprotein does influence the distribution of novel fluorescent compounds in solid tumour models', *Br J Cancer*, 89(8), pp. 1581-9.

Mathe, G., Schwarzenberg, L., Pouillart, P., Oldham, R., Weiner, R., Jasmin, C., Rosenfeld, C., Hayat, M., Misset, J.L., Musset, M., Schneider, M., Amiel, J.L. and De Vassal, F. (1974) 'Two epipodophyllotoxin derivatives, VM 26 and VP 16213, in the treatment of leukemias, hematosarcomas, and lymphomas', *Cancer*, 34(4), pp. 985-92.

Matsui, Y., Nakayama, Y., Okamoto, M., Fukumoto, Y. and Yamaguchi, N. (2012) 'Enrichment of cell populations in metaphase, anaphase, and telophase by synchronization using nocodazole and blebbistatin: a novel method suitable for examining dynamic changes in proteins during mitotic progression', *Eur J Cell Biol*, 91(5), pp. 413-9.

Mauer, A.M., Cohen, E.E., Ma, P.C., Kozloff, M.F., Schwartzberg, L., Coates, A.I., Qian, J., Hagey, A.E. and Gordon, G.B. (2008) 'A phase II study of ABT-751 in patients with advanced non-small cell lung cancer', *J Thorac Oncol*, 3(6), pp. 631-6.

McBlane, J.F., van Gent, D.C., Ramsden, D.A., Romeo, C., Cuomo, C.A., Gellert, M. and Oettinger, M.A. (1995) 'Cleavage at a V(D)J recombination signal requires only RAG1 and RAG2 proteins and occurs in two steps', *Cell*, 83(3), pp. 387-95.

McCarroll, J.A., Gan, P.P., Liu, M. and Kavallaris, M. (2010) 'betaIII-tubulin is a multifunctional protein involved in drug sensitivity and tumorigenesis in non-small cell lung cancer', *Cancer Res*, 70(12), pp. 4995-5003.

McGuire, T.C. and Poppie, M.J. (1973) 'Hypogammaglobulinemia and thymic hypoplasia in horses: a primary combined immunodeficiency disorder', *Infect Immun*, 8(2), pp. 272-7.

McIlwraith, M.J., Vaisman, A., Liu, Y., Fanning, E., Woodgate, R. and West, S.C. (2005) 'Human DNA polymerase eta promotes DNA synthesis from strand invasion intermediates of homologous recombination', *Mol Cell*, 20(5), pp. 783-92.

McIlwraith, M.J., Van Dyck, E., Masson, J.Y., Stasiak, A.Z., Stasiak, A. and West, S.C. (2000) 'Reconstitution of the strand invasion step of double-strand break repair using human Rad51 Rad52 and RPA proteins', *J Mol Biol*, 304(2), pp. 151-64.

McKinnon, P.J. (2004) 'ATM and ataxia telangiectasia', *EMBO Rep*, 5(8), pp. 772-6.

McManus, K.J. and Hendzel, M.J. (2005) 'ATM-dependent DNA damage-independent mitotic phosphorylation of H2AX in normally growing mammalian cells', *Mol Biol Cell*, 16(10), pp. 5013-25.

Meek, K., Gupta, S., Ramsden, D.A. and Lees-Miller, S.P. (2004) 'The DNA-dependent protein kinase: the director at the end', *Immunol Rev*, 200, pp. 132-41.

Meek, K., Kienker, L., Dallas, C., Wang, W., Dark, M.J., Venta, P.J., Huie, M.L., Hirschhorn, R. and Bell, T. (2001) 'SCID in Jack Russell terriers: a new animal model of DNA-PKcs deficiency', *J Immunol*, 167(4), pp. 2142-50.

Meena, A.S., Sharma, A., Kumari, R., Mohammad, N., Singh, S.V. and Bhat, M.K. (2013) 'Inherent and acquired resistance to paclitaxel in hepatocellular carcinoma: molecular events involved', *PLoS One*, 8(4), p. e61524.

Meyn, M.S. (1995) 'Ataxia-telangiectasia and cellular responses to DNA damage', *Cancer Res*, 55(24), pp. 5991-6001.

Mi, Y.J., Liang, Y.J., Huang, H.B., Zhao, H.Y., Wu, C.P., Wang, F., Tao, L.Y., Zhang, C.Z., Dai, C.L., Tiwari, A.K., Ma, X.X., To, K.K., Ambudkar, S.V., Chen, Z.S. and Fu, L.W. (2010) 'Apatinib (YN968D1) reverses multidrug resistance by inhibiting the efflux function of multiple ATP-binding cassette transporters', *Cancer Res*, 70(20), pp. 7981-91.

Michieli, M., Damiani, D., Ermacora, A., Masolini, P., Raspadori, D., Visani, G., Scheper, R.J. and Baccarani, M. (1999) 'P-glycoprotein, lung resistance-related protein and multidrug resistance associated protein in de novo acute non-lymphocytic leukaemias: biological and clinical implications', *Br J Haematol*, 104(2), pp. 328-35.

Mickisch, G.H., Licht, T., Merlino, G.T., Gottesman, M.M. and Pastan, I. (1991) 'Chemotherapy and chemosensitization of transgenic mice which express the human multidrug resistance gene in bone marrow: efficacy, potency, and toxicity', *Cancer Res*, 51(19), pp. 5417-24.

Mielke, S., Sparreboom, A. and Mross, K. (2006) 'Peripheral neuropathy: a persisting challenge in paclitaxel-based regimes', *Eur J Cancer*, 42(1), pp. 24-30.

Milas, L., Hunter, N.R., Mason, K.A., Kurdoglu, B. and Peters, L.J. (1994) 'Enhancement of tumor radioresponse of a murine mammary carcinoma by paclitaxel', *Cancer Res*, 54(13), pp. 3506-10.

Miles, P.D., Treuner, K., Latronica, M., Olefsky, J.M. and Barlow, C. (2007) 'Impaired insulin secretion in a mouse model of ataxia telangiectasia', *Am J Physiol Endocrinol Metab*, 293(1), pp. E70-4.

Mimori, T., Hardin, J.A. and Steitz, J.A. (1986) 'Characterization of the DNA-binding protein antigen Ku recognized by autoantibodies from patients with rheumatic disorders', *J Biol Chem*, 261(5), pp. 2274-8.

Mirzoeva, O.K. and Petrini, J.H.J. (2001) 'DNA damage-dependent nuclear dynamics of the Mre11 complex (vol 21, pg 281, 2001)', *Molecular and Cellular Biology*, 21(5), pp. 1898-1898.

Mitchell, J.B., Choudhuri, R., Fabre, K., Sowers, A.L., Citrin, D., Zabludoff, S.D. and Cook, J.A. (2010) 'In vitro and in vivo radiation sensitization of human tumor cells by a novel checkpoint kinase inhibitor, AZD7762', *Clin Cancer Res*, 16(7), pp. 2076-84.

Mitchison, T. and Kirschner, M. (1984) 'Dynamic instability of microtubule growth', *Nature*, 312(5991), pp. 237-42.

Mitchison, T.J. (1989) 'Polewards microtubule flux in the mitotic spindle: evidence from photoactivation of fluorescence', *J Cell Biol*, 109(2), pp. 637-52.

Modok, S., Mellor, H.R. and Callaghan, R. (2006) 'Modulation of multidrug resistance efflux pump activity to overcome chemoresistance in cancer', *Curr Opin Pharmacol*, 6(4), pp. 350-4.

Morse, D.L., Gray, H., Payne, C.M. and Gillies, R.J. (2005) 'Docetaxel induces cell death through mitotic catastrophe in human breast cancer cells', *Mol Cancer Ther*, 4(10), pp. 1495-504.

Mostoslavsky, R. (2008) 'DNA repair, insulin signaling and sirtuins: at the crossroads between cancer and aging', *Front Biosci*, 13, pp. 6966-90.

Mould, E., Berry, P., Jamieson, D., Hill, C., Cano, C., Tan, N., Elliott, S., Durkacz, B., Newell, D. and Willmore, E. (2014) 'Identification of dual DNA-PK MDR1 inhibitors for the potentiation of cytotoxic drug activity', *Biochem Pharmacol*, 88(1), pp. 58-65.

Munafo, D.B. and Colombo, M.I. (2001) 'A novel assay to study autophagy: regulation of autophagosome vacuole size by amino acid deprivation', *J Cell Sci*, 114(Pt 20), pp. 3619-29.

Neal, J.A., Dang, V., Douglas, P., Wold, M.S., Lees-Miller, S.P. and Meek, K. (2011) 'Inhibition of homologous recombination by DNA-dependent protein kinase requires kinase activity, is titratable, and is modulated by autophosphorylation', *Mol Cell Biol*, 31(8), pp. 1719-33.

New, J.H., Sugiyama, T., Zaitseva, E. and Kowalczykowski, S.C. (1998) 'Rad52 protein stimulates DNA strand exchange by Rad51 and replication protein A', *Nature*, 391(6665), pp. 407-10.

Niero, A., Emiliani, E., Monti, G., Pironi, F., Turci, L., Valenti, A.M. and Marangolo, M. (1999) 'Paclitaxel and radiotherapy: sequence-dependent efficacy--a preclinical model', *Clin Cancer Res*, 5(8), pp. 2213-22.

Nimonkar, A.V., Ozsoy, A.Z., Genschel, J., Modrich, P. and Kowalczykowski, S.C. (2008) 'Human exonuclease 1 and BLM helicase interact to resect DNA and initiate DNA repair', *Proc Natl Acad Sci U S A*, 105(44), pp. 16906-11.

Nogales, E., Wolf, S.G., Khan, I.A., Luduena, R.F. and Downing, K.H. (1995) 'Structure of tubulin at 6.5 A and location of the taxol-binding site', *Nature*, 375(6530), pp. 424-7.

Noguchi, T., Shibata, T., Fumoto, S., Uchida, Y., Mueller, W. and Takeno, S. (2002) 'DNA-PKcs expression in esophageal cancer as a predictor for chemoradiation therapeutic sensitivity', *Ann Surg Oncol*, 9(10), pp. 1017-22.

Nussenzweig, A., Chen, C., da Costa Soares, V., Sanchez, M., Sokol, K., Nussenzweig, M.C. and Li, G.C. (1996) 'Requirement for Ku80 in growth and immunoglobulin V(D)J recombination', *Nature*, 382(6591), pp. 551-5.

Nutley, B.P., Smith, N.F., Hayes, A., Kelland, L.R., Brunton, L., Golding, B.T., Smith, G.C., Martin, N.M., Workman, P. and Raynaud, F.I. (2005) 'Preclinical pharmacokinetics and metabolism of a novel prototype DNA-PK inhibitor NU7026', *Br J Cancer*, 93(9), pp. 1011-8.

Oettinger, M.A., Schatz, D.G., Gorka, C. and Baltimore, D. (1990) 'RAG-1 and RAG-2, adjacent genes that synergistically activate V(D)J recombination', *Science*, 248(4962), pp. 1517-23.

Oricchio, E., Saladino, C., Iacovelli, S., Soddu, S. and Cundari, E. (2006) 'ATM is activated by default in mitosis, localizes at centrosomes and monitors mitotic spindle integrity', *Cell Cycle*, 5(1), pp. 88-92.

Orr-Weaver, T.L. and Weinberg, R.A. (1998) 'A checkpoint on the road to cancer', *Nature*, 392(6673), pp. 223-4.

Osmak, M., Miljanic, S. and Kapitanovic, S. (1994) 'Low doses of gamma-rays can induce the expression of mdr gene', *Mutat Res*, 324(1-2), pp. 35-41.

Ouyang, H., Nussenzweig, A., Kurimasa, A., Soares, V.C., Li, X., Cordon-Cardo, C., Li, W., Cheong, N., Nussenzweig, M., Iliakis, G., Chen, D.J. and Li, G.C. (1997) 'Ku70 is required for DNA repair but not for T cell antigen receptor gene recombination In vivo', *J Exp Med*, 186(6), pp. 921-9.

Palazzo, L., Della Monica, R., Visconti, R., Costanzo, V. and Grieco, D. (2014) 'ATM controls proper mitotic spindle structure', *Cell Cycle*, 13(7), pp. 1091-100.

Pallis, A.G., Syrigos, K., Kotsakis, A., Karachaliou, N., Polyzos, A., Chandrinos, V., Varthalitis, I., Christophyllakis, C., Ardavanis, A., Vamvakas, L., Vardakis, N., Saridaki, Z., Samonis, G., Giassas, S., Georgoulias, V. and Agelaki, S. (2011) 'Second-line paclitaxel/carboplatin versus vinorelbine/carboplatin in patients who have advanced non-small-cell lung cancer pretreated with non-platinum-based chemotherapy: a multicenter randomized phase II study', *Clin Lung Cancer*, 12(2), pp. 100-5.

Parker, A.L., Kavallaris, M. and McCarroll, J.A. (2014) 'Microtubules and their role in cellular stress in cancer', *Front Oncol*, 4, p. 153.

Paull, T.T., Rogakou, E.P., Yamazaki, V., Kirchgessner, C.U., Gellert, M. and Bonner, W.M. (2000) 'A critical role for histone H2AX in recruitment of repair factors to nuclear foci after DNA damage', *Curr Biol*, 10(15), pp. 886-95.

Petronczki, M., Lenart, P. and Peters, J.M. (2008) 'Polo on the Rise-from Mitotic Entry to Cytokinesis with Plk1', *Dev Cell*, 14(5), pp. 646-59.

Pihan, G.A., Purohit, A., Wallace, J., Knecht, H., Woda, B., Quesenberry, P. and Doxsey, S.J. (1998) 'Centrosome defects and genetic instability in malignant tumors', *Cancer Res*, 58(17), pp. 3974-85.

Pittman, S.M., Kavallaris, M. and Stewart, B.W. (1993) 'Karyotypic analysis of CCRF-CEM and drug-resistant cell lines with stable and unstable ploidy', *Cancer Genet Cytogenet*, 66(1), pp. 54-62.

Pizzo, P.A., Henderson, E.S. and Leventhal, B.G. (1976) 'Acute myelogenous leukemia in children: a preliminary report of combination chemotherapy', *J Pediatr*, 88(1), pp. 125-30.

Povirk, L.F. (2006) 'Biochemical mechanisms of chromosomal translocations resulting from DNA double-strand breaks', *DNA Repair (Amst)*, 5(9-10), pp. 1199-212.

Price, B.D. and Youmell, M.B. (1996) 'The phosphatidylinositol 3-kinase inhibitor wortmannin sensitizes murine fibroblasts and human tumor cells to radiation and blocks induction of p53 following DNA damage', *Cancer Res*, 56(2), pp. 246-50.

Pyun, B.J., Seo, H.R., Lee, H.J., Jin, Y.B., Kim, E.J., Kim, N.H., Kim, H.S., Nam, H.W., Yook, J.I. and Lee, Y.S. (2013) 'Mutual regulation between DNA-PKcs and Snail1 leads to increased genomic instability and aggressive tumor characteristics', *Cell Death Dis*, 4, p. e517.

Rainey, M.D., Charlton, M.E., Stanton, R.V. and Kastan, M.B. (2008) 'Transient inhibition of ATM kinase is sufficient to enhance cellular sensitivity to ionizing radiation', *Cancer Res*, 68(18), pp. 7466-74.

Ramachandra, M., Ambudkar, S.V., Chen, D., Hrycyna, C.A., Dey, S., Gottesman, M.M. and Pastan, I. (1998) 'Human P-glycoprotein exhibits reduced affinity for substrates during a catalytic transition state', *Biochemistry*, 37(14), pp. 5010-9.

Ravelli, R.B., Gigant, B., Curmi, P.A., Jourdain, I., Lachkar, S., Sobel, A. and Knossow, M. (2004) 'Insight into tubulin regulation from a complex with colchicine and a stathmin-like domain', *Nature*, 428(6979), pp. 198-202.

Regina, A., Demeule, M., Che, C., Lavallee, I., Poirier, J., Gabathuler, R., Beliveau, R. and Castaigne, J.P. (2008) 'Antitumour activity of ANG1005, a conjugate between paclitaxel and the new brain delivery vector Angiopep-2', *Br J Pharmacol*, 155(2), pp. 185-97.

Reiman, A., Srinivasan, V., Barone, G., Last, J.I., Wootton, L.L., Davies, E.G., Verhagen, M.M., Willemsen, M.A., Weemaes, C.M., Byrd, P.J., Izatt, L., Easton, D.F., Thompson, D.J. and Taylor, A.M. (2011) 'Lymphoid tumours and breast cancer in ataxia telangiectasia; substantial protective effect of residual ATM kinase activity against childhood tumours', *Br J Cancer*, 105(4), pp. 586-91.

Reini, K., Uitto, L., Perera, D., Moens, P.B., Freire, R. and Syvaoja, J.E. (2004) 'TopBP1 localises to centrosomes in mitosis and to chromosome cores in meiosis', *Chromosoma*, 112(7), pp. 323-30.

Rendic, S. and Guengerich, F.P. (2012) 'Summary of information on the effects of ionizing and non-ionizing radiation on cytochrome P450 and other drug metabolizing enzymes and transporters', *Curr Drug Metab*, 13(6), pp. 787-814.

Renwick, A., Thompson, D., Seal, S., Kelly, P., Chagtai, T., Ahmed, M., North, B., Jayatilake, H., Barfoot, R., Spanova, K., McGuffog, L., Evans, D.G., Eccles, D., Breast Cancer Susceptibility, C., Easton, D.F., Stratton, M.R. and Rahman, N. (2006) 'ATM mutations that cause ataxia-telangiectasia are breast cancer susceptibility alleles', *Nat Genet*, 38(8), pp. 873-5.

Rieder, C.L. and Cole, R.W. (1998) 'Entry into mitosis in vertebrate somatic cells is guarded by a chromosome damage checkpoint that reverses the cell cycle when triggered during early but not late prophase', *J Cell Biol*, 142(4), pp. 1013-22.

Risinger, A.L., Giles, F.J. and Mooberry, S.L. (2009) 'Microtubule dynamics as a target in oncology', *Cancer Treat Rev*, 35(3), pp. 255-61.

Risinger, A.L., Jackson, E.M., Polin, L.A., Helms, G.L., LeBoeuf, D.A., Joe, P.A., Hopper-Borge, E., Luduena, R.F., Kruh, G.D. and Mooberry, S.L. (2008) 'The taccalonolides: microtubule stabilizers that circumvent clinically relevant taxane resistance mechanisms', *Cancer Res*, 68(21), pp. 8881-8.

Robert, F., Harper, K., Ackerman, J. and Gupta, S. (2010) 'A phase I study of larotaxel (XRP9881) administered in combination with carboplatin in chemotherapy-naive patients with stage IIIB or stage IV non-small cell lung cancer', *Cancer Chemother Pharmacol*, 65(2), pp. 227-34.

Rogakou, E.P., Pilch, D.R., Orr, A.H., Ivanova, V.S. and Bonner, W.M. (1998) 'DNA double-stranded breaks induce histone H2AX phosphorylation on serine 139', *J Biol Chem*, 273(10), pp. 5858-68.

Roth, D.M., Moseley, G.W., Glover, D., Pouton, C.W. and Jans, D.A. (2007) 'A microtubule-facilitated nuclear import pathway for cancer regulatory proteins', *Traffic*, 8(6), pp. 673-86.

Rottenberg, S., Nygren, A.O., Pajic, M., van Leeuwen, F.W., van der Heijden, I., van de Wetering, K., Liu, X., de Visser, K.E., Gilhuijs, K.G., van Tellingen, O., Schouten, J.P., Jonkers, J. and Borst, P. (2007) 'Selective induction of chemotherapy resistance of mammary tumors in a conditional mouse model for hereditary breast cancer', *Proc Natl Acad Sci U S A*, 104(29), pp. 12117-22.

Ruis, B.L., Fattah, K.R. and Hendrickson, E.A. (2008) 'The catalytic subunit of DNA-dependent protein kinase regulates proliferation, telomere length, and genomic stability in human somatic cells', *Mol Cell Biol*, 28(20), pp. 6182-95.

Ryu, J.S., Um, J.H., Kang, C.D., Bae, J.H., Kim, D.U., Lee, Y.J., Kim, D.W., Chung, B.S. and Kim, S.H. (2004) 'Fractionated irradiation leads to restoration of drug sensitivity in MDR cells that correlates with down-regulation of P-gp and DNA-dependent protein kinase activity', *Radiat Res*, 162(5), pp. 527-35.

Sahenk, Z., Barohn, R., New, P. and Mendell, J.R. (1994) 'Taxol neuropathy. Electrodiagnostic and sural nerve biopsy findings', *Arch Neurol*, 51(7), pp. 726-9.

Salimi, M., Mozdarani, H. and Majidzadeh, K. (2012) 'Expression pattern of ATM and cyclin D1 in ductal carcinoma, normal adjacent and normal breast tissues of Iranian breast cancer patients', *Med Oncol*, 29(3), pp. 1502-9.

Sampson, J.H., Carter, J.H., Jr., Friedman, A.H. and Seigler, H.F. (1998) 'Demographics, prognosis, and therapy in 702 patients with brain metastases from malignant melanoma', *J Neurosurg*, 88(1), pp. 11-20.

San Filippo, J., Sung, P. and Klein, H. (2008) 'Mechanism of eukaryotic homologous recombination', *Annu Rev Biochem*, 77, pp. 229-57.

Sanchez, A.M., Barrett, J.T. and Schoenlein, P.V. (1998) 'Fractionated ionizing radiation accelerates loss of amplified MDR1 genes harbored by extrachromosomal DNA in tumor cells', *Cancer Res*, 58(17), pp. 3845-54.

Sarkaria, J.N., Busby, E.C., Tibbetts, R.S., Roos, P., Taya, Y., Karnitz, L.M. and Abraham, R.T. (1999) 'Inhibition of ATM and ATR kinase activities by the radiosensitizing agent, caffeine', *Cancer Res*, 59(17), pp. 4375-82.

Sartori, A.A., Lukas, C., Coates, J., Mistrik, M., Fu, S., Bartek, J., Baer, R., Lukas, J. and Jackson, S.P. (2007) 'Human CtIP promotes DNA end resection', *Nature*, 450(7169), pp. 509-14.

Sasai, K., Katayama, H., Stenoien, D.L., Fujii, S., Honda, R., Kimura, M., Okano, Y., Tatsuka, M., Suzuki, F., Nigg, E.A., Earnshaw, W.C., Brinkley, W.R. and Sen, S. (2004) 'Aurora-C kinase is a novel chromosomal passenger protein that can complement Aurora-B kinase function in mitotic cells', *Cell Motil Cytoskeleton*, 59(4), pp. 249-63.

Sauna, Z.E. and Ambudkar, S.V. (2000) 'Evidence for a requirement for ATP hydrolysis at two distinct steps during a single turnover of the catalytic cycle of human P-glycoprotein', *Proc Natl Acad Sci U S A*, 97(6), pp. 2515-20.

Savitsky, K., Bar-Shira, A., Gilad, S., Rotman, G., Ziv, Y., Vanagaite, L., Tagle, D.A., Smith, S., Uziel, T., Sfez, S., Ashkenazi, M., Pecker, I., Frydman, M., Harnik, R., Patanjali, S.R., Simmons, A., Clines, G.A., Sartiel, A., Gatti, R.A., Chessa, L., Sanal, O., Lavin, M.F., Jaspers, N.G., Taylor, A.M., Arlett, C.F., Miki, T., Weissman, S.M., Lovett, M., Collins, F.S. and Shiloh, Y. (1995) 'A single ataxia telangiectasia gene with a product similar to PI-3 kinase', *Science*, 268(5218), pp. 1749-53.

Sen, R., Natarajan, K., Bhullar, J., Shukla, S., Fang, H.B., Cai, L., Chen, Z.S., Ambudkar, S.V. and Baer, M.R. (2012) 'The novel BCR-ABL and FLT3 inhibitor ponatinib is a potent inhibitor of the MDR-associated ATP-binding cassette transporter ABCG2', *Mol Cancer Ther*, 11(9), pp. 2033-44.

Shaheen, F.S., Znojek, P., Fisher, A., Webster, M., Plummer, R., Gaughan, L., Smith, G.C., Leung, H.Y., Curtin, N.J. and Robson, C.N. (2011) 'Targeting the DNA double strand break repair machinery in prostate cancer', *PLoS One*, 6(5), p. e20311.

Shang, Z., Yu, L., Lin, Y.F., Matsunaga, S., Shen, C.Y. and Chen, B.P. (2014) 'DNA-PKcs activates the Chk2-Brca1 pathway during mitosis to ensure chromosomal stability', *Oncogenesis*, 3, p. e85.

Shang, Z.F., Huang, B., Xu, Q.Z., Zhang, S.M., Fan, R., Liu, X.D., Wang, Y. and Zhou, P.K. (2010) 'Inactivation of DNA-dependent protein kinase leads to spindle disruption and mitotic catastrophe with attenuated checkpoint protein 2 Phosphorylation in response to DNA damage', *Cancer Res*, 70(9), pp. 3657-66.

Shareef, M.M., Brown, B., Shajahan, S., Sathishkumar, S., Arnold, S.M., Mohiuddin, M., Ahmed, M.M. and Spring, P.M. (2008) 'Lack of P-glycoprotein expression by low-

dose fractionated radiation results from loss of nuclear factor-kappaB and NF-Y activation in oral carcinoma cells', *Mol Cancer Res*, 6(1), pp. 89-98.

Sharpless, N.E., Ferguson, D.O., O'Hagan, R.C., Castrillon, D.H., Lee, C., Farazi, P.A., Alson, S., Fleming, J., Morton, C.C., Frank, K., Chin, L., Alt, F.W. and DePinho, R.A. (2001) 'Impaired nonhomologous end-joining provokes soft tissue sarcomas harboring chromosomal translocations, amplifications, and deletions', *Mol Cell*, 8(6), pp. 1187-96.

Shelby, R.D., Hahn, K.M. and Sullivan, K.F. (1996) 'Dynamic elastic behavior of alpha-satellite DNA domains visualized in situ in living human cells', *J Cell Biol*, 135(3), pp. 545-57.

Shen, K.C., Heng, H., Wang, Y., Lu, S., Liu, G., Deng, C.X., Brooks, S.C. and Wang, Y.A. (2005) 'ATM and p21 cooperate to suppress aneuploidy and subsequent tumor development', *Cancer Res*, 65(19), pp. 8747-53.

Shi, Z., Peng, X.X., Kim, I.W., Shukla, S., Si, Q.S., Robey, R.W., Bates, S.E., Shen, T., Ashby, C.R., Jr., Fu, L.W., Ambudkar, S.V. and Chen, Z.S. (2007) 'Erlotinib (Tarceva, OSI-774) antagonizes ATP-binding cassette subfamily B member 1 and ATP-binding cassette subfamily G member 2-mediated drug resistance', *Cancer Res*, 67(22), pp. 11012-20.

Shi, Z., Tiwari, A.K., Shukla, S., Robey, R.W., Singh, S., Kim, I.W., Bates, S.E., Peng, X., Abraham, I., Ambudkar, S.V., Talele, T.T., Fu, L.W. and Chen, Z.S. (2011) 'Sildenafil reverses ABCB1- and ABCG2-mediated chemotherapeutic drug resistance', *Cancer Res*, 71(8), pp. 3029-41.

Shigeta, T., Takagi, M., Delia, D., Chessa, L., Iwata, S., Kanke, Y., Asada, M., Eguchi, M. and Mizutani, S. (1999) 'Defective control of apoptosis and mitotic spindle checkpoint in heterozygous carriers of ATM mutations', *Cancer Res*, 59(11), pp. 2602-7.

Shiloh, Y. (2003) 'ATM and related protein kinases: safeguarding genome integrity', *Nat Rev Cancer*, 3(3), pp. 155-68.

Shinohara, E.T., Geng, L., Tan, J., Chen, H., Shir, Y., Edwards, E., Halbrook, J., Kesicki, E.A., Kashishian, A. and Hallahan, D.E. (2005) 'DNA-dependent protein kinase is a molecular target for the development of noncytotoxic radiation-sensitizing drugs', *Cancer Res*, 65(12), pp. 4987-92.

Shintani, S., Mihara, M., Li, C., Nakahara, Y., Hino, S., Nakashiro, K. and Hamakawa, H. (2003) 'Up-regulation of DNA-dependent protein kinase correlates with radiation resistance in oral squamous cell carcinoma', *Cancer Sci*, 94(10), pp. 894-900.

Shirakawa, T., Sasaki, R., Gardner, T.A., Kao, C., Zhang, Z.J., Sugimura, K., Matsuo, M., Kamidono, S. and Gotoh, A. (2001) 'Drug-resistant human bladder-cancer cells are more sensitive to adenovirus-mediated wild-type p53 gene therapy compared to drug-sensitive cells', *Int J Cancer*, 94(2), pp. 282-9.

Sikic, B.I., Fisher, G.A., Lum, B.L., Halsey, J., Beketic-Oreskovic, L. and Chen, G. (1997) 'Modulation and prevention of multidrug resistance by inhibitors of P-glycoprotein', *Cancer Chemother Pharmacol*, 40 Suppl, pp. S13-9.

Singer, W.D., Jordan, M.A., Wilson, L. and Himes, R.H. (1989) 'Binding of vinblastine to stabilized microtubules', *Mol Pharmacol*, 36(3), pp. 366-70.

Sirzen, F., Nilsson, A., Zhivotovsky, B. and Lewensohn, R. (1999) 'DNA-dependent protein kinase content and activity in lung carcinoma cell lines: correlation with intrinsic radiosensitivity', *Eur J Cancer*, 35(1), pp. 111-6.

Skowronska, A., Parker, A., Ahmed, G., Oldreive, C., Davis, Z., Richards, S., Dyer, M., Matutes, E., Gonzalez, D., Taylor, A.M., Moss, P., Thomas, P., Oscier, D. and Stankovic, T. (2012) 'Biallelic ATM inactivation significantly reduces survival in patients treated on the United Kingdom Leukemia Research Fund Chronic Lymphocytic Leukemia 4 trial', *J Clin Oncol*, 30(36), pp. 4524-32.

Sluder, G., Thompson, E.A., Miller, F.J., Hayes, J. and Rieder, C.L. (1997) 'The checkpoint control for anaphase onset does not monitor excess numbers of spindle poles or bipolar spindle symmetry', *J Cell Sci*, 110 (Pt 4), pp. 421-9.

Soderlund Leifler, K., Queseth, S., Fornander, T. and Askmalm, M.S. (2010) 'Low expression of Ku70/80, but high expression of DNA-PKcs, predict good response to radiotherapy in early breast cancer', *Int J Oncol*, 37(6), pp. 1547-54.

Someya, M., Sakata, K., Matsumoto, Y., Yamamoto, H., Monobe, M., Ikeda, H., Ando, K., Hosoi, Y., Suzuki, N. and Hareyama, M. (2006) 'The association of DNA-dependent protein kinase activity with chromosomal instability and risk of cancer', *Carcinogenesis*, 27(1), pp. 117-22.

Someya, M., Sakata, K.I., Matsumoto, Y., Kamdar, R.P., Kai, M., Toyota, M. and Hareyama, M. (2011) 'The association of DNA-dependent protein kinase activity of peripheral blood lymphocytes with prognosis of cancer', *Br J Cancer*, 104(11), pp. 1724-9.

Soulas-Sprauel, P., Le Guyader, G., Rivera-Munoz, P., Abramowski, V., Olivier-Martin, C., Goujet-Zalc, C., Charneau, P. and de Villartay, J.P. (2007) 'Role for DNA repair factor XRCC4 in immunoglobulin class switch recombination', *J Exp Med*, 204(7), pp. 1717-27.

Stanton, R.A., Gernert, K.M., Nettles, J.H. and Aneja, R. (2011) 'Drugs that target dynamic microtubules: a new molecular perspective', *Med Res Rev*, 31(3), pp. 443-81.

Stolarczyk, E.I., Reiling, C.J. and Paumi, C.M. (2011) 'Regulation of ABC transporter function via phosphorylation by protein kinases', *Curr Pharm Biotechnol*, 12(4), pp. 621-35.

Stracker, T.H. and Petrini, J.H. (2011) 'The MRE11 complex: starting from the ends', *Nat Rev Mol Cell Biol*, 12(2), pp. 90-103.

Strebhardt, K. and Ullrich, A. (2008) 'Paul Ehrlich's magic bullet concept: 100 years of progress', *Nat Rev Cancer*, 8(6), pp. 473-80.

Stucki, M., Clapperton, J.A., Mohammad, D., Yaffe, M.B., Smerdon, S.J. and Jackson, S.P. (2005) 'MDC1 directly binds phosphorylated histone H2AX to regulate cellular responses to DNA double-strand breaks', *Cell*, 123(7), pp. 1213-26.

Sullivan, K.F. and Cleveland, D.W. (1986) 'Identification of conserved isotype-defining variable region sequences for four vertebrate beta tubulin polypeptide classes', *Proc Natl Acad Sci U S A*, 83(12), pp. 4327-31.

Svendsen, J.M., Smogorzewska, A., Sowa, M.E., O'Connell, B.C., Gygi, S.P., Elledge, S.J. and Harper, J.W. (2009) 'Mammalian BTBD12/SLX4 assembles a Holliday junction resolvase and is required for DNA repair', *Cell*, 138(1), pp. 63-77.

Swain, S.M. and Arezzo, J.C. (2008) 'Neuropathy associated with microtubule inhibitors: diagnosis, incidence, and management', *Clin Adv Hematol Oncol*, 6(6), pp. 455-67.

Szakacs, G., Paterson, J.K., Ludwig, J.A., Booth-Genthe, C. and Gottesman, M.M. (2006) 'Targeting multidrug resistance in cancer', *Nat Rev Drug Discov*, 5(3), pp. 219-34.

Takagi, M., Delia, D., Chessa, L., Iwata, S., Shigeta, T., Kanke, Y., Goi, K., Asada, M., Eguchi, M., Kodama, C. and Mizutani, S. (1998) 'Defective control of apoptosis, radiosensitivity, and spindle checkpoint in ataxia telangiectasia', *Cancer Res*, 58(21), pp. 4923-9.

Takaki, T., Trenz, K., Costanzo, V. and Petronczki, M. (2008) 'Polo-like kinase 1 reaches beyond mitosis--cytokinesis, DNA damage response, and development', *Curr Opin Cell Biol*, 20(6), pp. 650-60.

Tavecchio, M., Munck, J.M., Cano, C., Newell, D.R. and Curtin, N.J. (2012) 'Further characterisation of the cellular activity of the DNA-PK inhibitor, NU7441, reveals potential cross-talk with homologous recombination', *Cancer Chemother Pharmacol*, 69(1), pp. 155-64.

Taya, T., Kobayashi, T., Tsukahara, K., Uchibayashi, T., Naito, K., Hisazumi, H. and Kuroda, K. (1977) '[In vitro culture of malignant tumor tissues from the human urinary tract (author's transl)]', *Nihon Hinyokika Gakkai Zasshi*, 68(11), pp. 1003-10.

Terasima, T. and Tolmach, L.J. (1963) 'Variations in several responses of HeLa cells to x-irradiation during the division cycle', *Biophys J*, 3, pp. 11-33.

Thompson, D., Duedal, S., Kirner, J., McGuffog, L., Last, J., Reiman, A., Byrd, P., Taylor, M. and Easton, D.F. (2005) 'Cancer risks and mortality in heterozygous ATM mutation carriers', *J Natl Cancer Inst*, 97(11), pp. 813-22.

Thornberry, N.A., Rano, T.A., Peterson, E.P., Rasper, D.M., Timkey, T., Garcia-Calvo, M., Houtzager, V.M., Nordstrom, P.A., Roy, S., Vaillancourt, J.P., Chapman, K.T. and Nicholson, D.W. (1997) 'A combinatorial approach defines specificities of members of the caspase family and granzyme B. Functional relationships established for key mediators of apoptosis', *J Biol Chem*, 272(29), pp. 17907-11.

Tichy, A., Durisova, K., Salovska, B., Pejchal, J., Zarybnicka, L., Vavrova, J., Dye, N.A. and Sinkorova, Z. (2014) 'Radio-sensitization of human leukaemic MOLT-4 cells by DNA-dependent protein kinase inhibitor, NU7441', *Radiat Environ Biophys*, 53(1), pp. 83-92.

Tonegawa, S. (1983) 'Somatic generation of antibody diversity', *Nature*, 302(5909), pp. 575-81.

Toso, R.J., Jordan, M.A., Farrell, K.W., Matsumoto, B. and Wilson, L. (1993) 'Kinetic stabilization of microtubule dynamic instability in vitro by vinblastine', *Biochemistry*, 32(5), pp. 1285-93.

Toulany, M., Kasten-Pisula, U., Brammer, I., Wang, S., Chen, J., Dittmann, K., Baumann, M., Dikomey, E. and Rodemann, H.P. (2006) 'Blockage of epidermal growth factor receptor-phosphatidylinositol 3-kinase-AKT signaling increases radiosensitivity of K-RAS mutated human tumor cells in vitro by affecting DNA repair', *Clin Cancer Res*, 12(13), pp. 4119-26.

Tritarelli, A., Oricchio, E., Ciciarello, M., Mangiacasale, R., Palena, A., Lavia, P., Soddu, S. and Cundari, E. (2004) 'p53 localization at centrosomes during mitosis and postmitotic checkpoint are ATM-dependent and require serine 15 phosphorylation', *Mol Biol Cell*, 15(8), pp. 3751-7.

Tsang, T.Y., Tsang, S.W., Lai, K.P., Tsang, W.P., Co, N.N. and Kwok, T.T. (2009) 'Facilitation of drug resistance development by gamma-irradiation in human cancer cells', *Oncol Rep*, 22(4), pp. 921-6.

Tsuchida, R., Yamada, T., Takagi, M., Shimada, A., Ishioka, C., Katsuki, Y., Igarashi, T., Chessa, L., Delia, D., Teraoka, H. and Mizutani, S. (2002) 'Detection of ATM gene mutation in human glioma cell line M059J by a rapid frameshift/stop codon assay in yeast', *Radiat Res*, 158(2), pp. 195-201.

Tsuruo, T., Iida, H., Nojiri, M., Tsukagoshi, S. and Sakurai, Y. (1983) 'Circumvention of vincristine and Adriamycin resistance in vitro and in vivo by calcium influx blockers', *Cancer Res*, 43(6), pp. 2905-10.

Tsuruo, T., Iida, H., Tsukagoshi, S. and Sakurai, Y. (1981) 'Overcoming of vincristine resistance in P388 leukemia in vivo and in vitro through enhanced cytotoxicity of vincristine and vinblastine by verapamil', *Cancer Res*, 41(5), pp. 1967-72.

Tsvetkov, L., Xu, X., Li, J. and Stern, D.F. (2003) 'Polo-like kinase 1 and Chk2 interact and co-localize to centrosomes and the midbody', *J Biol Chem*, 278(10), pp. 8468-75.

Tu, W.Z., Li, B., Huang, B., Wang, Y., Liu, X.D., Guan, H., Zhang, S.M., Tang, Y., Rang, W.Q. and Zhou, P.K. (2013) 'gammaH2AX foci formation in the absence of DNA damage: mitotic H2AX phosphorylation is mediated by the DNA-PKcs/CHK2 pathway', *FEBS Lett*, 587(21), pp. 3437-43.

Uziel, T., Lerenthal, Y., Moyal, L., Andegeko, Y., Mittelman, L. and Shiloh, Y. (2003) 'Requirement of the MRN complex for ATM activation by DNA damage', *Embo Journal*, 22(20), pp. 5612-5621.

van de Weerdt, B.C. and Medema, R.H. (2006) 'Polo-like kinases: a team in control of the division', *Cell Cycle*, 5(8), pp. 853-64.

van der Burg, M., Ijspeert, H., Verkaik, N.S., Turul, T., Wiegant, W.W., Morotomi-Yano, K., Mari, P.O., Tezcan, I., Chen, D.J., Zdzienicka, M.Z., van Dongen, J.J. and van Gent, D.C. (2009) 'A DNA-PKcs mutation in a radiosensitive T-B- SCID patient inhibits Artemis activation and nonhomologous end-joining', *J Clin Invest*, 119(1), pp. 91-8.

van der Kolk, D.M., de Vries, E.G., van Putten, W.J., Verdonck, L.F., Ossenkoppele, G.J., Verhoef, G.E. and Vellenga, E. (2000) 'P-glycoprotein and multidrug resistance protein activities in relation to treatment outcome in acute myeloid leukemia', *Clin Cancer Res*, 6(8), pp. 3205-14.

Vecchio, D., Daga, A., Carra, E., Marubbi, D., Raso, A., Mascelli, S., Nozza, P., Garre, M.L., Pitto, F., Ravetti, J.L., Vagge, S., Corvo, R., Profumo, A., Baio, G., Marcello, D. and Frosina, G. (2014) 'Pharmacokinetics, pharmacodynamics and efficacy on pediatric tumors of the glioma radiosensitizer KU60019', *Int J Cancer*.

Veuger, S.J., Curtin, N.J., Richardson, C.J., Smith, G.C. and Durkacz, B.W. (2003) 'Radiosensitization and DNA repair inhibition by the combined use of novel inhibitors of DNA-dependent protein kinase and poly(ADP-ribose) polymerase-1', *Cancer Res*, 63(18), pp. 6008-15.

Vlahos, C.J., Matter, W.F., Hui, K.Y. and Brown, R.F. (1994) 'A specific inhibitor of phosphatidylinositol 3-kinase, 2-(4-morpholinyl)-8-phenyl-4H-1-benzopyran-4-one (LY294002)', *J Biol Chem*, 269(7), pp. 5241-8.

Wang, C. and Lees-Miller, S.P. (2013) 'Detection and repair of ionizing radiation-induced DNA double strand breaks: new developments in nonhomologous end joining', *Int J Radiat Oncol Biol Phys*, 86(3), pp. 440-9.

Wang, H., Vo, T., Hajar, A., Li, S., Chen, X., Parissenti, A.M., Brindley, D.N. and Wang, Z. (2014) 'Multiple mechanisms underlying acquired resistance to taxanes in selected docetaxel-resistant MCF-7 breast cancer cells', *BMC Cancer*, 14, p. 37.

Wang, H., Wang, M., Wang, H., Bocker, W. and Iliakis, G. (2005) 'Complex H2AX phosphorylation patterns by multiple kinases including ATM and DNA-PK in human cells exposed to ionizing radiation and treated with kinase inhibitors', *J Cell Physiol*, 202(2), pp. 492-502.

Wang, S.Y., Peng, L., Li, C.P., Li, A.P., Zhou, J.W., Zhang, Z.D. and Liu, Q.Z. (2008a) 'Genetic variants of the XRCC7 gene involved in DNA repair and risk of human bladder cancer', *Int J Urol*, 15(6), pp. 534-9.

Wang, X., Szabo, C., Qian, C., Amadio, P.G., Thibodeau, S.N., Cerhan, J.R., Petersen, G.M., Liu, W. and Couch, F.J. (2008b) 'Mutational analysis of thirty-two double-strand DNA break repair genes in breast and pancreatic cancers', *Cancer Res*, 68(4), pp. 971-5.

Wani, M.C., Taylor, H.L., Wall, M.E., Coggon, P. and McPhail, A.T. (1971) 'Plant antitumor agents. VI. The isolation and structure of taxol, a novel antileukemic and antitumor agent from Taxus brevifolia', *J Am Chem Soc*, 93(9), pp. 2325-7.

Weiss, E. and Winey, M. (1996) 'The Saccharomyces cerevisiae spindle pole body duplication gene MPS1 is part of a mitotic checkpoint', *J Cell Biol*, 132(1-2), pp. 111-23.

White, J.S., Choi, S. and Bakkenist, C.J. (2008) 'Irreversible chromosome damage accumulates rapidly in the absence of ATM kinase activity', *Cell Cycle*, 7(9), pp. 1277-84.

Williamson, C.T., Muzik, H., Turhan, A.G., Zamo, A., O'Connor, M.J., Bebb, D.G. and Lees-Miller, S.P. (2010) 'ATM deficiency sensitizes mantle cell lymphoma cells to poly(ADP-ribose) polymerase-1 inhibitors', *Mol Cancer Ther*, 9(2), pp. 347-57.

Willmore, E., de Caux, S., Sunter, N.J., Tilby, M.J., Jackson, G.H., Austin, C.A. and Durkacz, B.W. (2004) 'A novel DNA-dependent protein kinase inhibitor, NU7026, potentiates the cytotoxicity of topoisomerase II poisons used in the treatment of leukemia', *Blood*, 103(12), pp. 4659-65.

Willmore, E., Elliott, S.L., Mainou-Fowler, T., Summerfield, G.P., Jackson, G.H., O'Neill, F., Lowe, C., Carter, A., Harris, R., Pettitt, A.R., Cano-Soumillac, C., Griffin, R.J., Cowell, I.G., Austin, C.A. and Durkacz, B.W. (2008) 'DNA-dependent protein kinase is a therapeutic target and an indicator of poor prognosis in B-cell chronic lymphocytic leukemia', *Clin Cancer Res*, 14(12), pp. 3984-92.

Wilmes, A., O'Sullivan, D., Chan, A., Chandrahasen, C., Paterson, I., Northcote, P.T., La Flamme, A.C. and Miller, J.H. (2011) 'Synergistic interactions between peloruside A and other microtubule-stabilizing and destabilizing agents in cultured human ovarian carcinoma cells and murine T cells', *Cancer Chemother Pharmacol*, 68(1), pp. 117-26.

Wilson, L., Jordan, M.A., Morse, A. and Margolis, R.L. (1982) 'Interaction of vinblastine with steady-state microtubules in vitro', *J Mol Biol*, 159(1), pp. 125-49.

Wong, R.H., Chang, I., Hudak, C.S., Hyun, S., Kwan, H.Y. and Sul, H.S. (2009) 'A role of DNA-PK for the metabolic gene regulation in response to insulin', *Cell*, 136(6), pp. 1056-72.

Woodbine, L., Neal, J.A., Sasi, N.K., Shimada, M., Deem, K., Coleman, H., Dobyns, W.B., Ogi, T., Meek, K., Davies, E.G. and Jeggo, P.A. (2013) 'PRKDC mutations in a SCID patient with profound neurological abnormalities', *J Clin Invest*, 123(7), pp. 2969-80.

Woods, C.M., Zhu, J., McQueney, P.A., Bollag, D. and Lazarides, E. (1995) 'Taxol-induced mitotic block triggers rapid onset of a p53-independent apoptotic pathway', *Mol Med*, 1(5), pp. 506-26.

Wu, J., Zhang, X., Zhang, L., Wu, C.Y., Rezaeian, A.H., Chan, C.H., Li, J.M., Wang, J., Gao, Y., Han, F., Jeong, Y.S., Yuan, X., Khanna, K.K., Jin, J., Zeng, Y.X. and Lin, H.K. (2012) 'Skp2 E3 ligase integrates ATM activation and homologous recombination repair by ubiquitinating NBS1', *Mol Cell*, 46(3), pp. 351-61.

Wu, Z.H., Shi, Y., Tibbetts, R.S. and Miyamoto, S. (2006) 'Molecular linkage between the kinase ATM and NF-kappaB signaling in response to genotoxic stimuli', *Science*, 311(5764), pp. 1141-6.

Xing, J., Wu, X., Vaporciyan, A.A., Spitz, M.R. and Gu, J. (2008) 'Prognostic significance of ataxia-telangiectasia mutated, DNA-dependent protein kinase catalytic

subunit, and Ku heterodimeric regulatory complex 86-kD subunit expression in patients with nonsmall cell lung cancer', *Cancer*, 112(12), pp. 2756-64.

Yajima, H., Lee, K.J. and Chen, B.P. (2006) 'ATR-dependent phosphorylation of DNA-dependent protein kinase catalytic subunit in response to UV-induced replication stress', *Mol Cell Biol*, 26(20), pp. 7520-8.

Yang, C., Tang, X., Guo, X., Niikura, Y., Kitagawa, K., Cui, K., Wong, S.T., Fu, L. and Xu, B. (2011) 'Aurora-B mediated ATM serine 1403 phosphorylation is required for mitotic ATM activation and the spindle checkpoint', *Mol Cell*, 44(4), pp. 597-608.

Yang, D.Q. and Kastan, M.B. (2000) 'Participation of ATM in insulin signalling through phosphorylation of eIF-4E-binding protein 1', *Nat Cell Biol*, 2(12), pp. 893-8.

Yang, W., Soares, J., Greninger, P., Edelman, E.J., Lightfoot, H., Forbes, S., Bindal, N., Beare, D., Smith, J.A., Thompson, I.R., Ramaswamy, S., Futreal, P.A., Haber, D.A., Stratton, M.R., Benes, C., McDermott, U. and Garnett, M.J. (2013) 'Genomics of Drug Sensitivity in Cancer (GDSC): a resource for therapeutic biomarker discovery in cancer cells', *Nucleic Acids Res*, 41(Database issue), pp. D955-61.

Yoo, S. and Dynan, W.S. (1999) 'Geometry of a complex formed by double strand break repair proteins at a single DNA end: recruitment of DNA-PKcs induces inward translocation of Ku protein', *Nucleic Acids Res*, 27(24), pp. 4679-86.

Yvon, A.M., Wadsworth, P. and Jordan, M.A. (1999) 'Taxol suppresses dynamics of individual microtubules in living human tumor cells', *Mol Biol Cell*, 10(4), pp. 947-59.

Zhai, Y., Kronebusch, P.J., Simon, P.M. and Borisy, G.G. (1996) 'Microtubule dynamics at the G2/M transition: abrupt breakdown of cytoplasmic microtubules at nuclear envelope breakdown and implications for spindle morphogenesis', *J Cell Biol*, 135(1), pp. 201-14.

Zhang, A.L., Russell, P.J., Knittel, T. and Milross, C. (2007a) 'Paclitaxel enhanced radiation sensitization for the suppression of human prostate cancer tumor growth via a p53 independent pathway', *Prostate*, 67(15), pp. 1630-40.

Zhang, S., Hemmerich, P. and Grosse, F. (2007b) 'Centrosomal localization of DNA damage checkpoint proteins', *J Cell Biochem*, 101(2), pp. 451-65.

Zhao, Y., Thomas, H.D., Batey, M.A., Cowell, I.G., Richardson, C.J., Griffin, R.J., Calvert, A.H., Newell, D.R., Smith, G.C. and Curtin, N.J. (2006) 'Preclinical evaluation of a potent novel DNA-dependent protein kinase inhibitor NU7441', *Cancer Res*, 66(10), pp. 5354-62.

Zhou, B.B. and Bartek, J. (2004) 'Targeting the checkpoint kinases: chemosensitization versus chemoprotection', *Nat Rev Cancer*, 4(3), pp. 216-25.

Zhu, M.L., Horbinski, C.M., Garzotto, M., Qian, D.Z., Beer, T.M. and Kyprianou, N. (2010) 'Tubulin-targeting chemotherapy impairs androgen receptor activity in prostate cancer', *Cancer Res*, 70(20), pp. 7992-8002.

Zieve, G.W., Turnbull, D., Mullins, J.M. and McIntosh, J.R. (1980) 'Production of large numbers of mitotic mammalian cells by use of the reversible microtubule inhibitor nocodazole. Nocodazole accumulated mitotic cells', *Exp Cell Res*, 126(2), pp. 397-405.

Zumer, K., Low, A.K., Jiang, H., Saksela, K. and Peterlin, B.M. (2012) 'Unmodified histone H3K4 and DNA-dependent protein kinase recruit autoimmune regulator to target genes', *Mol Cell Biol*, 32(8), pp. 1354-62.